1-1-2002

Characterization of microbial aggregates in relation to membrane biofouling in submerged membrane bioreactors

Heather Elizabeth Kraemer
Ryerson University

In compliance with the
Canadian Privacy Legislation
some supporting forms
may have been removed from
this dissertation.

While these forms may be included
in the document page count,
their removal does not represent
any loss of content from the dissertation.

Characterization of Microbial Aggregates in Relation to Membrane Biofouling in Submerged Membrane Bioreactors

by

Heather Elizabeth Kraemer, B.Sc. (Hons) (Waterloo, 2000)

A thesis presented to Ryerson University in partial fulfillment of the requirement for the degree of Master of Applied Science in Environmental Applied Science and Management

Toronto, Ontario, Canada, 2002

Your file Votre référence
ISBN: 0-612-87159-2
Our file Notre référence
ISBN: 0-612-87159-2

I hereby declare that I am the sole author of this thesis.

I authorize Ryerson University to lend this thesis to other institutions or individuals for the purpose of scholarly research.

Heather Kraemer

I further authorize Ryerson University to reproduce this thesis by photocopying or by other means, in total or in part, at the request of other institutions or individuals for the purpose of scholarly research.

Heather Kraemer

Ryerson University requires the signatures of all persons using or photocopying this thesis. Please sign below and give address and date.

Signature of Borrower	Address	Date

Characterization of Microbial Aggregates in Relation to Membrane Biofouling in Submerged Membrane Bioreactors

ABSTRACT

The purpose of this study was to characterize microbial aggregates and extracellular polymeric substances (EPS) that contribute to biofouling of submerged polymeric microfiltration membranes. Two issues were addressed in this study, 1) the influence operational and recovery cleanings of membranes have on biofouling amelioration and 2) the influence physicochemical properties of microbial flocs have on biofouling.

The experiments in this study employed two pilot scale ZeeWeed™ membrane bioreactors (MBRs). In one MBR, a ZW-10 module was installed to treat secondary municipal wastewater at a sludge retention time (SRT) of 30 days and operated under permeate/relaxation conditions. In the other MBR, two ZW-10 modules were installed to treat secondary municipal wastewater at an SRT of 12 days. One module operated under permeate/relaxation conditions, while the other operated under permeate/backwash conditions. Sludge samples from the MBRs were characterized by measuring the surface charge, hydrophobicity, and EPS composition of the microbial flocs. Membrane fibre samples were collected from each ZW-10 module during permeation and after recovery cleanings. The biofoulant on the membrane was analyzed using confocal laser scanning microscopy (CLSM) after simultaneous staining with the lectins concanavalin A (ConA), wheat germ agglutinin (WGA), and soybean agglutinin (SBA).

The CLSM analysis of the membrane fibres sampled showed that the biofoulant on the membrane was composed of a heterogeneous colonization of microbes and EPS known to contain glucose, mannose, *N*-acetylglucosamine, and galactose. The dominant carbohydrate in the biofoulant was shown to be *N*-acetylglucosamine, which is part of both the cell wall of bacteria and the extracellular matrix. The reversible biofoulant was composed of individual cells, aggregates of cells, and EPS. The major constituent of the irreversible biofoulant was inferred to be EPS, which was observed as a fibrous network of material that remained adhered to the membrane after recovery cleaning the modules with a 2000 ppm hypochlorite solution. By using a permeate backwash rather than relaxation as an operational cleaning method, the rate of biofouling may be reduced. The rate of biofoulant accumulation on hydrophilic membranes may be reduced at higher SRTs because the biomass at higher SRTs has a higher hydrophobicity when compared to the biomass at lower SRTs.

ACKNOWLEDGEMENTS

I would first like to express my appreciation to my supervisor, Dr. Steven Liss, for being very supportive and patient throughout my thesis. I would like to thank Dr. Steven Liss for the financial support for this project provided by CRESTech and Zenon Environmental Inc. I would also like to thank the School of Graduate Studies at Ryerson University for awarding me a Program Scholarship.

I acknowledge the employees at Zenon Environmental Inc., especially Dr. Hadi Hussain, Henry Behmann, Mike Russell, Mike Moorhead, Samira Nawar, and Natasha Stojanovic, for making this research possible by operating the reactors, performing the standard wastewater analysis, and providing assistance and expertise.

A special thanks to all of my colleagues, both in the Biotechnology Lab and in the Environmental Applied Science and Management program at Ryerson University, especially Eva, Dean, Deborah, Heather, Jamie, Jennifer, Joe, Margaret, Morgan, and Penny for their friendship, advice, and continual support. Thanks to Moses Akingbade for his hard work at assisting me with the analytical experiments, especially the DNA analysis.

Finally, I would like to express my sincere gratitude to my mother, father, Salvatore, and all of my family and friends whose unconditional love, patience, and support throughout my personal and professional development has helped me reach this important goal.

TABLE OF CONTENTS

LIST OF TABLES

LIST OF FIGURES

NOMENCLATURE

AF	Alexa Fluor
AFM	atomic force microscopy
BS	*Bandeiraea simplicifolia*
CLSM	confocal laser scanning microscopy
COM	conventional optical microscopy
ConA	concanavalin A
CPS	capsular polymeric substances
DNA	deoxyribonucleic acid
DO	dissolved oxygen
EPS	extracellular polymeric substances
Fl	fluorescein
HRT	hydraulic residence time
LPS	lipopolysaccharide
MATH	microbial adherence to hydrocarbons
MBR	membrane bioreactor
MLSS	mixed liquor suspended solids
PBS	phosphate buffered saline
RCM	Raman confocal microspectroscopy
SBA	soybean agglutinin
SRT	sludge retention time
SEM	scanning electron microscopy
TEM	transmission electron microscopy
TMP	transmembrane pressure
tmr	tetramethylrhodamine
WGA	wheat germ agglutinin

1.0 INTRODUCTION

1.1 Background and Objectives

Membrane separation technologies have gained widespread use in the treatment of wastewaters. The conventional activated sludge process is being modified in that a membrane bioreactor replaces the secondary clarifier for the separation of mixed liquor and effluent (Cicek *et al.*, 1998). Membrane bioreactors (MBRs) offer numerous advantages over the conventional activated sludge process including superior quality effluent, reduced land requirements, total retention of biomass, high volumetric loading, longer sludge retention times (SRT), and less sludge production (Owen *et al.*, 1995; Liu *et al.*, 2000b; Novachis, 2000; Parameshwaran *et al.*, 2001). However, the most significant limitation in membrane technology is membrane fouling, in particular biofouling. When membrane fouling occurs, the process performance of a MBR is dramatically reduced which leads to high energy consumption, and frequent membrane cleaning or replacement.

With respect to membrane technology, biofouling is the interaction between the membrane and the activated sludge matrix, which is composed of bacterial cells, microbial aggregates, and extracellular polymers (Chang and Lee, 1998). The microbes within the MBR aggregate together either in suspension to form flocs or on the membrane to form a biofilm. As the microbes reproduce, metabolize, and grow they are continuously synthesizing extracellular polymers. Previous studies have shown that when the SRT is varied, the physicochemical properties of microbial aggregates change. The extracellular polymeric substances (EPS) composition is also expected to change, in turn affecting the performance of MBRs. Biofouling of membranes tends to be both reversible and irreversible. Deposition or attachment of particulate matter is often reversible and is characterized as external fouling of the membrane surface by the accumulation of aggregated cells, cell debris, and other rejected particles (Ma *et al.*, 2000; Wakeman and Williams, 2002). Irreversible fouling is characterized as internal fouling of the membrane pores by the deposition and adsorption of solute and colloid materials, which are similar in size to the pore diameter of the membrane (Ma *et al.*, 2000; Wakeman and Williams, 2002). EPS play a major role in reversible and irreversible fouling (Nagaoka *et al.*, 1996 and 1998; Chang and Lee, 1998). The soluble and bound EPS have the ability to accumulate within the pore structure as well as on the membrane surface.

Other factors that affect biofouling of membranes include hydrodynamic conditions, membrane module design, and membrane surface chemistry.

In order to maintain operability of MBRs, strategies have been implemented to control biofouling. Biofouling is controlled by methods that attempt to prevent biofouling and methods to alleviate biofouling when already present. Common methods to prevent membrane biofouling include operational cleaning methods such as backwashing, backpulsing, and relaxation. The most common practice to alleviate biofouling is by recovery cleaning. Recovery cleaning is performed in order to destroy any foulants that have adhered to the membrane surface or within its pore structure. Oxidizing biocides, specifically chlorine, have been used extensively for recovery cleaning of fouled membranes (Gander *et al.*, 2000). Chlorine has been known to weaken the sludge cake by reacting with proteins and EPS (Flemming *et al.*, 1996).

Previous studies have examined the hydrodynamics of MBRs, in particular those associated with improving membrane performance; however, studying these concepts exclusively is insufficient to understand the whole MBR system. Therefore, it is also important to research the biological conditions in conjunction with the hydrodynamics of the system.

The purpose of this study was to characterize microbial aggregates and their associated extracellular polymers that contribute to biofouling of submerged polymeric microfiltration membranes. The objectives of this study were threefold: 1) to study the influence physicochemical properties of microbial flocs have on biofouling; 2) to assess the influence operational cleaning methods in MBRs have on biofouling; and 3) to investigate the effect recovery cleaning of membrane modules has on biofouling amelioration.

1.2 Thesis Outline

The next section of this report is a review of the literature relevant to this study. The information provides background on membrane technology, its use in aerobic municipal wastewater treatment, membrane biofouling and control, mechanisms for microbial adherence to surfaces, and physicochemical properties of microbial aggregates and EPS. Additionally, microscopic techniques are reviewed with emphasis on confocal laser scanning microscopy (CLSM) since it was used extensively in this study.

Chapter 3 explains the experimental approach applied in this study and outlines the techniques used. In Chapter 4 the results obtained using microscopic and analytical techniques to study biofouling in MBRs are presented and summarized. Chapter 5 contains a discussion of the results. Chapters 6 summarizes the conclusions of this study and provides recommendations for biofouling management and future research. Detailed protocols and experimental results are given in the appendices.

2.0 LITERATURE REVIEW

2.1 Conventional Wastewater Treatment

Wastewater treatment generally employs a multi-stage process that includes preliminary, primary, secondary, and tertiary treatment (Metcalf and Eddy, Inc., 1991). The goal is to reduce or remove organic matter, solids, nutrients, disease-causing organisms and other pollutants from wastewater (Rittmann and McCarty, 2000). The preliminary stage eliminates materials that may interfere with the physical operation of the system. Treatment equipment such as bar screens, comminutors and grit chambers are used when the wastewater first enters a treatment plant. Primary treatment is the second step in treatment in which suspended solids or insoluble matter is removed from the wastewater via screening or settling tanks. The remaining effluent contains soluble organic matter and fine particles that cannot be released into the environment due to regulatory requirements. The most efficient way to remove organic matter from wastewater is by utilizing biological treatment systems. Thus, secondary treatment uses microbes to degrade the organic matter to inert solids, water, and gases (either carbon dioxide if aerobic or carbon dioxide and methane if anaerobic) through biochemical reactions (Stephenson *et al.*, 2001).

Approaches used to accomplish secondary treatment include fixed film and suspended growth systems. Fixed film systems (trickling filters, rotating biological contactors, and sand filters) grow microorganisms on substrates such as rocks, sand or plastic. The wastewater flows past the film of microorganisms fixed to the substrate and organic matter and nutrients are degraded (Rittmann and McCarty, 2000). Suspended growth systems are the most widely used in municipal and industrial wastewater treatment and include an aerated bioreactor, a settling tank, a solids recycle from the settling tank to the bioreactor, and a sludge wasting line. The bioreactor contains a mixture of organics and microbial aggregates, or flocs, of microorganisms termed the activated sludge (Rittmann and McCarty, 2000). The various microorganisms include prokaryotes (bacteria) and eukaryotes (protozoa, rotifers, and nematodes) (Rittmann and McCarty, 2000). Bacteria play a key role in nitrification, denitrification, and converting soluble and particulate organic compounds into biomass and gaseous waste. The bacteria present in activated sludge are predominantly Gram negative when compared to Gram positive bacteria at sludge retention times (SRT) ranging from 2 to 30

days (Cicek *et al.*, 2001). The higher microbes consume particulate organic matter and also scavenge bacteria (Stephenson *et al.*, 2001). The protozoa are important because they can be used as indicator organisms of process performance (Rittmann and McCarty, 2000). In order to grow, survive and function, microbes need specific environmental conditions including sufficient nutrients, neutral pH, and ambient temperature control. The final stage of treatment focuses on removal of disease-causing organisms from wastewater. This is accomplished by disinfection of the treated wastewater either by adding chlorine or by using ultraviolet light.

While the activated sludge process is widely used, it also has many problems. One of the major problems is poor settling sludge. When this occurs, the effluent contains suspended solids that often exceed regulatory requirements and the desired SRT cannot be maintained. Poor settling sludge can be a result of filamentous bulking, non-filamentous bulking, dispersed growth, pinpoint flocs, and/or foaming or scum formation (Rittmann and McCarty, 2000). Filamentous bulking occurs when filamentous organisms extend out from the flocs and interfere with compaction and settling. Non-filamentous bulking occurs when microbes are present in large amounts of extracellular polymeric substances (EPS). When microorganisms are unable to form flocs they are dispersed and only form small clusters of individual cells. Similarly, pinpoint flocs are small, compact, and spherical which settle much more slowly than large, irregular shaped flocs. Finally, foaming or scum formation occurs in the presence of *Nocardia* sp. and/or *Microthrix parvicella* or by non-degradable surfactants.

2.2 Membrane Technology

Membrane separation technologies have recently gained widespread use in the treatment of drinking water, industrial wastewater, and municipal wastewater. A membrane can be defined as a material through which one type of substance can pass more readily than others (Stephenson *et al.*, 2001) and its primary goal is to retain solids (Gander *et al.*, 2000). In general, membranes can be categorized by a number of factors including pore size, molecular weight cut off, whether the membrane is dense or porous, or whether the membrane is organic (polymeric) or inorganic (ceramic or metallic) (Stephenson *et al.*, 2001). In wastewater applications, ultrafiltration or microfiltration membranes with pore sizes ranging from 0.04 μm to 0.45 μm are often employed (Stephenson *et al.*, 2001). The geometry of membranes is also

important in process performance. The configurations are based on planar or cylindrical geometry and include pleated filter cartridge, plate-and-frame, spiral wound, tubular, and hollow fibre membranes (Stephenson *et al.*, 2001).

Combining membrane technology with biological reactors for the treatment of wastewaters has led to the development of three generic membrane bioreactors (MBRs). These MBRs are used for separation and retention of solids, for bubble-less aeration within the bioreactor, and for extraction of priority organic pollutants from industrial wastewater (Brindle and Stephenson, 1996). Biomass separation MBRs are the most common type of membrane technology and have been developed to address the solids separation issue in conventional activated sludge treatment. The MBR process modifies the activated sludge process in that the secondary clarifier is eliminated and sludge settling no longer becomes problematic (Defrance *et al.*, 2000; Novachis, 2000). Instead, ultra- or microfiltration membrane modules are used together with a biological reactor to separate the mixed liquor and effluent (Smith *et al.*, 1969; Cicek *et al.*, 1998; Cote and Thompson, 2000; Lee *et al.*, 2001; Rosenberger *et al.*, 2002).

In the treatment of wastewater, aerated MBRs fall into two types, a crossflow external MBR and a submerged MBR (Liu *et al.*, 2000a; Ozaki and Yamamoto, 2001). In a crossflow external MBR the membrane module is located outside the bioreactor and a recirculating pump is used to transfer the mixed liquor to the membrane module where the biomass is separated (Ozaki and Yamamoto, 2001). In a submerged MBR the module is immersed directly into the bioreactor and the effluent exits the aerated bioreactor either by a vacuum pump or by gravity (Liu *et al.*, 2001a; Ozaki and Yamamoto, 2001). The use of submerged modules has reduced the power consumption of MBRs significantly (Rosenberger *et al.*, 2002). Consequently, submerged MBRs have become the most common system for the treatment of municipal wastewater (Gander *et al.*, 2000; Stephenson *et al.*, 2001).

2.2.1 Applications of Aerobic MBRs in Municipal Wastewater Treatment

The application of MBRs to treat municipal wastewater has been a subject of recent research in both laboratory and pilot-scale reactors. This research has shown MBRs to offer numerous advantages over the conventional activated sludge process including superior quality effluent,

reduced land requirements, total retention of biomass, high volumetric loading, longer SRTs, and less sludge production (Owen *et al.*, 1995; Liu *et al.*, 2000b; Novachis, 2000; Parameshwaran *et al.*, 2001). Additionally, in biomass separation MBRs the SRT is independent of the hydraulic residence time (HRT). Therefore the MBR can be run at a low HRT with long SRTs without biomass washout, which is common in a conventional activated sludge process (Stephenson *et al.*, 2001). Furthermore, the overall operating costs of MBRs decrease because they can be easily automated which minimizes maintenance time and the reduction in sludge production reduces sludge disposal (Gander *et al.*, 2000; Parameshwaran *et al.*, 2001).

In aerated MBRs, oxygen is supplied by surface aeration, coarse air bubble diffusers, fine air bubble diffusers, and jet aeration (Novachis, 2000; Stephenson *et al.*, 2001). In addition to providing oxygen, shear stress and air scouring are important hydrodynamic conditions that help to prevent sludge accumulation on the membrane surface. Ozaki and Yamamoto (2001) studied the hydraulic effect of sludge accumulation on the membrane surface in bubble and non-bubble driven crossflow filtration. They observed that sludge accumulation on the membrane surface is dependent on aeration intensity which can be explained by shear stress. Shear stress caused by crossflow velocity and recirculation velocity has an impact on cake formation as well as on floc properties in the MBR. Tardieu *et al.* (1998) observed that at a low recirculation velocity of 0.5 m/sec, the flocs accumulated rapidly onto the membrane surface to form a cake deposit. Conversely, at a high recirculation velocity of 4 m/sec, they observed an absence of flocs accumulating at the membrane surface. They concluded that high recirculation velocities appear to prevent sludge deposition on membrane surfaces. However, Wisniewski and Grasmick (1998) found that shear stress from recirculation destructures the composition and characteristics of flocs in the biological suspension. In their experiments, when the recirculation velocity was increased from 0.5 m/sec to 5 m/sec, they observed a decrease in mean particle size from 125 μm to 20 μm respectively. This decrease in floc size resulted in a decrease of the settleable fraction and the release of EPS which can also reduce the settleability of the biological suspension. Bouhabila *et al.* (2001) found that increasing the air flow rate over the membrane surface from 1.2 $m^3/m^2/hr$ to 3.6 $m^3/m^2/hr$ resulted in a decrease in total resistance of the membrane, thus increasing the filtrate flux by a ratio of 3.

While shear stress and air scouring are favorable hydrodynamic conditions to maintain membrane filterability, they are high in energy consumption which can increase operating costs.

The operating flux in aerobic MBR systems has been studied extensively due to the fact that MBR performance is directly related to the hydrodynamic condition. Flux rates are known to range from 5 to 300 $L/m^2/hr$ (Stephenson *et al.*, 2001). The exact permeation flux at which a system operates is dependent on complex interrelated parameters including transmembrane pressure (TMP), shear forces, crossflow velocity, pore size, membrane configuration, and biomass characteristics. There is also the concept of critical flux. Field *et al.* (1995) hypothesized that critical flux is a flux that does not decline for a period of time after start-up. If the TMP and flux are below the critical flux, the steady-state flux will increase linearly with the TMP which controls filtration. If the flux is above the critical flux, the TMP increases rapidly and the flux may even decrease (Tardieu *et al.*, 1998). MBRs are conventionally operated at a constant flux while monitoring TMP; however, on occasion TMP is kept constant while flux is monitored.

The volumetric loading rates have been reported between 1.2 kg $COD/m^3/day$ to 3.2 kg $COD/m^3/day$ with chemical oxygen demand (COD) removal efficiencies >90% (Stephenson *et al.*, 2001). With respect to COD removal, performance appears to be relatively insensitive to HRT with values of HRT ranging from 2 to 24 hours resulting in very high removal percentages. Typical mixed liquor suspended solids (MLSS) concentrations in aerobic MBRs range from 10 to 20 g/L. High biomass concentrations could play a significant role in membrane fouling. A higher MLSS concentration correlates to a higher TMP or a lower permeate flux due to sludge cake formation on the membrane surface (Nagaoka *et al.*, 1996). Typically, SRTs vary between 5 and 30 days for all MBR applications (Stephenson *et al.*, 2001). Since MBRs are able to operate well at longer SRTs, the sludge produced is often less than with conventional activated sludge processes because aerobic digestion is allowed to occur within the system (Gander *et al.*, 2000; Novachis, 2000). However, the characteristics of a microbial community change with varying SRT in turn affecting the filterability of the sludge

(Liss *et al.*, 1996; Cicek *et al.*, 2001; Liao *et al.*, 2001; Rosenberger *et al.*, 2002; Witzig *et al.*, 2002).

2.2.2 Sludge Retention Time

The age of sludge is determined by the amount of time the biomass is retained within a bioreactor. When SRT is varied, the sludge characteristics are affected. These characteristics include changes in floc settling properties, EPS composition, flocculation capability, and dewaterability (Liao *et al.*, 2001). In general, low SRTs are associated with a rapid rate of microbial growth and higher rates of sludge production, while high SRTs are associated with slow growing microbes and low rates of sludge production. Cicek *et al.* (2001) compared the biomass in a pilot-scale MBR treating synthetic wastewater containing high molecular weight compounds under SRTs varying from 2 to 30 days. They concluded that the biomass production rate and biomass viability increased with decreasing SRT, but the overall enzymatic activity did not change significantly.

Since floc properties change with varying SRT, one would also expect the EPS composition to change, in turn affecting the performance of MBRs. Studies that have examined the influence of SRT on EPS composition have produced contradictory results. Frølund *et al.* (1994) found that the total polysaccharide content was higher at low sludge age when compared to high sludge age. Conversely, Liao *et al.* (2001) found that the total EPS content was independent of SRT and it was the EPS composition that changed with SRT. The protein to carbohydrate ratio increased when the SRT was increased from 4 to 12 days and leveled off at SRTs above 12 days. Eriksson *et al.* (1992) proposed that the difference between sludge ages is due to the fact that central, older parts of flocs are embedded in a strong EPS matrix, while the periphery is surrounded by weak chains of microorganisms joined by EPS bridges. In the central part of flocs, the binding and cross linking of the polymers may be due to electrostatic bridging or polyvalent metal ions with strong complexing ability. In the outer parts of flocs, the cells are flocculated with few cell-cell contacts due to the structure and partly because of weak binding due to the limited amount of polymers. Therefore, new flocs would be composed mainly of the weakly linked chains, while the older flocs would contain a higher proportion of the tightly bound material (Eriksson *et al.*, 1992).

Recently, studies have been conducted to explain the role of SRT in controlling membrane biofouling (Chang and Lee, 1998; Fan *et al.*, 2000; Bouhabila *et al.*, 2001). Chang and Lee (1998) used membranes with varying pore sizes and hydrophobicity and found that when the SRT was increased from 3 and 8 days to 33 days a significant increase in sustainable flux resulted. They attribute this to a lower concentration of EPS at higher SRTs. Fan *et al.* (2000) came to a similar conclusion after studying MBRs at 5, 10, and 20 day SRTs. They reported that cleaning was not required for the MBR having a 20 day SRT for the first 70 days of operation; however, the MBR having a 5 day SRT required cleaning after 3 to 5 days of operation. Furthermore, Bouhabila *et al.* (2001) fractioned the sludge suspension into suspended solids, colloids, solutes and investigated fouling at 10, 20, and 30 day SRTs. They concluded that at all SRTs colloids and solutes were dominant in controlling filtration resistance.

2.3 Biofouling

Although the use of MBRs in wastewater treatment is emerging as a desirable technology with advantages over conventional treatment methods, there continue to be inherent problems with this innovative technology. The most significant limitation is membrane fouling, in particular biofouling. Membrane fouling occurs when the process performance of a MBR is dramatically reduced due to a rapid increase in TMP or a rapid decrease in flux, which leads to high energy consumption, and frequent membrane cleaning or replacement (Wisniewski and Grasmick, 1998; Defrance *et al.*, 2000; Bouhabila *et al.*, 2001; Chang *et al.*, 2001; Ozaki and Yamamoto, 2001; Wakeman and Williams, 2002).

Biofouling is related to the interaction of biosolids with the membrane in a MBR treating wastewater. Biofouling is a consequence arising from the formation of a biofilm. Biofilms are ubiquitous in both natural and engineered environments. They have been researched in many different fields including biofouling, biocorrosion, medicine, and limnology (van Loosdrecht *et al.*, 1995). These aggregates are well known to develop at liquid-solid interfaces, but they can also form at water-air and solid-air interfaces (Flemming *et al.*, 2000). A biofilm is an aggregation of microbial cells and their associated extracellular polymers adhered to a substratum and separated by interstitial voids (Davey and O'Toole, 2000; Lewandowski,

2000). These hydrated complex structures range from being a discrete group of microcolonies to a thin, dense layer of cells, to a well developed heterogeneous microenvironment (Okabe *et al.*, 1998; Donlan, 2000; Davey and O'Toole, 2000).

Commercially, biofilms are important in that they provide valuable processes; however, biofilms can also reveal their destructive abilities that have proven detrimental and costly (McFeters *et al.*, 1984). Biofilms are beneficial in the removal of soluble and particulate matter from natural streams and rivers and in wastewater treatment facilities. They can also determine water quality by influencing dissolved oxygen levels and serve as a sink for toxic and hazardous materials (Characklis, 1984). Conversely, biofilms cause biofouling. Biofouling is the undesirable deposition and accumulation of microorganisms, extracellular polymers, and cell debris on substrates (Flemming *et al.*, 1996; Baker and Dudley, 1998). Biofilms are a disadvantage when the performance of an engineered system, such as a MBR, declines and leads to the deterioration of materials and an increase in capital and operating costs.

2.3.1 Biofilm Development

The structure of a biofilm is influenced by numerous factors including the type of substratum it adheres to, flow rate, organic loading, temperature, suspended solids levels, and shear stress (van Loosdrecht *et al.*, 1995; Donlan, 2000). Despite these factors the developmental stages of a biofilm are similar in all liquid-solid interfaces and follow a sequential pattern of colonization, maturation, and detachment (McFeters *et al.*, 1984).

The substratum may play an important role in biofilm attachment and stability. According to researchers, surface roughness enhances the biofilm development (Characklis, 1984; McFeters *et al.*, 1984; van Loosdrecht *et al.*, 1995). Prolonged attachment of microbes to rough surfaces may be more likely than to smooth surfaces because microbes adhere to areas on the surface where they are shielded from shear forces (Characklis, 1984; McFeters *et al.*, 1984; van Loosdrecht *et al.*, 1995). Furthermore the attachment rates may increase on rough surfaces since the microbes have a larger surface area to make contact with (Characklis, 1984).

Before microbial adhesion occurs, the substrate is conditioned rapidly, often in minutes, with organic material, proteins, and polysaccharides (McFeters *et al.*, 1984; Wimpenny, 2000). When bacterial cells approach the surface they do so randomly until they come close to the surface at which point they contact the surface by diffusion, convective transport, or active movement (Newby *et al.*, 2000). Once contact between the cells and the surface has been made, adhesion can take place. At first the microbes are attached to the surface loosely by van der Waals and electrostatic forces. Eventually, they become more firmly attached by fimbriae, and pili, and by secreting EPS which serve as an adhesive substance (Wimpenny, 2000). As the microbes reproduce, metabolize and grow, they form a monolayer, then microcolonies develop. The microbes synthesize EPS which serve as a site for nutrient adsorption, maintains the structural integrity of the biofilm, protects the biofilm from environmental stresses, and bridges one microcolony to another (McFeters *et al.*, 1984; Lewandowski, 2000). Numerous interstitial voids are evident within the biofilm in which water moves freely providing nutrients and oxygen. The biofilm also traps nutrients from the surrounding environment and continues to grow and become thicker until maturation is reached. The biofilm is considered mature when changes occur within the microenvironment such as in anaerobic zones. Anaerobic zones arise because the older layers become more dense and thick and less hydrated leading to a lack of oxygen (McFeters *et al.*, 1984). Often, detachment of biofilm material is thought of as the final stage in biofilm development. However, according to Characklis (1984) detachment occurs from the moment of initial attachment. At all stages of biofilm development detachment is influenced by shear forces, cell death and lysis, and lack of stability (Characklis 1984; McFeters *et al.*, 1984; Wimpenny, 2000). Detachment may occur as shearing, a continuous removal of small portions of the biofilm, or as sloughing, a massive removal of biofilm usually due to lack of nutrients or oxygen (Characklis, 1984).

2.3.2 Biofouling in Membrane Bioreactors

During filtration, the mixed liquor and soluble components of the biological suspension are rejected by the membrane surface. A concentration gradient or polarization layer is developed, that is, a higher concentration of retained particles is formed at the membrane surface compared to that of the bulk suspension (Tardieu *et al.*, 1998; Gander *et al.*, 2000; Silva *et al.*, 2000; Stephenson *et al.*, 2001). Simultaneously, suspended solids, colloids, and solutes are

transported away from the membrane via three different backtransport mechanisms including shear-induced diffusion, inertial lift, and surface transport (Tardieu *et al.*, 1998). Therefore the onset of membrane fouling arises when the membrane resistance increases, which is known to occur in the early stages of filtration, especially within the first few hours of start-up (Gander *et al.*, 2000). Furthermore, in feedwater with particle size distribution, the smaller particles deposit preferentially to the membrane surface because hydrodynamic backtransport increases with particle size (Fane *et al.*, 2000).

Biofouling is the interaction between the membrane and the activated sludge matrix, which is composed of bacterial cells, microbial aggregates, and extracellular polymers (Chang *et al.*, 1998). Biofouling of membranes tends to be both reversible and irreversible. Deposition or adhesion of particulate matter is often reversible and is characterized as external fouling of the membrane surface by the accumulation of aggregated cells, cell debris, and other rejected particles (Ma *et al.*, 2000; Wakeman and Williams, 2002). Irreversible fouling is characterized as internal fouling of the membrane pores by the deposition and adsorption of solute and colloid materials, which are similar in size to the pore diameter of the membrane (Ma *et al.*, 2000; Wakeman and Williams, 2002). Since particle deposition (sludge cake formation) creates an additional layer of resistance to permeate flow and pore blocking increases membrane resistance by decreasing the surface area of the membrane pores, these two phenomena can be classified as mechanisms of biofouling in MBRs.

EPS play a major role in reversible and irreversible fouling and can be classified as its own biofouling mechanism (Nagaoka *et al.*, 1996 and 1998; Chang and Lee, 1998). The EPS has the ability to accumulate within the pore structure as well as on the membrane surface leading to a decrease in filterability. Numerous studies have examined the relationship between EPS production and biofouling of membrane surfaces. A larger EPS content is related to a higher fouling rate or a decrease in membrane performance (Hodgson *et al.*, 1993). Nagaoka *et al.* (1996) found that the accumulation of EPS in the aeration tank and on the membrane surface resulted in an increase in viscosity of the MLSS and an increase in the filtration resistance of the membrane. Recent studies have quantified biofouling by examining each fraction of the activated sludge matrix (Tardieu *et al.*, 1998; Defrane *et al.*, 2000; Wisniewski *et al.*, 2000;

Bouhabila *et al.*, 2001). Tardieu *et al.* (1998) fractioned the organic matter from suspension into suspended solids (1 μm – 1000 μm), colloids (0.001 μm to 1 μm), and solutes (< 0.001 μm). In all studies, the researchers concluded that colloids are of prime importance in the biofouling process. EPS production is also related to activated sludge flocculation, settling, and dewatering properties (Horan and Eccles, 1986; Figueroa and Silverstein, 1989; Frølund *et al.*, 1996; Palmgren and Nielsen, 1996; Bura *et al.*, 1998; Jorand *et al.*, 1998; Liao *et al.*, 2001).

Other factors that affect biofouling of membranes include hydrodynamic conditions, membrane module design, and membrane surface chemistry. However, Ma *et al.* (2000) conducted research on the surface chemistry of various membranes and concluded that fouling was primarily due to the physical deposition of bacterial cells on the membrane surface regardless of its surface chemistry.

2.3.3 Biofouling Control

Strategies to control biofouling can be classified as methods to prevent biofouling and methods to alleviate biofouling when already present. Methods to prevent fouling include backwashing, backpulsing, relaxation, pretreating the feedwater, optimizing the activated sludge process, optimizing the hydrodynamics of the MBR system, and choosing or developing the most applicable membrane module design and membrane material (Fane *et al.*, 2000; Ma *et al.*, 2000; Bouhabila *et al*,. 2001; Wakeman and Williams, 2002).

Backwashing is an effective way to maintain MBR performance (Silva *et al.*, 2000; Bouhabila *et al.*, 2001; Wakeman and Williams, 2002). Backwashing is a common practice whereby the permeate (filtrate) is pumped back through the membrane at periodic intervals. This process is effective at removing loosely adhered foulant from the membrane; however, backwashing has proven to be ineffective when the sludge cake is adhered strongly to the membrane or if the pores are blocked with foulant (Bouhabila *et al.*, 2001; Wakeman and Williams, 2002). Backpulsing is similar to backwashing, but is shorter in duration ($\leq$ 0.1 seconds) and may be operated continuously or periodically (Silva *et al.*, 2000; Wakeman and Williams, 2002). Backpulsing has been particularly useful at minimizing the adherence of colloids (Wakeman

and Williams, 2002). Relaxation is not a common practice, but allows for periods of filtration relief which is intended to prolong the permeability of the membrane.

Feed pretreatment can involve physical and chemical processes. Physical processes include prefiltration or centrifugation to remove foulants that may cause a decrease in process performance (Wakeman and Williams, 2002). However, the feasibility of this option is limited since it is the foulants that form a large part of the organic load which the MBR is intended to treat (Stephenson *et al.*, 2001). Chemical processes include the addition of coagulants thereby promoting the formation of larger particles (Ma *et al.*, 2000). As compared to smaller particles, larger particles are thought to adhere less to the membrane surface due to backtransport mechanisms and settleability.

The biological suspension in the MBR can be manipulated in order to reduce the impacts of biofouling. For example MLSS concentration and SRT are two factors that are known to change the physicochemical properties of activated sludge and can be utilized to assist in maximizing membrane permeability.

By optimizing the hydrodynamic conditions in the MBR, the rate at which biofouling occurs can be reduced. The critical flux and aeration intensity and frequency should be determined experimentally for each application according to the nature of the feedwater. Aeration within the MBR can be efficient for biofouling reduction by inducing turbulence at and near the membrane surface. On the other hand, inducing aeration for this purpose can add to operating costs.

Both the membrane material and module design have an effect on the hydrodynamics of the system which in turn influence biofouling to a great extent. Once filtration begins, the initial rate of particle deposition is partly dependent on the membrane material; however, once the foulant layer is developed, the material is insignificant until after the membrane has been cleaned (Wakeman and Williams, 2002). Therefore, choosing the appropriate membrane material and module design can minimize the onset of pore blocking and cake formation and may also make membrane cleaning less intensive (Wakeman and Williams, 2002).

The most common practice to alleviate biofouling is by chemical cleaning. Acids, bases, and oxidants have been used for maintenance cleaning and recovery cleaning of membrane modules (Baker and Dudley, 1998). Maintenance cleaning is effective at maintaining flux so that recovery cleanings are minimized. Recovery cleaning is performed in order to destroy any foulants that have adhered to the membrane surface or within its pore structure. Oxidizing biocides, specifically chlorine, have been used extensively for recovery cleaning of fouled membranes (Gander *et al.*, 2000). Chlorine is known to weaken the sludge cake by reacting with proteins and EPS (Flemming *et al.*, 1996). Thereafter the foulant can be removed from the membrane by mechanical forces such as ultrasonics, wiping, or rinsing with water, air, steam or a combination of these methods (Flemming *et al.*, 1996). The use of chlorine may not always alleviate biofouling and may even worsen biofouling potential (Baker and Dudley, 1998). After recovery cleaning, it is inevitable that some bacteria will have survived disinfection because they are protected by EPS. As a defense mechanism the bacteria may produce an increased amount of EPS thereby becoming resistant to the chlorine solution. Therefore the sludge cake on the membrane surface will be more difficult to eliminate since it will be composed of a high proportion of EPS (Baker and Dudley, 1998).

In most cases, a membrane module can never be cleaned to its original state. McDonogh *et al.* (1994) showed that removal of an accumulated biofilm on the surface of a microfiltration membrane is rarely achieved by standard cleaning techniques. The amount of foulant left on the membrane surface provides favourable conditions for rapid regrowth of the sludge cake. Thus after a short period of time, recovery cleaning will be required which creates the well known 'saw-tooth curve' (Flemming *et al.*, 1996). Furthermore, in order to be effective, the selection of cleaning agent will depend on the nature of the foulants and the membrane material and should be determined by experience and laboratory testing.

2.4 Methods for Characterizing Microbial Aggregates in Wastewater

Studying microbial flocs by analytical and microscopic methods is important for understanding the effects of physical, chemical, and microbiological conditions of the activated sludge. In this study, the physicochemical characteristics of microbial flocs were quantified by measuring their EPS composition, surface charge, and hydrophobicity.

2.4.1 Extracellular Polymeric Substances

EPS originate from microbial metabolism, cell lysis, and biosorption of organic materials (Urbain *et al.*, 1993; Jorand *et al.*, 1998). The amount and composition of EPS produced varies and may range from 10 to 90% of the total organic matter depending on growth conditions and environmental stresses (Christensen and Characklis, 1990). Additionally, the chemical composition of EPS is very heterogeneous. The major components include carbohydrates and proteins (Flemming, 2000; Liao *et al.*, 2001), as well as other macromolecules such as acidic polysaccharides, lipids, humic substances, and DNA (Horan and Eccles, 1986; Jorand *et al.*, 1998; Spaeth and Wuertz, 2000).

In association with microbial aggregates, EPS are involved in structural integrity, cohesion forces, adsorption of organic and inorganic materials, and spatial heterogeneity. Van der Waals forces, electrostatic forces, and hydrogen bonds contribute to the cohesiveness and stability of EPS (Flemming *et al.*, 1995; Spaeth and Wuertz, 2000). In addition, it has been proposed that hydrophobic and hydrophilic regions within EPS interact with the surfaces of cells thereby reinforcing the stability of the aggregate (Jorand *et al.*, 1998). Divalent cations such as Ca^{2+} and Mg^{2+} are thought to contribute to microbial aggregate stability since they bind to the negatively charged groups present within EPS and on cell surfaces (Urbain *et al.*, 1993; Flemming *et al.*, 2000; Spaeth and Wuertz, 2000). These cations form bridges between acidic polysaccharide chains, which aid in the development of the fibrillar gel-like matrix. It has been reported that flocs and biofilms became destabilized when divalent cations were extracted from the biomass and replaced by monovalent cations (Rudd *et al.*, 1983; Frølund *et al.*, 1996).

EPS can be classified as capsular EPS (bound) and slime EPS (soluble). The bound EPS is attached tightly to the exterior cell wall, while the soluble EPS is the loosely attached or unattached 'slime' material that can be washed away by centrifugation (Gehr and Henry, 1983; Spaeth and Wuertz, 2000). In order to analyze the composition of bound EPS without inducing cell lysis, a variety of extraction methods have been developed. Brown and Lester (1980) have compared bacterial EPS extraction methods from other sources including chemical methods such as ammonium hydroxide, sodium hydroxide, EDTA, sulfuric acid, and boiling benzene. Mechanical extraction methods such as high-speed centrifugation, ultrasonication, and boiling

or autoclaving were also investigated. Rudd *et al.* (1983) and Frølund *et al.* (1996) found that a cation exchange resin (CER), utilizing both a mechanical and chemical means of extraction, was the most successful in terms of minimal cell lysis and non-disruptive effects on the EPS. This extraction method removes divalent cations such as Ca^{2+} and Mg^{2+} from the EPS matrix and replaces them with monovalent cations. By removing the divalent cations the EPS becomes less stable thereby allowing the EPS to separate from the cellular material. Subsequent to capsular EPS extraction, proteins (Lowry *et al.*, 1951), carbohydrates (Gaudy, 1962), acidic polysaccharides (Filisetti-Cozzi and Carpita, 1991), and DNA can be measured.

2.4.2 Surface Properties

Surface properties are important in activated sludge floc and biofilm interactions. Surface charge and hydrophobicity at the cell surface influence the early stages of aggregate formation. Despite the fact that microbial biofilms and flocs are hydrated, their surfaces possess hydrophobic areas (Magnusson, 1980; Urbain *et al.*, 1993). Hydrophobic regions are due to side chains of amino acids, methyl groups in polysaccharides, and long-chain carbon groups in lipids. Due to the nature of these hydrophilic and hydrophobic regions, ionizable groups such as carboxyl, phosphate, and amino groups are present in the EPS matrix and at the cell surface creating a densely charged surface. The surface carries a net negative charge with a zeta potential ranging from –10 mV to –30 mV in sludge flocs (Horan and Eccles, 1986).

2.4.2.1 Surface Charge

Bacteria vary due to the physical and chemical nature of their cell surface structure; however, whether bacteria are Gram positive or Gram negative, their surfaces are negatively charged at neutral pH. This is attributed to the ionizable groups found at the cell surface (Beveridge *et al.*, 1997). The dominant ionizable groups of Gram positive bacteria at pH ~ 7 are the carboxylates present in the peptidoglycan layer, teichuronic acids and proteins, and the phosphates present in teichoic acids (Beveridge *et al.*, 1997). Because the surfaces of Gram positive bacteria are anionic, these cells are capable of sequestering dilute metal ions. If the cell possesses a high electronegative surface charge, then it is possible that the entire cell surface will become covered in minerals (Beveridge *et al.*, 1997).

The cell walls of Gram negative bacteria are more complex than their Gram positive counterparts. These bacteria possess a thin peptidoglycan layer surrounded by dense periplasm of the periplasmic space with an asymmetric lipid bilayer over top. The lipid bilayer is composed mostly of lipopolysaccharides (LPS) with membrane proteins, phospholipids and lipoproteins intermingled (Beveridge *et al.*, 1997). The physicochemical properties are controlled by the LPS. Long, highly charged O-polysaccharide chains which are strain specific may be attached to the LPS molecule and will dominate the surface chemistry. Conversely, if the bacteria lack these chains, the inner core polysaccharide groups and the lipid A regions will dominate the surface chemistry (Beveridge *et al.*, 1997).

Bacterial structures, other than the cell wall, can contribute to surface charge. These structures include capsules, sheaths, S-layers, and EPS. At neutral pH, these structures are also anionic due to polymeric substances with chemical reactive sites such as glycosaminoglycans, polypeptides and proteins, and glycoproteins (Flemming, 1995; Beveridge *et al.*, 1997). Although the negative charge on bacterial surfaces is dominant, there are also regions of localized positive charges. According to Flemming (1995) these positive charges are attributed to amino groups in sugars, sugar acids, and proteins, which can act as binding sites for anions.

As reviewed by Liss (2002), methods used in the past to determine microbial surface charge include attachment to charge-modified polystyrene, fluorescent probe ion exchange resin, and electrophoretic mobility. At present, the most common and reproducible method to determine surface charge density of microbial aggregates is by a colloid titration (Morgan *et al.*, 1990; Liao *et al.*, 2001).

2.4.2.2 Hydrophobicity

Hydrophobic interactions may play an important role in bioflocculation and biofilm development (Urbain *et al.*, 1993; Zita and Hermannsson, 1997; Liao *et al.*, 2001). Hydrophobic interactions (hydrophobic effect), result from the behaviour of entities (particles or molecules) incapable of interacting electrostatically or establishing hydrogen bonds with water and are therefore drawn together when put in an aqueous phase (Magnusson, 1980). In the case of microbial cells in aqueous media, the bound water layer near the cell surface

accounts for the hydrophobic or hydrophilic interaction (Urbain *et al.*, 1993; Zita and Hermannsson, 1997). When two hydrophobic surfaces approach each other, the bound water layers overlap, displacing the intervening layers of water to the bulk solution. This displacement reaction causes a decrease in entropy resulting in a favourable condition for aggregation. In the case of hydrophilic surfaces, the opposite is true in that entropy increases resulting in repulsion of cells. Therefore, any alteration to the cell surface that increases its hydrophobicity will favour flocculation.

Numerous methods have been reported in the literature for determining hydrophobic interactions of cells and have been summarized by Liss (2002). These include methods that measure actual binding to a hydrophobic ligand such as microbial adhesion to hydrocarbons (MATH) and those giving an estimate of an overall surface property, such as salt aggregation test and contact angle measurement of dry cell layers.

This study employed the MATH method because it is a simple method to rapidly quantify cell surface hydrophobicity (Rosenberg *et al.*, 1980). This method is based on the partitioning of cells possessing hydrophobic surface characteristics at the interface of a biphasic hydrocarbon-aqueous system after brief mixing. There is a limitation to this method when determining hydrophobicity of microbial cells because microbes in activated sludge are aggregated and this method has been developed for testing dispersed cultures. This limitation can be overcome by dispersion of microbial cells by sonication and by using samples from similar treatment systems having closely related bacterial strains (Rosenberg *et al.*, 1980; Jorand *et al.*, 1995).

2.5 Microscopic Techniques

Characterization of foulants is essential to understanding biofouling in MBRs. While membrane biofouling may not be avoidable, information about the structural and chemical properties of the foulant will provide assistance in managing this problem more effectively. Currently, applications to analyze membrane biofouling are emerging. In particular, recent advances in microscopy have enabled researchers to non-destructively visualize the spatial distribution, thickness, and physiological activities of biofilms and their response to biofouling control agents (Yu and McFeters, 2000). Fane *et al.* (2000) developed optical techniques to analyze foulants directly on the membrane surface through a destructive autopsy. Bouhabila *et*

al. (2001) employed microscopic techniques to observe the existence of a thin biofilm layer that they describe is equivalent to one or two layers of filamentous bacteria. Other microscopic techniques have been used to analyze biofouling and include conventional optical microscopy (COM), epifluorescence microscopy, confocal laser scanning microscopy (CLSM), two-photon laser scanning microscopy (2P-LSM), atomic force microscopy (AFM), Raman confocal microspectroscopy (RCM), scanning electron microscopy (SEM), environmental scanning electron microscopy (ESEM), and transmission electron microscopy (TEM). The microscope techniques employed in this research are described below.

2.5.1 Conventional Optical Microscopy

All forms of microscopy rely on user interpretation. While this may be somewhat subjective, microscopy can provide beneficial information about microorganisms (Maier *et al.*, 2000). The basic light microscope is still a necessary instrument in every microbiology laboratory (Maier *et al.*, 2000). Conventional optical microscopy (COM) has been the most common method for analyzing gross morphology of biological structures (Droppo *et al.*, 1996b). By varying lenses COM can be subdivided into bright field, dark field, and phase contrast microscopy. Bright field microscopy is the most common type of microscope whereby light is transmitted through the specimen. Dark field microscopy can be used to increase contrast of the transparent specimen. Phase contrast microscopy is utilized to identify internal structures of the specimen by relying on the fact that cell components have different densities and therefore interact differently with light (Maier *et al.*, 2000).

The images obtained by COM show the whole picture of particular biological structures and observations of size, shape, volume, gross composition, density, and porosity can be achieved (Liss *et al.*, 1996). However, the microscopist should be aware that using COM for structural analysis could lead to erroneous observations due to its limited resolution (Liss *et al.*, 1996). Liss *et al.* (1996) examined a floc using COM and reported that large voids appeared to be devoid of structure. However, when visualized with a higher resolution microscope such as TEM they concluded these voids were filled with EPS. Therefore, the use of COM alone can be limited, but when used in combination with higher resolution microscopes, it is an excellent tool for comparison purposes.

2.5.2 Epifluorescence Microscopy

Fluorescence microscopy is a form of light microscopy in which the specimens are stained with fluorescent dyes that emit visible light (Maier *et al.*, 2000). Epifluorescence microscopy is the most common type of fluorescence microscopy. This technique is advantageous for visualizing bacteria on opaque surfaces (Lawrence *et al.*, 1997). Morris *et al.* (1997) investigated biofilms on leaf surfaces using epifluorescence microscopy and found that microbial aggregates were embedded in an exopolymeric matrix when stained with acridine orange. The biofilm images on broad-leaved endive revealed the best resolution when examined either directly on a flat portion of leaf or when mounted under a coverslide with the cuticle peeled from the leaf surface.

The studies that use epifluorescence microscopy alone to examine biological structures are limited possibly due to the fact that the primary limitation of this technique is its spatial resolution of 0.2 μm laterally (in the image plane) and 0.6 μm axially (focus) (Gustafsson, 1999). Furthermore, the advances in fluorescence microscopy to fluorescent *in situ* hybridization, CLSM, and 2P-LSM have exceeded the resolution limits of epifluorescence microscopy (Gustafsson, 1999). Similar to COM, epifluorescence microscopy can also be a useful tool when used in conjunction with other microscope techniques.

2.5.3 Confocal Laser Scanning Microscopy

Since the introduction of CLSM in 1957, significant advancements have been made with respect to biotechnology (Periasamy *et al.*, 1999). In particular, CLSM has gained wide acceptance for its ability to provide detailed visualization of optical thin sectioning while eliminating out-of-focus information from above and below the plane of focus (Caldwell *et al.*, 1992) by using a pinhole aperture in the emission path (Periasamy *et al.*, 1999). Since CLSM has the ability to scan at various depths of a specimen, the information can be combined to form three-dimensional images. Because CLSM is a novel technique for creating three-dimensional images, the thickness of relatively thin biofilms can be measured with accuracy (Silyn-Roberts and Lewis, 1997). Hydrated biofilms kept intact with the substrate can be examined over a large area at various depths using CLSM. This non-destructive technique provides an average thickness of the biofilm and a distance at which optimal growth occurs.

This information is useful because it can be used to estimate biofilm maturity and architecture as well as growth over time (Silyn-Roberts and Lewis, 1997).

While CLSM is advantageous in visualizing biological structures and interfaces, it also has some disadvantages. One important disadvantage is the limitation of depth penetration by CLSM. This results in unattainable images of relatively thick biofilms (Stewart *et al.*, 1995). Scattering and absorption by the excitation and emission wavelengths result in a loss of signal, hence the inability to penetrate further into the sample (Gerritsen and De Grauw, 1999). Secondly, the illumination light excites the whole specimen. Therefore, background emission is introduced into the plane of focus, which increases photobleaching and photodamage to the cell (Periasamy *et al.*, 1999). Finally, any number of parameters relating directly to the instrument can cause reduced resolution. Pawley (2000) has summarized an extensive list of variables that affect spatial resolution when using CLSM in fluorescence mode. Some notable variables include the adjustment of the numerical aperture which affects the amount of light passing through the objective when emitted from the specimen, scan speed which can affect the signals to and from the sample, and laser alignment which is important because it should coincide with the pinhole after focusing on the specimen and then refocusing through the optical system. Many of the disadvantages associated with CLSM can be resolved by 2P-LSM. In this research, CLSM was chosen because the thickness of the foulant layer was well within the depth resolution of the microscope and as such the ability to penetrate the sample was not problematic.

2.5.4 Stabilization of Biological Structures

In order to stabilize and preserve the spatial arrangement of biological structures, studies have used Nanoplast and agar-embedding techniques. In this way, sections can be visualized using COM and CLSM successfully. Decho and Kawaguchi (1998) embedded microbial cells and EPS in Nanoplast, a hydrophilic resin. The lectin concanavalin A was conjugated with the stain fluorescein isothiocyanate (ConA-FITC) and was employed to image EPS using CLSM. The results showed that EPS was observed throughout the substrate and within the interstitial spaces. In addition, a 2 μm scanning thickness was sufficient to observe ConA-FITC fluorescently labeled EPS. However, they found inhomogeneous fluorescence throughout the

EPS matrix, which suggests that EPS may consist of varying compositions and/or distinct channels. The stabilization method used in their study resulted in a relatively simple imaging technique to visualize the EPS matrix in hydrated biofilms.

Ganczarczyk *et al.* (1992) physically stabilized microbial aggregates in solidified agar for light microscopy studies. They were able to rapidly measure the size of individual cells as well as evaluate some morphologic properties of the activated sludge flocs. Droppo *et al.* (1996a) compared observations between flocs stabilized in low melting point agarose and non-stabilized flocs. Essentially, their observations revealed that no obvious structural or compositional differences in the flocs were evident. Since the agarose did not appear to generate erroneous results, they concluded that flocs stabilized in agarose minimized the limitations of handling, preparing, and examining floc structures that were not stabilized. Both embedding techniques allowed for an extended period of observation and sample storage.

2.5.5 Fluorescent Staining

In the past, fluorescent stains were quite limited, but today, there seems to be a continuous development of new stains. In total there are approximately 2000 different fluorescent compounds available for use with CLSM to analyze biological samples. These fluorescent probes are able to target biomolecules such as proteins, nucleic acids, polysaccharides, cell organelles, and antibodies (Neu, 2000). The only limitation of using fluorescent stains is the range of wavelengths and filter sets available in the visible spectrum. Nevertheless, multi-colour labelling has been accomplished using up to 7 probes (Neu, 2000).

Most CLSM work in microbiology originated from Lawrence and colleagues. They examined hydrated microbial biofilms that had been stained with fluorescein and acridine orange using CLSM. They obtained images of intact biofilms in the horizontal (xy) and sagittal (xz) scanning directions. The sagittal sectioning (0.2 μm intervals) revealed more detail of the biofilm structure including voids and interstitial spaces (Lawrence *et al.*, 1991; Caldwell *et al.*, 1992). In general, they found that biofilms are highly hydrated, open structures, consisting of heterogeneous species arranged distinctly in a matrix of EPS.

Recently, multispectral imaging of biofilms and EPS was introduced by employing autofluorescence, nucleic acid stains, and lectin-conjugate stains (Neu and Lawrence, 1997; Lawrence *et al.*, 1998). While autofluorescence can sometimes interfere with a fluorescent stain of interest, it can also be advantageous in that the same specimens have the ability to fluoresce without the addition of a fluorescent stain (Hibbs, 2000). For example algae and specific bacterial groups may be visualized through the fluorescence of chlorophyll and other fluorescent biomolecules when the appropriate filters are used (Lawrence *et al.*, 1998). There are many nucleic acid stains available; however, Neu and Lawrence (1997) found that the SYTO series, specifically SYTO 9, was the most effective stain showing minimal non-specific binding during staining of complex biofilm communities.

Although quantitative estimations of EPS in biofilms have been traditionally accomplished through extraction and chemical methods, fluorescent probes are also suitable for estimating EPS in situ. In the past, Calcofluor White M2R was used to measure exopolysaccharide production in single bacterial strains such as *Azospirillum*, *Pseudomonas aeruginosa* and *Klebsiella pneumoniae* (Del Gallo *et al.*, 1989; Stewart *et al.*, 1995). Similarly, congo red was employed for general light microscopy staining of polysaccharides (Allison and Sutherland, 1984). More recently researchers have begun to use fluorescently labeled lectins as a method to probe the spatial relationships of EPS within thick heterogeneous biofilm communities (Michael and Smith, 1995; Lawrence *et al.*, 1998; Wolfaardt *et al.*, 1998; Johnsen *et al.*, 2000). Lectins are a large group of glycoproteins that bind to specific carbohydrates. They are prevalent in nature and are present in plants, bacteria, animals, and humans (Sharon and Lis, 1989). Plant lectins have been used as both specific and general stains to estimate EPS in biofilms as well as to characterize the EPS left on surfaces after the removal of microbes (Neu and Marshall, 1991; Michael and Smith, 1995; Lawrence *et al.*, 1998; Wolfaardt *et al.*, 1998). Lawrence *et al.* (1998) concluded that lectins derived from *Canavalia ensiformis* (concanavalin A, ConA) or *Triticum vulgaris* (wheat germ agglutinin, WGA) with a broad range of carbohydrate specificity for residues including glucose, mannose, and *N*-acetyl-D-glucosamine were well suited to general staining of EPS in biofilms. Michael and Smith (1995) investigated biofouling in marine environments by employing lectins from ConA and *Limulus polyphemus* (limulin) to detect and describe the distribution of glycoconjugates on inert and living surfaces.

Wolfaardt *et al.* (1998) investigated the organization of exopolymers in the presence of chlorinated organics. By employing 9 different lectins, they discovered that diclofop and its metabolites accumulated in EPS nonuniformly when biofilms were grown with diclofop as the sole carbon source, but not in the presence of a labile carbon source. The lectin-conjugates employed were selected based on other studies that have shown EPS to contain mannose, glucose, galactose, glucosamine, N-acetyl-α-galactosamine, fucose and other carbohydrate residues. Because lectin-conjugates have been shown to be useful tools to investigate the spatial relationships of EPS within biofilms, lectin-conjugates were also employed in the present study to investigate the distribution of EPS in the biofoulant attached to hollow fibre microfiltration membranes.

3.0 EXPERIMENTAL

3.1 Experimental Approach

The purpose of this study was to investigate biofouling of hollow fibre polymeric microfiltration membranes used to filter and treat secondary municipal wastewater. The experimental work was carried out in collaboration with Zenon Environmental Inc. at the Wastewater Technology Centre, Environment Canada, in Burlington, Ontario. Biomass samples and membrane fibre samples from each ZeeWeed™ (ZW) membrane bioreactor (MBR) were taken to the laboratory for analysis at Ryerson University, Toronto, Ontario.

A preliminary study was performed whereby ZeeWeed™ (ZW) microfiltration membranes, manufactured by Zenon Environmental Inc., were constructed into simple loops and immersed into an existing pilot scale MBR. The ZeeWeed™ membrane characteristics are given in Table 3.1. The reactor was operated under permeate/relaxation conditions. Membrane fibre samples were collected for microscopic analysis after 0, 3, 30, and 69 days of filtration.

Table 3.1. ZeeWeed™ Membrane Properties

Permeation Configuration	Outside-in supported hollow fibre
Nominal Outer/Inner Diameter (mm)	1.9/1.0
Nominal membrane pore diameter (μm)	0.04
Molecular Weight Cut-off (Daltons)	200,000
Maximum permeation transmembrane pressure (bar)	0.83
Typical operating transmembrane pressure (bar)	0.07 - 0.55
Maximum backpulse transmembrane pressure (bar)	0.55
Maximum operating temperature (°C)	40
Maximum cleaning temperature (°C)	40
Operating pH range	5 - 9.5
Cleaning pH range	2 - 11 (< 30°C), 2 - 9 (30 – 40°C)
Maximum OCl- exposure (lifetime contact time)	1,000,000 ppm-hours
Maximum concentration for OCl- cleaning	1000 - 2000 ppm (< 30°C), 500 ppm (30 – 40°C)
Nominal module pure water permeability (at 51 L/m^2/hr, corrected to 20 °C)	300 – 400 L/m^2/hr/bar

The core study was conducted by employing two pilot scale ZeeWeed™ MBRs. In reactor 1, one ZW-10 module was installed to treat wastewater at a sludge retention time (SRT) of 30 days. This membrane module operated under permeate/relaxation conditions. In reactor 2, two ZW-10 modules were installed to treat wastewater at an SRT of 12 days. One membrane module operated under permeate/relaxation conditions, while the other operated under permeate/backwash conditions. The specifications of a ZW-10 module are shown in Figure 3.1. For municipal sewage applications, a typical net flux for a ZW-10 module ranges from 20 to 30 $L/m^2/hr$ at 15 to 20°C and the transmembrane pressure (TMP) ranges from -10 to -50 kPa. In this experiment, single membrane fibre samples were collected at specified times from each ZW-10 module for microscopic analysis until each module reached a critical TMP near -60 kPa. At that point, the ZW-10 modules were recovery cleaned overnight in a 2000 ppm hypochlorite solution and reinstalled into the reactors. Membrane samples were also collected following recovery cleaning. This procedure was performed three times described as Runs 1, 2, and 3.

In all experiments, the ZW-MBRs were set up and maintained by Zenon Environmental Inc. at the Wastewater Technology Centre, Environment Canada, in Burlington, Ontario. All reactors were fed municipal wastewater and the operating conditions in the reactors were kept constant. The biomass within each reactor was collected and analyzed bimonthly by microscopy and physicochemical methods.

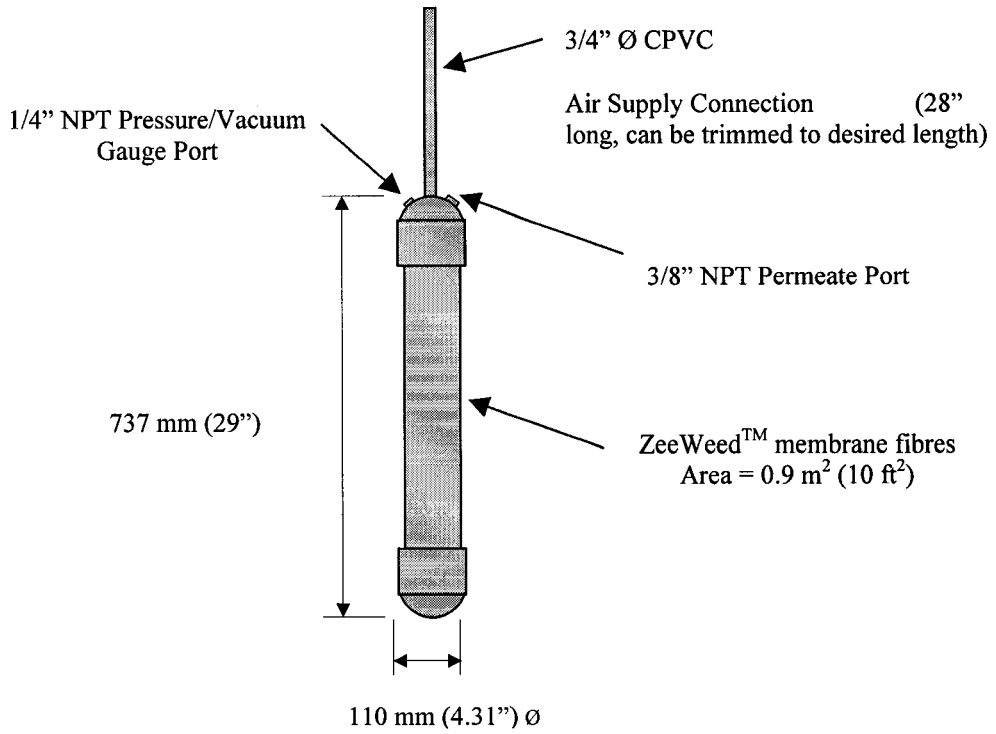

Figure 3.1. Schematic of a ZW-10 Module and its specifications

3.2 Preliminary Study

A preliminary experiment was required to assure the workability and quality of microscopic analysis of hollow fibre polymeric membranes. In this experiment simple membrane loops were constructed and immersed within an existing pilot scale MBR. While in the reactor, the secondary municipal wastewater was filtered at a constant pressure using a suction duty pump with periodic relaxation intervals. Aeration was supplied to the system by coarse air bubbles at the base of the MBR. After 0, 3, 30, and 69 days of operation membrane samples were collected and taken to the laboratory for analysis. The membrane samples were analyzed by confocal laser scanning microscopy (CLSM). On a monthly basis, sludge samples were collected from the pilot-scale reactor and taken to the laboratory for physicochemical analysis.

3.2.1. Experimental Design

Figure 3.2 illustrates a single constructed ZeeWeed™ membrane loop one metre in length with a surface area of 6.28×10^{-3} m^2.

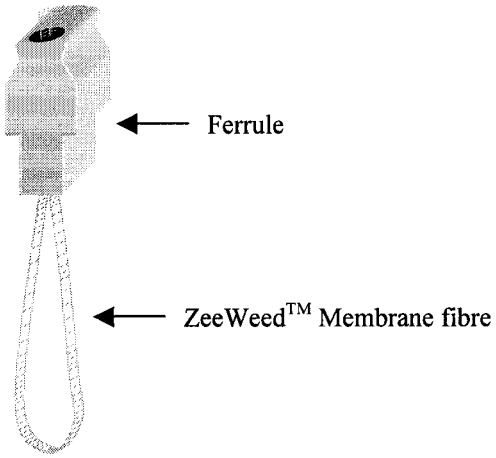

Figure 3.2. Illustration of a single constructed membrane loop

Each loop was constructed by threading the ends of the membrane fibre through a ferrule. The fibre was made air-tight by sealing the void space within the ferrule with hot glue from a glue gun. To ensure filterability, a leak test was performed on each membrane loop. This test was performed by hooking up each loop to a peristaltic pump via swage fittings and locks. The loop was immersed in clean water and the pump was set at 33.8 kPa (10 in Hg) to push air through the membrane fibre. If air bubbles were observed the membrane loop was defective and the loop was reconstructed. Conversely, if air bubbles were absent, the membrane loop was acceptable for filtration. An initial flux was measured by filtering clean water through the membrane fibre. The volume of filtrate was measured for one minute at –16.9 kPa (5 in Hg) and at –33.8 kPa (10 in Hg) and the membrane permeability, corrected to 25°C, was calculated using the following formula (Bouhabila *et al.*, 2001):

$$\text{Permeability} = J/P \qquad \textbf{[3-1]}$$

where J represents flux ($L/m^2/hr$) and P represents pressure (bar).

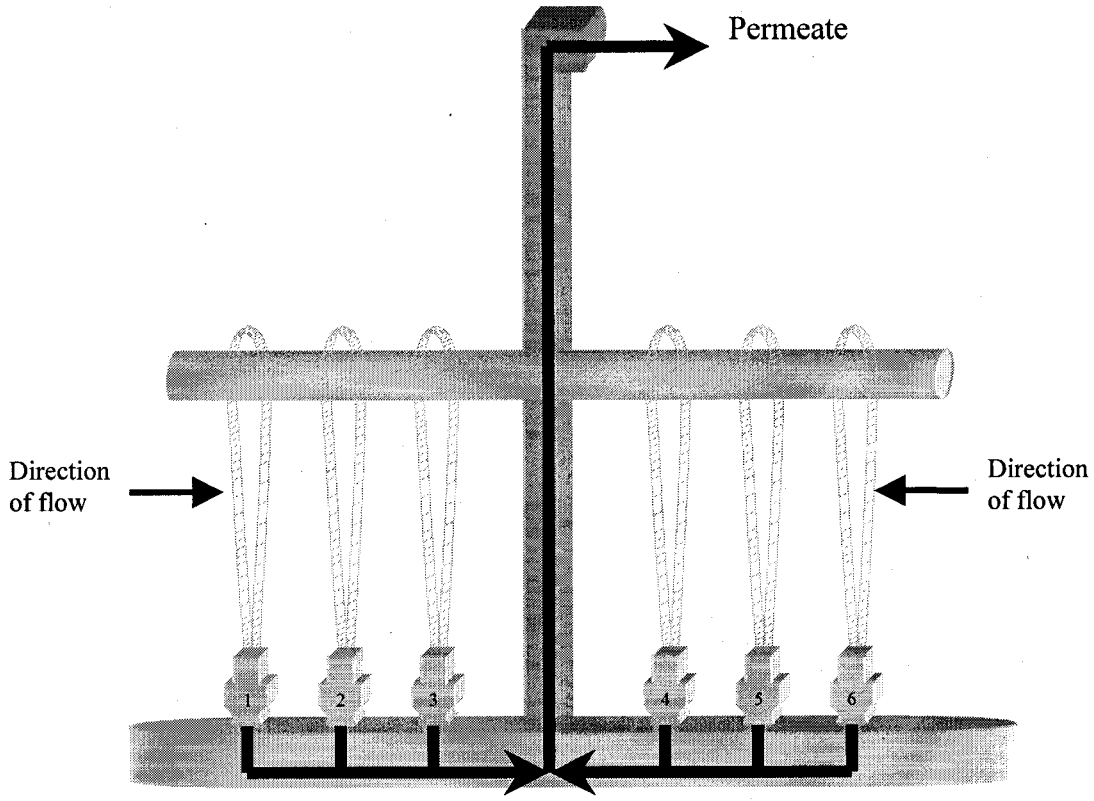

Figure 3.3. Illustration of the manifold used for the preliminary study

Each loop was numbered and attached to the manifold via swage fittings and locks as illustrated in Figure 3.3. The apparatus was immersed into the existing pilot scale MBR (18,000 L capacity) and hooked up to an existing suction duty pump for filtration of secondary wastewater. At each sampling period, two membrane loops were removed from the manifold for analysis and replaced by two virgin membrane loops. Table 3.2 indicates the position of each membrane loop on the manifold and the time each loop was sampled. Immediately after sampling, the final flux of each membrane loop was measured by the same method as the initial flux and the membrane permeability was calculated.

Table 3.2. Membrane Loop Position on the Manifold and Days in Operation in the MBR

Membrane Loop No.	Days in Operation	Manifold Position
4744.08	3 days	1
4744.16	3 days	6
4744.13	30 days	5
4744.17	30 days	2
4744.10	69 days	3
4744.12	69 days	4

3.3 Core Study

This research focused on investigating biofouling of ZeeWeed™ microfiltration polymeric membranes used in MBR technology. In this study three runs were accomplished over a period of 64 days in which membrane fibre samples were collected periodically for CLSM analysis. Each Run was terminated when the TMP reached a critical pressure near -60 kPa with the exception of Run 3 which was terminated when the TMP reached -30 kPa. The use of pilot scale MBRs enabled SRT and operational parameters to be altered. SRT was altered to 12 days and 30 days in order to study the relationship between sludge properties and biofouling. Two operational cleaning methods were used in this study and included relaxation and backwashing. A constant flux was maintained at 35 $L/m^2/hr$ for Runs 1 and 2 and 20 $L/m^2/hr$ for Run 3. At critical TMP, each ZW-10 module was removed from the bioreactor and recovery cleaned overnight in a 2000 ppm hypochlorite solution. After recovery cleaning, a membrane fibre sample was collected for CLSM analysis and each ZW-10 module was reinstalled into the reactor for the next run.

3.3.1 Membrane Bioreactor Design

Two pilot scale ZeeWeed™ MBRs were set up and maintained by Zenon Environmental Inc. at the Wastewater Technology Centre, Environment Canada, in Burlington, Ontario. Each ZW-10 module was constructed with numerous polymeric hollow fibre microfiltration membranes to yield a 0.9 m^2 filtration area. The system was operated under the conditions described in Table 3.3.

Table 3.3. Operating Conditions for the MBR System

	Reactor 1	Reactor 2	Reactor 2
Membrane Module	1	2	3
Operational Cleaning	relaxation	relaxation	permeate backwash
SRT (days)	30	12	12
Feed (municipal)	raw sewage	raw sewage	raw sewage
Tank Size/Capacity	16" diameter, 26.5" operating height (87 L)	22" diameter, 30" operating height (187 L)	22" diameter, 30" operating height (187 L)
Membrane Module Area	0.9 m^2 (10 ft^2)	0.9 m^2 (10 ft^2)	0.9 m^2 (10 ft^2)
Aeration (scfm)	2	2	2
Wastewater Flux ($L/m^2/hr$)	35 for Runs 1 and 2, 20 for Run 3	35 for Runs 1 and 2, 20 for Run 3	35 for Runs 1 and 2, 20 for Run 3
Cycle Time	9.5 minute permeate, 0.5 minute relax	9.5 minute permeate, 0.5 minute relax	9.5 minute permeate, 0.5 minute backwash
Manual Waste Flow (once/day)	2.9 L/day	15.6 L/day	15.6 L/day

The experimental MBR system is illustrated in Figure 3.4. The reactors were first filled with mixed liquor from an existing MBR which is fed fresh mixed liquor from the Skyway Wastewater Treatment Plant after passing through a 1 mm bar screen. The Skyway Wastewater Treatment Plant in Burlington, Ontario provides municipal wastewater treatment for the City of Burlington urban area. In order to maintain MLSS concentrations, each MBR was operated on a permeate-to-drain basis with permeate recycle which allowed HRT to vary. The average MLSS concentration in Reactor 1 and Reactor 2 was 18.1 g/L and 18.9 g/L respectively. Within Reactor 1, one ZW-10 module (Module 1) was installed and operated at a 30 day SRT under permeate/relaxation conditions. In Reactor 2, two ZW-10 modules were installed. Both were run at a 12 day SRT and one module operated under permeate/relaxation conditions (Module 2), while the other module operated under permeate/backwash conditions (Module 3). Each module was continuously aerated to provide turbulence to the external surface of the membrane fibres and to provide biological oxygen at a constant rate of 2

standard cubic feet per minute (scfm). The TMP was monitored daily before and after operational cleaning methods. The permeability of the membrane modules filtering clean water and wastewater was calculated using equation [3-1] and corrected to 25°C. The feed sewage was analyzed for total suspended solids (TSS), total phosphorus (P) and ammonia (N), pH, total chemical oxygen demand (TCOD), and soluble COD (FCOD) (Table 3.4). The temperature, MLSS, pH, COD, and dissolved oxygen were monitored in each reactor on a regular basis and are summarized in Table 3.5.

Table 3.4. Summary of Feed Sewage Analytical Data (February 11 – April 16, 2002)

Parameter	Feed Sewage
Average TSS (mg/L)	301 ± 62.2
Average Feed pH	7.24 ± 0.175
Average Feed TCOD (mg/L)	660 ± 386
Average Feed FCOD (mg/L)	67 ± 21
Average Total P (mg/L)	25.5 ± 9.86
Average Ammonia N (mg/L)	15.6 ± 3.97

Table 3.5. Summary of Reactor Analytical Data (February 11 – April 16, 2002)

Parameter	Reactor 1	Reactor 2	
Average Operating Temperature (°C)	10 ± 1.9	10 ± 1.9	
Average MLSS Concentration (g/L)	18.1 ± 3.42	18.9 ± 3.01	
Average Dissolved Oxygen (mg/L)	3.7 ± 1.3	4.1 ± 1.6	
ZW-10 Module‡	Module 1	Module 2	Module 3
Average Permeate pH	7.24 ± 0.087	7.25 ± 0.121	7.26 ± 0.109
Average Permeate COD (mg/L)	12.5 ± 6.3	14 ± 7.7	14 ± 9.3

‡Modules 1, 2, and 3 represent SRT 30 Permeate/Relax; SRT 12 Permeate/Relax, SRT 12 Permeate/Backwash respectively.

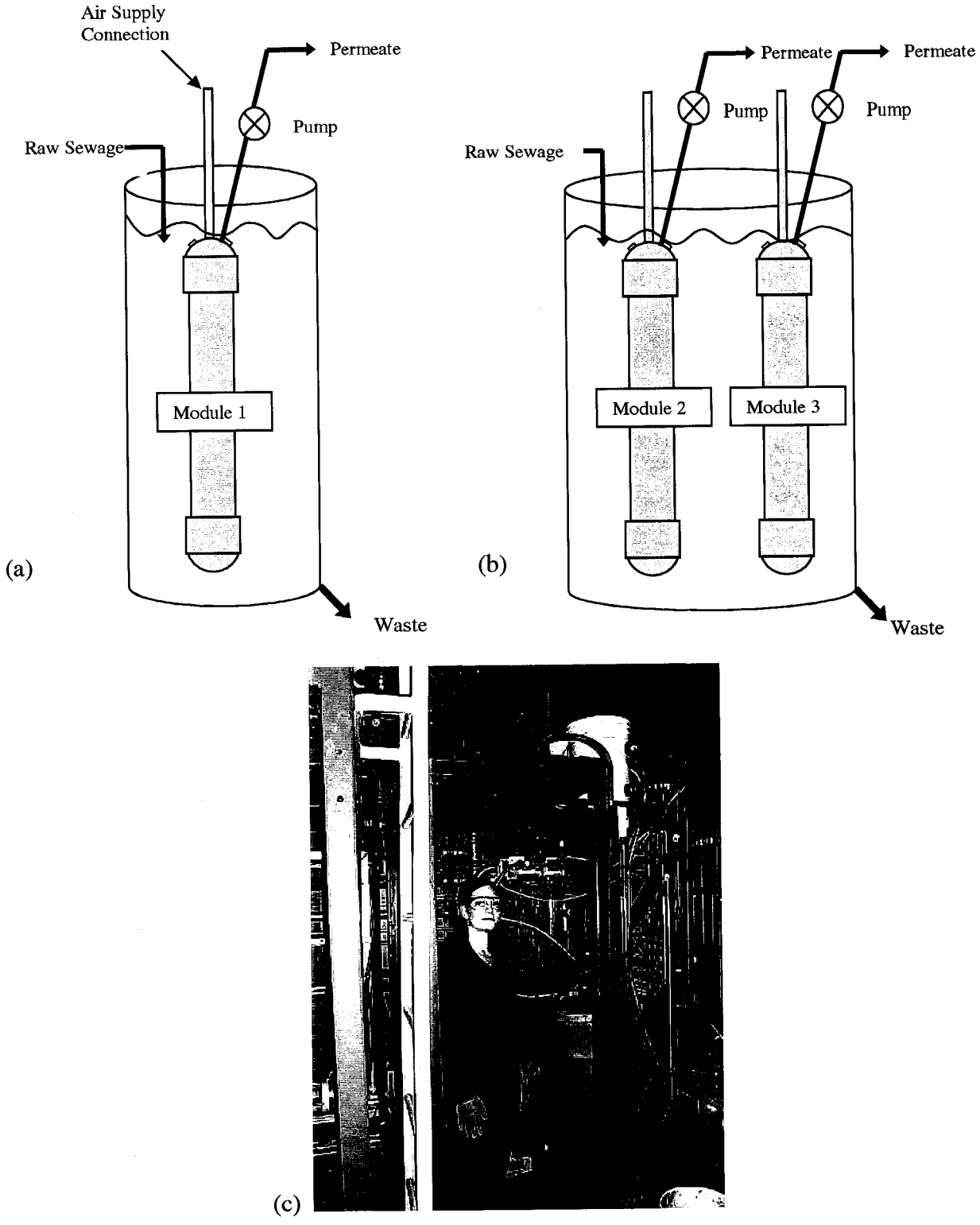

Figure 3.4. Illustration of Experimental MBR System operating at the Wastewater Technology Centre in Burlington, Ontario: (a) Reactor 1, SRT 30: Module 1 - permeate/relaxation; (b) Reactor 2, SRT 12: Module 2 - permeate/relaxation, Module 3 - permeate/backwash; (c) Picture of Experimental MBR System.

3.3.2 Membrane Fibre Sample Collection

Each membrane fibre sample was collected as described in Table 3.6.

Table 3.6. Collection Schedule of Membrane Fibre Samples

Run No.[†]	Flux ($L/m^2/h$)	Day No.	ZW-10 Module[‡]	Collection Time[*]
1	35	0	All modules	Virgin membrane
1	35	0	All modules	2 hours
1	35	3	All modules	3 days
1	35	15	All modules	15 days
1	35	18	Module 2	At critical TMP
1	35	21	Modules 1 and 3	At critical TMP
2	35	22	All modules	After first recovery cleaning
2	35	22	All modules	2 hours
2	35	25	All modules	3 days
2	35	29	Module 2	At critical TMP
3	20	30	Module 2	After second recovery cleaning
3	20	30	Module 2	2 hours
2	35	31	Module 3	At critical TMP
3	20	32	Module 3	After second recovery cleaning
3	20	32	Module 3	2 hours
2	35	35	Module 1	At critical TMP
3	20	36	Module 1	After second recovery cleaning
3	20	36	Module 1	2 hours
3	20	43	Module 2	13 days
3	20	45	Module 3	13 days
3	20	49	Module 1	13 days
3	20	64	Module 1 after 28 days Module 2 after 34 days Module 3 after 32 days,	At shutdown
3	20	65	All modules	After final recovery cleaning

[†]Each Run was terminated when critical TMP was reached with the exception of Run 3 which was terminated near –30 kPa.

[‡]Modules 1, 2, and 3 represent SRT 30 permeate/relaxation, SRT 12 permeate/relaxation, SRT 12 permeate/backwash respectively.

[*]Critical TMP is defined as near –60kPa. Recovery cleaning is defined as soaking the module overnight in 2000 ppm NaOCl.

Each membrane fibre sample was collected by disconnecting each ZW-10 module from the reactor. The membrane was immersed in clean water to maintain moisture while the membrane fibre was clipped from the module with scissors. The remaining membrane fibre attached to the module was sealed with silicone so that further operation did not disrupt the filtration process. Each clipped membrane fibre sample was stored in a round Ziploc™

container enclosed with moistened filter paper and transported to the laboratory at Ryerson University, Toronto, Ontario. All samples were stored at + 4°C and were analyzed by CLSM within 48 hours, but not later than two weeks after collection. The preliminary study demonstrated that as long as moisture was maintained, the foulant on the membrane fibres showed no significant change over time.

3.3.3 Clean Water Flux

Subsequent to each membrane fibre collection, a clean water flux was performed on each ZW-10 module. A clean water flux is measured by acquiring TMP readings after 4 minutes of clean water filtration. This test was typically performed at fluxes between 38 and 43 $L/m^2/hr$. Permeability of the membrane modules filtering clean water was calculated using equation [3-1] and corrected to 25°C.

3.4 Standard Wastewater Analysis

3.4.1 Mixed Liquor Suspended Solids and pH

MLSS was measured daily and the feed and permeate pH were measured weekly. The methods used were those described in Standard Methods for Examination of Water and Wastewater 15^{th} edition, 1980.

3.4.2 Dissolved Oxygen

Dissolved oxygen (DO) was measured frequently throughout the course of the experiment. DO was measured *in situ* using a YSI Model 50B dissolved oxygen meter.

3.4.3 Chemical Oxygen Demand

The feed TCOD and FCOD and the permeate COD from each ZW-10 module were measured on a weekly basis. The method used was # 8000 for water, wastewater and sea water in Hach DR/4000 Spectrophotometer Analytical Procedures Handbook.

3.5 Physical Analysis of Biomass

3.5.1 Surface Charge

The surface charge of microbial flocs was determined by colloidal titration (Morgan *et al.*, 1990). The surface charge of a biomass sample was measured by mixing a known amount of sludge with a known amount of positively charged polymer, polybrene, and titrating the solution with a negatively charged polymer, polyanetholsulfonic acid. The endpoint volume of the titration is compared with the endpoint volume of a blank sample. This experiment was modified in that polyvinyl sulphate was replaced by polyanetholsulfonic acid.

A grab sample of sludge was collected from each reactor and brought to Ryerson University for immediate analysis. Due to high MLSS concentrations, each sample was diluted to approximately 1/5 of the original concentration. Each sample of sludge was washed once with distilled and deionized water and centrifuged at 3000 *g* for 5 minutes at + 4°C. Each sample was washed again with distilled and deionized water at pH 7.0 and centrifuged at 3000 *g* for 5 minutes at + 4°C. In 40.0 mL of pH-balanced distilled and deionized water, 2.0 mL of washed sludge was mixed with 4.0 mL of excess polybrene. A standard solution of polyanetholsulfonic acid was used to titrate with the excess polybrene using toluidine blue as the indicator. A blank was also titrated whereby the 2.0 mL washed sludge sample was replaced by 2.0 mL of pH-balanced distilled and deionized water. The surface charge of each sample was calculated using the following formula:

$$\text{Surface Charge} = \frac{-(V_o - V) * N * 10^9}{2 * \text{MLSS}} \qquad \textbf{[3-2]}$$

where N = 0.001 eq/L, V = volume of polyanetholsulfonic acid (L) required to reach the endpoint, and V_o = volume of polyanetholsulfonic acid (L) to reach the endpoint for a blank solution. MLSS is measured in mg/L.

3.5.2 Hydrophobicity

The Microbial Adherence To Hydrocarbons (MATH) method was employed for determining relative % hydrophobicity of microbial flocs (Rosenberg *et al.*, 1980). Upon mixing, hydrophobics in the microbial sludge suspension adhere to the hydrocarbon at the

hydrocarbon-aqueous interface. The absorbance of the aqueous phase was subsequently measured to estimate the relative hydrophobicity of the sample.

A grab sample of sludge was collected from each reactor and brought to Ryerson University for immediate analysis. Due to high MLSS concentrations, each sample was diluted to approximately 1/5 of the original concentration. Each sludge sample was washed twice with distilled and deionized water and centrifuged at 3000 *g* for 5 minutes at + 4°C after each washing. Samples were shaken gently to resuspend the pellet, then sonicated for 30 seconds using a MSE Soniprep Ultrasonic Disintegrator (Johns Scientific, Toronto, Ontario). The initial absorbance of the dispersed suspension (I_o) was adjusted to 1.3 $\pm$ 0.30 at 400 nm, using distilled and deionized water for dilution. 10 mL of the adjusted sludge suspension was mixed with 1.0 mL of hexadecane using a vortex mixer for 2 minutes. The hydrophobic and hydrophilic phases were left to separate for 10 minutes in a separatory funnel. The aqueous phase was collected and absorbance (I) was measured at 400 nm (Spectronic® 20^+, Spectronic Instruments, Rochester, NY, USA). Relative hydrophobicity was calculated using the following formula:

$$\% \text{ Hydrophobicity} = (I_o - I)/I_o * 100 \qquad \textbf{[3-3]}$$

3.6 Chemical Analysis of Extracellular Polymeric Substances

3.6.1 Extraction of EPS

The extraction of EPS was performed by a cation exchange resin (CER) method (Frølund *et al.*, 1996; Liao *et al.*, 2001). A duplicate sample of sludge at SRT 12 and 30 days, diluted to approximately 1/5 of the original MLSS concentration, was washed three times with extraction buffer (2 mN Na_3PO_4, 4 mN NaH_2PO_4, 9 mN NaCl, 1 mN KCl in 1 L of distilled and deionized water at pH 7) and centrifuged at 2000 *g* for 5 minutes at + 4°C. The MLSS of the washed sample was measured and the amount of CER (DOWEX® HCR-W2 Cation Exchange Resin) in the sodium form was determined and added to each washed sample based on 80 g of resin per g of MLSS. Prior to addition, the CER was washed with buffer solution until the liquid was clear. The mixture of each sample and CER was stirred at a constant rate (247 RPM) for two hours at + 4°C. Each sample was then decanted into high speed centrifuge tubes

and centrifuged for 20 minutes at 9500 *g* at + 4°C. The supernatant was decanted into new centrifuge tubes and stored at – 20°C for future analysis of carbohydrates, proteins, acidic polysaccharides, and DNA. When each sample was thawed for analysis, the samples were centrifuged if required at 3500 *g* at + 4°C to remove any remaining floc particles.

3.6.2 Carbohydrates

The carbohydrate concentration within the EPS was quantified utilizing the Anthrone method, as described by Gaudy (1962). A standard solution of D-glucose was used to prepare a standard calibration curve. From each thawed sample a 2.0 mL aliquot was added to each test tube in triplicate. At 60 second intervals, 5.0 mL of ice cold Anthrone reagent (0.2 g anthrone dissolved in 100 mL 95% H_2SO_4) was added to each test tube, mixed with a vortex mixer for 30 seconds, and placed in a boiling water bath for 15 minutes. Each sample was sequentially cooled to room temperature in an ice bath and analyzed for spectrophotometric absorbance at 625 nm (Spectronic® 20^+, Spectronic Instruments, Rochester, NY, USA).

3.6.3 Proteins

The protein concentration within the EPS is quantified by colorimetry using the Folin reaction (Lowry *et al.*, 1951; Liao *et al.*, 2001). A standard solution of bovine serum albumin was used to prepare a standard calibration curve. From each thawed sample a 1.0 mL aliquot was added to each test tube in triplicate. At 30 second intervals, 5.0 mL of a prepared reagent (20 g Na_2CO_3 in 1 L of 0.1 N NaOH, mixed with 0.25 g $CuSO_4 \cdot 5H_2O$ dissolved in 50 mL of 1 % (w/v) aqueous solution of sodium tartrate, in a ratio of 25:1) was added to each test tube, mixed with a vortex mixer for 15 seconds, and allowed to stand for 10 minutes at room temperature. Finally, a 0.5 mL aliquot of Folin reagent (Folin and Ciocalteu's phenol reagent diluted to a ratio of 1:1 with distilled and deionized water) was added to each test tube, mixed with a vortex mixer for 15 seconds, and allowed to stand for 30 minutes at room temperature. The samples were analyzed for spectrophotometric absorbance at 750 nm (Spectronic® 20^+, Spectronic Instruments, Rochester, NY, USA).

3.6.4 Acidic Polysaccharides

The uronic acid determination within the EPS was quantified utilizing a colorimetric method as described by Filisetti-Cozzi and Carpita (1991). A standard solution of D-glucuronic acid was used to prepare a standard calibration curve. From each thawed sample a 0.8 mL aliquot was added to each test tube in triplicate. 80 μL of 4 M sulfamic acid – potassium sulfamate (pH 1.6 adjusted with saturated KOH at + 4°C) was added to each test tube and mixed with a vortex mixer for 20 seconds. Subsequently, a 4.8 mL aliquot of ice cold analytical grade (96.4 %) H_2SO_4 containing 75 mM sodium tetraborate was added at 60 seconds intervals to each test tube, mixed again using a vortex mixer for 30 seconds, and placed in a near boiling water bath for 20 minutes. Each sample was sequentially cooled to room temperature in an ice bath. Finally 160 μL of 0.15 % (w/v) *m*-hydroxydiphenyl in 0.5 % (w/v) NaOH at + 4°C was added to each test tube and mixed with a vortex mixer for 15 seconds. Samples were analyzed after 10 minutes by spectrophotometric absorbance at 525 nm (Spectronic® 20^+, Spectronic Instruments, Rochester, NY, USA).

3.6.5 DNA

DNA was quantified by utilizing a standard fluorescent DNA quantitation kit (BIO-RAD Laboratories, Hercule, CA). Calf thymus DNA was used to prepare a standard calibration curve. Each sample was thawed to + 4°C. Hoest dye was added to each sample in triplicate and measurements were taken using a 360 nm excitation filter and a 460 nm emission filter.

3.7 Microscopic Analysis

3.7.1 Conventional Optical Microscopy

A Zeiss Axiovert 200M inverted microscope equipped with a CCD camera (Carl Zeiss Inc., Toronto, Ontario) and Northern Eclipse Version 6.0 software (Empix Imaging, Inc., Mississauga, Ontario) was used for direct observation of microbial flocs. Typically, wet mounts were visualized using phase contrast microscopy at 200X magnification using a Zeiss 20X/0.5 NA Plan Neofluar objective. Each image was digitally rendered to examine the gross morphology of microbial flocs.

3.7.2 Confocal Laser Scanning Microscopy

A Zeiss Axioplan LSM 510 (Carl Zeiss Inc., Toronto, Ontario) was employed to analyze flocs and hollow fibre microfiltration membrane samples embedded in low melting point agarose. Lectins conjugated with fluorescent dyes were used to identify specific polysaccharides within the floc matrix and on the membrane fibres. Lectins are proteins that selectively bind to specific carbohydrate components to form a glycoconjugate. Each lectin is conjugated with a fluorescent dye in order to allow visualization when excited by a laser source such as an argon or helium-neon laser. Lectins were selected on the basis of observations from other studies that have shown EPS to contain mannose, glucose, galactose, *N*-acetylglucosamine, *N*-acetylgalactosamine and other residues. These lectins included those derived from *Canavalia ensiformis* (concanavalin A, ConA), *Triticum vulgaris* (wheat germ agglutinin, WGA), *Glycine max* (soybean agglutinin, SBA), and *Griffonia simplicifolia* (formerly *Bandeiraea simplicifolia*, BS-I). The lectin-conjugate stains used for analysis, their carbohydrate specificity, and applications are given in Table 3.7.

Table 3.7. Lectin-conjugates used for CLSM Analysis

Lectin-conjugate	**Abs/Em*[1]**	**Carbohydrate Specificity**	**Applications**
Concanavalin[1] A-Fluorescein; Alexa Fluor 647; Alexa Fluor 633	494/518; 650/668; 632/647	α-mannopyranosyl and α-glucopyranosyl residues	EPS detection in *Sphingomonas* biofilms[3], and ocean[4,5], river[6], and degradative[7] microbial biofilms
Wheat Germ Agglutinin[1]-Texas Red; Tetramethylrhodamine	595/615; 555/580	*N*-acetylglucosaminyl residues	EPS detection in *Sphingomonas* biofilms[3] and microbial biofilms[8]
Soybean Agglutinin[1]-Alexa Fluor 488	496/519	α and β-*N*-acetylgalactosaminyl and galactopyranosyl residues	EPS detection in bacterial species of *Azospirillum*[9]
BS-I-TRITC[2]	554/576	1° affinity for α-D-galactosyl residues, 2° affinity for *N*-acetyl-α-D-galactosaminyl residues	EPS detection in river microbial biofilms[6]

* Approximate absorption (Abs) and fluorescence emission (Em) maxima in nm.
[1] Supplied by Molecular Probes, Inc. Eugene, Oregon, USA; [2] supplied by Sigma-Aldrich Co., Canada; [3] Johnsen *et al.*, 2000; [4] Decho and Kawaguchi, 1999; [5] Michael and Smith, 1995; [6] Neu and Lawrence, 1997; [7] Wolfaardt *et al.*, 1998; [8] Lawrence *et al.*, 1998; [9] Del Gallo *et al.*, 1989.

A stock solution for each lectin-conjugate was prepared at selected concentrations and stored at –20°C. The solution used for each lectin-conjugate stain and their working concentrations are given in Table 3.8. Prior to use, the stains were thawed and centrifuged for 2 minutes at 14,000 *g* to remove any aggregates.

Table 3.8. Required Solutions and Working Concentrations for Lectin-conjugates

Lectin-conjugate	**Working Concentration (μg/mL)**	**Solution**
Concanavalin A[1]-Fluorescein, Alexa Fluor 647, Alexa Fluor 633	100	0.1 M $NaHCO_3$ containing 1mM Mn^{2+} and 1mM Ca^{2+} at pH 8.3
Wheat Germ Agglutinin[1]-Texas Red, Tetramethylrhodamine	10	PBS at pH 7.4 or 0.1 M $NaHCO_3$ containing 1mM Mn^{2+} and 1mM Ca^{2+} at pH 8.3
Soybean Agglutinin[1]-Alexa Fluor 488	10	Stock solution: distilled and deionized H_2O, working solution: 0.1 M $NaHCO_3$ containing 1mM Mn^{2+} and 1mM Ca^{2+} at pH 8.3
BS-I-TRITC[2]	10	PBS at pH 7.4 containing 1mM Ca^{2+}

[1] supplied by Molecular Probes, Inc. Eugene, Oregon
[2] supplied by Sigma-Aldrich Co., Canada

To retain moisture and maintain stability, both biomass and membrane fibre samples were embedded in low melting point agarose. To prepare the biomass sample for CLSM analysis, a 0.2 mL aliquot of biomass was added to 0.65 mL of low melting point agarose in a 1.5 mL microcentrifuge tube. After mixing by inversion, the mixture was poured into a plankton chamber and allowed to gel. A 1.0 mL working solution was made with the appropriate volume of lectin-conjugate in solution and poured over the flocs embedded in agarose. The sample was incubated at room temperature in the dark for 10 minutes. The sample was washed three times with buffer solution and incubated for 10 minutes after each washing (see Appendix B for a detailed protocol).

For each membrane fibre sample, three 1.0 cm longitudinal sections and three 1.5 mm cross-sections were excised using a sterile scalpel. The same methodology that was employed to stain flocs was employed to stain the membrane fibre sections with the exception that the

membrane fibre sections were immersed in the 1.0 mL staining solution first and then embedded in low melting point agarose following washings (see Appendix A for a detailed protocol). The preliminary study employed single and double lectins with various fluorescent conjugates. The core study employed three lectin-conjugates (Con A-AF647/AF633, WGA-tmr, and SBA-AF488) which were chosen based on the results of the preliminary study (see Appendix D for image data recorded from the preliminary study).

For comparison purposes, floc samples were imaged in fluorescence and reflectance mode. The fluorescent images were captured using the lectin-conjugates Con A-AF633, WGA-tmr, and SBA-AF488. The reflected images were captured by detecting scattered light from the sample, rather than fluorescent light.

In an effort to examine the nucleic acids in the biofoulant attached to the membrane fibres, LIVE *Bac*Light™ Bacterial Gram Stain, supplied by Molecular Probes Inc., was employed in combination with CLSM. This kit contains SYTO 9 which binds to nucleic acids found on and within bacterial cells. The protocol supplied by the manufacturer was followed when performing the LIVE *Bac*Light™ Bacterial Gram Stain on the membrane fibre sections (see Appendix C for a detailed protocol).

The CLSM analysis was performed using a Zeiss Axioplan LSM 510 (Carl Zeiss, Toronto, Ontario) equipped with an argon laser (excitation line 488), and helium-neon lasers (excitation lines 543 and 633). For each experiment, the argon laser was set at 50% of its total power. When collecting images, the argon laser was operated at 50% transmission power. The total power of the helium-neon lasers was not adjustable; however, each laser was operated at 100% transmission power. Samples were scanned by using three channels at selected z-intervals through the thickness of the flocs embedded in agarose or foulant adhered to the membrane fibre. For all images collected in the core study, channels 1, 2, and 3 represent the fluorescently labeled lectins Con A (blue), SBA (green), and WGA (red) respectively. Typically, scans were captured using a Zeiss 63X/1.2 NA water immersion C-Apochromat objective or a Zeiss 63X/0.9 NA water immersion Achroplan objective, a scan speed of 8.96 μs/pixel, and line averaging of 2. For each objective used, the pinhole diameter varied.

Therefore for a 63X/1.2 NA water immersion C-Apochromat objective the pinhole diameter for channels 1, 2, and 3 was set at 146 μm, 111 μm, and 129 μm respectively. Similarly, for a 63X/0.9 NA water immersion Achroplan objective the pinhole diameter for channels 1, 2, and 3 was set at 191 μm, 146 μm, and 169 μm respectively. To optimize each image, the brightest and darkest pixels were detected by adjusting the detector gain, amplitude gain, and amplitude offset for each channel (see Appendix J for image data recorded from the core study).

LSM 510 Release 2.3 software (Carl Zeiss, Toronto, Ontaro) was utilized to create gallery images, projections and depth-coded images for each z-stacked image. Gallery images were created by displaying sequential z-sections side by side. A projection was created by adding a sequence of consecutive z-sections together. When the projection was viewed at numerous angles on a computer screen, a three-dimensional impression was generated. The depth of a sequence of z-sections was visualized by employing depth coding. A colour scale bar provided information about the various components of the image at varying depths. The digital images were analyzed to determine parameters such as foulant coverage over the membrane surface, and regions containing microbial aggregates and EPS at various depths. Images could also be displayed using a split channel image. In the core study, a split channel image represented the three individual lectin-conjugates employed and a combined lectin-conjugate image. In all split channel images presented, the upper left, upper right, lower left, and lower right quadrants represent ConA (channel 1, blue), SBA (channel 2, green), WGA (channel 3, red), and combined lectins respectively.

3.8 Statistical Analysis

Variability in measurements was calculated using the standard deviation of the average and is shown as mean $\pm$ standard deviation. When studying the effect of SRT on the physicochemical properties of biomass, a t-test was used to determine the significance between treatment means. All calculations were performed by using Microsoft Excel (for Windows 2000). The null hypothesis that there is no significant difference in the physicochemical properties at the 12 and 30 day SRTs was tested using a two tailed t-test. If the probability for the calculated t-statistic was ≤ 0.05, then the null hypothesis was rejected and the two samples at SRT 12 days and 30 days were concluded to be different and statistically significant.

4.0 RESULTS

In this section, the results obtained using microscopic and analytical techniques to study biofouling in membrane bioreactors (MBRs) are presented. Preliminary results, presented in Section 4.1, were obtained by analyzing the constructed membrane loops sampled over time using confocal laser scanning microscopy (CLSM). Additionally, the physicochemical properties of the microbial flocs were determined from monthly sampling of the mixed liquor within the existing MBR. Section 4.2 details the performance of the MBRs used in this study including the physicochemical properties of the biomass at different sludge retention times (SRT). Section 4.3 describes the influence SRT, operational cleaning, and recovery cleaning had on membrane biofouling.

4.1 Preliminary Results of Biofouling

The primary purpose of the preliminary study was to evaluate the use of lectin-conjugate stains to analyze biofouling of polymeric microfiltration membranes by CLSM. Additionally, analytical techniques were employed to characterize the physicochemical properties of the biomass.

4.1.1 Membrane Bioreactor Performance

The preliminary experiments were run for two months (August 21, 2001 to October 29, 2001) in an existing pilot scale MBR treating municipal wastewater. The MBR was operated under steady state conditions until October at which point it was switched from automatic to manual operation due to sewage feeding problems. This resulted in intermittent permeation of wastewater through the membrane fibres. During manual operation, the temperature was stable at 20°C and aeration was continuous in the MBR.

While the performance of the MBR was not the focus of the preliminary study, various parameters were monitored. The MBR was run at an SRT of 20 days with a mixed liquor suspended solids (MLSS) concentration between 12–15 g/L and the temperature averaged 20.8°C. Although the dissolved oxygen concentration averaged 2.23 mg/L, the levels increased in October as shown in Figure 4.1.

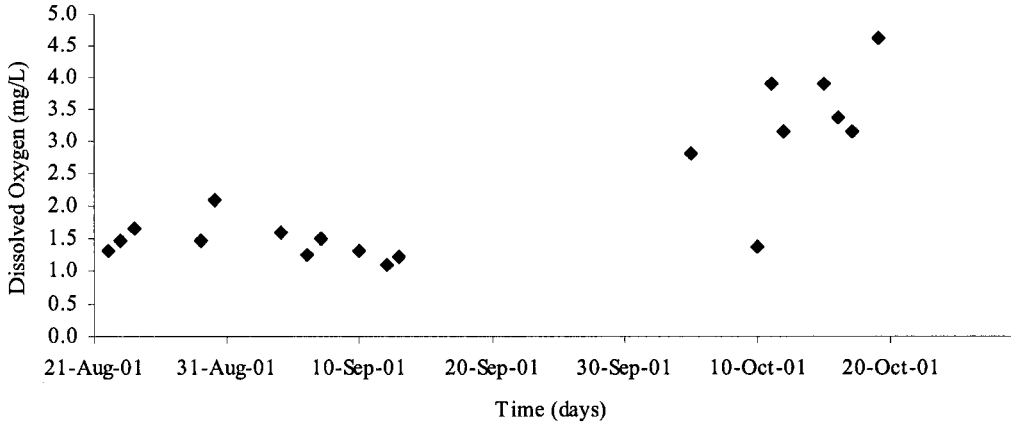

Figure 4.1. Dissolved oxygen concentration profile in the MBR for the duration of the preliminary study.

The initial and final permeability of each membrane loop was calculated and corrected to 25°C using equation [3-1]. As expected, over the range of 3 to 69 days of operation, the percent decrease in permeability increased with the amount of time the membrane loop operated in the MBR (Figure 4.2). However, there was no significant difference in permeability when measured at –16.9 kPa (5 in Hg) and at –33.8 kPa (10 in Hg) (t-test, $p > 0.05$).

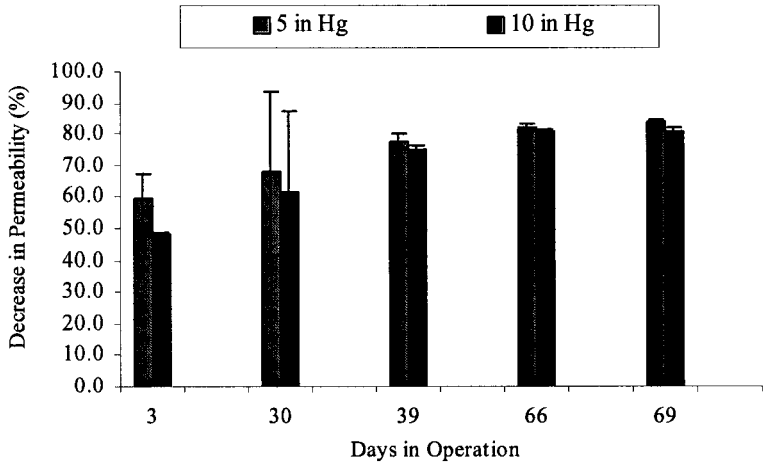

Figure 4.2. Average % decrease in permeability of membrane loops corrected to 25°C. The error bars represent the standard deviation within samples.

4.1.2 Characterization of Microbial Aggregates in Wastewater

Due to the high solids concentration in the MBR, the results of the first physicochemical analysis could not be obtained. Therefore, the mixed liquor was diluted to approximately one fifth of its original concentration. The physical properties of the mixed liquor included surface charge and hydrophobicity and were calculated using equations [2] and [3] respectively. Grab samples of the mixed liquor were sampled monthly from August to October, 2001. Surface charge and hydrophobicity were measured in triplicate with the exception of the samples taken in August which was measured only once due to sample loss. As illustrated in Figure 4.3 the surface charge was reasonably stable with an average of -0.322 ± 0.057 meq/g MLSS. On the other hand the relative % hydrophobicity was variable with an average of 36.7 ± 17.5 % as shown in Figure 4.4. The hydrophobicity increased significantly in the October sample which may be due to the change in MBR performance.

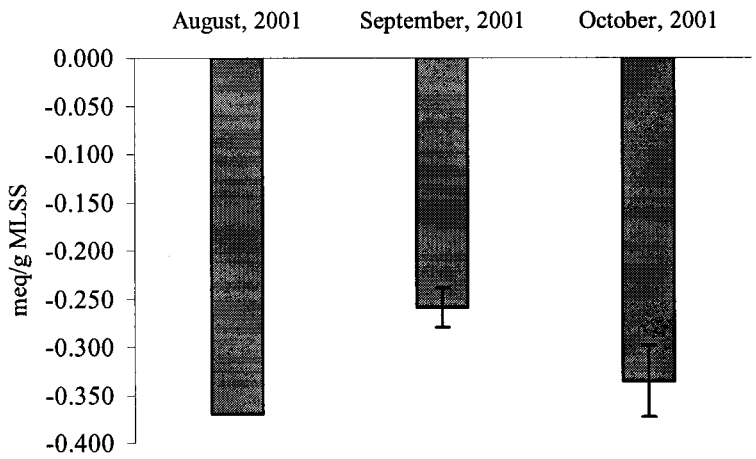

Figure 4.3. Surface charge of the microbial flocs in the MBR for the duration of the preliminary study. The error bars represent the standard deviation within samples.

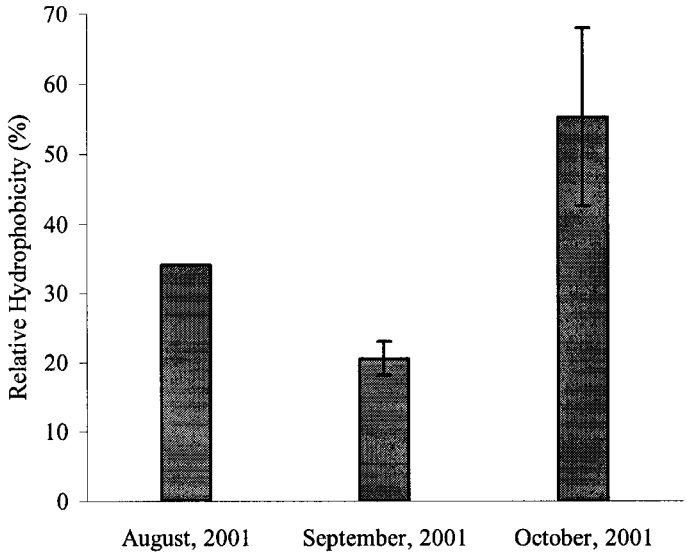

Figure 4.4. Relative % hydrophobicity of the microbial flocs in the MBR for the duration of the preliminary study. The error bars represent the standard deviation within samples.

From the extracted EPS, proteins, carbohydrates, uronic acids, and DNA were measured as shown in Figure 4.5. All EPS components were measured monthly with the exception of DNA which was measured only in October. Within the total EPS, proteins showed the highest concentration over all sampling periods. The uronic acids represent acidic polysaccharides in the EPS which showed a slightly higher concentration than the carbohydrate concentration except in the October sample whereby the uronic acids decreased to the lowest concentration of the total EPS. Since the total carbohydrate concentration includes acidic polysaccharides, it would not be possible for the uronic acids concentration to be higher than the carbohydrate concentration. Therefore the results obtained for uronic acids can be attributed to experimental error; however, the results demonstrate that acidic polysaccharides contributed to a large portion of the total carbohydrate concentration. The DNA concentration represented a small portion of the total EPS.

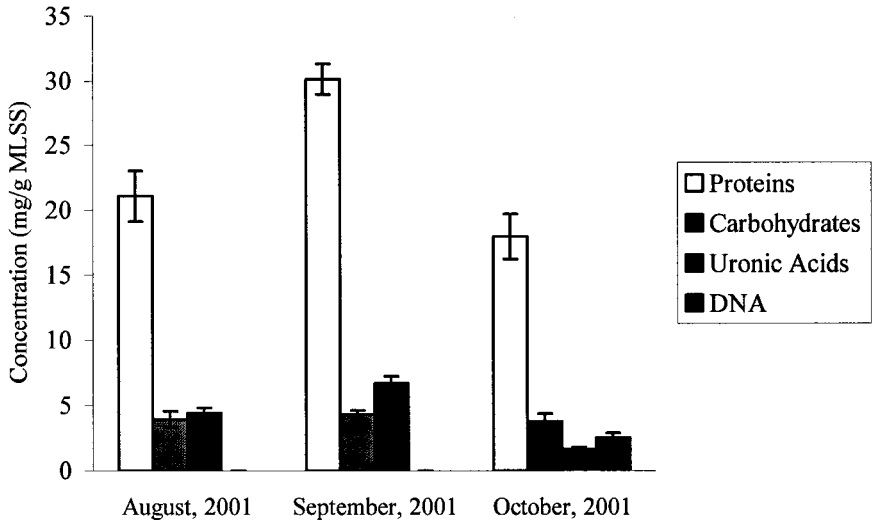

Figure 4.5. EPS composition and concentration for the duration of the preliminary study. The error bars represent the standard deviation within samples.

4.1.3 Microbial Community Analysis

Typical samples of the microbial flocs within the pilot scale MBR are depicted in Figure 4.6. The phase contrast images illustrated compact flocs containing a diversity of microbes including filamentous bacteria and higher organisms including stalked ciliates (Figure 4.6a), rotifers, and spirochetes (Figure 4.6b).

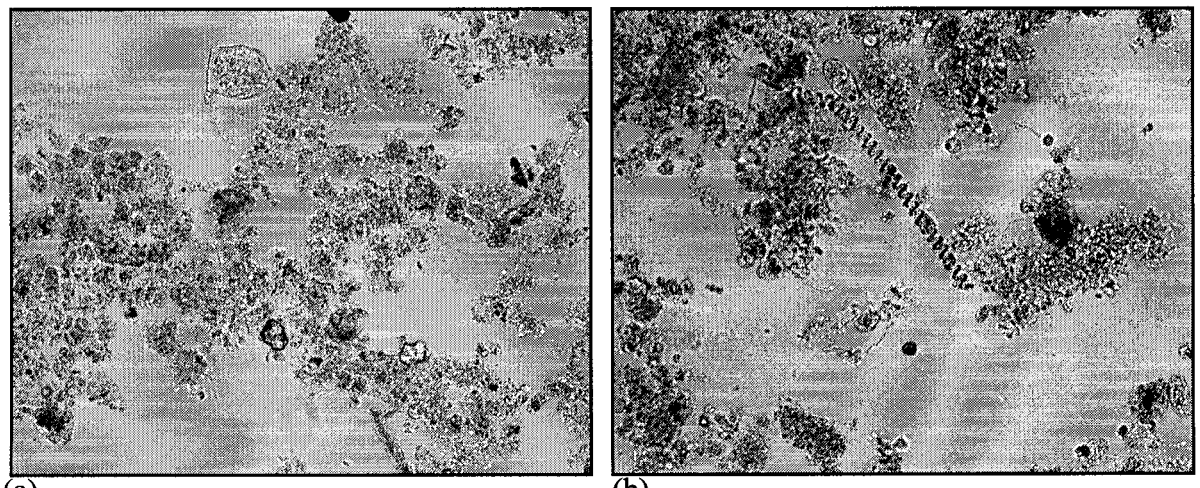

Figure 4.6. Wet mounts of microbial flocs observed in the pilot scale MBR obtained using phase contrast microscopy (20X, 0.50 NA objective).

4.1.4 CLSM Analysis of Microfiltration Membranes

In an effort to visualize the biological foulant on the surface of the membrane fibres, various lectin-conjugate stains were employed using CLSM (Table 3.7 and 3.8). The lectins were chosen based on previous studies as well as for their carbohydrate specificity. The initial results showed that the membrane fibre itself is autofluorescent at wavelengths in the visible spectrum above 488 nm. Autofluorescence of the membrane fibre proved to be advantageous because it served as a reference point.

After 3 days of filtration of municipal wastewater, microbial aggregates possessing α-mannopyranosyl and α-glucopyranosyl residues were observed. The sample was stained with concanavalin A conjugated with the fluorophore fluorescein (ConA-Fl). After 30 days of filtering municipal wastewater, the aggregation of microbes and EPS production became prevalent on the membrane fibres. Samples were stained with the lectins wheat germ agglutinin, conjugated with the fluorophore tetramethylrhodamine (WGA-tmr), and ConA-Fl. After 69 days of filtration, microbial aggregates continued to be prevalent on the membrane fibres sampled. Additionally, a layer of fibrous material was widely distributed over the surface of the membrane. Furthermore, the membrane itself had a mottled appearance due to a loss of autofluorescence. which may indicate that a chemical foulant was associated with the membrane.

4.2 Membrane Bioreactor System Performance

In the core study, two MBRs were set up and operated simultaneously, one at an SRT of 12 days (Reactor 2) and the other at an SRT of 30 days (Reactor 1). At start-up the reactors were filled with mixed liquor from an existing MBR that was operating at an SRT of 15-20 days. Throughout the experiment, both MBRs were operated on a permeate-to-drain basis to maintain a constant biomass level in the reactor. The reactors were fed fresh mixed liquor from the Skyway Wastewater Treatment Plant in Burlington, Ontario after passing through a 1 mm bar screen. In practice, to achieve steady-state operating conditions a bioreactor is typically operated for three times the length of the SRT; however, due to time constraints, this acclimation period was not established. The time constraints were a result of difficulty in maintaining mixed liquor suspended solids (MLSS) concentrations in the MBRs. Once the

necessary modifications were made to the reactors, new ZeeWeed™ (ZW) 10 modules were installed and the MBRs were operated under the conditions outlined in Table 3.3. The MBRs were run continuously for 64 days with the exception of sampling membrane fibres, clean water flux measurements, and recovery cleaning periods whereby each ZW-10 module was physically removed from the bioreactor. During sampling of membrane fibres and clean water flux measurements, the modules were outside of the reactor for no more than 2 hours. During recovery cleanings, the modules were outside of the reactor for no more than 24 hours. Additionally, when outside the reactor the moisture of each module was maintained by immersing it in clean water.

To monitor the stability and operability of the MBRs, various parameters were measured including temperature, pH, MLSS concentrations, dissolved oxygen concentrations, influent and permeate chemical oxygen demand (COD), and transmembrane pressure (TMP).

4.2.1 Analytical Data

The temperature, pH, MLSS concentrations, dissolved oxygen concentrations, and COD were monitored in each reactor on a regular basis and are summarized in Table 3.4 and Table 3.5. In both reactors the temperature was maintained at $10^{o}C \pm 1.9$ as shown in Figure 4.7.

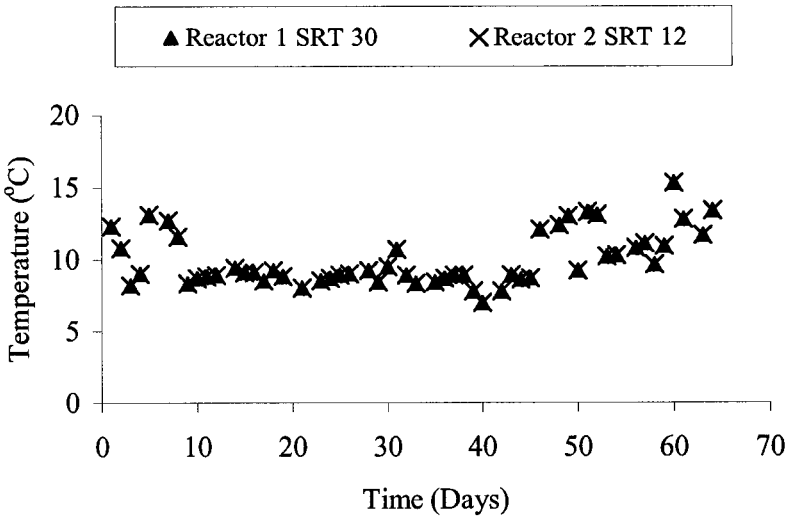

Figure 4.7. Temperature profile in Reactors 1 and 2 for the duration of the core study.

As illustrated in Figure 4.8 the pH was stable in both the feed and permeate of all ZW-10 modules.

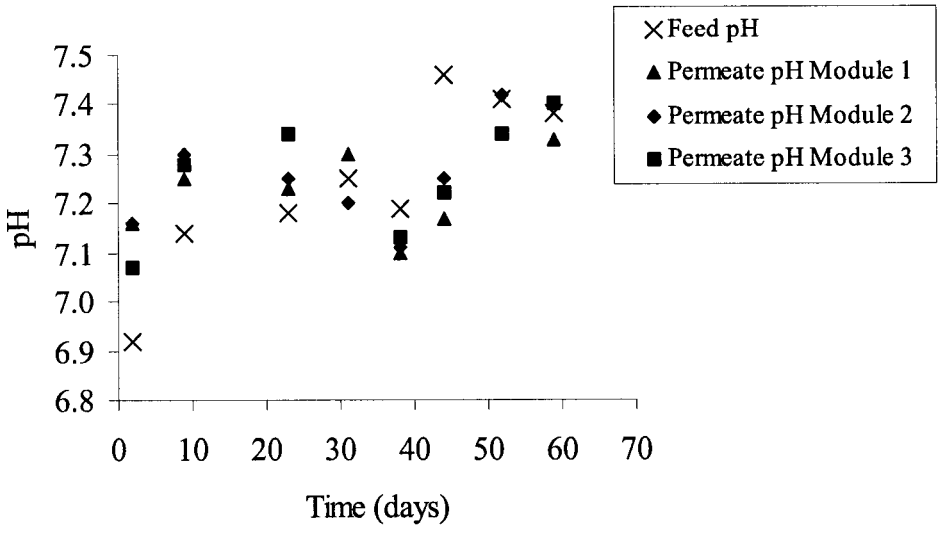

Figure 4.8. pH versus time measured in the feed and permeate of ZW-10 Modules 1, 2, and 3. Modules 1, 2, and 3 represent Reactor 1 SRT 30 permeate/relaxation; Reactor 2 SRT 12 permeate/relaxation, and Reactor 2 SRT 12 permeate/backwash respectively.

As illustrated in Figure 4.9, the MLSS concentration ranged between 11.54 g/L and 28.35 g/L in Reactor 1 and between 9.79 g/L and 27.94 g/L in Reactor 2. In both reactors the SRT was controlled only by the amount of sludge wasted per day as shown in Table 3.3. Therefore, the MLSS concentrations fluctuated with waste flow. Despite the apparent wide range of MLSS values, the average MLSS concentrations in Reactors 1 and 2 were 18.1 $\pm$ 3.42 g/L and 18.9 $\pm$ 3.01 g/L respectively.

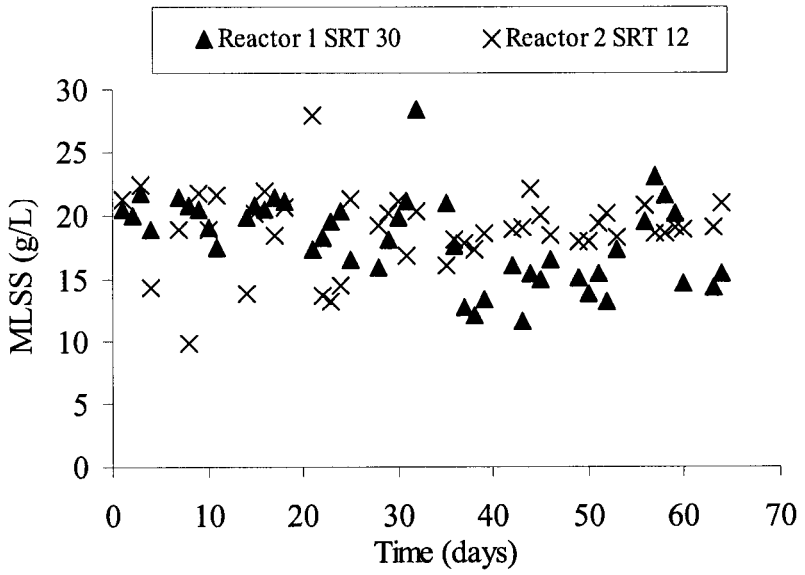

Figure 4.9. Mixed liquor suspended solids concentration profile in Reactors 1 and 2 for the duration of the core study.

As illustrated in Figure 4.10, the dissolved oxygen levels fluctuated between 1.4 mg/L and 5.2 mg/L in Reactor 1 and between 1.2 mg/L and 7.5 mg/L in Reactor 2 with average concentrations of 3.7 $\pm$ 1.3 mg/L and 4.1 $\pm$ 1.6 mg/L respectively.

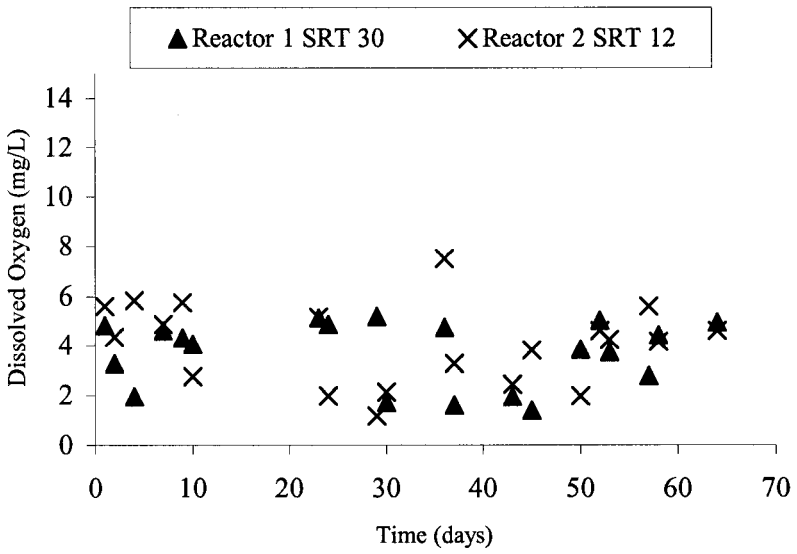

Figure 4.10. Dissolved oxygen concentration profile in Reactors 1 and 2 for the duration of the core study.

Figure 4.11 displays the influent (feed) COD concentrations measured as total COD (TCOD) and soluble COD (FCOD). The permeate COD concentrations were also measured for ZW-10 Modules 1, 2, and 3. For each module, the percent COD removal was calculated based on the influent FCOD. As illustrated in Figure 4.12, the FCOD removal for Modules 1, 2, and 3 was between 54.2 and 86.6%, 62.5 and 93.2%, and 69.0 and 92.5% respectively.

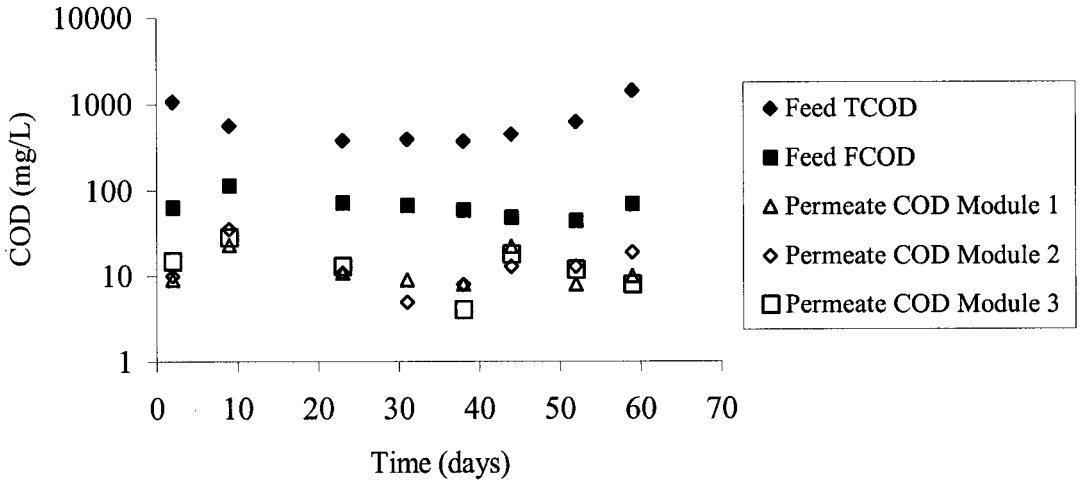

Figure 4.11. COD concentrations in the influent and permeate of ZW-10 Modules 1, 2, and 3 for the duration of the core study.

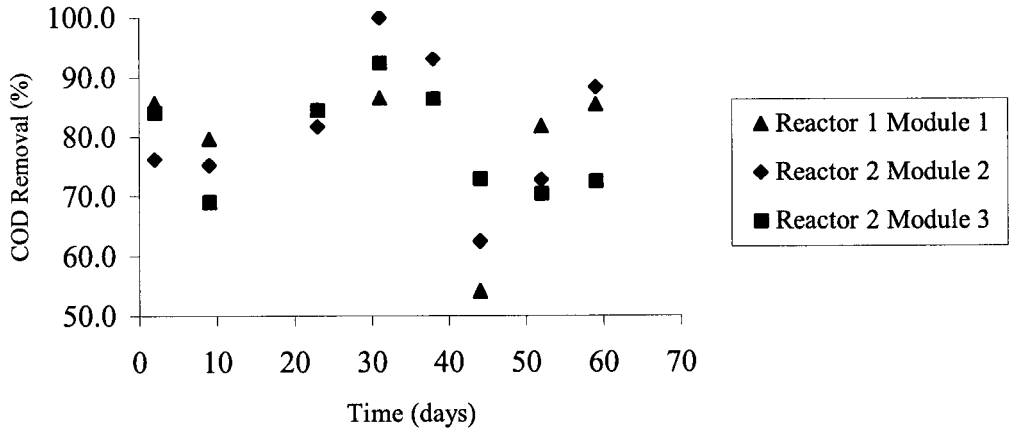

Figure 4.12. Percent FCOD removal for ZW-10 Modules 1, 2, and 3 for the duration of the core study.

4.2.2 Hydrodynamics

For municipal sewage applications, a typical net flux for a ZW-10 module ranges from 20 to 30 $L/m^2/hr$ at 15 to 20°C and the TMP ranges from -10 to -50 kPa. In order to intentionally biofoul the membranes, the ZW-10 modules in this study were operated at a higher flux (35 $L/m^2/hr$) for Run 1 and Run 2. In Run 1, Modules 1, 2, and 3 reached a critical TMP set near –60 kPa after 21, 18, and 21 days of operation respectively. Run 2 was operated under the same flux conditions; however, Modules 1, 2, and 3 reached critical TMP after only 13, 7, and 9 days of operation respectively. Therefore, to prolong the operation time of the ZW-10 modules, the flux was lowered to 20 $L/m^2/hr$ for Run 3. Modules 1, 2, and 3 were operated at this lower flux for 28, 34, and 32 days respectively at which point the experiment was terminated due to space limitations. The operational parameters and conditions of the MBR system are summarized in Table 3.3.

For each run, TMP values were recorded before and after each operational cleaning method, either relaxation or backwash, as shown for each ZW-10 module in Figure 4.13 (see recorded data in Appendix N). The measurement of TMP over time was based on the average TMP derived from measurements before and after operational cleaning. This was based on the observation that the TMP did not differ before and after operational cleaning.

In addition to TMP measurements, membrane permeability can be calculated during filtration of clean water or during filtration of wastewater. The permeability for each ZW-10 module filtering clean water and wastewater was calculated and corrected to 25°C using equation [3-1] and is illustrated in Figure 4.14 and Figure 4.15 respectively (see data in Appendix N and O).

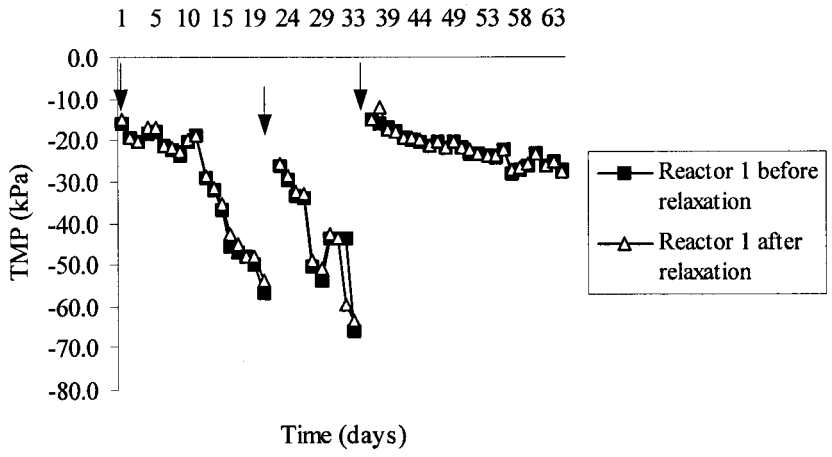

(a)

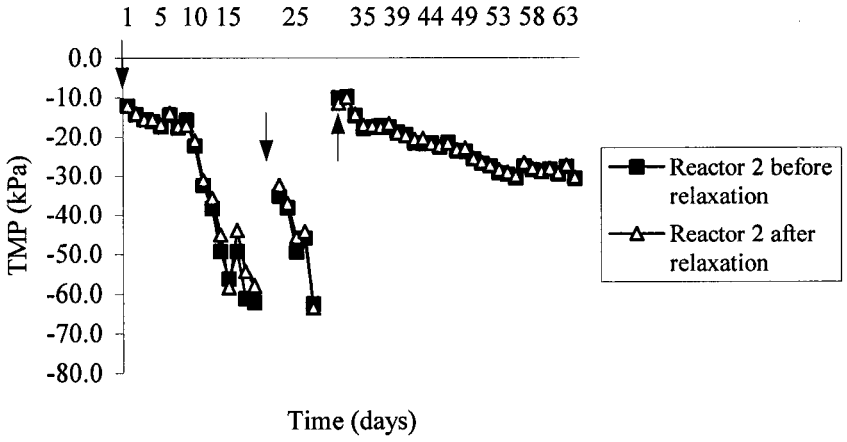

(b)

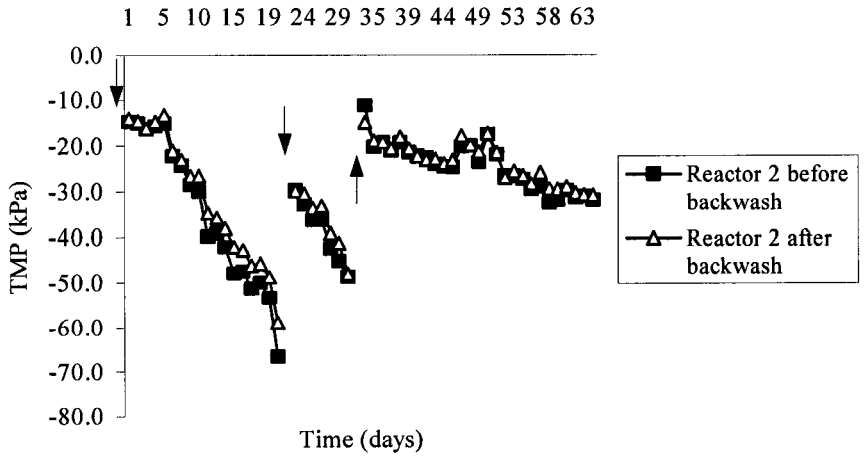

(c)

Figure 4.13. TMP versus time before and after operational cleaning for Runs 1, 2, and 3 (each run begins at the indicated arrow), (a) Module 1 SRT 30 permeate/relaxation, (b) Module 2 SRT 12 permeate/relaxation, (c) Module 3 SRT 12 permeate/backwash.

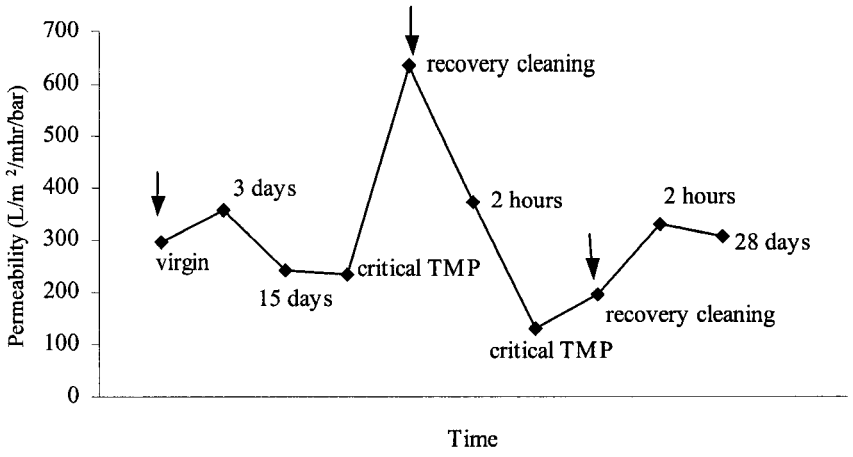

(a)

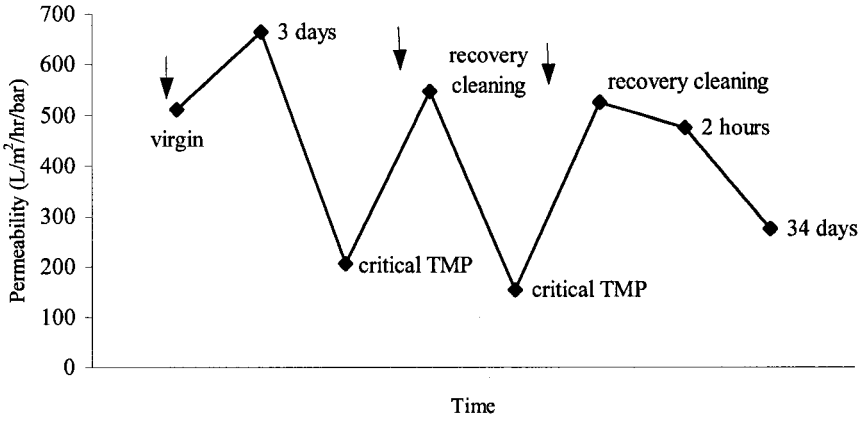

(b)

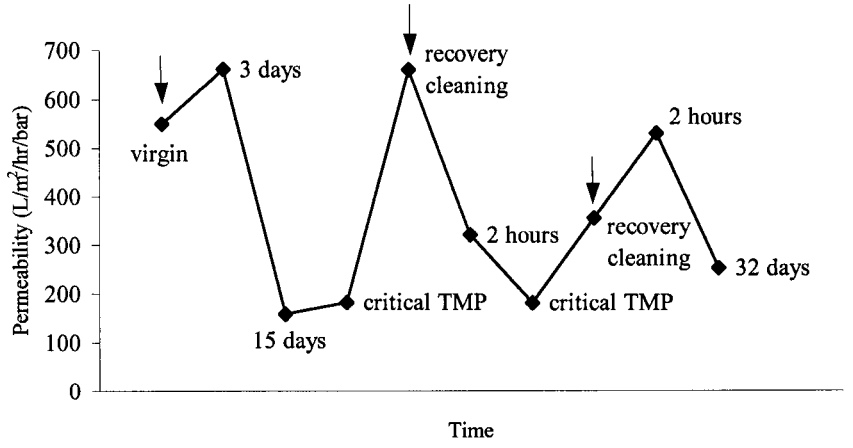

(c)

Figure 4.14. Clean water membrane permeability versus time for Runs 1, 2, and 3 corrected to 25°C (each run begins at the indicated arrow), (a) Module 1 SRT 30 permeate/relaxation, (b) Module 2 SRT 12 permeate/relaxation, (c) Module 3 SRT 12 permeate/backwash.

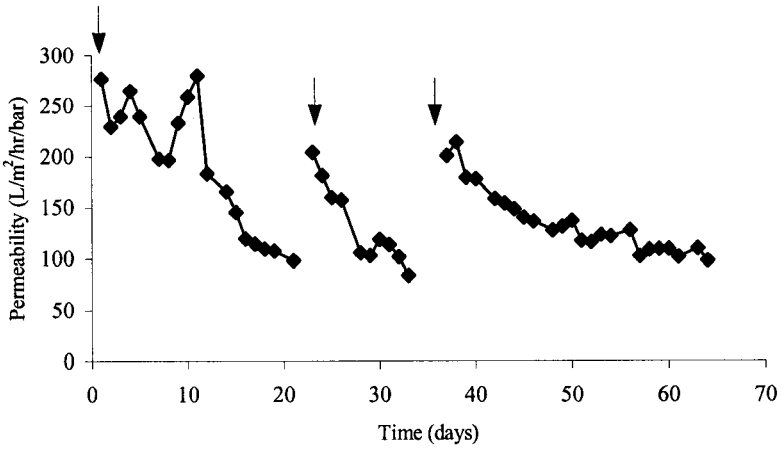

(a)

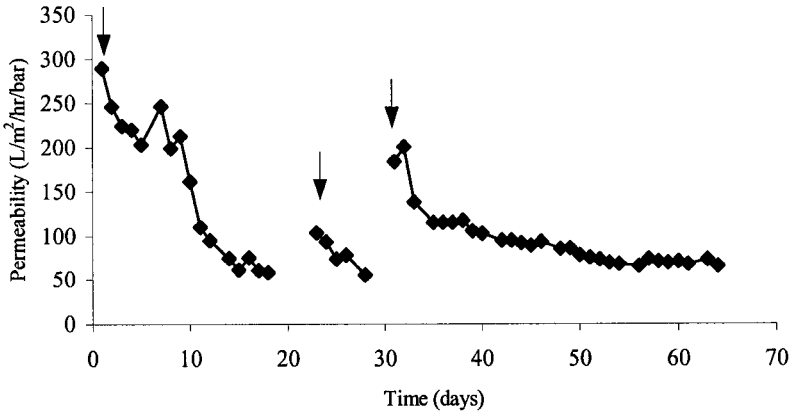

(b)

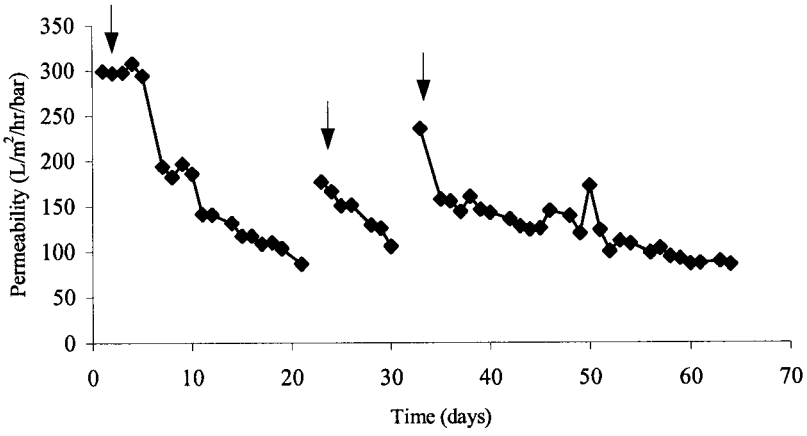

(c)

Figure 4.15. Wastewater membrane permeability versus time for Runs 1, 2, and 3 corrected to 25°C (each run begins at the indicated arrow), (a) Module 1 SRT 30 permeate/relaxation, (b) Module 2 SRT 12 permeate/relaxation, (c) Module 3 SRT 12 permeate/backwash.

4.2.3 Microbial Community Analysis

Typical samples of the microbial flocs within the MBRs are depicted which represent Reactor 1 operating at an SRT of 30 days (Figure 4.16 and Figure 4.18) and Reactor 2 operating at an SRT of 12 days (Figure 4.17 and Figure 4.19). In order to visualize individual flocs using conventional optical microscopy, the biomass was diluted because of its high MLSS concentration. Figure 4.16 and Figure 4.17 represent images that were captured in phase contrast and magnified 200X. At this magnification, significant differences are not observed between the flocs at SRT 12 and 30 days. In both reactors the flocs appeared to be irregular in shape and densely packed together containing filamentous bacteria. The noticeable dark areas may be a result of iron accumulation which is known to be in high concentrations in the feed sewage.

Figure 4.18 and Figure 4.19 represent images that were captured using CLSM in fluorescence and reflection mode. The microbial flocs were embedded in agarose and stained with lectin-conjugates as outlined in Appendix B. In order to gain a better understanding of the composition of microbial flocs, three lectins were utilized and include *Canavalia ensiformis* (concanavalin A, ConA) specific for α-mannopyranosyl and α-glucopyranosyl residues, *Triticum vulgaris* (wheat germ agglutinin, WGA) specific for *N*-acetylglucosaminyl residues, and *Glycine max* (soybean agglutinin, SBA) specific for α and β-*N*-acetylgalactosaminyl and galactopyranosyl residues. Images obtained in reflection mode corroborated the images obtained in fluorescence mode (Figure 4.18 b and d and Figure 4.19 b and d). At both SRTs, the spatial distribution of lectin-binding residues were highly heterogeneous. However, there was a difference in individual lectin distribution within the flocs at SRT 12 and 30 days. The 12 day SRT flocs had a specificity for ConA that appeared to be concentrated in the outer regions whereas the 30 day SRT flocs had specificity for ConA that was more dominant in the interior regions. Furthermore, the flocs at the 12 day SRT appeared to have a higher affinity for SBA when compared to the flocs at the 30 day SRT. At both SRTs, WGA was the principle lectin showing that the flocs affinity for WGA was dominant in both the interior and exterior regions.

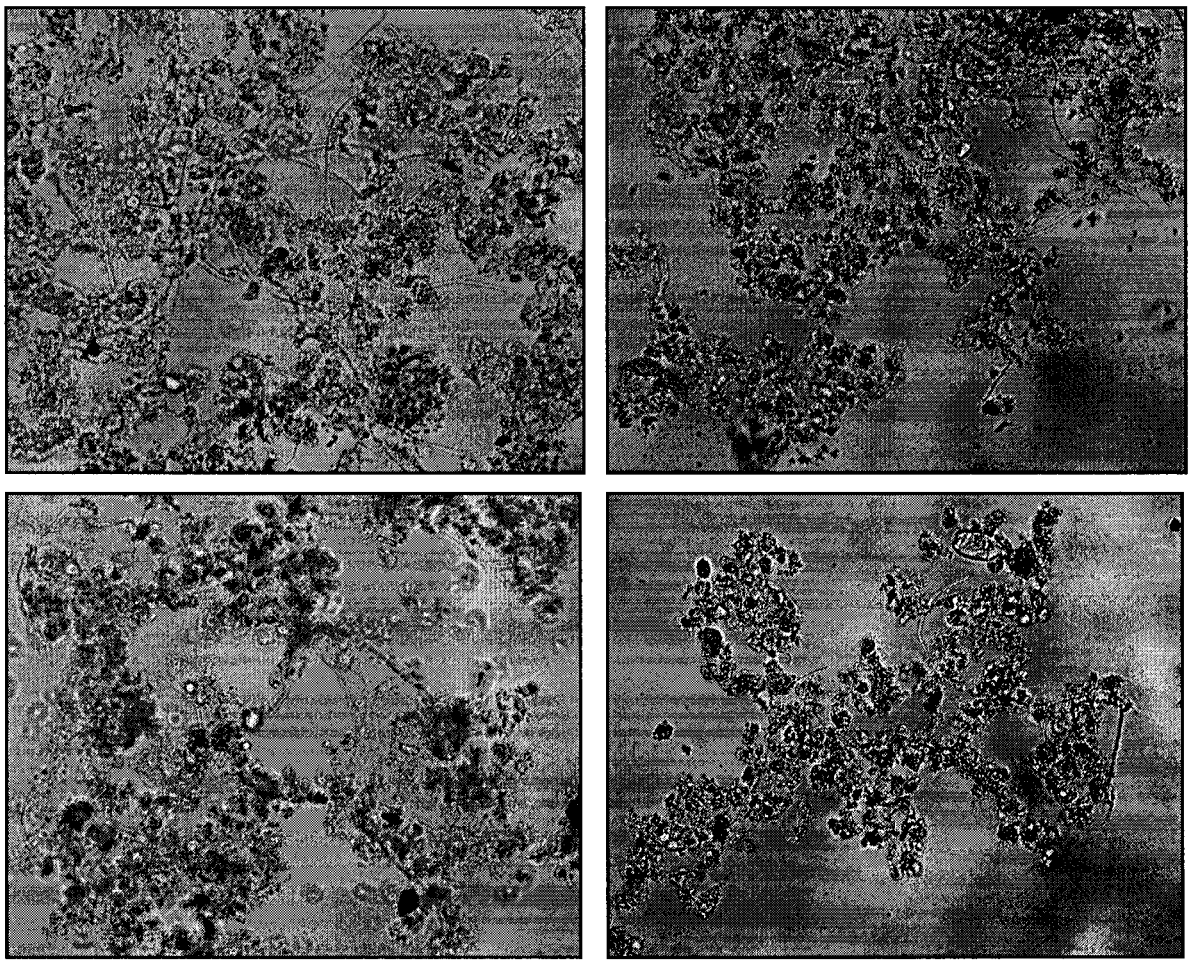

Figure 4.16. Wet mounts of microbial flocs observed by phase contrast microscopy in Reactor 1 operating at a 30 day SRT (20X, 0.50 NA objective).

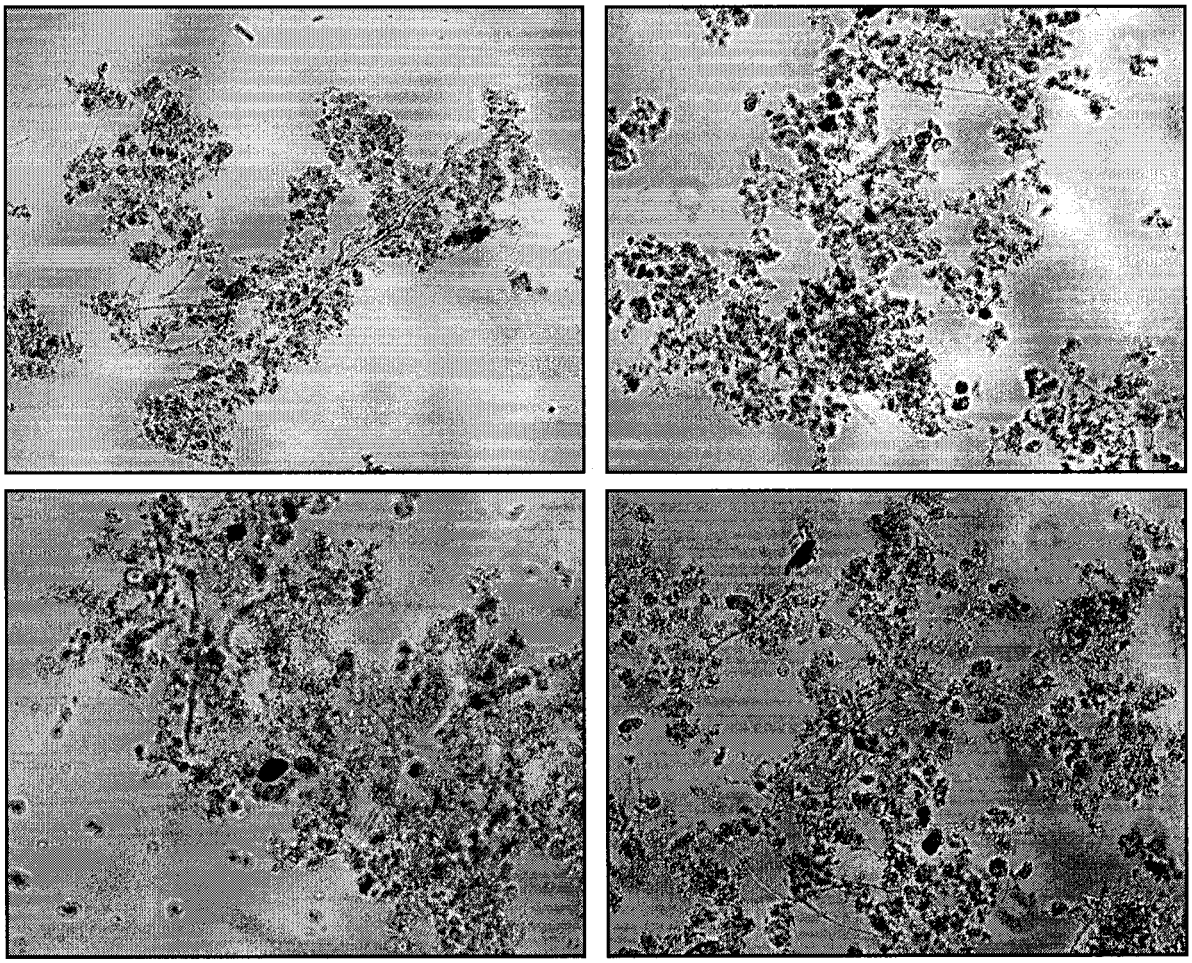

Figure 4.17. Wet mounts of microbial flocs observed by phase contrast microscopy in Reactor 2 operating at a 12 day SRT (20X, 0.50 NA objective).

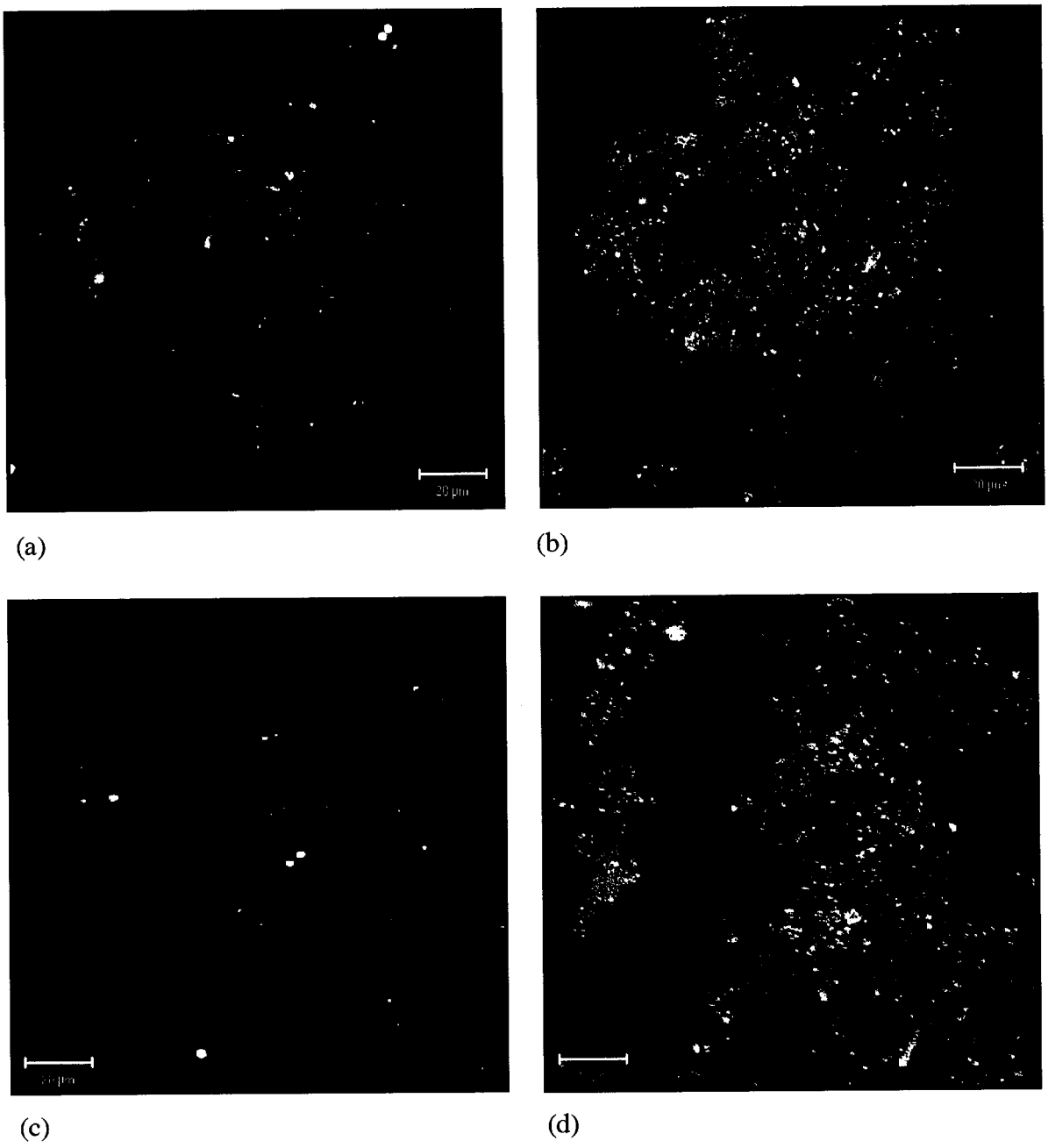

Figure 4.18. CLSM micrographs (63X/0.9 W objective, scale bar = 20 μm) showing the composition of microbial flocs at a 30 day SRT in fluorescence (a and c) and reflection mode (b and d). In the fluorescent images, blue represents ConA-AF633, green represents SBA-AF488, and red represents WGA-tmr. (a) and (b) were captured as a single plane. (c) and (d) are projections of a z-stack 16.5 μm in depth.

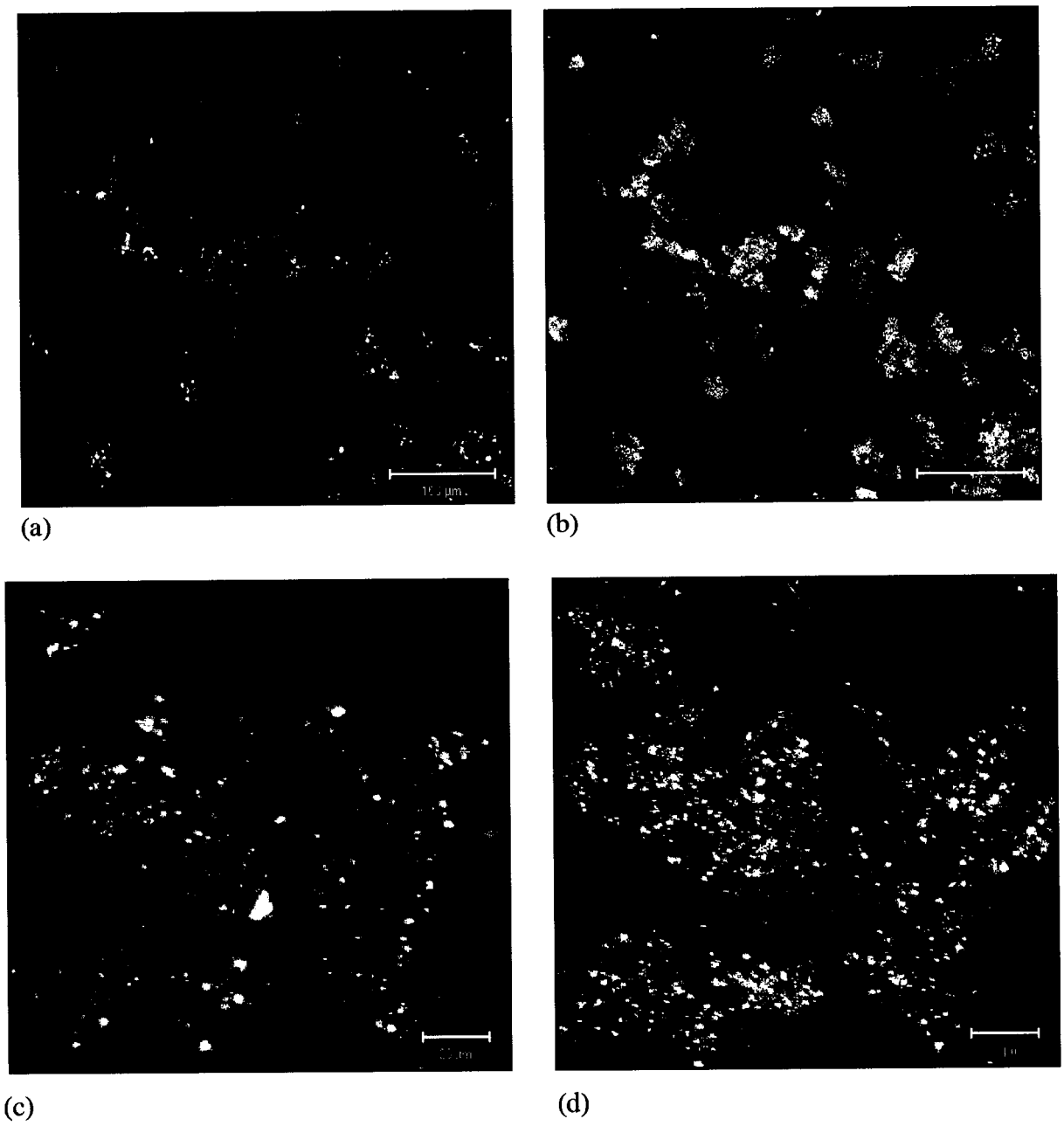

Figure 4.19. CLSM micrographs showing the composition of microbial flocs at a 12 day SRT in fluorescence (a and c) and reflection mode (b and d). In the fluorescent images, blue represents ConA-AF633, green represents SBA-AF488, and red represents WGA-tmr. (a) and (b) were captured as a single plane (20X/0.75 objective, scale bar = 100 μm). (c) and (d) are projections of a z-stack 30.0 μm in depth (63X/0.9 W objective, scale bar = 20 μm).

4.2.4 Characterization of Microbial Aggregates in Wastewater

The MLSS in the MBRs in the core study shared similar characteristics with the MLSS in the pilot scale reactor in the preliminary study. Since reliable results were obtained in the preliminary study by diluting the mixed liquor to approximately one fifth of its original concentration, the same approach was employed in the core study for surface charge, hydrophobicity, and EPS composition analyses.

4.2.4.1 Surface Charge

As illustrated in Figure 4.20, the surface charge of microbial flocs was less negative with increasing SRT. However, there was no significant difference between the samples measured the 12 day SRT and 30 day SRT (t-test, $p > 0.05$).

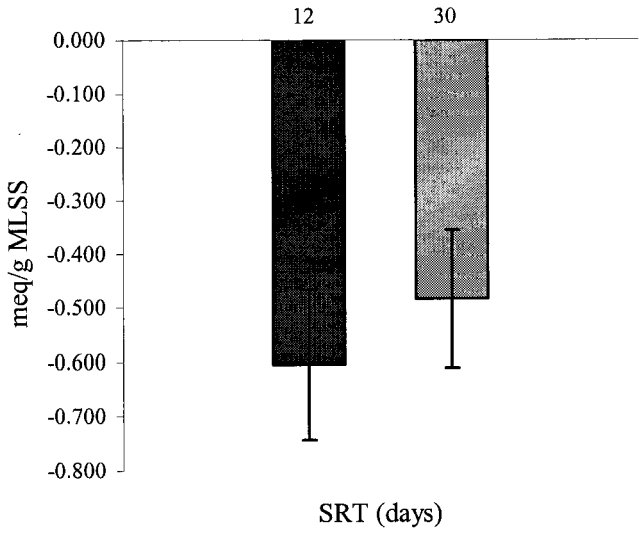

Figure 4.20. The relationship between surface charge of microbial flocs and SRT.

4.2.4.2 Hydrophobicity

The relationship between hydrophobicity of microbial flocs and SRT is illustrated in Figure 4.21. Hydrophobicity increased with increasing SRT, which is inversely correlated to surface charge. However, there was no significant difference between the samples measured at the 12 day SRT and 30 day SRT (t-test, $p > 0.05$).

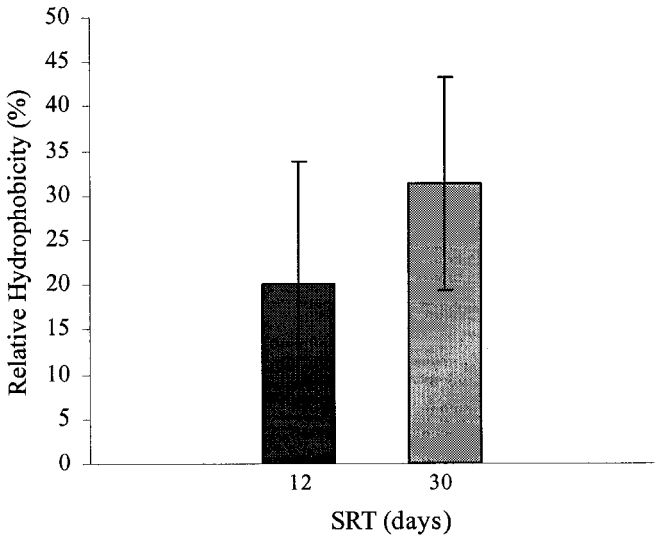

Figure 4.21. The relationship between hydrophobicity of microbial flocs and SRT.

4.2.4.3 EPS Composition

Figure 4.22 shows the concentration of individual EPS components (proteins, carbohydrates, uronic acids, and DNA) within the mixed liquor at the 12 and 30 day SRTs. At both SRTs, proteins showed the highest concentration and uronic acids showed the lowest concentration over all sampling periods (Figure 4.23a). Figure 4.23a showed that the DNA concentration at both SRTs contributed a considerable proportion of the total EPS which is contrary to previous studies (Bura *et al.*, 1998; Liao *et al.*, 2001). When compared to the DNA concentration, the carbohydrate concentration was higher at the 12 day SRT and lower at the 30 day SRT (Figure 4.23a). There was no significant difference in the concentrations of the individual EPS components between the 12 day and 30 day SRTs (t-test, $p > 0.05$). The total EPS was

considered to be the sum of all individual EPS components and was higher at the 30 day SRT (Figure 4.23b). However, there was no significant difference in the total EPS components between the 12 day and 30 day SRTs (t-test, $p > 0.05$). Similarly, the protein:carbohydrate ratio did not significantly differ between the 12 day and 30 day SRTs (t-test, $p > 0.05$).

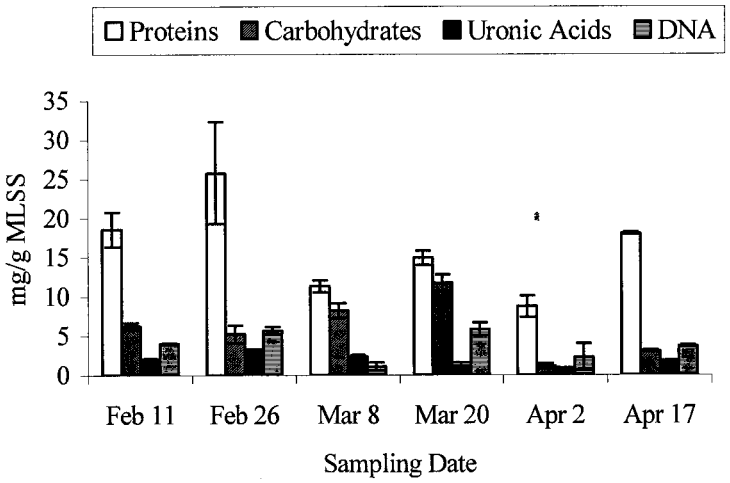

(a)

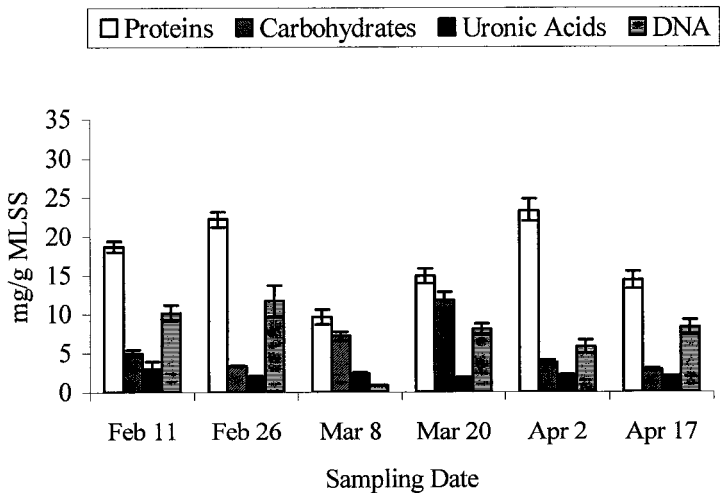

(b)

Figure 4.22. EPS composition and concentration for SRT 12 days (a) and SRT 30 days (b).

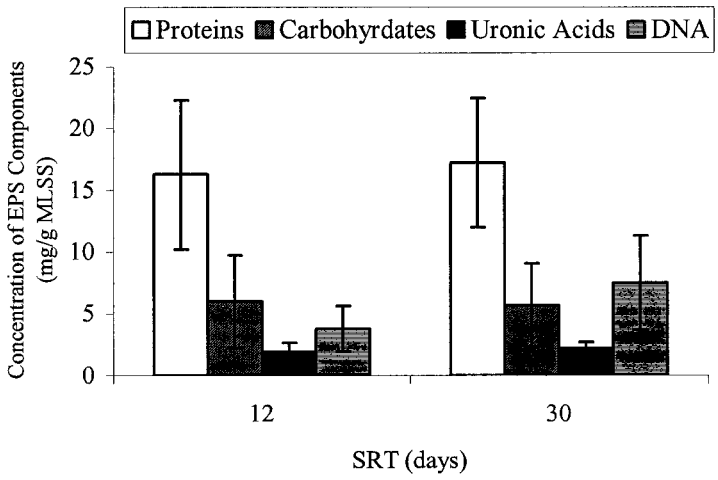

(a)

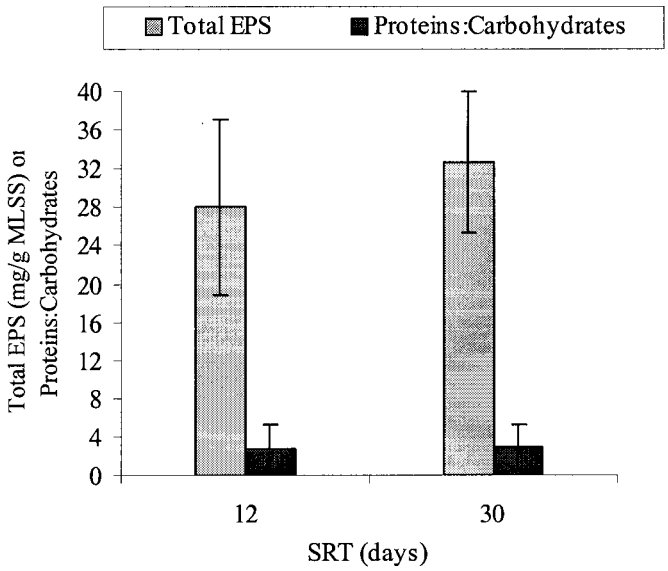

(b)

Figure 4.23. (a) Effect of SRT on the production of individual EPS components; (b) effect of SRT on the total EPS and protein:carbohydrate ratio.

4.3 Analysis of Membrane Biofouling by CLSM

This section presents the images captured by CLSM of the sampled microfiltration membrane fibres. Table 3.6 summarizes the sampling schedule of each membrane fibre from the ZW-10 modules. Numerous images were collected in an effort to investigate membrane biofouling. Unfortunately due to the large number of images collected, not all will be presented; however, all the image data is catalogued in Appendix J. The images that are presented show a representative development of the biofoulant on the membrane surface over time for Runs 1, 2, and 3 and after recovery cleanings. All images were captured using three lectin-conjugates, ConA, WGA, and SBA as outlined in Section 3.7.2 and Section 4.2.3.

As discovered from the preliminary study, the membrane fibres are autofluorescent. Therefore, samples of unstained virgin membrane fibres were imaged as a control and to illustrate its structural morphology. Figure 4.24 shows a longitudinal projection of a virgin membrane fibre. The bright fluorescent areas in Figure 4.24 were inferred to be artifacts in the image since they were visible at all depths of the z-stack.

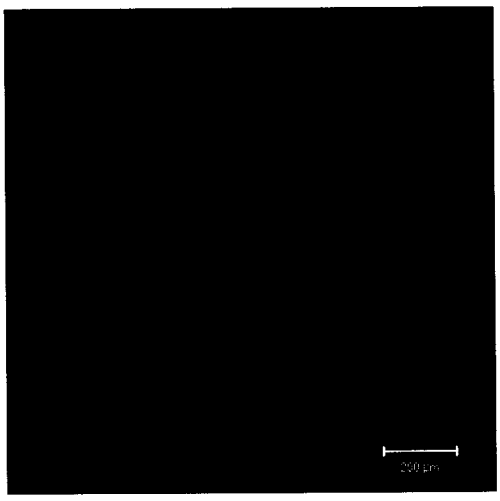

Figure 4.24. CLSM micrograph of a virgin membrane fibre showing its autofluorescence (longitudinal projection 138 μm in depth,10X/0.25 objective, scale bar = 200 μm).

After the installation of the three ZW-10 modules in Reactors 1 and 2, the first samples of membrane fibres were collected after two hours of operation. Previous studies have shown that fouling is known to occur within the first few hours of start up (Gander *et al.*, 2000). Therefore, as expected heterogeneous microbial aggregates had begun to adhere to the membrane fibres sampled from Module 2 (Figure 4.25a) and Module 3 (Figure 4.25b); however, these aggregates were observed to be sparse. The depth coded image (Figure 4.25c) showed evidence that the aggregate was attached to the membrane and was between 10 μm and 12 μm thick. Observations of the membrane fibres sampled from Module 1 showed an absence of microbial attachment to the membrane as indicated by lack of fluorescence.

Similarly, after 3 days of filtration the CLSM analysis of the membrane fibres showed that microbial aggregates were not abundant on the membrane's surface (Figure 4.26). When comparing the membrane fibres sampled from Modules 1 and 3, it appeared that the microbial aggregates had a high affinity for SBA and were closely associated with the membrane surface. In contrast, the membrane fibres sampled from Module 2 had a high affinity for WGA and appeared to be located just above the membrane's surface.

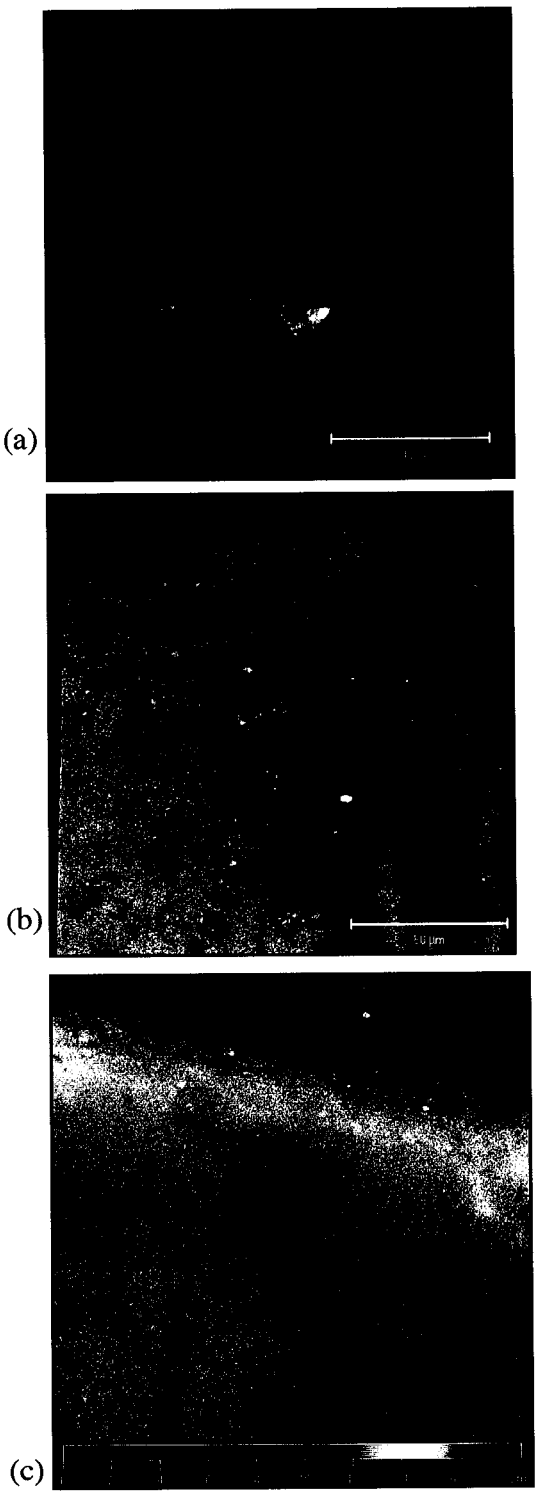

Figure 4.25. CLSM micrographs of longitudinal sections of membrane fibres sampled after 2 hours of filtration (scale bar = 50 μm), (a) Module 2 - SRT12 permeate/relaxation (63X/0.9 W objective), (b) Module 3 - SRT12 permeate/backwash, depth = 19 μm (63X/1.2 W objective), and (c) depth coded image of (b) (scale = 0-18 μm from blue to red).

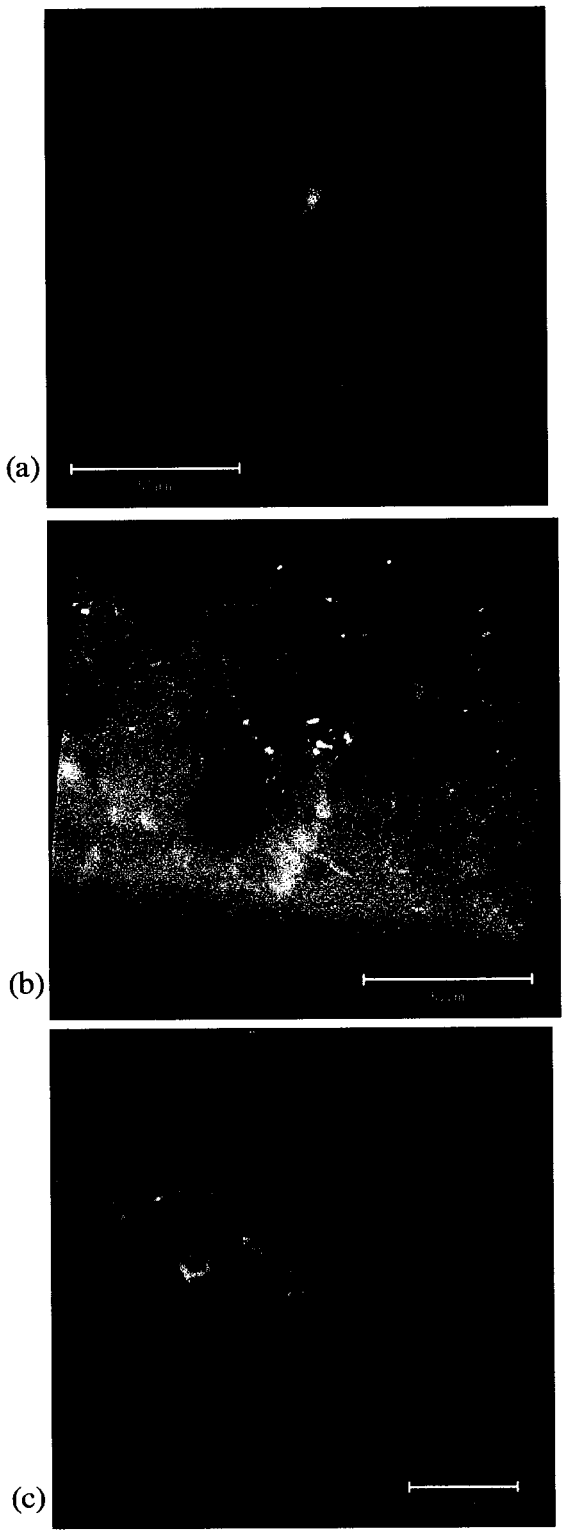

Figure 4.26. CLSM micrographs of longitudinal projections of membrane fibres sampled after 3 days of filtration (scale bars = 50 μm), (a) Module 1 - SRT 30 permeate/relaxation, depth = 17.5 μm (63X/0.9 W objective), (b) Module 2 - SRT12 permeate/relaxation, depth = 34 μm (63X/1.2 W objective), (c) Module 3 - SRT12 permeate/backwash, depth = 7.8 μm (63X/1.2 W objective).

After 15 days of filtration, a biofoulant had developed and was widely distributed over the surface of the membrane fibres sampled from all modules. As shown in Figure 4.27a, the biofoulant on the membrane fibres sampled from Module 1 consisted of a fibrous material specific for ConA which was observed faintly in blue. As shown by the distribution of lectins employed, there was a heterogeneous aggregation of microbes attached to the membrane fibres sampled from Module 2 (Figure 4.27b). However, WGA appeared to be dominant as indicated by a large quantity of *N*-acetylglucosaminyl residues were present in the aggregate. The aggregates were also observed to be densely packed together as shown by the dark shadowed area on the surface of the membrane (Figure 4.27b). The biofoulant observed on the membrane fibres sampled from Module 3 was comprised of large, dense microbial aggregates, which seemed to be either homogeneous (Figure 4.28a) or heterogeneous (Figure 4.28b) in glycoconjugate composition.

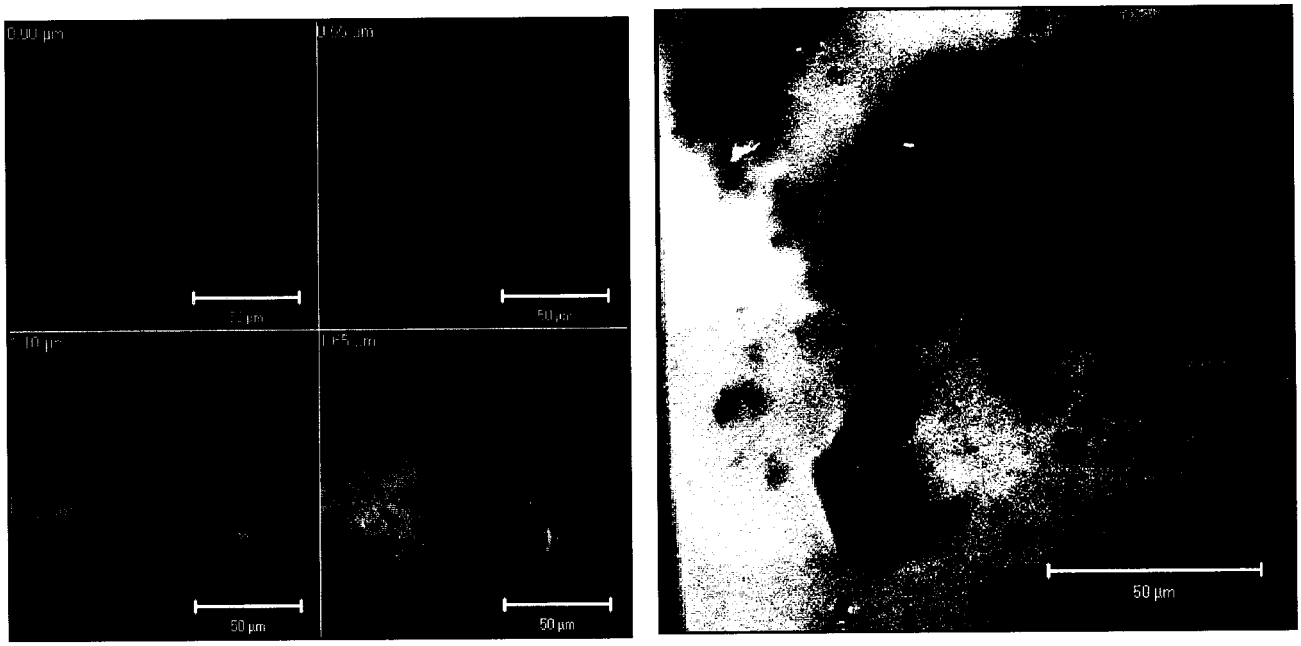

(a) (b)

Figure 4.27. CLSM micrographs of longitudinal sections of membrane fibres sampled after 15 days of filtration (scale bars = 50 µm) (a) gallery of images from Module 1 taken at 0.55 µm z-intervals (63X/1.2 W objective), (b) projection from Module 2, depth = 39 µm (63X/1.2 W objective).

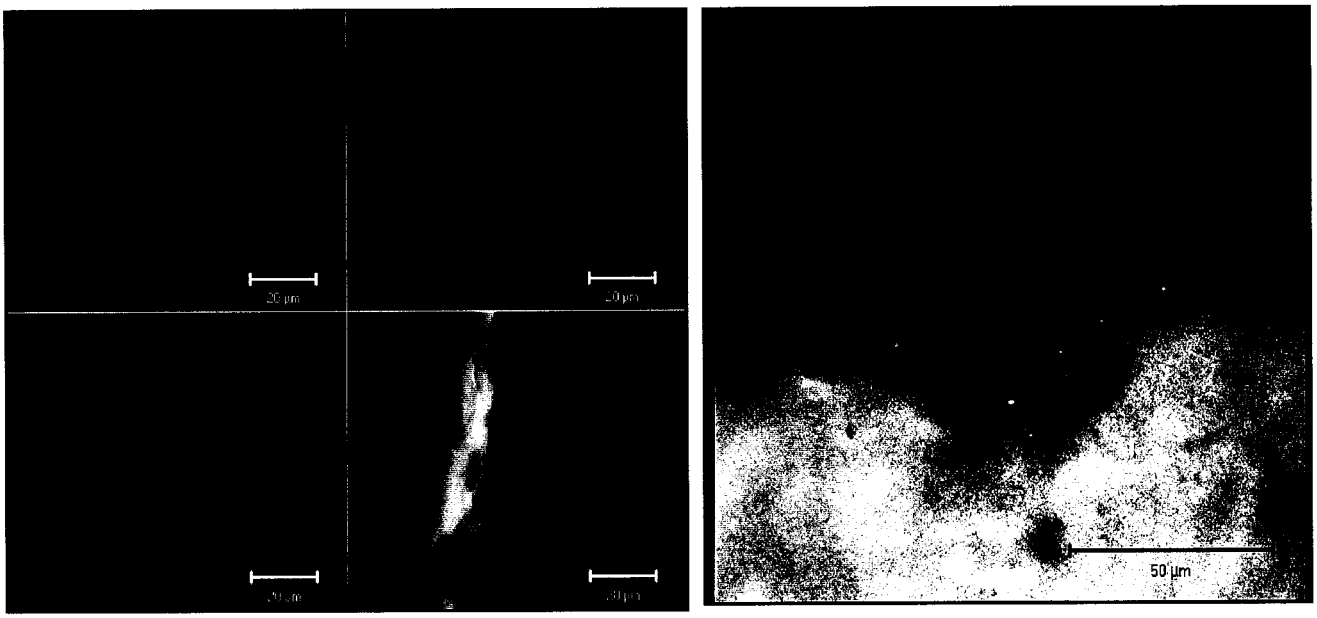

(a) (b)

Figure 4.28. CLSM micrographs of longitudinal projections of membrane fibres sampled from Module 3 after 15 days of filtration (a) split channel image (blue = ConA, green = SBA, red = WGA) showing a homogeneous microbial aggregate specific to WGA, depth = 50.8 µm (63X/0.9 W objective, scale bar = 20 µm), (b) heterogeneous microbial aggregate observed at the membrane surface, depth = 29.4 µm (63X/0.9 W objective, scale bar = 50 µm).

When each ZW-10 module reached critical TMP a membrane fibre was sampled and the modules were recovery cleaned. Module 2 reached critical TMP on day 18 and the other modules followed on day 21. When observing the membrane fibres sampled from Module 2 and Module 3, a significant amount of biofoulant was widely distributed over the surface of the membrane (Figure 4.29). In Module 2, the biofoulant was heterogeneous, but in some observations there was a dominant specificity for ConA (Figure 4.29a) whereas in others there was a dominant specificity for WGA (Figure 4.29b). In Module 3, the heterogeneity of the glycoconjugates appeared to have equal binding capacity for all lectins (ConA, WGA, and SBA) (Figure 4.29c). A network of fibrous material specific for ConA was also observed on the surface of the membrane fibres sampled from all modules (Figure 4.30).

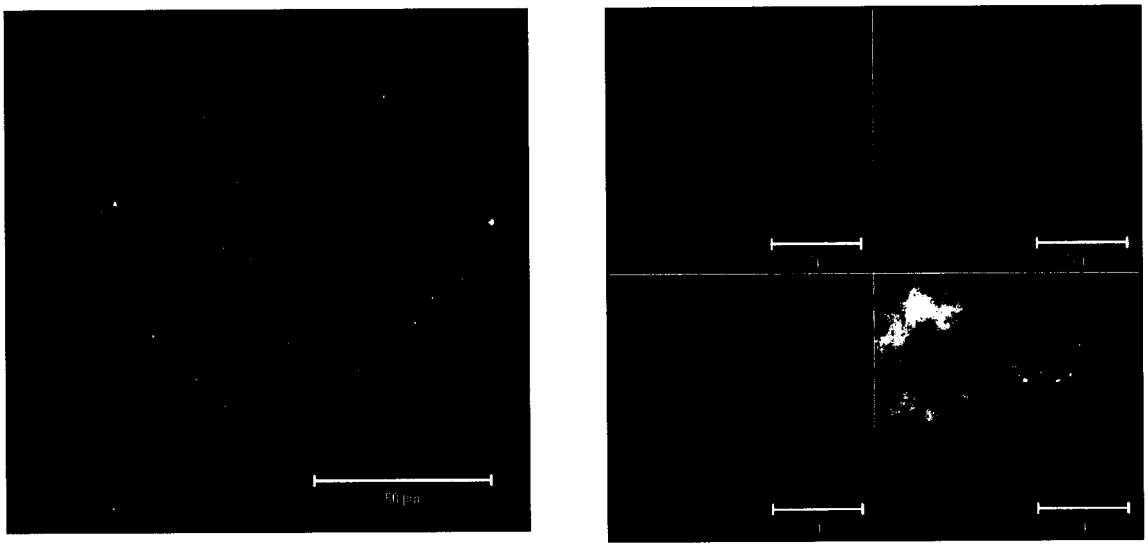

(a) (b)

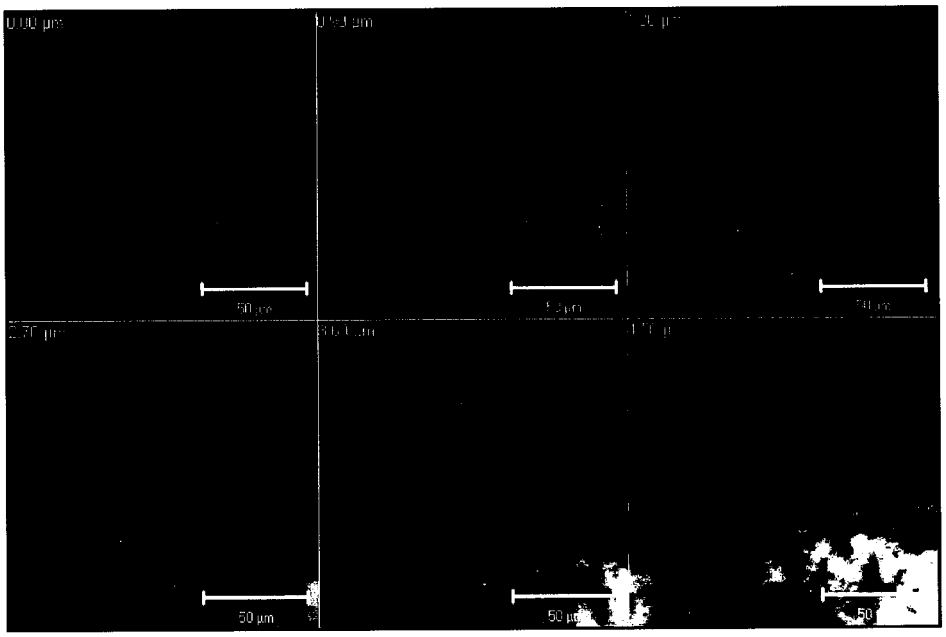

(c)

Figure 4.29. CLSM micrographs of longitudinal sections of membrane fibres sampled at critical TMP (scale bars = 50 μm), (a) projection image from Module 2, depth = 18 μm (63X/1.2 W objective), (b) split channel image (blue = ConA, green = SBA, red = WGA) from Module 2, depth = 15.0 μm (63X/1.2 W objective), (c) gallery of images from Module 3 taken at 0.90 μm z-intervals (63X/1.2 W objective).

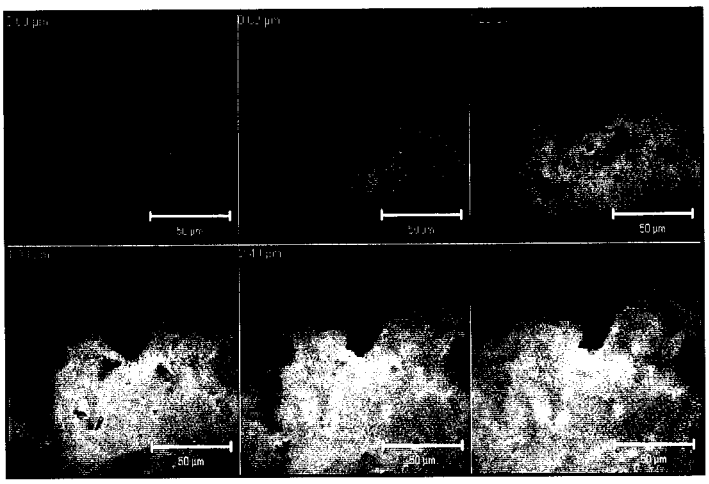

(a)

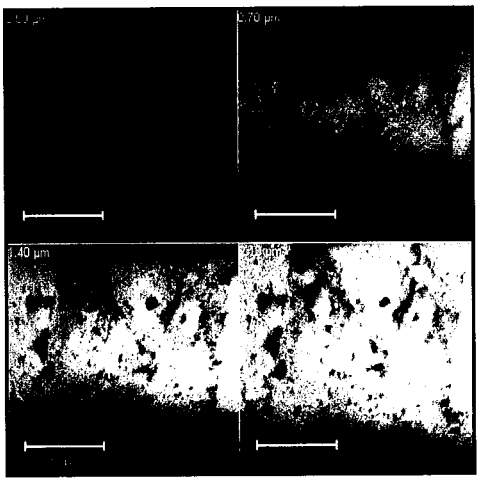

(b)

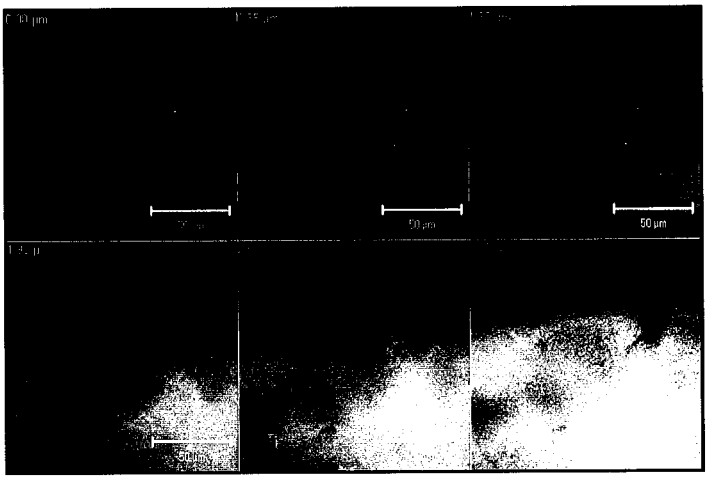

(c)

Figure 4.30. CLSM micrographs of longitudinal sections of membrane fibres sampled at critical TMP showing a fibrous matrix specific for ConA (63X/1.2 W objective, scale bars = 50 μm), (a) gallery of images from Module 1 taken at 0.60 μm z-intervals, (b) gallery of images from Module 2 taken at 0.70 μm z-intervals, (c) gallery of images from Module 3 taken at 0.65 μm z-intervals.

Membrane fibres were sampled after the ZW-10 modules were recovery cleaned overnight in a 2000 ppm hypochlorite solution. Observations from the CLSM analysis showed that in all membrane fibres sampled, a fibrous material specific to ConA in Modules 1 and 2 and WGA in Module 3 was attached to the surface of the membrane (Figure 4.31). Additionally, there appeared to be microbial aggregates still present, yet specific to different lectin-conjugates in all modules (Figure 4.31). The depth coded images in Figure 4.31 illustrated that the thickness of the biofoulant from Modules 1, 2, and 3 was 6.0 μm, 12.1 μm, and 8.5 μm respectively. Prior to recovery cleaning the modules, the biofoulant thickness ranged from 20 μm to 50 μm. Therefore, although recovery cleaning did not restore the membranes to their original state, it did appear to significantly reduce the biofouling layer.

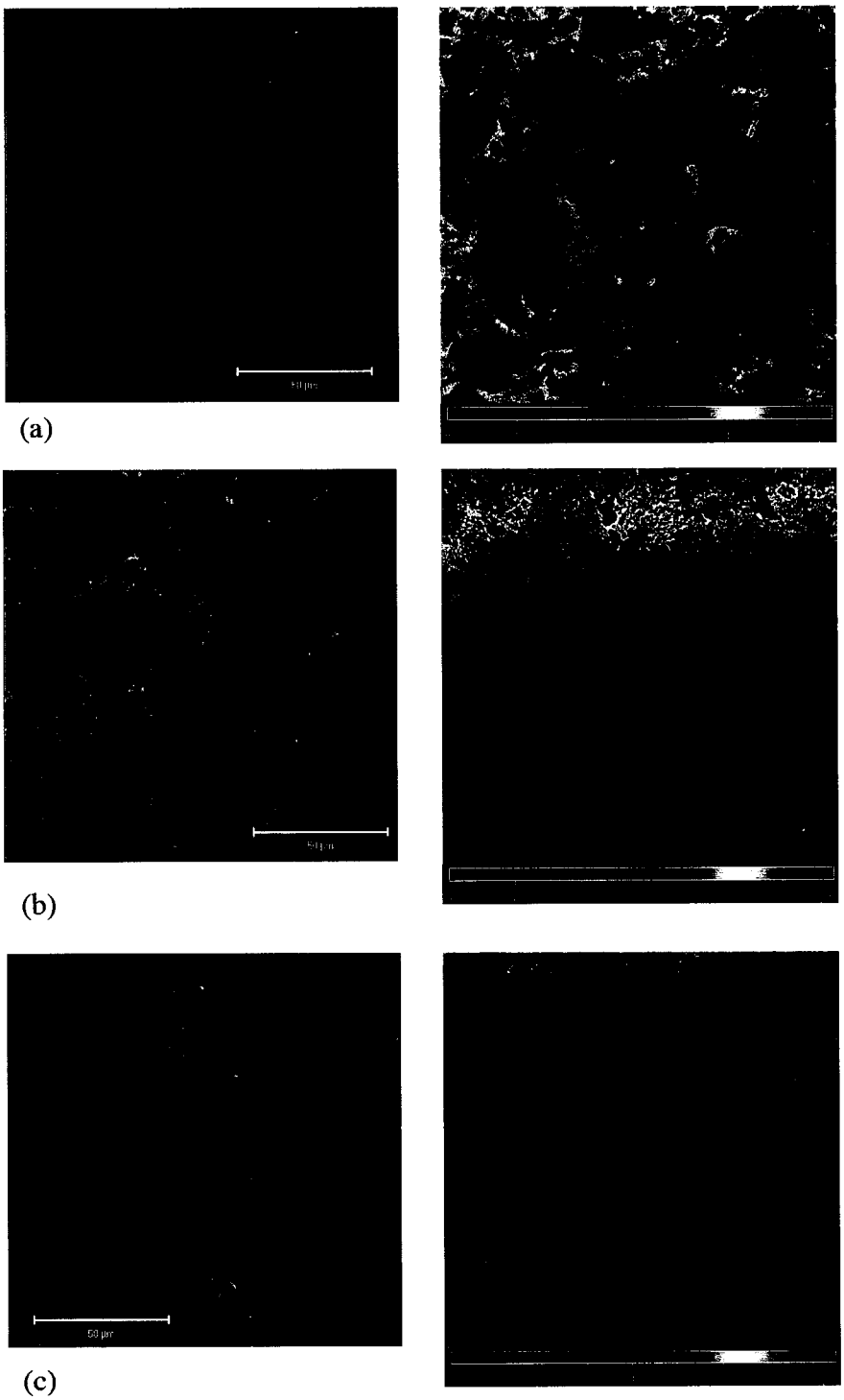

Figure 4.31. CLSM micrographs of longitudinal projections (left) (63X/1.2 W objective, scale bars = 50 μm) and depth coding (right) of membrane fibres sampled after recovery cleaning. (a) Module1 showing specificity for ConA and WGA, depth = 6.0 μm, (b) Module 2 showing specificity for ConA and SBA, depth = 12.1 μm, (c) Module 3 showing specificity for WGA and ConA, depth = 8.5 μm.

In Run 2, membrane fibres were sampled again at 2 hours, 3 days and at critical TMP. After 2 hours, the CLSM analysis of membrane fibres sampled from Module 2 (Figure 4.32a) and Module 3 (Figure 4.32b) showed that microbial aggregates had redeveloped on the membrane and resembled the amount of biofoulant observed after the first 15 days of operation in Run1. The aggregates observed on the membrane fibres sampled from Module 2 were dense and tended to be more cluster-specific to SBA and WGA rather than existing as a heterogeneous colony (Figure 4.32a). The membrane fibres sampled from Module 3 appeared to be comprised of scattered microcolonies on and above the membrane surface with high specificity for ConA and WGA (Figure 4.32b). In addition to the fibrous material on the membrane's surface, observations of the fibres sampled from Module 1 showed evidence of the beginning stages of microbial reattachment to the membrane which was specific to ConA and WGA (Figure 4.32c).

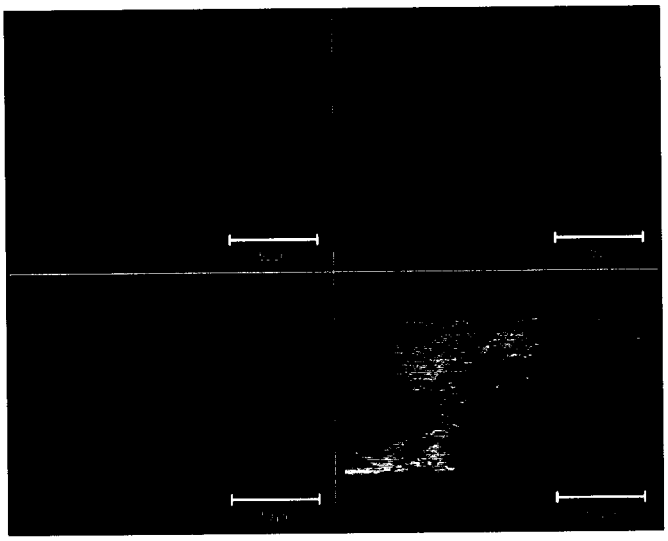

(a)

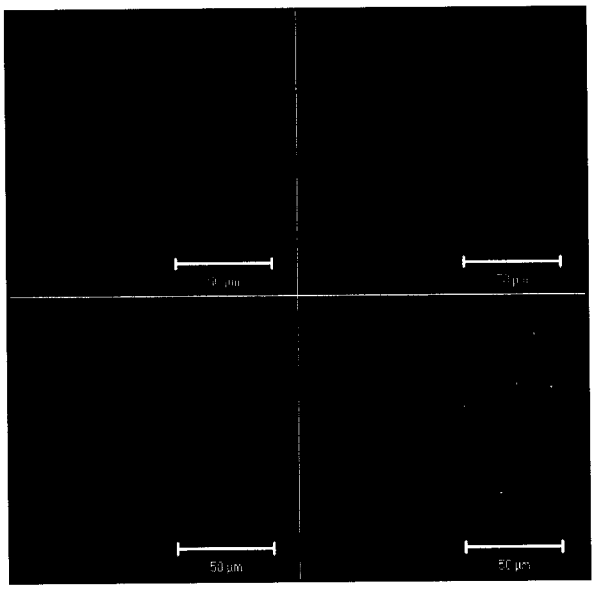

(b)

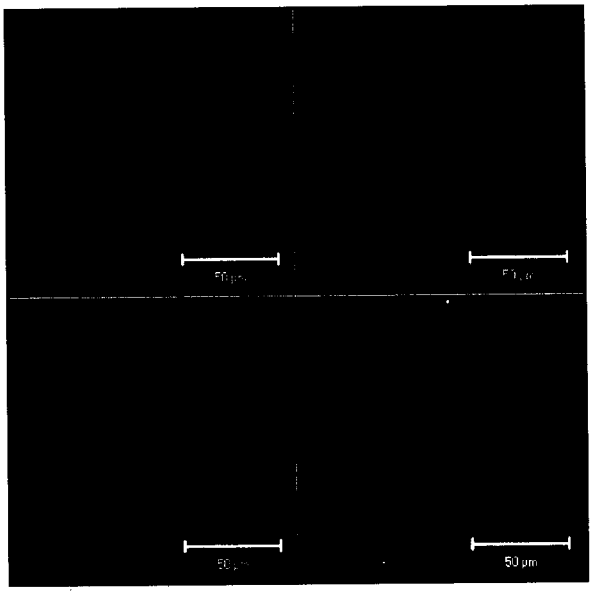

(c)

Figure 4.32. CLSM split channel micrographs of longitudinal projections of membrane fibres sampled after 2 hours of Run 2 (scale bars = 50 µm), (a) Module 2, depth =114.6 µm (63X/0.9 W objective), (b) Module 3, depth = 25.7 µm (63X/1.2 W objective), (c) Module 1, depth = 23.2 µm (63X/1.2 W objective).

After 3 days of filtration in Run 2 the membrane fibres sampled from Module 2 (Figure 4.33 a and b) and Module 3 (Figure 4.33 c and d) did not show significant changes from the 2 hour sampling period. On the other hand the membrane fibres sampled from Module 1 showed a large aggregation of microbes highly specific for WGA (Figure 4.34a). Individual cells were also observed that had a high specificity for SBA and WGA (Figure 4.34b). Although this was an isolated occurrence, it is evidence of a biofilm growing on the membrane surface.

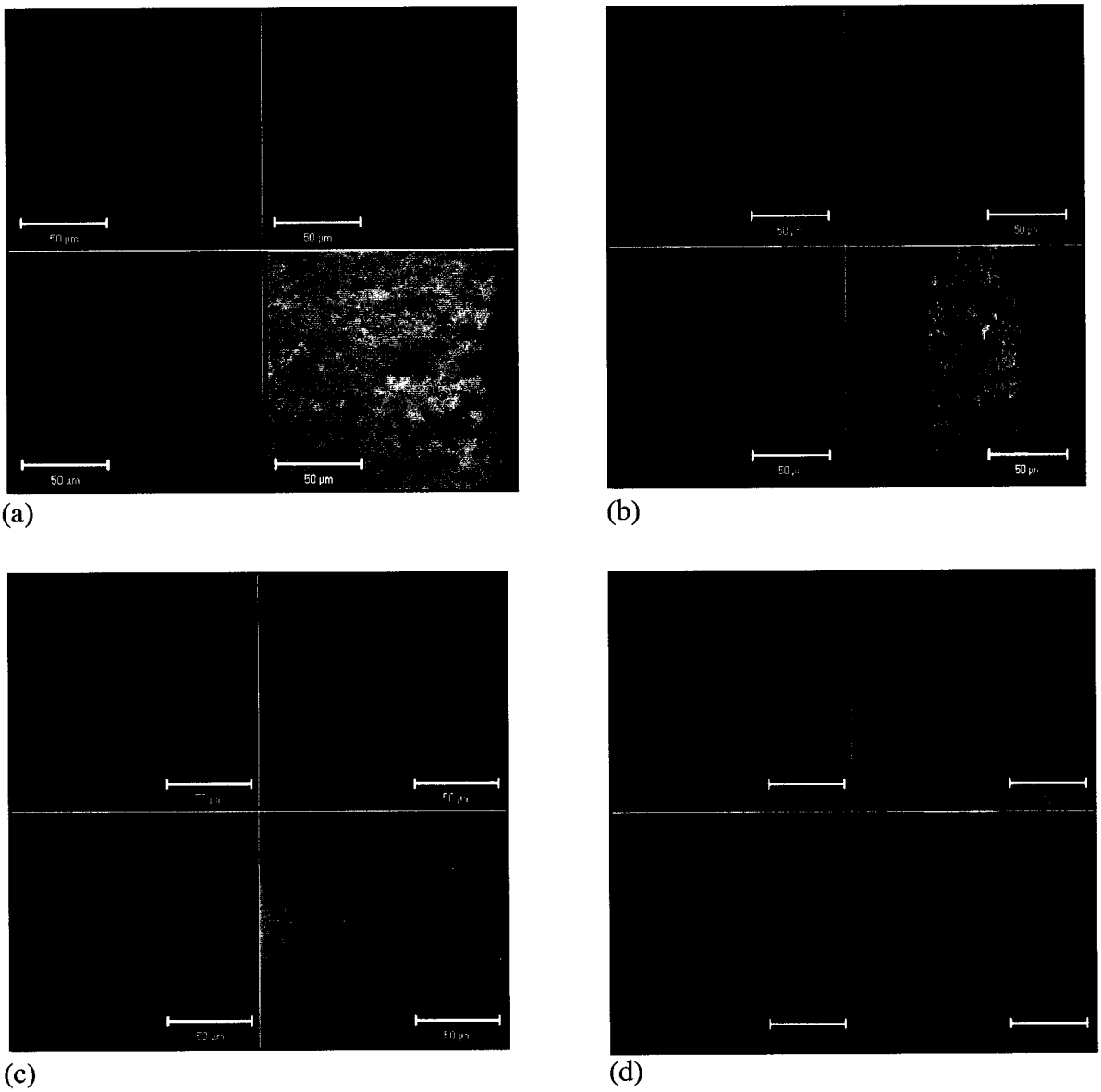

Figure 4.33. CLSM split channel micrographs of longitudinal projections of membrane fibres sampled after 3 days of Run 2 (63X/0.9 objective, scale bars = 50 µm), (a) Module 2, depth = 18.0 µm (63X/0.9 W objective), (b) Module 2, depth = 37.0 µm, (c) Module 3, depth = 6.0 µm, (d) Module 3, depth = 61.1 µm.

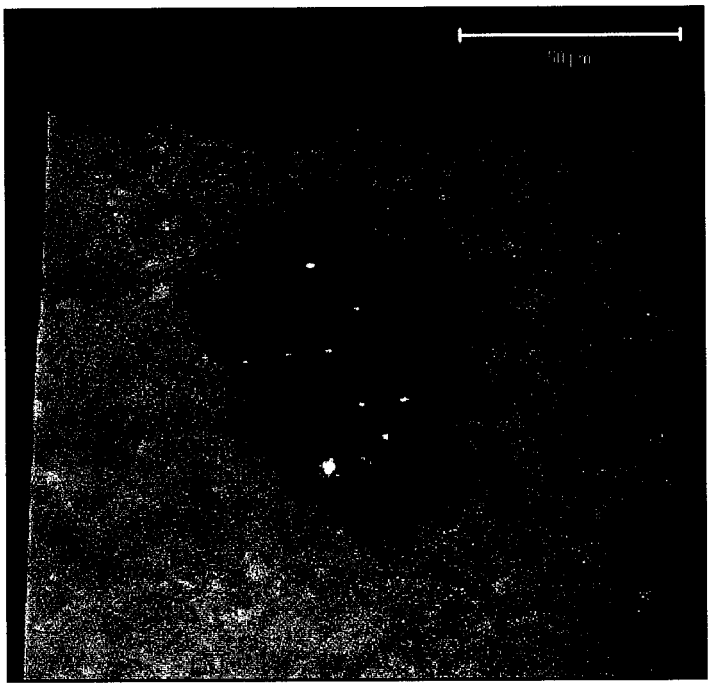

(a)

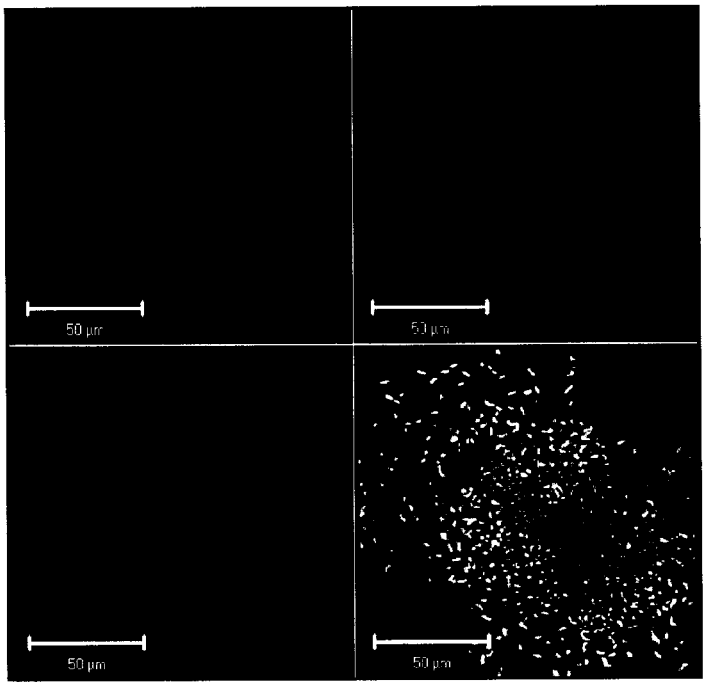

(b)

Figure 4.34. CLSM micrographs of longitudinal projections of membrane fibres sampled from Module 1 after 3 days of Run 2 (63X/0.9 objective, scale bars = 50 µm), (a) depth =58.9 µm, (b) split channel projection, depth = 30.0 µm.

Module 2 reached critical TMP after only 7 days of filtering municipal wastewater after the first recovery cleaning. Module 3 followed shortly thereafter, reaching critical TMP 9 days after the first recovery cleaning and Module 1 stayed in operation the longest, filtering municipal wastewater for 13 days before reaching critical TMP. At critical TMP the membrane fibres sampled from Module 1 (Figure 4.35a) and Module 3 (Figure 4.35b) showed large heterogeneous microbial aggregates with the greatest specificity for WGA. The membrane fibres sampled from Module 2 displayed a layer of biofoulant over the surface of the membrane, but there did not seem to be specificity for a particular lectin-conjugate (Figure 4.35 c and d). The thickness of the biofoulant attached to the membranes in ZW-10 Modules 1, 2, and 3 was 110 μm, 73.5 μm, and 41.0 μm respectively.

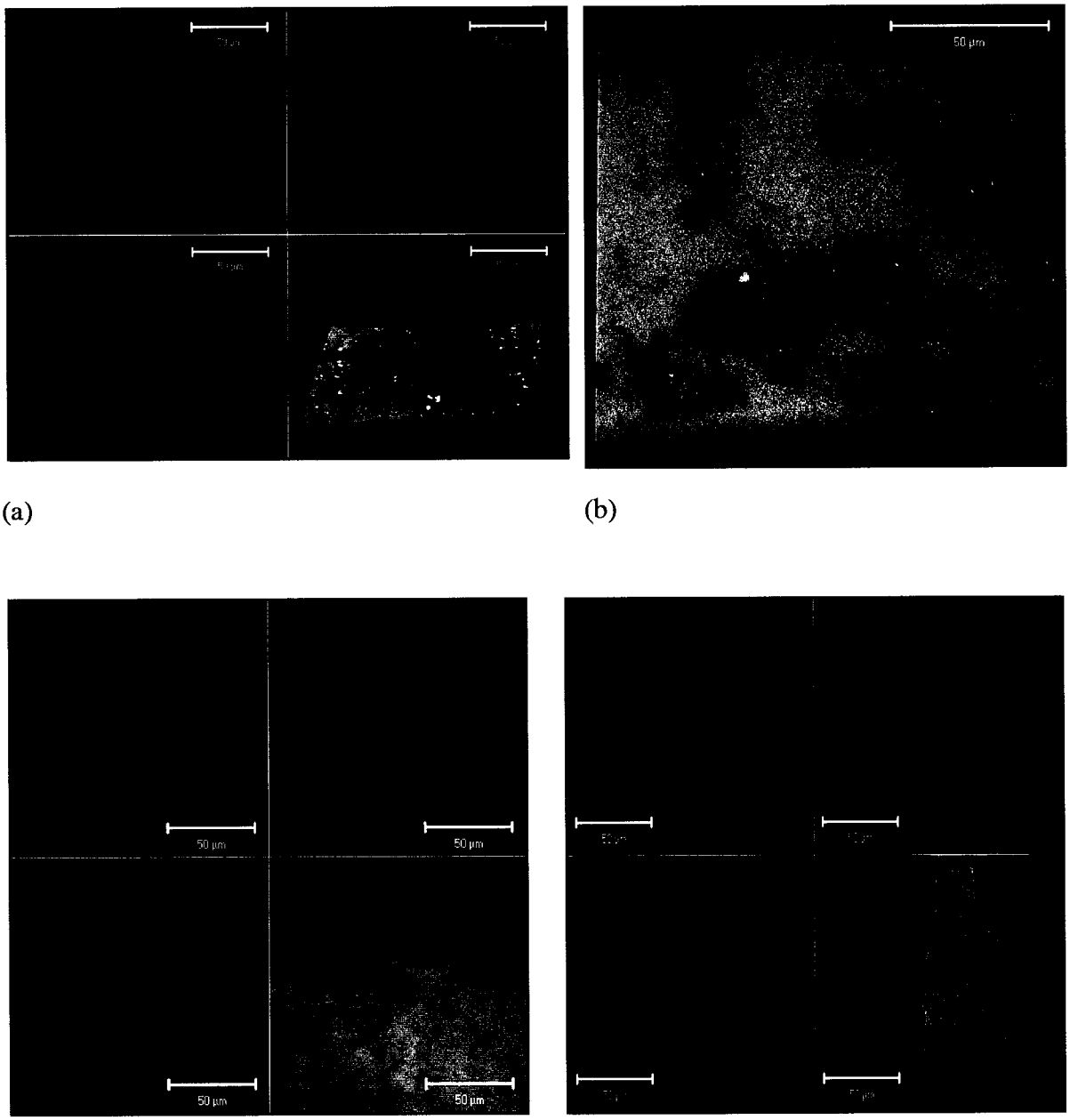

(a) (b)

(c) (d)

Figure 4.35. CLSM micrographs of longitudinal membrane fibres sampled at critical TMP in Run 2 (63X/0.9 objective, scale bars = 50 µm), (a) Module 1 split channel projection, depth = 110.0 µm (63X/0.9 W objective), (b) Module 3 projection, depth = 41.0 µm, (c) Module 2 single plane image, (d) Module 2, depth = 73.5 µm.

Unstained membrane fibres sampled from Run 2 at critical TMP and after the second recovery cleaning were imaged using CLSM (Figure 4.36) Observations from the analysis of the membrane fibres sampled at critical TMP showed a lack of microbial aggregation on the membrane surface (Figure 4.36a, b, c). Similarly, the fibrous material was not observed on the membrane fibres sampled after the second recovery cleaning (Figure 4.36d). These results are expected and verify that the fluorescence observed in the CLSM analysis was from the lectin-conjugate stains. However, even without staining, the chemical and biological foulant on the membrane was still apparent in that the autofluorescence of the membrane was masked by dark areas (Figure 4.36).

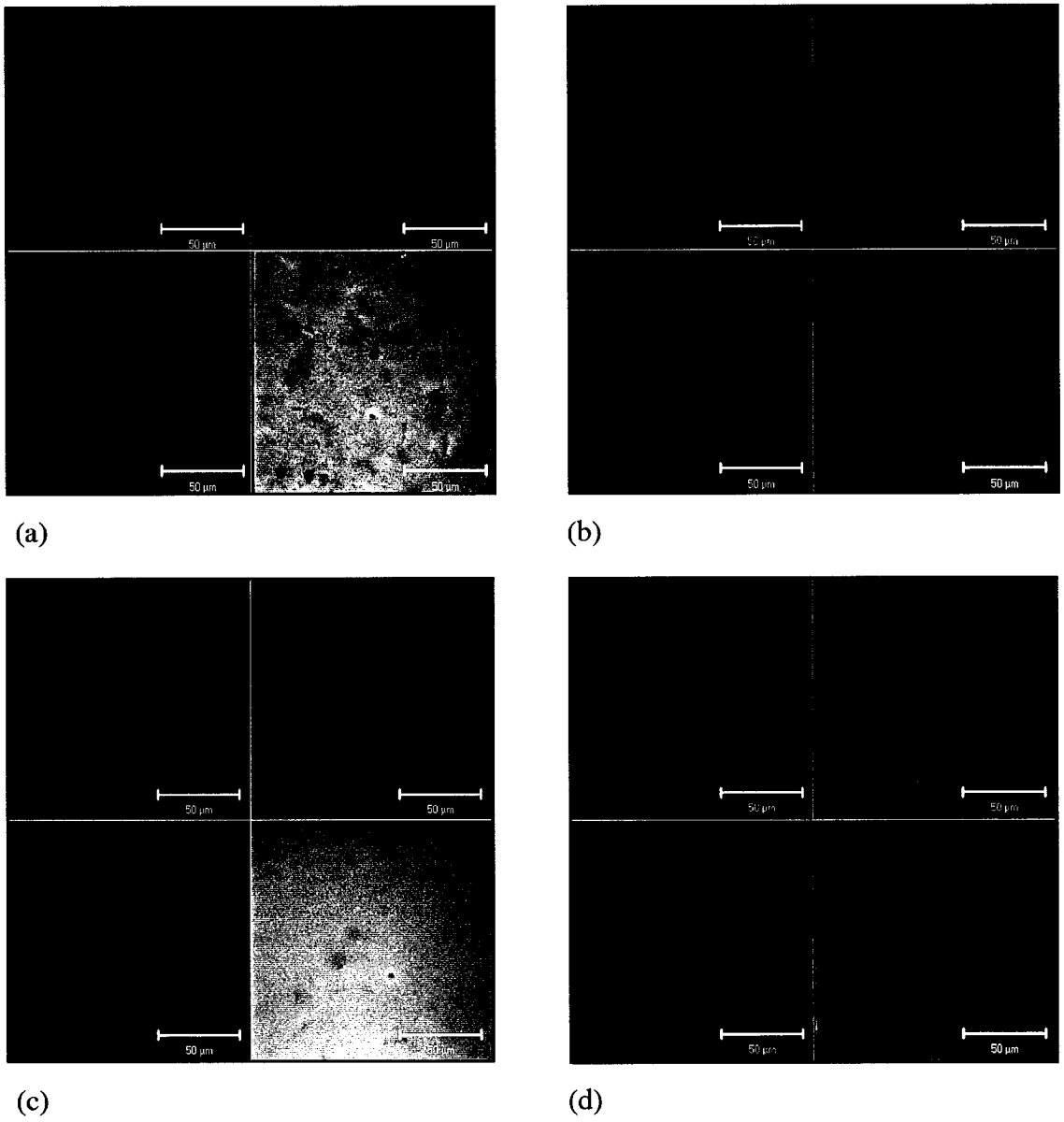

Figure 4.36. CLSM micrographs of longitudinal projections of unstained membrane fibres (63X/0.9 W objective, scale bars = 50 µm), (a) Module1 Run 2 at critical TMP, depth = 18.0 µm, (b) Module 2 Run 2 at critical TMP, depth = 17.9 µm, (c) Module 3 Run 2 at critical TMP, depth = 20.0 µm, (d) Module 3 after the second recovery cleaning, depth = 10.5 µm.

After a second recovery cleaning, membrane fibres were sampled again from all ZW-10 modules. The membrane fibres sampled from all ZW-10 modules showed a network of fibrous material that was adhered to and covered the surface of the membrane (Figure 4.37) This result was similar to the observations made of the membrane fibres sampled after the first recovery cleaning. Additionally, the recovery cleaning helped to ameliorate the biofoulant on the membranes of each module. The depth coded images in Figure 4.37 showed the thickness of the biofoulant on the membrane fibres sampled from Modules 1, 2, and 3 to be 11.5 μm, 10.8 μm and 9.0 μm respectively, which is a significant decrease from the thickness of the biofoulant attached to the membrane before recovery cleaning (Figure 4.35). The fibrous material showed specificity to ConA, WGA, and SBA (Figure 4.37). The network of fibrous material observed on the membrane fibres sampled from Modules 1 and 2 were similar (Figure 4.37a and b) whereas the network of fibrous material observed on the membrane fibres sampled from Module 3 did not appear to be as detailed, and showed less specificity for ConA in comparison (Figure 4.37c).

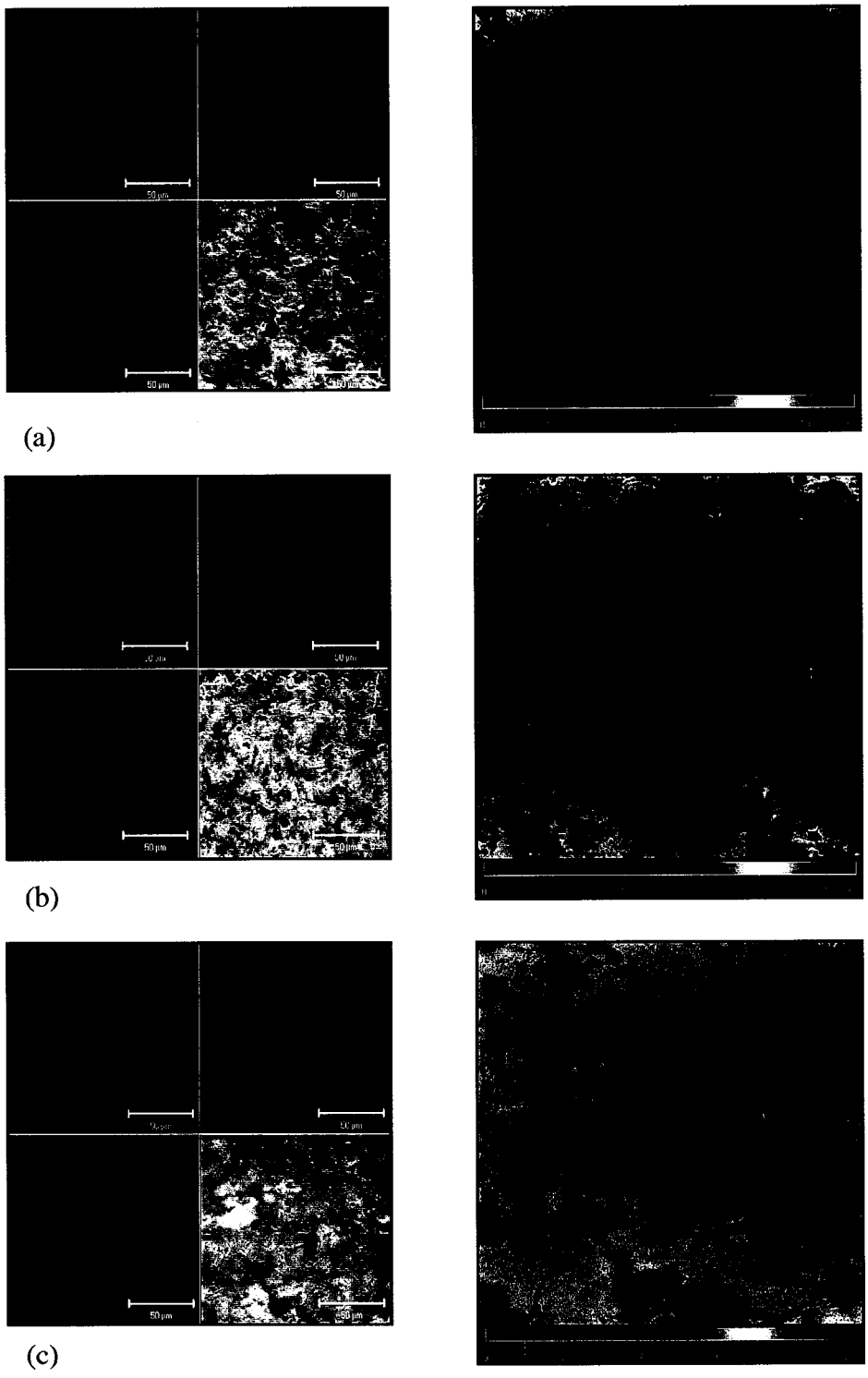

Figure 4.37. CLSM split channel micrographs of longitudinal projections (left) (63X/0.9 W objective, scale bars = 50 μm) and depth coding (right) of membrane fibres sampled after the second recovery cleaning, (a) Module1, depth = 11.5 μm, (b) Module 2, depth = 10.8 μm, (c) Module 3, depth = 9.0 μm.

In Run 3, the wastewater flux was decreased to 20 $L/m^2/hr$ from 35 $L/m^2/hr$ in Runs 1 and 2. The membrane fibres were sampled at 2 hours, 13 days, and at shutdown. As expected with a lower flux, after 2 hours of operation there was not a significant amount of biofoulant on the membrane fibres sampled from all modules (Figure 4.38). The membrane fibres sampled from Module 1 after 2 hours (Figure 4.38a) resembled the characteristics of the membrane fibres sampled from Module 2 after 2 hours in Run 2 (Figure 4.32b). In Figure 4.38c, observations of the membrane fibres sampled from Module 3 showed the most microbial aggregate redevelopment on the membrane which had a dominant specificity for WGA.

After 13 days of operation in Run 3, there was evidence of further microbial aggregate redevelopment on the membrane fibres sampled from Modules 1 and 3 (Figure 4.39a and c). The microbial aggregates attached to the membrane fibres sampled from Module 1 were highly specific for WGA (Figure 4.39a) whereas the microbial aggregates attached to the membrane fibres sampled from Module 3 were highly specific for ConA (Figure 4.39c). In addition, there were prominent small dark spots on the membrane fibres sampled from Modules 1 and 3 that could represent chemical fouling (Figure 4.39a and c). Observations of the membrane fibres sampled from Module 2 did not show microbial aggregation on the membrane, but rather a network of fibrous material that was highly specific for ConA in some areas and highly specific for SBA and WGA in other areas (Figure 4.39b).

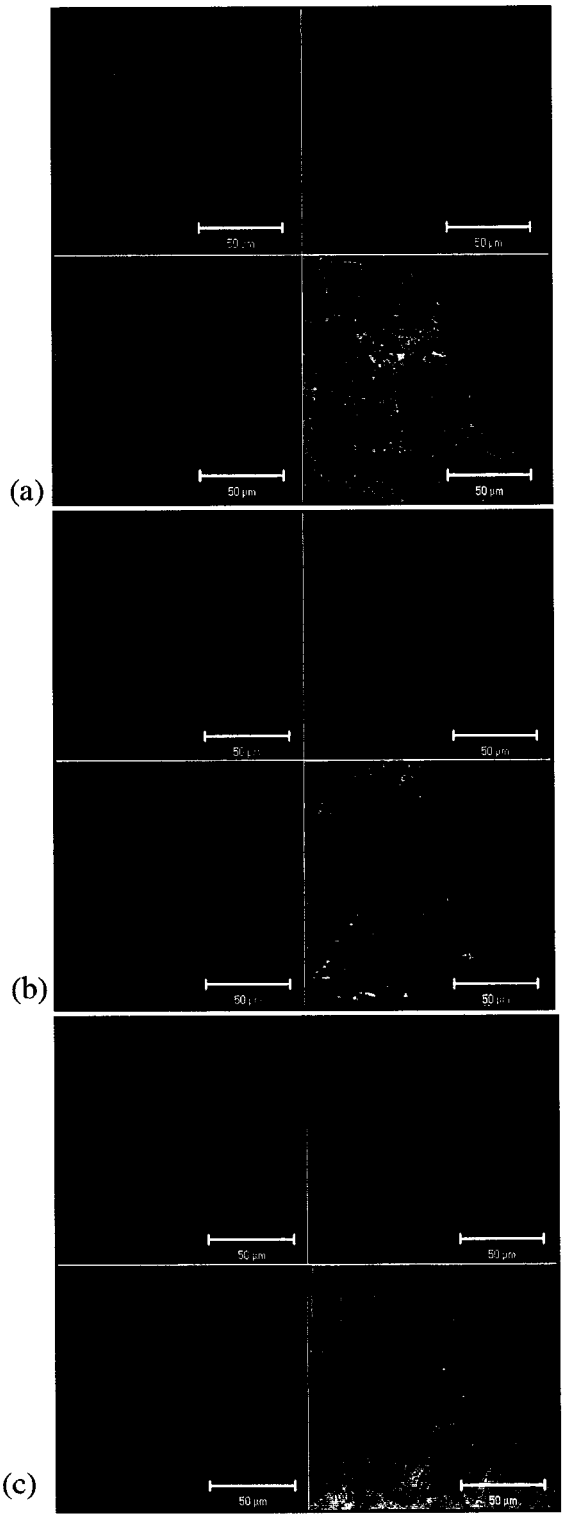

Figure 4.38. CLSM split channel micrographs of longitudinal projections of membrane fibres sampled after 2 hours of Run 3 (63X/0.9 W objective, scale bars = 50 μm), (a) Module1, depth = 13.2 μm, (b) Module 2, depth = 10.0 μm, (c) Module 3, depth = 22.4 μm.

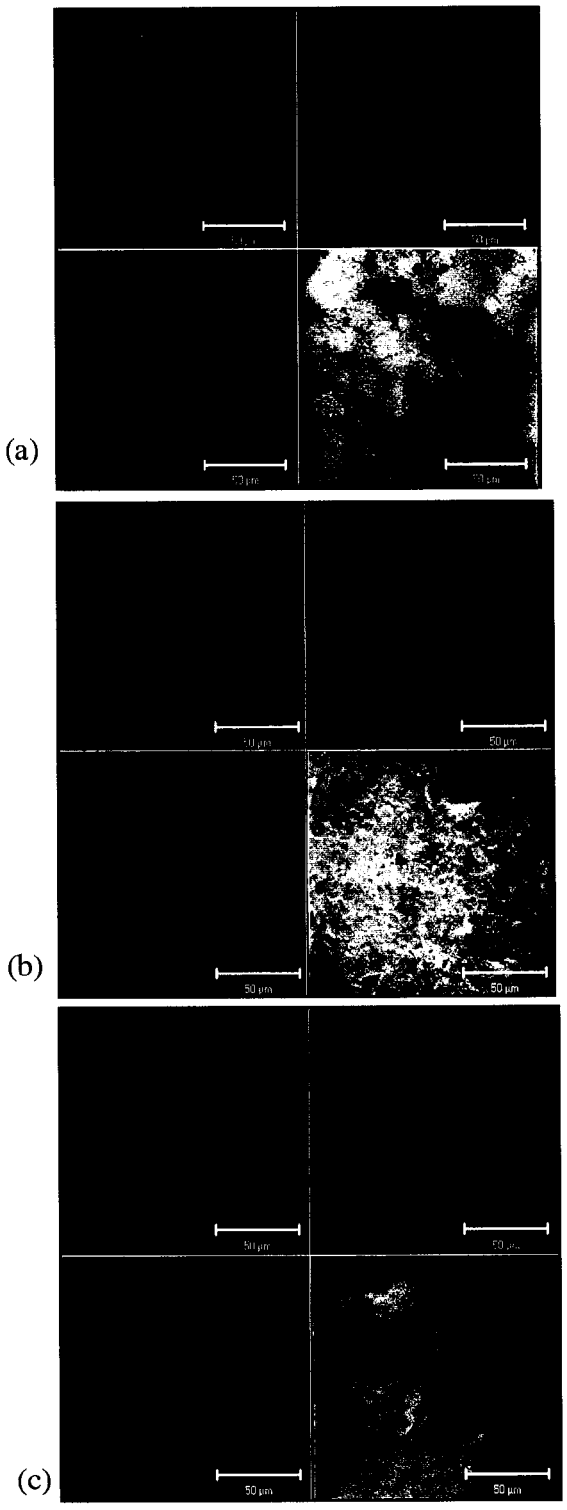

Figure 4.39. CLSM split channel micrographs of longitudinal projections of membrane fibres after 13 days of Run 3 (63X/0.9 W objective, scale bars = 50 μm), (a) Module1, depth = 28.0 μm, (b) Module 2, depth = 10.4 μm, (c) Module 3, depth = 20.8 μm.

At shutdown the membrane fibres were sampled at different stages of operation in Run 3. Modules 1, 2, and 3 had been in operation for 28, 34, and 32 days respectively. Furthermore, the Modules had not yet reached critical TMP, but were operating near –30 kPa. Nevertheless, the results showed that heterogeneous microbial aggregates were attached to the membrane fibres sampled from all ZW-10 modules (Figure 4.40). These microbial aggregates had a dominant specificity for WGA, some specificity for SBA, and little specificity for ConA (Figure 4.40). When compared to Modules 2 and 3, the microbial aggregates on the membrane fibres sampled from Module 1 appeared to be less developed as shown by the sparseness of lectin-specific areas (Figure 4.40).

After a final recovery cleaning was performed, membrane fibres were sampled from all ZW-10 modules. The results of the CLSM analysis continued to illustrate a confluent network of fibrous material that was adherent to and covered the surface of the membrane fibres sampled from Modules 1, 2, and 3 (Figures 4.41, 4.42, and 4.43). In Figures 4.41c and 4.43c, it appeared that the fibrous material was shielding microbial aggregates specific to SBA. This shielding effect is known to occur in biofilms existing in regions with high turbulence.

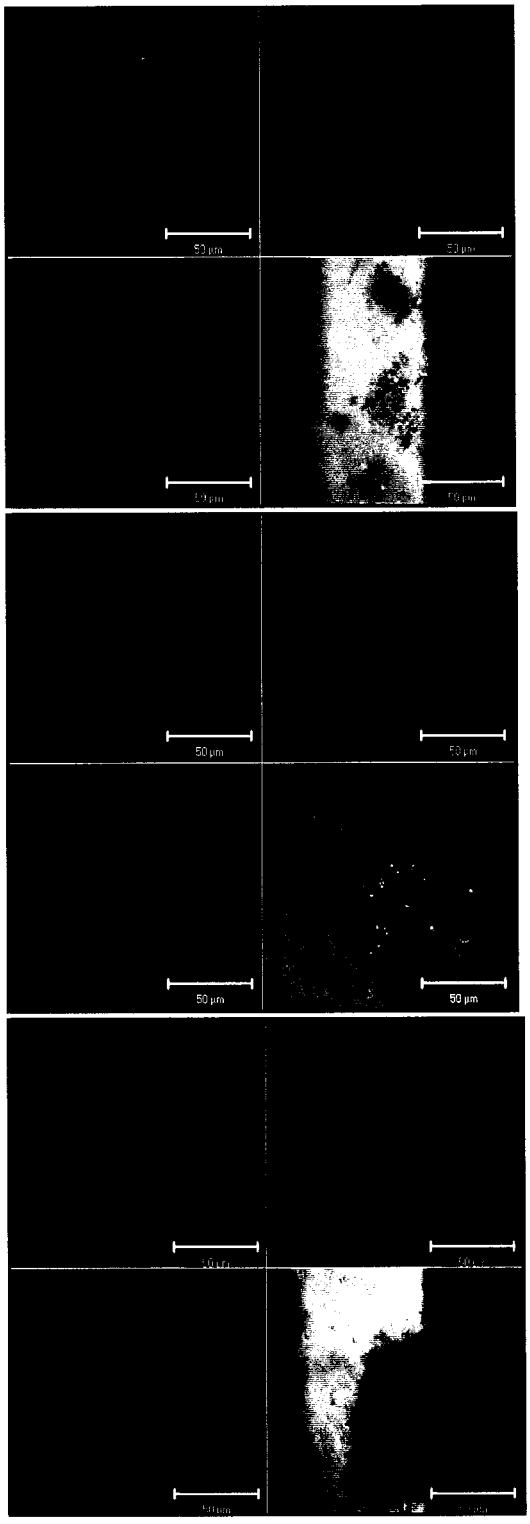

Figure 4.40. CLSM split channel micrographs of longitudinal projections of membrane fibres at shutdown of Run 3 (63X/0.9 W objective, scale bars = 50 μm), (a) Module1, depth = 30.0 μm, (b) Module 2, depth = 36.0 μm, (c) Module 3, depth = 39.6 μm.

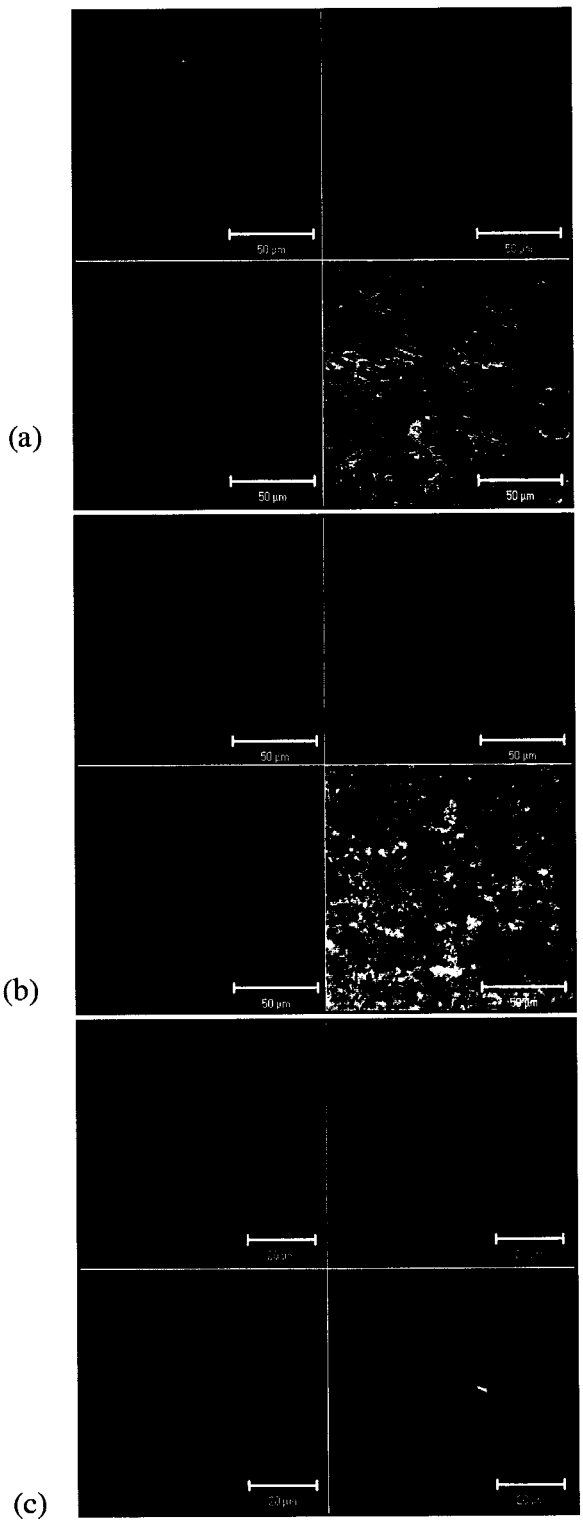

Figure 4.41. CLSM split channel micrographs of longitudinal projections of membrane fibres sampled from Module 1 after the final recovery cleaning (63X/0.9 W objective), (a) depth = 7.2 μm, scale bar = 50 μm, (b) depth = 7.2 μm, scale bar = 50 μm (c) image zoom = 2, depth = 9.6 μm, scale bar = 20 μm.

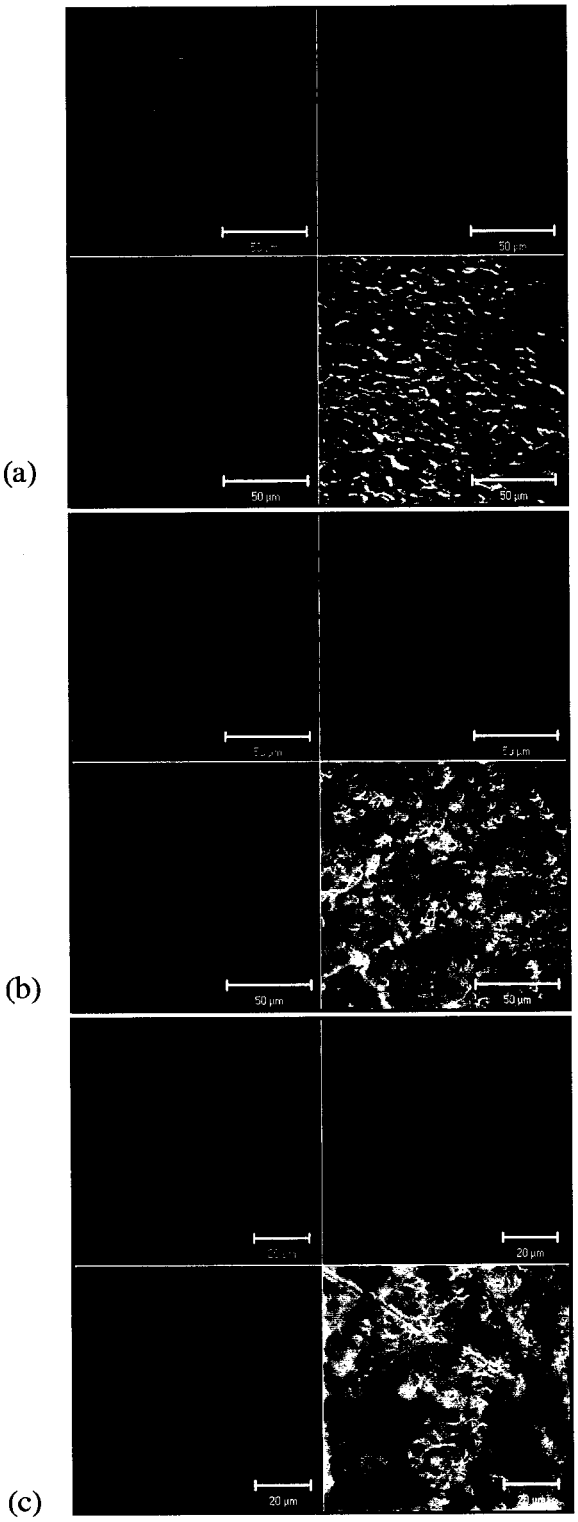

Figure 4.42. CLSM split channel micrographs of longitudinal projections of membrane fibres sampled from Module 2 after the final recovery cleaning (63X/0.9 W objective), (a) depth = 11.0 µm, scale bar = 50 µm, (b) depth = 6.8 µm, scale bar = 50 µm (c) image zoom = 1.7, depth = 8.8 µm, scale bar = 20 µm.

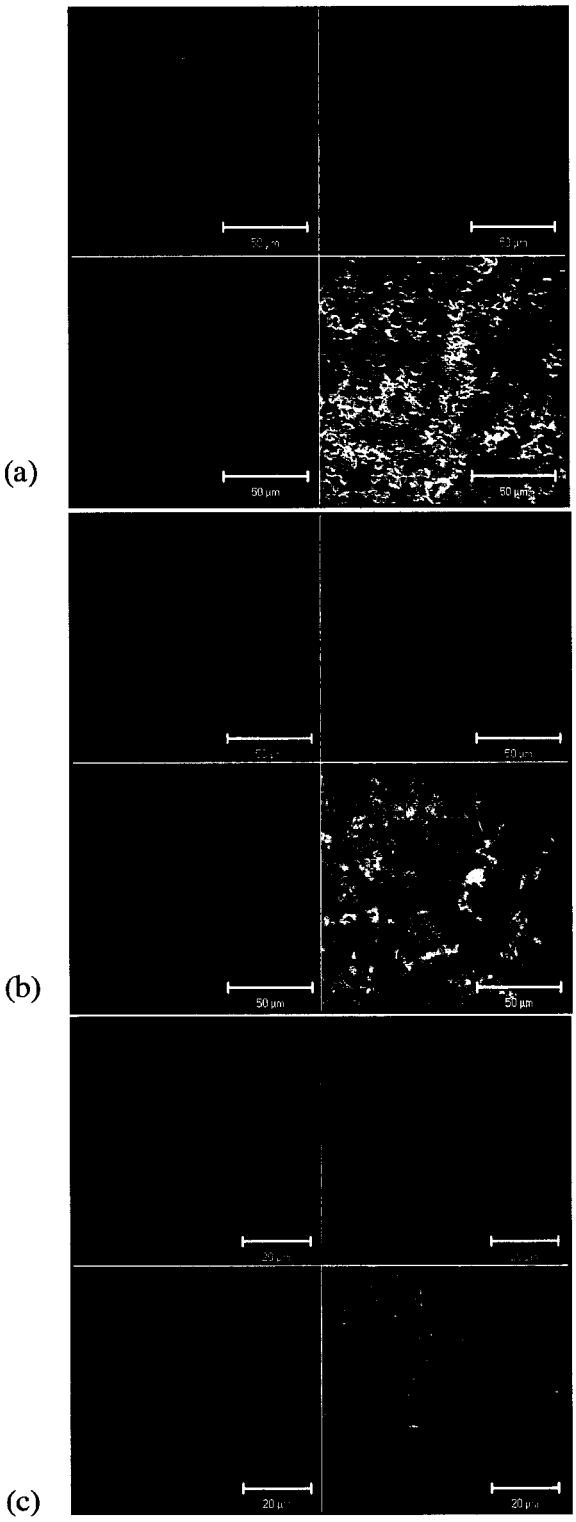

Figure 4.43. CLSM split channel micrographs of longitudinal projections of membrane fibres sampled from Module 3 after the final recovery cleaning (63X/0.9 W objective), (a) depth = 8.0 µm, scale bar = 50 µm, (b) depth = 10.5 µm, scale bar = 50 µm (c) image zoom = 2, depth = 9.8 µm, scale bar = 20 µm.

In an effort to gain further information about the biofoulant, a nucleic acid stain was employed. Membrane fibres taken from Run 2 at critical TMP were stained with SYTO 9, which is only available as part of the *Bac*Light™ Bacterial Gram Stain Kit from Molecular Probes Inc., Eugene, OR. As shown in Figure 4.44 the results of the CLSM analysis of all the membrane fibres sampled at critical TMP in Run 2 did not provide any new information about the biofoulant. All the membrane fibres sampled from all modules showed evidence of the fibrous material covering the surface of the membrane. This result was expected since DNA was measured as a portion of the total EPS content in the mixed liquor. When comparing the nucleic acid content in the fibrous material between ZW-10 modules, the membrane fibres sampled from Module 1 had the largest quantity followed by Modules 2 and 3. Furthermore, only one aggregate was observed (Figure 4.44d) from the membrane fibres sampled in all modules. This microbial aggregate was observed on the membrane fibre sampled from Module 3 and was different from the microbial aggregates observed using the lectin-conjugate stains in that the whole aggregate appeared to be much more concentrated and closely-packed suggesting fluorescence of cellular material.

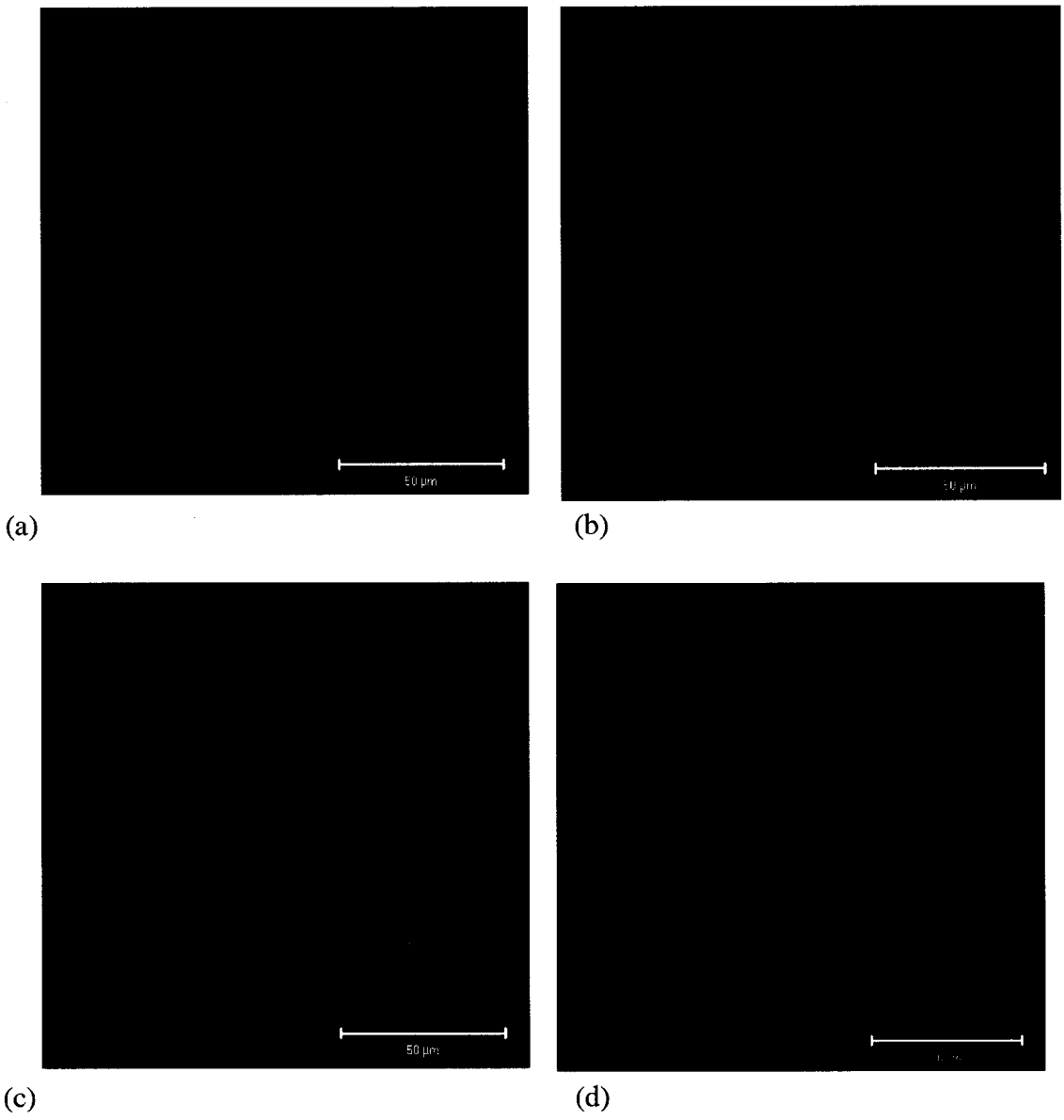

Figure 4.44. CLSM micrographs of longitudinal projections of membrane fibres stained with a nucleic acid stain SYTO 9 (63X/0.9 W objective, scale bars = 50 µm), (a) Module1, depth = 10.0 µm, (b) Module 2, depth = 12.5 µm, (c) Module 3, depth = 7.8 µm, (d) Module 3, depth = 68.0 µm.

5.0 DISCUSSION

The purpose of this study was to characterize the extent to which microbial aggregates and their extracellular components contribute to biofouling of submerged polymeric microfiltration membranes. The objectives of this study were threefold, 1) to study the influence physicochemical properties of microbial flocs have on biofouling; 2) to assess the influence operational cleaning methods in MBRs have on biofouling; and 3) to investigate the effect recovery cleaning of membrane modules has on biofouling amelioration. The first objective was accomplished by running two ZeeWeed™ (ZW) 10 MBRs at a sludge retention time (SRT) of 12 days and 30 days using relaxation as an operational cleaning method. The second objective was accomplished by running two ZW-10 modules in a MBR operating at an SRT of 12 days and using backwash and relaxation as operational cleaning methods. The third objective was accomplished by cleaning all the ZW-10 modules in a 2000 ppm hypochlorite solution overnight when the system reached critical transmembrane pressure (TMP) near – 60 kPa. Prior to investigating the objectives, a preliminary study was carried out to establish a reproducible method for analyzing microfiltration membrane fibres by confocal laser scanning microscopy (CLSM).

5.1 Preliminary Study

In the preliminary study, constructed membrane loops were attached to the manifold as illustrated in Figure 3.3. The manifold was installed into an existing pilot-scale MBR and was operated over a two month period under permeation/relaxation conditions. The results of this study provided important information about the characteristics of the polymeric microfiltration membranes. The observations from the CLSM analysis showed that the microfiltration membrane fibres were autofluorescent. This information is advantageous because the membrane's surface could be used as a reference point for detecting the deposition of foulants on the membrane. Biofouling was detected by analyzing the operational parameters and microscopic images. The decrease in percent permeability of each membrane loop increased over time (Figure 4.2) indicating that the resistance of the membrane increased due to sludge cake formation at the surface of the membrane. Staining the membrane fibres with three lectin-conjugates and analyzing them by CLSM revealed the presence of the sludge cake. The results showed that the sludge cake was composed of microbial aggregates and extracellular

polymers that were highly specific for α-mannopyranosyl, α-glucopyranosyl, and *N*-acetylglucosaminyl residues.

Over time, the biofoulant was observed at the surface of the membrane as a fibrous matrix of material known to be composed of extracellular polymeric substances (EPS). The fact that EPS is present is not surprising due to the fact that microbes are known to synthesize EPS through metabolism and cell lysis (Wimpenny, 2000), but there appears to be a large quantity of EPS. In an effort to prevent membrane biofouling, aeration is one of the mechanisms applied to promote shear stress and turbulence at the membrane surface. Consequently, the microorganisms that have adhered to the membrane surface are put in a state of stress. As a result the microbes protect themselves by producing a larger quantity of EPS as a defence mechanism (Baker and Dudley, 1998).

CLSM was employed using a single lectin-conjugate as well as double lectin-conjugates which was shown to work effectively in all cases. Therefore, a method was developed for staining microfiltration membrane fibre samples with multiple lectin-conjugates and was employed throughout this research to provide consistency in the results (see Appendix A for a detailed protocol). Subsequent to staining the sampled membrane fibres, there was a need to stabilize and maintain moisture in the membrane fibres during CLSM analysis. Previous studies have shown successful results when imaging microbial cells and EPS stabilized in Nanoplast, a hydrophilic resin (Decho and Kawaguchi, 1999), and low melting point agarose, which has properties similar to water (Droppo *et al.*, 1996b). In this study, both methods were attempted. The stained membrane fibre samples were embedded in Nanoplast resin and cross-sections were taken using a microtome. The microscopic analysis revealed that this stabilization technique failed in this study because the moisture content was unable to be maintained and the structural integrity of the membrane fibre was severely damaged when cross-sections were taken. Conversely, stabilizing the stained membrane fibre sections in low melting point agarose was shown to be successful at maintaining the membrane's moisture content as well as its structural integrity. Using this stabilization technique also allowed for long periods of microscopic observation.

Also in the preliminary study, the physicochemical properties of the microbial flocs in the pilot-scale membrane bioreactor (MBR) were studied. This was necessary because the sludge in MBRs differ from the sludge in conventional activated sludge processes in that MBRs use higher concentrations of mixed liquor suspended solids (MLSS). The first attempt to use conventional protocols (Section 3.5 and 3.6) to characterize the flocs failed for this reason. Therefore, the procedure was altered in that the sludge was centrifuged at low speed (1000 *g*) for 5 minutes to help settle the suspended solids. Subsequently, the sludge was diluted to approximately 1/5 of its original MLSS concentration. By modifying the conventional procedure, successful results were attained when characterizing the surface charge, hydrophobicity, and EPS composition of microbial flocs.

5.2 Core Study

The MBRs in the core study were operated for 64 days from February 11, 2002 to April 16, 2002 without any severe problems. The temperature in both MBRs was maintained at 10°C $\pm$ 1.9 (Figure 4.7). This temperature range is typical in winter and early spring conditions. The pH was stable ranging from 7.0 to 7.5 (Figure 4.8). The mixed liquor suspended solids (MLSS) showed minimal fluctuations and averaged 18.1 $\pm$ 3.42 g/L and 18.9 $\pm$ 3.01 g/L in Reactors 1 and 2 respectively (Figure 4.9). Similarly, the dissolved oxygen concentrations averaged 3.7 $\pm$ 1.3 mg/L and 4.1 $\pm$ 1.6 mg/L in Reactors 1 and 2 respectively (Figure 4.10). There was some fluctuation in the dissolved oxygen concentration, which may have occurred due to operational factors. Also, a fluctuation in dissolved oxygen may have occurred because not only does the substrate exert a demand for oxygen, but a higher MLSS concentration will also increase demand (Stephenson *et al.*, 2001). The influent soluble chemical oxygen demand (FCOD) was typically measured between 60 mg/L and 70 mg/L. The effluent COD in Module 1, 2, and 3 averaged 12.5 $\pm$ 6.3 mg/L, 14.0 $\pm$ 9.3 mg/L, and 14.0 $\pm$ 7.7 mg/L respectively (Figure 4.11). The percent FCOD removal for Modules 1, 2, and 3 ranged between 54.2 and 86.6%, 62.5 and 93.2%, and 69.0 and 92.5% respectively (Figure 4.12). At specific sampling periods there was a difference measured in the percent FCOD removal in Reactor 2 from Modules 2 and 3 (Figure 4.12). This may be related to the operational cleaning methods employed. Module 2 operated under filtration/relaxation conditions and Module 3 operated under filtration/backwash conditions. Therefore, it is possible that there would be more

accumulation of biological material on the membranes in Module 2 than in Module 3, which may result in a higher FCOD removal at the surface of the membranes in Module 2. The low percent FCOD removal could be due to operational variability in the MBR system, a change in sludge characteristics, or errors in measurements. Nonetheless, when considering the fact that effluent COD concentrations are a function of the FCOD concentrations, the COD removal in this study was considered good.

For each ZW-10 module, the TMP was monitored before and after each operational cleaning method (Figure 4.13). As expected, the TMP increased over time until critical TMP was reached at which point the ZW-10 module was said to be fouled and recovery cleaning took place. Recovery cleaning is a mechanism to ameliorate membrane fouling and is designed to restore a membrane's filtration efficiency to its original state; however, as shown in previous studies and in this study, recovery cleaning is not always effective (McDonogh, *et al.*, 1994). After the first recovery cleaning, the wastewater permeability was not recovered to its original state in all ZW-10 modules, but after the second recovery cleaning, the TMP was recovered in all ZW-10 modules (Figure 4.13). This can be attributed to a decrease in flux from 35 $L/m^2/hr$ to 20 $L/m^2/hr$, which substantiates the theory of critical flux.

Membrane biofouling can be associated with both the operational cleaning methods and the physical properties of the sludge. The results showed that Module 2 (SRT 12 permeate/relaxation) fouled first in both Runs 1 and 2, followed by Module 3 (SRT 12 permeate/backwash), which fouled second in Run 2, and finally by Module 1 (SRT 30 permeate/relaxation), which fouled last in Run 2. When the operational cleaning methods are compared, it can be concluded that backwashing is more effective than relaxation at an SRT of 12 days. When the MBR operating at a 12 day SRT is compared to the MBR operating at a 30 day SRT, the lower sludge age could result in a higher fouling rate regardless of which operational cleaning method is used. This result is supported by previous studies (Chang and Lee, 1998; Fan *et al.*, 2000). Furthermore, the rate of membrane fouling can be correlated to the hydrophobicity of microbial flocs. The polymeric microfiltration membranes used in this study have a hydrophilic surface. The hydrophobicity, though not significantly different in this study, began to show an increasing trend at higher SRTs. This trend has been shown in

previous studies (Liao *et al.*, 2001). Therefore, the flocs at the 12 day SRT would be more likely to become associated with the hydrophilic membrane surface before the flocs at the 30 day SRT thereby causing membrane fouling first. These results are supported by observations made when analyzing the membrane fibres by CLSM. After the first two hours of operation, microbial aggregates at the 12 day SRT began to adhere to the membrane surface, whereas no microbial aggregates at the 30 day SRT were observed at the membrane surface during that time (Figure 4.25).

Membrane permeability is a measure of filtration efficiency and can be used to estimate membrane fouling (Bouhabila *et al.*, 2001). Permeability is calculated during filtration of clean water or during filtration of wastewater. As expected, Figures 4.14 and 4.15 illustrate that after each recovery cleaning the permeability of each membrane module improved. As shown in Figure 4.14, the permeability of the membrane increased above its original value after 3 days of filtration. This may be attributed to operational cleaning methods, sampling periods, and recovery cleanings. Nonetheless, during each run there is a trend of decreasing permeability over time.

Perhaps a more common method to characterize membrane fouling quantitatively is by employing Darcy's Law:

$$J = \Delta P / \eta \cdot (R_m + R_c) \qquad \textbf{[5-1]}$$

where J is the clean water flux (m^3/m^2 s), ΔP is the TMP (Pa), η is the dynamic viscosity of the permeate (Pa s), R_m is the initial membrane resistance of the virgin membrane or recovery cleaned membrane (m^{-1}), R_c is the cake resistance formed by fouling phenomena (m^{-1}) (Bouhabila *et al.*, 2001). The dynamic viscosity was calculated as a function of temperature using the following equation (Roorda and van der Graaf, 2000):

$$\eta = 0.497/(T + 42.5)^{1.5} \qquad \textbf{[5-2]}$$

where T is the temperature of the water being filtered (°C). Many researchers have used Darcy's Law to calculate the total membrane resistance and have found that the cake resistance (R_c) is a major factor causing membrane fouling (Chang and Lee 1998 and 1999; Wisniewski and Grasmick, 1998; Bouhabila *et al.*, 2001; Parameshwaran *et al.*, 2001; Roorda and van der Graaf, 2000). In this study, the membrane resistance (R_m) and cake resistance (R_c) were calculated by adopting the same approach as Roorda and van der Graaf (2000) in which clean water flux data were used to accurately compare resistances found after various cleaning methods as shown in Table 5.1.

Table 5.1. Microfiltration Membrane Resistances

ZW-10 Module[a]	Run No.[b]	Wastewater Flux (L/m^2/hr)	R_m (10^{12} x m^{-1})[c]	R_c (10^{12} x m^{-1})[d]	R_t (10^{12} x m^{-1})[e]
1	1	35	1.21	0.343	1.56
1	2	35		1.57	2.79
1	3	20		-0.0553	1.16
2	1	35	0.790	1.16	1.95
2	2	35		1.85	2.64
2	3	20		0.670	1.46
3	1	35	0.733	1.48	2.21
3	2	35		1.49	2.22
3	3	20		0.859	1.59

[a] Modules 1, 2, and 3 represent SRT 30 Permeate/Relax, SRT 12 Permeate/Relax, SRT 12 Permeate/Backwash respectively.
[b] Each Run was terminated when critical TMP was reached with the exception of Run 3 which was terminated near –30 kPa.
[c] R_m was calculated for each virgin Module (Run 1).
[d] R_c was calculated for each Module when critical TMP (-60 kPa) was reached (Runs 1 and 2) and at shutdown (Run 3).
[e] R_t is the sum of R_m and R_c

When comparing the cake resistance (R_c) in Table 5.1 to the clean water membrane permeability at critical TMP and at shutdown (Figure 4.14), an inverse relationship exists. An increase in membrane resistance corresponds to a decrease in permeability. Additionally, it can be concluded that the wastewater flux is inversely proportional to the cake resistance (R_c). A reduction in flux from 35 L/m^2/hr in Runs 1 and 2 to 20 L/m^2/hr in Run 3 resulted in a lower cake resistance of each ZW-10 module. In fact, the cake resistance (R_c)cannot be accounted for in Module 1 in Run 3 as shown by a negative value (Table 5.1).

In this study, the microbial aggregates and associated extracellular polymers were characterized by physicochemical methods and microscopic methods. The results of the physicochemical analysis showed no significant difference between the total and individual EPS constituents at an SRT of 12 days and 30 days (Figure 4.22 and 4.23) (t-test, $p > 0.05$). However, this may be due to the fact that an acclimation period was not sufficient to observe a significant difference in the EPS composition between reactors. In practice, to achieve steady-state operating conditions, a bioreactor is typically operated for three times the length of the SRT. Nevertheless, the results from the physicochemical analysis are supported by CLSM. In all membrane fibres sampled from all ZW-10 modules, the biofoulant that formed on the surface of the membrane can be characterized as a patchy heterogeneous colonization of microbes and extracellular polymers. This was accomplished with the use of three lectins, namely concanavalin A (ConA), wheat germ agglutinin (WGA), and soybean agglutinin (SBA).

Previous studies have successfully utilized various lectin-conjugates to study extracellular polymers produced by bacterial cells (Del Gallo, 1989; Michael and Smith, 1995; Lawrence *et al.*, 1998; Wolfaardt *et al.*, 1998; Johnsen *et al.*, 2000). Of these lectins, ConA, WGA, and SBA were chosen in this study because of their specificity to common sugars. Glucose, mannose, and galactose are ubiquitous sugars in the environment and are prominently found as major constituents of bacterial extracellular polymers in sludge biomass (Dignac *et al.*, 1998). The polysaccharides produced by bacteria are associated with a bacterial cell in three manners: 1) as intracellular polysaccharides, 2) as capsular or bound polysaccharides (CPS), and 3) as extracellular or soluble polysaccharides (EPS) (Figueroa and Silverstein, 1989; Del Gallo *et al.*, 1989). It is assumed that lectins will have a higher binding affinity to the polysaccharides in the CPS and EPS. Therefore, the observations of fluorescence in the images obtained by CLSM can be inferred to be lectin-conjugates bound to the CPS and EPS. In this study, the CLSM analysis of the membrane fibres showed lectin binding to both the CPS and EPS. During filtration, although the CPS and EPS are both present, it appeared that the lectins were prominently bound to the CPS; however, when the bacterial cells were cleaned from the membrane during recovery cleanings, the lectins were bound to a fibrous network of material. This is inferred to be EPS.

Since the CPS is closely associated with the cell wall, it may be interpreted that the bacteria in the biofoulant were imaged. This may be significant because the CLSM analysis has shown that the biofoulant on all membrane fibres sampled is composed largely of *N*-acetylglucosaminyl residues (specific for WGA). This is an indication that the lectins may be binding to the bacterial cell wall of Gram positive and Gram negative bacteria. *N*-acetylglucosamine is one of the repeating amino sugars that forms the backbone in the bacterial cell wall. Furthermore, the lipopolysaccharide (LPS) which forms the outer membrane of the Gram negative cell wall also contains *N*-acetylglucosamine. Moreover, the LPS also contains glucose, mannose, and galactose (specific for ConA and SBA). This may indicate that in addition to binding to the CPS and EPS, the lectins are probably binding to areas that are not specific to extracellular polymers. Johnsen *et al.* (2000) studied the localization of EPS in *Sphingomonas* biofilms and suggested a similar conclusion.

After the ZW-10 modules were recovery cleaned there was an unequivocal biofoulant that uniformly covered the surface of the polymeric microfiltration membrane fibres. The biofoulant is composed of a network of fibrous material containing few bacterial cells but which shows equal specificity for all lectins employed. This fibrous material continues to be evident when filtration of wastewater is resumed and appears to become more concentrated after each successive recovery cleaning. This network of fibrous material is EPS that continues to adhere to the membrane after the removal of bacterial cells. This adhesive material serves as a beneficial site for redevelopment and colonization of microbial aggregates after filtration of wastewater is resumed. This finding is also supported by the hydrodynamics of the MBR system in that the wastewater permeability of each ZW-10 module could not be recovered to its original state after the first recovery cleaning. Additionally, all the ZW-10 modules fouled at a faster rate after filtration of wastewater was resumed in Run 2. Furthermore, when the membrane fibre samples were stained using a nucleic acid stain, SYTO 9, the fibrous material on the membrane was evident, but was not as intensely fluorescent (Figure 4.44). This result is expected since EPS contains DNA as shown in the chemical analysis of individual EPS constituents in this study (Figure 4.22 and 4.23). Also in support of this finding is that the network of fibrous material was absent when imaging unstained membrane fibre samples (Figure 4.36). Since the polymeric microfiltration membranes used in

this study are known to be autofluorescent, this indicates that the fibrous material is not part of the membrane itself.

5.3 Proposed Model of Biofoulant Accumulation on Membranes in Submerged MBRs

In a MBR system a biofoulant develops on the microfiltration membrane in a similar manner that a conventional biofilm develops on any moist surface in that, once a bacterial cell is in the vicinity of the surface, interactions can occur by diffusion, convective transport, or active movement of the cell (Newby *et al.*, 2000). However, the manner in which a cell is able to come into the vicinity of the surface differs in a MBR system. Because the primary purpose of an MBR system is to filter the wastewater, individual bacterial cells, microbial flocs, cell debris, and other materials in the reactor are directed toward the membrane rather than coming in contact with it by random interactions as in the formation of conventional biofilms. Therefore, in contrast to biofilm development, whole flocs may attach to the membrane surface in addition to individual cells that colonize at the surface (Figure 5.1a). In agreement with previous studies, biofouling of membranes is both reversible and irreversible. In this study, the reversible biological layer is largely composed of individual cells, aggregates of cells (i.e. flocs) and their associated extracellular material; however, the formation of this layer is not completely prevented by shear forces and operational cleaning methods (Figure 5.1b). Instead the reversible layer accumulates on the membrane creating an additional barrier until the membrane becomes fouled. The biofoulant that forms on the surface of the membrane and within the membrane's pores is directly related to the hydrodynamics of the system. Therefore, a MBR system operating at higher fluxes (i.e. above the critical flux) will result in an increased rate of the onset of biofouling. It is only after recovery cleaning that the majority of microbial aggregates are cleaned from the membrane (Figure 5.1c). Microbial cells remaining on the membrane after recovery cleaning may be present because the EPS serves as a protective layer against the recovery cleaning agent. In this study, the irreversible layer is the fibrous network of material, inferred to be EPS produced by microbes, that continues to adhere to the membrane after recovery cleaning (Figure 5.1c). This is the first reported evidence that EPS is a major constituent of the biofoulant deposited on microfiltration membranes following recovery cleaning.

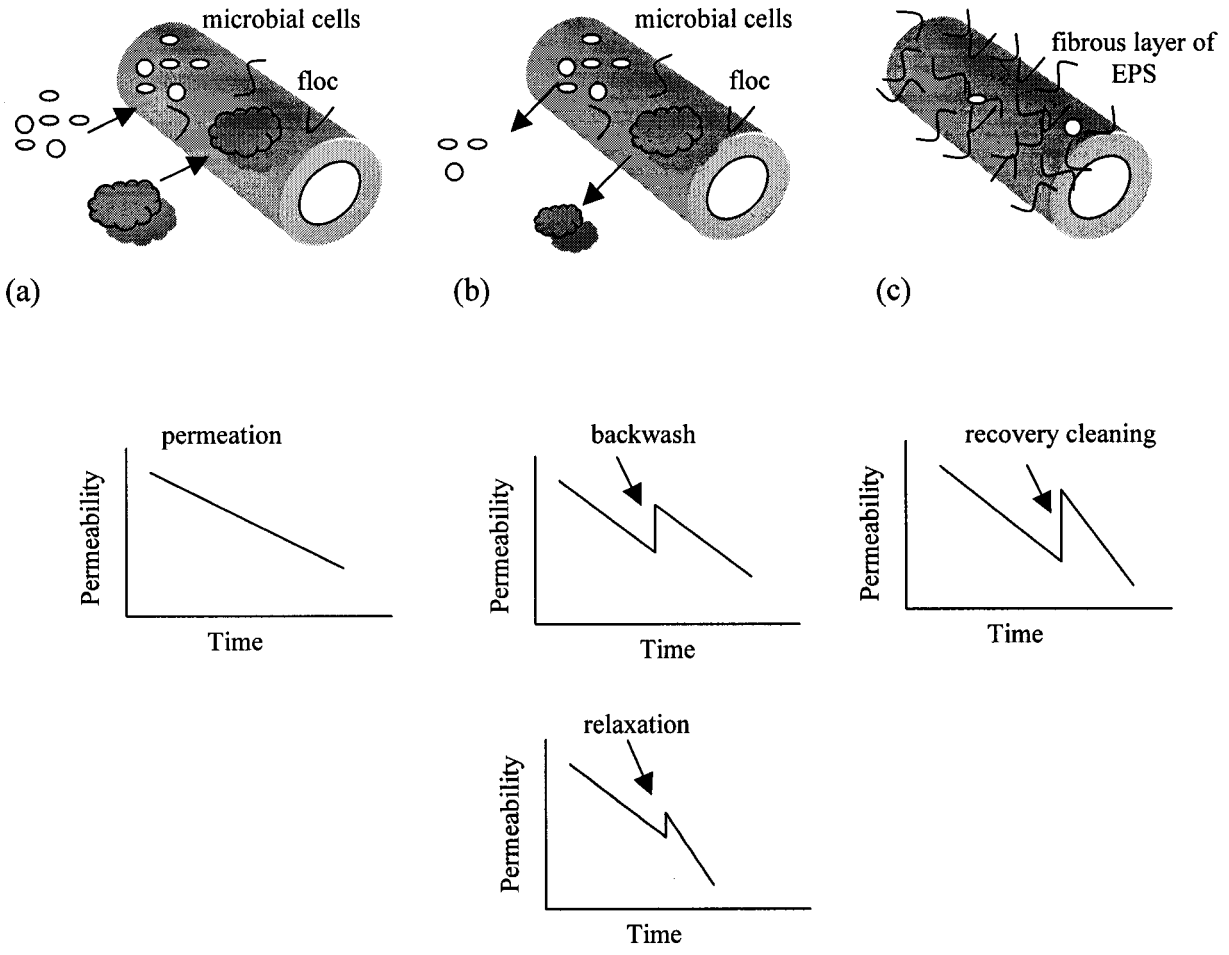

Figure 5.1. Proposed model of biofoulant accumulation on the membrane in a submerged MBR after (a) attachment of flocs and microbial cells during permeation, (b) partial removal of flocs and microbial cells during operational cleaning, and (c) irreversible fibrous layer of EPS after recovery cleaning. The graphs are a representation of (a) the decline in permeability during permeation, (b) the decline in permeability during backwash or relaxation, and (c) the decline in permeability before and after recovery cleaning.

6.0 CONCLUSIONS AND RECOMMENDATIONS

In an effort to better understand biofouling of polymeric microfiltration membranes, a comparative study of two pilot-scale ZeeWeed™ MBRs operating at two sludge retention times (SRT) (12 and 30 days) using two different operational cleaning methods (backwash and relaxation) and recovery cleanings has been conducted. Conclusions drawn from this study are as follows:

1. The CLSM analysis of the membrane fibres sampled showed that the biofoulant accumulation on the membrane during filtration of municipal wastewater can be characterized as a patchy heterogeneous colonization of microbes and extracellular polymers that are known to contain glucose, mannose, *N*-acetylglucosamine, and galactose.
2. The CLSM analysis of the membrane fibres sampled showed that *N*-acetylglucosamine was the dominant carbohydrate present in the biofoulant during filtration of municipal wastewater. Since *N*-acetylglucosamine is part of both the cell wall of Gram negative and Gram positive bacteria and the extracellular matrix, the lectins are probably binding to areas that are not specific to extracellular polymers.
3. Biofouling is both reversible and irreversible. In this study, the reversible layer is largely composed of individual cells, aggregates of cells (i.e. flocs) and their associated extracellular material. The irreversible layer is the EPS produced by microbes through metabolism and cell lysis that remains adhered to the membrane after recovery cleaning.
4. After recovery cleaning there is an unequivocal fibrous layer of biofoulant that uniformly covers the surface of the polymeric microfiltration membranes. The biofoulant is EPS and is composed of α-mannopyranosyl and α-glucopyranosyl residues, *N*-acetylglucosaminyl residues, and α and β-*N*-acetylgalactosaminyl and galactopyranosyl residues,
5. At lower SRTs membrane biofouling may be reduced by permeate backwashing rather than relaxation.
6. The rate of biofoulant accumulation on hydrophilic membranes may be reduced at higher SRTs because the biomass at higher SRTs has a higher hydrophobicity when compared to the biomass at lower SRTs.
7. Membrane permeability is inversely correlated with membrane resistance and both are dependent on flux. Recovery cleaning of ZW-10 modules using a hypochlorite solution

was effective at re-establishing membrane permeability, but did not return the membrane to its original state.

Recommendations for Biofouling Management and Future Research

Because biofoulant accumulation on membrane surfaces will likely never be completely prevented, biofouling of microfiltration membrane systems will need to be managed. In order to manage biofouling, it is important that each MBR system is tailored to meet the needs of the wastewater being treated because some methods to alleviate membrane fouling may be more effective than others. When using hydrophilic membranes in submerged MBRs treating municipal wastewater, biofouling may be reduced by operating the MBRs at longer sludge retention times. Furthermore, regardless of SRT, permeate backwashing may be a more effective operational cleaning method than relaxation for preventing the accumulation of biofoulant on the membrane. Continued research on operational cleaning methods would be beneficial to understanding both chemical and biological fouling of membranes. The use of a hypochlorite solution to recovery clean membranes is sufficient to reduce the thickness of the biofoulant; however, it is apparent that EPS is resistant to this cleaning agent. Additional research is needed to investigate methods to ameliorate the adherence of EPS to the membrane. In addition to operational and recovery cleaning methods, many other methods have been proposed to prevent and alleviate biofouling and are summarized by Wakeman and Williams (2002). Some notable methods include feed pretreatment, choice of membrane material, manipulation of flow through the membrane, gas sparging, electric fields, ultrasonic fields, or a combination of these.

While there may be numerous methods engineered to ameliorate biofouling, more research is required to understand the biology of membrane fouling. By understanding the biological properties of the foulant, it may be possible to make use of the biofoulant rather than trying to prevent it. By continuing to study membrane biofouling by employing CLSM in conjunction with fluorescently labeled probes, there is a tremendous amount of knowledge that can be gained regarding the composition of the biofoulant. In addition to CLSM, other microscopic techniques can be employed to investigate the biofouling phenomenon. By using Raman confocal microspectroscopy (RCM) and atomic force microscopy (AFM) in conjunction with

CLSM, a more comprehensive understanding of biofouling can be achieved. RCM is a non-destructive method that combines chemical information obtained through vibrational spectroscopy with the spatial distribution of chemical constituents within bulk, heterogeneous systems by confocal microscopy (Ljunglof *et al.*, 2000). AFM has proven to be a useful tool for visualizing and analyzing bacterial structures on solid surfaces and includes capabilities such as topographical imaging of microbial cells with nanometer resolution and adhesion measurements of microbial cells to surfaces using functionalized probes (Dufrene, 2001). Using correlative microscopy techniques such as CLSM, RCM, and AFM is advantageous because each one adds to and integrates the understanding of biological structures and interfaces.

7.0 REFERENCES

Allison, D.G., Sutherland, I.W. 1984. A staining technique for attached bacteria and its correlation to extracellular carbohydrates production. *Journal of Microbiological Methods*. 2:93-99.

APHA. 1980. Standard methods for the examination of water and wastewater, 15th edition. American Public Health Association, American Water Works Association and Water Pollution Control Federation, Washington, DC.

Baker, J.S., Dudley, L.Y. 1998. Biofouling in membrane systems - a review. *Desalination*. 118:81-90.

Beveridge, T.J., Makin, S.A., Kadurugamuwa, J.I., Zusheng, L. 1997. Interactions between biofilms and the environment. *FEMS Microbiology Reviews*. 20:291-303.

Bouhabila, E.H., Aim, R.B., Buisson, H. 2001. Fouling characterization in membrane bioreactors. *Separation and Purification Technology*. 22-23:123-132.

Brindle, K., Stephenson, T. 1996. The application of membrane biological reactors for the treatment of wastewaters. *Biotechnology and Bioengineering*. 49(6):601-610.

Bura, R., Cheung, M., Liao, B., Finlayson, J., Lee, B.C., Droppo, I.G., Leppard, G.G., Liss, S.N. 1998. Composition of extracellular polymeric substances in the activated sludge matrix. *Water Science and Technology*. 37(4-5):325-333.

Caldwell, D.E., Korber, D.R., Lawrence, J.R. 1992. Imaging of bacterial cells by fluorescence exclusion using scanning confocal laser microscopy. *Journal of Microbiological Methods*. 15:249-261.

Chang, I-S., Lee, C-H. 1998. Membrane filtration characteristics in membrane-coupled activated sludge system - the effect of physiological states of activated sludge on membrane fouling. *Desalination*. 120:221-233.

Chang, I-S., Lee, C-H., Ahn, K.H. 1999. Membrane filtration characteristics in membrane-coupled activated sludge system: the effect of floc structure on membrane fouling. *Separation Science and Technology*. 34(9):1743-1758.

Chang, I-S., Bag, S-O., Lee, C-H. 2001. Effects of membrane fouling on solute rejection during membrane filtration of activated sludge. *Process Biochemistry*. 36:855-860.

Characklis, W.G. 1984. Biofilm development: A process analysis. In K.C. Marshall (ed.), *Microbial Adhesion and Aggregation*. Dahlem Kanferenzen, Springer-Verlag, Berlin, p.137-157.

Christensen, B.E., Characklis, W.G. 1990. Physical and chemical properties of biofilms. In W.G. Characklis and K.C. Marshall (eds.), *Biofilms*. John Wiley and Sons, New York, p.93-130.

Cicek, N., Winnen, H., Suidan, M.T., Wrenn, B.E., Urbain, V., Manem, J. 1998. Effectiveness of the membrane bioreactor in the biodegradation of high molecular weight compounds. *Water Research*. 32(5):1553-1563.

Cicek, N., Macomber, J., Davel, J., Suidan, M.T., Audic, J., Genestet, P. 2001. Effect of solids retention time on the performance and biological characteristics of a membrane bioreactor. *Water Science and Technology*. 43(11):43-50.

Cote, P., Thompson, D. 2000. Wastewater treatment using membranes: the North American experience. *Water Science and Technology*. 41(10-11):209-215.

Davey, M.E., O'Toole, G.A. 2000. Microbial biofilms: from ecology to molecular genetics. *Microbiology and Molecular Biology Reviews*. Dec:847-867.

Decho, A.W., Kawaguchi, T. 1999. Confocal imaging of in situ natural microbial communities and their extracellular polymeric secretions using Nanoplast resin. *Biotechniques*. 27(6):1246-1252.

Defrance, L., Jaffrin, M.Y., Gupta, B., Paullier, P., Geaugey V. 2000. Contribution of various constituents of activated sludge to membrane bioreactor fouling. *Bioresource Technology*. 73:105-112.

Del Gallo, M., Negi, M., Neyra, C.A. 1989. Calcofluor- and lectin-binding exocellular polysaccharides of *Azospirillum brasilense* and *Azospirillum lipoferum*. *Journal of Bacteriology*. 171:3504-3510.

Dignac, M-F., Urbain, V., Rybacki, D., Bruchet, A., Snidaro, D., Scribe, P. 1998. Chemical description of extracellular polymers: implication of activated sludge floc structure. *Water Science and Technology*. 38(8-9):45-53.

Donlan, R.M. 2000. Biofilm control in industrial water systems: approaching an old problem in new ways. In Evans, L.V. (ed), *Biofilms: Recent Advances in their Study and Control*. Harwood Academic Publishers, Singapore, p.333-360.

Droppo, I.G., Flannigan, D.T., Leppard, G.G., Liss, S.N. 1996a. Floc stabilization for multiple microscopic techniques. *Applied and Environmental Microbiology*. Sept:3508-3515.

Droppo, I.G., Flannigan, D.T., Leppard, G.G., Liss, S.N. 1996b. Microbial floc stabilization and preparation for structural analysis by correlative microscopy. *Water Science and Technology*. 34(5-6):155-162.

Dufrene, Y.F. (2001). Application of atomic force microscopy to microbial surfaces: from reconstituted cell surface layers to living cells. *Micron*. 32: 153-165.

Eriksson, L., Steen, I., Tendaj, M. 1992. Evaluation of sludge properties at an activated sludge plant. *Water Science and Technology*. 25(6): 251-265.

Fan, X-J., Urbain V., Qian, Y., Manem, J. 2000. Ultrafiltration of activated sludge with ceramic membranes in a cross-flow membrane bioreactor process. *Water Science and Technology*. 41(10-11):243-250.

Fane, A.G., Beatson, P., Li, H. 2000. Membrane fouling and its control in environmental applications. *Water Science and Technology*. 41(10-11):303-308.

Field, R.W., Wu, D., Howell, J.A., Gupta, B.B. 1995. Critical Flux concept for microfiltration fouling. *Journal of Membrane Science*. 100:259-272.

Figueroa, L., Silverstein, J.A. 1989. Ruthenium red adsorption method for measurement of extracellular polysaccharides in sludge flocs. *Biotechnology and Bioengineering*. 33:941-947.

Filisetti-Cozzi, T.M., Carpita, N.C. 1991. Measurement of uronic acids without interference from neutral sugars. *Analytical Biochemistry*. 197:159-162.

Flemming, H-C. 1995. Sorption sites in biofilms. *Water Science and Technology*. 32(8):27-33.

Flemming, H-C., Griebe, T., Schaule, G. 1996. Antifouling strategies in technical systems - a short review. *Water Science and Technology*. 34(5-6):517-524.

Flemming, H-C., Wingender, J., Griebe, T., Mayer, C. 2000. Physico-chemical properties of biofilms. In Evans, L.V. (ed), *Biofilms: Recent Advances in their Study and Control*. Harwood Academic Publishers, Singapore, p.19-34.

Frølund, B., Keiding, K., Nielsen, P.H. 1994. A comparative study of biopolymers from a conventional and an advanced activated sludge treatment plant. *Water Science and Technology*. 29(7):137-141.

Frølund, B., Palmgren, R., Keiding, K., Nielsen, P.H. 1996. Extraction of extracellular polymers from activated sludge using a cation exchange resin. *Water Research*. 30(8):1749-1758.

Ganczarczyk, J.J., Zahid, W.M., Li, D-H. 1992. Physical stabilization and embedding of microbial aggregates for light microscopy studies. *Water Research*. 26(12):1695-1699.

Gander, M., Jefferson, B., Judd, S. 2000. Aerobic MBRs for domestic wastewater treatment: a review with cost consideration. *Separation and Purification Technology*. 18:119-130.

Gaudy, A.F. 1962. Colorimetric determination of protein and carbohydrate. *Industrial Water and Wastes*. Jan-Feb:17-22.

Gehr, R., Henry, J.G. 1983. Removal of extracellular materials: techniques and pitfalls. *Water Research*. 17(12):1743-1748.

Gerritsen, H.C., De Grauw, C.J. 1999. Imaging of optically thick specimen using two-photon excitation microscopy. *Microscopy Research and Technique*. 47(3):206-209.

Gustafsson, M.G. 1999. Extended resolution fluorescence microscopy. *Current Opinion Structural Biology*. 9(5):627-634.

Hibbs, A.R. 2000. Confocal microscopy for biologists: an intensive introductory course. Biocon, Australia, p.1-173.

Hodgson, P.H., Leslie, G.L., Schneider, R.P., Fane, A.G., Fell, C.J.D., Marshall, K.C. 1993. Cake resistance and solute rejection in bacterial microfiltration: the role of extracellular matrix. *Journal of Membrane Science*. 79:35-53.

Horan, N.J., Eccles, C.R. 1986. Purification and characterization of extracellular polysaccharide from activated sludges. *Water Research*. 20(11):1427-1432.

Johnsen, A.R., Hausner, M., Schnell, A., Wuertz, S. 2000. Evaluation of fluorescently labeled lectins for noninvasive localization of extracellular polymeric substances in *Sphingomonas* biofilms. *Applied and nvironmental Microbiology*. 66(8):3487-3491.

Jorand, F., Zartarian, F., Thomas, F., Block, J.C., Bottero, J.Y., Villemin, G., Urbain, V., Manem, J. 1995. Chemical and structural (2D) linkage between bacteria within activated sludge flocs. *Water Research*. 29(7)1639-1647.

Jorand, F., Boue-Bigne, F., Block, J.C., Urbain, V. 1998. Hydrophobic/Hydrophilic properties of activated sludge exopolymeric substances. *Water Science and Technology*. 37(4-5):307-315.

Lawrence, J.R., Korber, D.R., Hoyle, B.D., Costerton, J.W., Caldwell, D.E. 1991. Optical sectioning of microbial biofilms. *Journal of Bacteriology*. 173(20):6588-6567.

Lawrence, J.R., Wolfaardt, G.M., Korber, D.R., Caldwell, D.E. 1997. Analytical imaging and microscopy techniques. In C.J. Hurst, G.R. Knudsen, M.J. McInerney, L.D. Stetzenback, M.V. Walter (eds), *Manual of Environmental Microbiology*. American Society of Microbiology Press, Washington, DC, p.29-51.

Lawrence, J.R., New, T.R., Swerhone, G.D.W. 1998. Application of multiple parameter imaging for the quantification of algal, bacterial and exopolymer components of microbial biofilms. *Journal of Microbiological Methods*. 32:253-261.

Lee, J., Ahn, W-Y., Lee, C-H. 2001. Comparison of the filtration characteristics between attached and suspended growth micoorganisms in submerged membrane bioreactor. *Water Research.* 35(10):2435-2445.

Lewandowski, Z. 2000. Structure and function of biofilms In Evans, L.V. (ed.), *Biofilms: Recent Advances in their Study and Control.* Harwood Academic Publishers, Singapore, p.1-17.

Liao, B.Q., Allen, D.G., Droppo, I.G., Leppard, G.G., Liss, S.N. 2001. Surface properties of sludge and their role in bioflocculation and settleability. *Water Research.* 35(2):339-350.

Liss, S.N., Droppo, I.G., Flannigan, D.T., Leppard G.G. 1996. Floc architecture in wastewater and natural riverine systems. *Environmental Science and Technology.* 30(2):680-686.

Liss, S.N. 2002. Microbial flocs suspended biofilms. In Flemming, H-C., Bitton, G. (eds.), *Biofilms, The Encyclopedia of Environmental Microbiology.* John Wiley and Sons, New York, NY. in press.

Liu, R., Huang, X., Wanc, C., Chen, L., Qian, Y. 2000a. A pilot study on a submerged membrane bioreactor for domestic wastewater treatment. *Journal of Environmental Science and Health, Part A.* 35(10):1761-1772.

Liu, R., Huang, X., Wang, C., Chen, L., Qian, Y. 2000b. Study of hydraulic characteristics in a submerged membrane bioreactor process. *Process Biochemistry.* 36:249-254.

Ljunglof, A., Larsson, M., Knuuttila, K.G., Lindgren, J. (2000). Measurement of ligand distribution in individual adsorbent particles using confocal scanning laser microscopy and confocal micro-Raman spectroscopy. *Journal of Chromatography A.* 896(2): 235-244.

Lowry, O.H., Rosenbrough, N.J., Farr, A.L., Randall, R.J. 1951. Protein Measurement with the Folin phenol reagent. *Journal of Biological Chemistry.* 193:265-275.

Ma, H., Bowman, C.N., Davis, R.H. 2000. Membrane fouling reduction by backpulsing and surface modification. *Journal of Membrane Science.* 173:191-200.

Magnusson, K.E. 1980. The hydrophobic effect and how it can be measured with relevance for cell-cell interactions. *Scandinavian Journal of Infectious Diseases Suppl.* 24:131-134.

Maier, R.M., Pepper, I.L., Gerber, C.P. 2000. Chapter 9 Microscopic Techniques. In *Environmental Microbiology.* Academic Press, San Diego, CA, p.195-211.

McDonogh, R.M., Schaule, G., Flemming, H.C. 1994. The permeability of biofouling layers on membranes. *Journal of Membrane Science.* 87:199-217.

McFeters, G.A., Bazin, M.J., Bryers, J.D., Caldwell, D.E., Characklis, W.G., Lund, D.B., Mirelman, D., Mitchell, R., Schubert, R.H.W., Tanaka, T., White, D.C. 1984. Biofilm development and its consequences. In K.C. Marshall (ed), *Microbial Adhesion and Aggregation*. Dahlem Kanferenzen, Springer-Verlag, Berlin, p.109-124.

Metcalf and Eddy, Inc. 1991. Wastewater engineering : treatment, disposal, and reuse. 3rd ed. McGraw-Hill, New York, NY.

Michael, T., Smith, C.M. 1995. Lectins probe molecular films in biofouling: characterization of early films on non-living and living surfaces. *Marine Ecology Progress Series*. 119(1-3):229-236.

Morgan, J.W., Forster, C.F., Evison, L. 1990. A comparative study of the nature of biopolymers extracted from anaerobic and activated sludges. *Water Research*. 24(6):743-751.

Morris, C.E., Monier, J-M., Jacques, M-A. 1997. Methods for observing microbial biofilms directly on leaf surfaces and recovering them for isolation of culturable microorganisms. *Applied and Environmental Microbiology*. 63(4):1570-1576.

Nagaoka, H., Ueda, S., Miya, A. 1996. Influence of extracellular polymers on membrane separation activated sludge process. *Water Science and Technology*. 34(9):165-172.

Nagaoka, H., Yamanishi, S., Miya, A. 1998. Modeling of biofouling by extracellular polymers in a membrane separation activated sludge system. *Water Science and Technology*. 38(4-5):497-504.

Neu, T.R., Marshall, K.C. 1991. Microbial 'footprints' - A new approach to adhesive polymers. *Biofouling*. 3:101-112.

Neu, T.R., Lawrence, J. R. 1997. Development and structure of microbial biofilms in river water studied by confocal laser scanning microscopy. *FEMS Microbial Ecology*. 24(1):11-25.

Neu, T.R. 2000. Confocal laser scanning microscopy (CLSM) of biofilms. In H-C. Flemming, U. Szewzyk, T. Griebe (eds.), *Biofilms: Investigative Methods and Applications*. Technomic Publishing Company Inc., Lancaster, Pennsylvania, p.211-224.

Newby, D.T., Pepper, I.L., Maier, R.M. 2000. Chapter 7 Microbial Transport. In *Environmental Microbiology*. Academic Press, San Diego, CA, p.147-175.

Novachis, L. 2000. Design and operation of membrane bioreactor technology for industrial and municipal wastewater treatment. In *Membrane Technologies for Industrial and Municipal Wastewater Treatment and Reuse*. Water Environment Federation, Alexandria, VA, p. 32-46.

Okabe, S., Kuroda, H., Watanabe, Y. 1998. Significance of Biofilm Structure on Transport of Inert Particulates into Biofilms. *Water Science and Technology.* 38(8-9):163-170.

Owen, G., Bandi, M., Howell, J.A., Churchouse, S.J. 1995. Economic assessment of membrane processes for water and waste water treatment. *Journal of Membrane Science.* 102:77-91.

Ozaki, N., Yamamoto, K. 2001. Hydraulic effects on sludge accumulation on membrane surface in crossflow filtration. *Water Research.* 35(13):3137-3146.

Pagano, M., Gauvreau, K. 1993. Principles of Biostatistics. Duxbury Press, Belmont, California, USA.

Palmgren, R., Nielsen, P.H. 1996. Accumulation of DNA in the exopolymeric matrix of activated sludge and bacterial cultures. *Water Science and Technology.* 34(5-6):233-240.

Parameshwaran, K., Fane, A.G., Cho, B.D., Kim, K.J. 2001. Analysis of microfiltration performance with constant flux processing of secondary effluent. *Water Research.* 35(18):4349-4358.

Pawley, J. 2000. The 39 Steps: A cautionary tale of quantitative 3-D fluorescence microscopy. *Biotechniques.* 28(5):884-887.

Periasamy, A., Skoglund, P., Noakes, C., Keller, R. 1999. An evaluation of two-photon excitation versus confocal and digital deconvolution fluorescence microscopy. *Microscopy Research and Technique.* 47(3):172-181.

Rittmann, B.E., McCarty, P.L. 2000. Chapter 6. Activated sludge process. In *Environmental Biotechnology: Principles and Applications.* McGraw-Hill Companies Inc., New York, NY, p.307-393.

Roorda, J.H., van der Graaf, J.H.J.M. 2000. Understanding membrane fouling in ultrafiltration of WWTP-effluent. *Water Science and Technology.* 41(10-11):345-353.

Rosenberg, M., Gutnick, D., Rosenberg, E. 1980. Adherence of bacteria to hydrocarbons: a simple method for measuring cell-surface hydrophobicity. *FEMS Microbiology Letters.* 9:29-33.

Rosenberger, S., Kruger, U., Witzig, R., Manz, W., Szewzyk, U., Kraume, M. 2002. Performance of a bioreactor with submerged membranes for aerobic treatment of municipal waste water. *Water Research.* 36:413-420.

Rudd, T., Sterritt, R.M., Lester, J.N. 1983. Extraction of extracellular polymers from activated sludge. *Biotechnology Letters.* 5(5):327-332.

Sharon, N., Lis, H. 1989. Lectins. Chapman and Hall, New York, NY, p. 1-127.

Silva, C.M., Reeve, D.W., Husain, H., Rabie, H.R., Woodhouse, K.A. 2000. Model for flux prediction in high-shear microfiltration systems. *Journal of Membrane Science.* 173:87-98.

Silyn-Roberts, G., Lewis, G. 1997. A technique in confocal laser microscopy for establishing biofilm coverage and thickness. *Water Science and Technology.* 36(10):117-124.

Smith, C. V., Di Gregorio, D., Talcott, R. M. 1969. The use of ultrafiltration membranes for activated sludge separation. *24th Proceedings - Industrial Waste Conference.* 60:1300-1310.

Spaeth, R., Wuertz, S. 2000. Extraction and quantification of extracellular polymeric substances from wastewater. In H-C. Flemming, U. Szewzyk, T. Griebe (eds.), *Biofilms: Investigative Methods and Applications.* Technomic Publishing Company Inc., Lancaster, Pennsylvania, p.51-68.

Stephenson, T., Judd, S., Jefferson, B., Brindle, K. 2001. Membrane bioreactors for wastewater treatment. IWA Publishing, London, UK, p. 1-176.

Stewart, P.S., Murga, R., Srinivasan, R., de Beer, D. 1995. Biofilm structural heterogeneity visualized by three microscopic methods. *Water Research.* 29(8):2006-2009.

Tardieu, E., Grasmick, A., Geaugey, V., Manem, J. 1998. Hydrodynamic control of bioparticle deposition in a MBR applied to wastewater treatment. *Journal of Membrane Science.* 147:1-12.

Thompson, D., Mourato, D., Penny, J. 2000. Demonstration of the ZenoGem® process for municipal wastewater treatment. In *Membrane Technologies for Industrial and Municipal Wastewater Treatment and Reuse.* Water Environment Federation, Alexandria, VA, p.403-412.

Urbain, V., Block, J.C., Manem, J. 1993. Bioflocculation in activated sludge: an analytic approach. *Water Research.* 27:829-838.

van Loosdrecht, M.C.M., Eikelboom, D., Gjaltema, A., Mulder, A., Tijhuis, L., Heijnen, J.J. 1995. Biofilm structures. *Water Science and Technology.* 32(8):35-43.

Wakeman, R.J., Williams, C.J. 2002. Additional techniques to improve microfiltration. *Separation and Purification Technology.* 26:3-18.

Wimpenny, J. 2000. Structural determinants in biofilm formation. In Evans, L.V. (ed.), *Biofilms: Recent Advances in their Study and Control.* Harwood Academic Publishers, Singapore, p.35-49.

Wisniewski, C., Grasmick, A. 1998. Floc size distribution in a membrane bioreactor and consequences for membrane fouling. *Colloids and Surfaces A: Physicochemical and Engineering Aspects.* 138:403-411.

Wisniewski, C., Grasmick, A., Cruz, A.L. 2000. Critical particle size in membrane bioreactors Case of a denitrifying bacterial suspension. *Journal of Membrane Science.* 178:141-150.

Witzig, R., Manz, W., Rosenberger, S., Kruger, U., Kraume, M., Szewzyk, U. 2002. Microbiological aspects of a bioreactor with submerged membranes for aerobic treatment of municipal wastewater. *Water Research.* 36:394-402.

Wolfaardt, G.M., Lawrence, J.R., Robarts, R.D., Caldwell, D.E. 1998. In situ characterization of biofilm exopolymers involved in the accumulation of chlorinated organics. *Microbial Ecology.* 35:213-223.

Yu, F.P., McFeters, G.A. 2000. Study of biofouling control with fluorescent probes and image analysis. In Evans, L.V. (ed.), *Biofilms: Recent Advances in their Study and Control.* Harwood Academic Publishers, Singapore, p.401-418.

Zita, A., Hermannsson, M. 1997. Effects of bacterial cell surface structure and hydrophobicity on attachment to activated sludge flocs. *Applied and Environmental Microbiology.* 63(3):1168-1170.

APPENDIX A: CLSM Analysis of Hollow Fibre Microfiltration Membrane Samples

1. Prepare each lectin-conjugate stain according to the stock concentration listed below.

Lectin - conjugate	Stock Concentration	Working Concentration
Wheat germ agglutinin – tetramethylrhodamine	1 - 2 mg/mL in 0.1 M $NaHCO_3$ containing 1mM Mn^{2+} and 1mM Ca^{2+} at pH 8.3	10 µg/mL in 0.1 M $NaHCO_3$ containing 1 mM Mn^{2+} and 1 mM Ca^{2+} at pH 8.3
Concanavalin A - Alexa Fluor 647	2 mg/mL in 0.1 M $NaHCO_3$ containing 1mM Mn^{2+} and 1mM Ca^{2+} at pH 8.3	100 µg/mL in 0.1 M $NaHCO_3$ containing 1 mM Mn^{2+} and 1 mM Ca^{2+} at pH 8.3
Soybean agglutinin - Alexa Flour 488	2 mg/mL in distilled deionized water	10 µg/mL in 0.1 M $NaHCO_3$ containing 1 mM Mn^{2+} and 1 mM Ca^{2+} at pH 8.3

2. Centrifuge each lectin-conjugate for 2 minutes at 14 000 g.

3. Using 1.5 mL microcentrifuge tubes wrapped in aluminum foil, add the appropriate volume of lectin-conjugate to 0.1 M $NaHCO_3$ containing 1 mM Mn^{2+} and 1 mM Ca^{2+} at pH 8.3 to make a 1 mL working solution.

4. Slice 3 longitudinal sections and 3 cross sections of each membrane sample with a sterile scalpel blade.

5. Immerse membrane sections in 1 mL working solution and mix thoroughly by pipetting up and down several times.

6. Incubate at room temperature in the dark for 10 minutes.

7. Draw off working solution with a pipet or dropper.

8. Wash membrane sections three times with 1 mL 0.1 M $NaHCO_3$ containing 1 mM Mn^{2+} and 1 mM Ca^{2+} at pH 8.3 and incubate again for 10 minutes each at room temperature in the dark.

9. Embed stained membrane sections in low melting point agarose in plankton chambers.

10. Observe samples by CLSM using the FITC, Rhodamine, and Cy 5 configurations installed with the Zeiss LSM 510 Release 2.3 software.

APPENDIX B: CLSM Analysis of Flocs

1. Prepare each lectin-conjugate stain according to the stock concentration listed below.

Lectin - conjugate	Stock Concentration	Working Concentration
Wheat germ agglutinin – tetramethylrhodamine	1 - 2 mg/mL in 0.1 M $NaHCO_3$ containing 1mM Mn^{2+} and 1mM Ca^{2+} at pH 8.3	10 µg/mL in 0.1 M $NaHCO_3$ containing 1 mM Mn^{2+} and 1 mM Ca^{2+} at pH 8.3
Concanavalin A - Alexa Fluor 647	2 mg/mL in 0.1 M $NaHCO_3$ containing 1mM Mn^{2+} and 1mM Ca^{2+} at pH 8.3	100 µg/mL in 0.1 M $NaHCO_3$ containing 1 mM Mn^{2+} and 1 mM Ca^{2+} at pH 8.3
Soybean agglutinin - Alexa Flour 488	2 mg/mL in distilled deionized water	10 µg/mL in 0.1 M $NaHCO_3$ containing 1 mM Mn^{2+} and 1 mM Ca^{2+} at pH 8.3

2. Centrifuge each lectin-conjugate for 2 minutes at 14 000 g.

3. Using a wide mouth pipet, add 0.2 – 0.35 mL of sludge sample to 0.6 – 0.65 mL of low melting point agarose in a 1.5 mL microcentrifuge tube.

4. Mix thoroughly by inverting the tube several times.

5. Pour mixture in a plankton chamber and allow to agarose to gel.

6. Using 1.5 mL microcentrifuge tubes wrapped in aluminum foil, add the appropriate volume of lectin-conjugate to 0.1 M $NaHCO_3$ containing 1 mM Mn^{2+} and 1 mM Ca^{2+} at pH 8.3 to make a 1 mL working solution.

7. Pour the working solution over the floc embedded in agarose.

8. Incubate at room temperature in the dark for 10 minutes.

9. Wash three times with 1 mL 0.1 M $NaHCO_3$ containing 1 mM Mn^{2+} and 1 mM Ca^{2+} at pH 8.3 and incubate again for 10 minutes each at room temperature in the dark.

10. Observe samples by CLSM using the FITC, Rhodamine, and Cy 5 configurations installed with the Zeiss LSM 510 Release 2.3 software.

APPENDIX C: LIVE *Bac*Light™ Bacterial Gram Stain

1. Staining Membrane Fibre Samples for Nucleic Acid Analysis

2. Prepare a combined reagent mixture in a 1.5 mL microcentrifuge tube by adding 5 μL of Component A to 5 μL of Component B and Vortex for 1 minute to mix thoroughly.

3. Add 3 μL of the combined reagent mixture to each of the three samples taken at critical transmembrane pressure (12 day SRT Relax, 12 day SRT Back wash, 30 day SRT Relax) and mix thoroughly by pipetting up and down several times.

4. Incubate at room temperature in the dark for 15 minutes.

5. Wash membrane sections three times with 1 mL of distilled deionized water and incubate again for 10 minutes each at room temperature in the dark

6. Embed sample in low melting point agarose in plankton chambers

7. Observe samples by CLSM using the FITC, Rhodamine, and Cy 5 configurations installed with the Zeiss LSM 510 Release 2.3 software. Live gram-negative bacteria fluoresce green and live gram-positive bacteria fluoresce red. Any dead bacteria present may stain variably.

Appendix D: Preliminary Study - CLSM Image Data

Date	File Name	Specimen	Obj/NA	Averaging	Zoom	Speed (us/pixel)	Image Size	
							Pixels	Microns
29-Mar-01	controlMar29	clean membrane sample	20X/0.75	1	1	8.6	1024 x 1024	460.6 x 460.6
05-Jul-01	Test1	test membrane sample	20X/0.75	1	1	1.76	512 x 512	460.6 x 460.6
05-Jul-01	Test2	test membrane sample	20X/0.75	1	1	1.76	512 x 512	460.6 x 460.6
05-Jul-01	Test3	test membrane sample	20X/0.75	1	1	1.76	512 x 512	460.6 x 460.6
05-Jul-01	wholemembrane	test membrane sample	20X/0.75	1	1	1.76	512 x 512	460.6 x 460.6
10-Jul-01	xsection	test membrane sample	20X/0.75	1	1	1.76	512 x 512	460.6 x 460.6
17-Jul-01	clean_xsection	clean membrane sample	20X/0.75	1	1	1.76	512 x 512	460.6 x 460.6
17-Jul-01	clean_xsection2	clean membrane sample	20X/0.75	1	1	1.76	512 x 512	460.6 x 460.6
17-Jul-01	clean_xsection3	clean membrane sample	20X/0.75	1	1	8.96	512 x 512	460.6 x 460.6
17-Jul-01	clean_xsection4	clean membrane sample	20X/0.75	1	1	17.92	512 x 512	460.6 x 460.6
17-Jul-01	clean_xsection5	clean membrane sample	20X/0.75	1	1	4.48	512 x 512	460.6 x 460.6
17-Jul-01	clean_xsection6	clean membrane sample	63X/0.9 W	1	1	35.84	512 x 512	146.2 x 146.2
17-Jul-01	clean_xsection7	clean membrane sample	63X/0.9 W	1	1	35.84	512 x 512	146.2 x 146.2
17-Jul-01	clean_xsection8	clean membrane sample	63X/0.9 W	1	1	35.84	512 x 512	146.2 x 146.2
17-Jul-01	clean_zstack	clean membrane sample	63X/0.9 W	1	1	35.84	512 x 512	146.2 x 146.2
29-Aug-01	Sample2	3 day filtration/relaxation expt	20X/0.75	2	1	17.92	512 x 512	460.6 x 460.6
29-Aug-01	Sample2b	3 day filtration/relaxation expt	40X/0.6	2	1	17.92	512 x 512	230.3 x 230.3
29-Aug-01	Sample2c	3 day filtration/relaxation expt	40X/0.6	1	1	8.96	512 x 512	230.3 x 230.3
30-Aug-01	Sample2d	3 day filtration/relaxation expt	63X/0.9 W	2	1	17.92	512 x 512	146.2 x 146.2
30-Aug-01	Sample2e	3 day filtration/relaxation expt	63X/0.9 W	1	1	4.48	512 x 512	146.2 x 146.2
30-Aug-01	Sample3a	3 day filtration/relaxation expt	63X/0.9 W	2	0.7	17.92	512 x 512	146.2 x 146.2
30-Aug-01	Sample3b	3 day filtration/relaxation expt	63X/0.9 W	2	0.7	4.48	512 x 512	206.8 x 206.8
28-Sep-01	744.13_single1	30 day filtration/relaxation expt	20X/0.75	4	1	35.84	512 x 512	460.6 x 460.6
28-Sep-01	744.13ds_single	30 day filtration/relaxation expt	63X/0.9 W	2	1	17.92	512 x 512	146.2 x 146.2
28-Sep-01	744.13ds_single2	30 day filtration/relaxation expt	63X/0.9 W	2	1	17.92	512 x 512	146.2 x 146.2
28-Sep-01	744.13ds_single3	30 day filtration/relaxation expt	63X/0.9 W	2	2.3	17.92	512 x 512	
28-Sep-01	744.17ds_single1	30 day filtration/relaxation expt	10X/0.25	2	2.3	35.84	512 x 512	
28-Sep-01	744.17ds_stack	30 day filtration/relaxation expt	63X/0.9 W	2	1	8.96	512 x 512	146.2 x 146.2
02-Oct-01	744.17_Iia	30 day filtration/relaxation expt	63X/0.9 W	2	1	35.84	512 x 512	146.2 x 146.2
02-Oct-01	744.17_Iia_zstack	30 day filtration/relaxation expt	63X/0.9 W	2	1	8.96	512 x 512	146.2 x 146.2
02-Oct-01	744.17_IIB	30 day filtration/relaxation expt	63X/0.9 W	2	1	8.96	512 x 512	146.2 x 146.2
02-Oct-01	744.17_IIB	30 day filtration/relaxation expt	63X/0.9 W	2	1	8.96	512 x 512	146.2 x 146.2
02-Oct-01	744.17_IIB	30 day filtration/relaxation expt	63X/0.9 W	2	1	35.84	512 x 512	146.2 x 146.2
02-Oct-01	744.17_IIB	30 day filtration/relaxation expt	63X/0.9 W	2	1	8.96	512 x 512	146.2 x 146.2
02-Oct-01	744.17_IIC	30 day filtration/relaxation expt	63X/0.9 W	2	1	35.84	512 x 512	146.2 x 146.2
02-Oct-01	744.17_IIC	30 day filtration/relaxation expt	63X/0.9 W	2	1	8.96	512 x 512	146.2 x 146.2
02-Oct-01	744.17_IID	30 day filtration/relaxation expt	63X/0.9 W	2	1	35.84	512 x 512	146.2 x 146.2
02-Oct-01	744.17_IID	30 day filtration/relaxation expt	63X/0.9 W	2	1	8.96	512 x 512	146.2 x 146.2

Appendix D: Preliminary Study - CLSM Image Data

Date	File Name	Specimen	Dye/Lectin			Abs/Ex λ		
			Ch 1	Ch 2	Ch 3	Ch 1	Ch 2	Ch 3
29-Mar-01	controlMar29	clean membrane sample	FITC			494/518		
05-Jul-01	Test1	test membrane sample	WGA-Tr	ConA-Fl		595/615	494/518	
05-Jul-01	Test2	test membrane sample	WGA-Tr	ConA-Fl		595/615	494/518	
05-Jul-01	Test3	test membrane sample	WGA-Tr	ConA-Fl		595/615	494/518	
05-Jul-01	wholemembrane	test membrane sample	WGA-Tr	ConA-Fl		595/615	494/518	
10-Jul-01	xsection	test membrane sample	WGA-Tr	ConA-Fl		595/615	494/518	
17-Jul-01	clean_xsection	clean membrane sample	none			Rhod. Settings		
17-Jul-01	clean_xsection2	clean membrane sample	none			Rhod. Settings		
17-Jul-01	clean_xsection3	clean membrane sample	none			FITC settings		
17-Jul-01	clean_xsection4	clean membrane sample	none			Rhod. Settings		
17-Jul-01	clean_xsection5	clean membrane sample	none	none		Rhod. Settings	FITC settings	
17-Jul-01	clean_xsection6	clean membrane sample	none			Rhod. Settings		
17-Jul-01	clean_xsection7	clean membrane sample	none			Cy 5 settings		
17-Jul-01	clean_xsection8	clean membrane sample	none			FITC settings		
17-Jul-01	clean_zstack	clean membrane sample	none			FITC settings		
29-Aug-01	Sample2	3 day filtration/relaxation expt	ConA-Fl			494/518		
29-Aug-01	Sample2b	3 day filtration/relaxation expt	ConA-Fl			494/518		
29-Aug-01	Sample2c	3 day filtration/relaxation expt	ConA-Fl			494/518		
30-Aug-01	Sample2d	3 day filtration/relaxation expt	ConA-Fl			494/518		
30-Aug-01	Sample2e	3 day filtration/relaxation expt	ConA-Fl			494/518		
30-Aug-01	Sample3a	3 day filtration/relaxation expt	WGA-Tr			595/615		
30-Aug-01	Sample3b	3 day filtration/relaxation expt	WGA-Tr			595/615		
28-Sep-01	744.13_single1	30 day filtration/relaxation expt	WGA-tmr			used FITC settings		
28-Sep-01	744.13ds_single	30 day filtration/relaxation expt	WGA-tmr	ConA-Fl		555/580	494/518	
28-Sep-01	744.13ds_single2	30 day filtration/relaxation expt	WGA-tmr	ConA-Fl		555/580	494/518	
28-Sep-01	744.13ds_single3	30 day filtration/relaxation expt	WGA-tmr	ConA-Fl		555/580	494/518	
28-Sep-01	744.17ds_single1	30 day filtration/relaxation expt	WGA-tmr	ConA-Fl		555/580	494/518	
28-Sep-01	744.17ds_stack	30 day filtration/relaxation expt	WGA-tmr	ConA-Fl		555/580	494/518	
02-Oct-01	744.17_Iia	30 day filtration/relaxation expt	WGA-tmr	ConA-Fl		555/580	494/518	
02-Oct-01	744.17_Iia_zstack	30 day filtration/relaxation expt	WGA-tmr	ConA-Fl		555/580	494/518	
02-Oct-01	744.17_IIB	30 day filtration/relaxation expt	WGA-tmr	ConA-Fl		555/580	494/518	
02-Oct-01	744.17_IIB	30 day filtration/relaxation expt		ConA-Fl			494/518	
02-Oct-01	744.17_IIB	30 day filtration/relaxation expt	WGA-tmr	ConA-Fl		555/580	494/518	
02-Oct-01	744.17_IIB	30 day filtration/relaxation expt	WGA-tmr	ConA-Fl		555/580	494/518	
02-Oct-01	744.17_IIC	30 day filtration/relaxation expt	WGA-tmr	ConA-Fl		555/580	494/518	
02-Oct-01	744.17_IIC	30 day filtration/relaxation expt	WGA-tmr	ConA-Fl		555/580	494/518	
02-Oct-01	744.17_IID	30 day filtration/relaxation expt	WGA-tmr	ConA-Fl		555/580	494/518	
02-Oct-01	744.17_IID	30 day filtration/relaxation expt	WGA-tmr	ConA-Fl		555/580	494/518	

Appendix D: Preliminary Study - CLSM Image Data

Date	File Name	Specimen	Filters			Laser Power		
			Ch 1	Ch2	Ch 3	Ch 1	Ch 2	Ch 3
29-Mar-01	controlMar29	clean membrane sample	BP505-530			76% of 10%		
05-Jul-01	Test1	test membrane sample	LP 560	BP 505-530		HeNe1 11%	Ar 10% of 50%	
05-Jul-01	Test2	test membrane sample	LP 560	BP 505-530		HeNe1 10%	Ar 11% of 50%	
05-Jul-01	Test3	test membrane sample	LP 560	BP 505-530		HeNe1 9%	Ar 10% of 50%	
05-Jul-01	wholemembrane	test membrane sample	LP 560	BP 505-530		HeNe1 10%	Ar 10% of 50%	
10-Jul-01	xsection	test membrane sample	LP 560	BP 505-530		HeNe1 15%	Ar 15% of 50%	
17-Jul-01	clean_xsection	clean membrane sample	LP 560			HeNe1 30%		
17-Jul-01	clean_xsection2	clean membrane sample	LP 560			HeNe1 30%		
17-Jul-01	clean_xsection3	clean membrane sample	LP 505			Ar 10% of 50%		
17-Jul-01	clean_xsection4	clean membrane sample	LP 560			HeNe1 50%		
17-Jul-01	clean_xsection5	clean membrane sample	LP 560	BP 505-530		HeNe1 50%	Ar 40% of 50%	
17-Jul-01	clean_xsection6	clean membrane sample	LP 560			HeNe1 30%		
17-Jul-01	clean_xsection7	clean membrane sample	LP 650			HeNe2 30%		
17-Jul-01	clean_xsection8	clean membrane sample	LP 505			Ar 10% of 50%		
17-Jul-01	clean_zstack	clean membrane sample	LP 505			Ar 20% of 50%		
29-Aug-01	Sample2	3 day filtration/relaxation expt	LP 505			Ar 10% of 50%		
29-Aug-01	Sample2b	3 day filtration/relaxation expt	LP 505			Ar 10% of 50%		
29-Aug-01	Sample2c	3 day filtration/relaxation expt	LP 505			Ar 10% of 50%		
30-Aug-01	Sample2d	3 day filtration/relaxation expt	LP 505			Ar 10% of 50%		
30-Aug-01	Sample2e	3 day filtration/relaxation expt	LP 505			Ar 10% of 50%		
30-Aug-01	Sample3a	3 day filtration/relaxation expt	LP 560			HeNe1 30%		
30-Aug-01	Sample3b	3 day filtration/relaxation expt	LP 560			HeNe1 30%		
28-Sep-01	744.13_single1	30 day filtration/relaxation expt	LP 505			Ar 10% of 50%		
28-Sep-01	744.13ds_single	30 day filtration/relaxation expt	LP 560	BP 505-530		HeNe1 0%	Ar 10% of 50%	
28-Sep-01	744.13ds_single2	30 day filtration/relaxation expt	LP 560	BP 505-530		HeNe1 100%	Ar 10% of 50%	
28-Sep-01	744.13ds_single3	30 day filtration/relaxation expt	LP 560	BP 505-530		HeNe1 100%	Ar 10% of 50%	
28-Sep-01	744.17ds_single1	30 day filtration/relaxation expt	LP 560	BP 505-530		HeNe1 100%	Ar 10% of 50%	
28-Sep-01	744.17ds_stack	30 day filtration/relaxation expt	LP 560	BP 505-530		HeNe1 100%	Ar 10% of 50%	
02-Oct-01	744.17_Iia	30 day filtration/relaxation expt	LP560	BP 505-530		HeNe1 100%	Ar 10% of 50%	
02-Oct-01	744.17_Iia_zstack	30 day filtration/relaxation expt	LP560	BP 505-530		HeNe1 100%	Ar 10% of 50%	
02-Oct-01	744.17_IIB	30 day filtration/relaxation expt	LP560	BP 505-530		HeNe1 100%	Ar 10% of 50%	
02-Oct-01	744.17_IIB	30 day filtration/relaxation expt		BP 505-530			Ar 10% of 50%	
02-Oct-01	744.17_IIB	30 day filtration/relaxation expt	LP560	BP 505-530		HeNe1 100%	Ar 10% of 50%	
02-Oct-01	744.17_IIB	30 day filtration/relaxation expt	LP560	BP 505-530		HeNe1 100%	Ar 10% of 50%	
02-Oct-01	744.17_IIC	30 day filtration/relaxation expt	LP560	BP 505-530		HeNe1 100%	Ar 10% of 50%	
02-Oct-01	744.17_IIC	30 day filtration/relaxation expt	LP560	BP 505-530		HeNe1 100%	Ar 10% of 50%	
02-Oct-01	744.17_IID	30 day filtration/relaxation expt	LP560	BP 505-530		HeNe1 100%	Ar 10% of 50%	
02-Oct-01	744.17_IID	30 day filtration/relaxation expt	LP560	BP 505-530		HeNe1 100%	Ar 10% of 50%	

Appendix D: Preliminary Study - CLSM Image Data

Date	File Name	Specimen	Pinhole (um)		Detector Gain		Amplitude Offset		Amplitude Gain	
			Ch 1	Ch 2	Ch 1	Ch 2	Ch 1	Ch 2	Ch 1	Ch 2
29-Mar-01	controlMar29	clean membrane sample	1000		?		?		?	
05-Jul-01	Test1	test membrane sample	65	60	?	?	?	?	?	?
05-Jul-01	Test2	test membrane sample	65	60	?	?	?	?	?	?
05-Jul-01	Test3	test membrane sample	65	60	?	?	?	?	?	?
05-Jul-01	wholemembrane	test membrane sample	65	60	?	?	?	?	?	?
10-Jul-01	xsection	test membrane sample	65	60	?	?	?	?	?	?
17-Jul-01	clean_xsection	clean membrane sample	78		?		?		?	
17-Jul-01	clean_xsection2	clean membrane sample	78		?		?		?	
17-Jul-01	clean_xsection3	clean membrane sample	68		?		?		?	
17-Jul-01	clean_xsection4	clean membrane sample	68		?		?		?	
17-Jul-01	clean_xsection5	clean membrane sample	76	56	?	?	?	?	?	?
17-Jul-01	clean_xsection6	clean membrane sample	166		?		?		?	
17-Jul-01	clean_xsection7	clean membrane sample	214		?		?		?	
17-Jul-01	clean_xsection8	clean membrane sample	153		?		?		?	
17-Jul-01	clean_zstack	clean membrane sample	158		?		?		?	
29-Aug-01	Sample2	3 day filtration/relaxation expt	57		793		-0.0670		1	
29-Aug-01	Sample2b	3 day filtration/relaxation expt	142		931		-0.0675		1	
29-Aug-01	Sample2c	3 day filtration/relaxation expt	142		931		-0.0425		1	
30-Aug-01	Sample2d	3 day filtration/relaxation expt	153		744		-0.0690		1	
30-Aug-01	Sample2e	3 day filtration/relaxation expt	153		744		-0.0690		1	
30-Aug-01	Sample3a	3 day filtration/relaxation expt	169		795		-0.0690		1.54	
30-Aug-01	Sample3b	3 day filtration/relaxation expt	169		818		-0.0470		1	
28-Sep-01	744.13_single1	30 day filtration/relaxation expt	57		965		-0.1495		1	
28-Sep-01	744.13ds_single	30 day filtration/relaxation expt	166	146	860	933	-0.1080	-0.0900	1.05	1
28-Sep-01	744.13ds_single2	30 day filtration/relaxation expt	166	146	785	893	0.0220	-0.0150	1	1
28-Sep-01	744.13ds_single3	30 day filtration/relaxation expt	166	146	817	1000	-0.1120	-0.0990	1	1
28-Sep-01	744.17ds_single1	30 day filtration/relaxation expt	110	209	981	860	-1.0565	-0.6665	1.57	1.68
28-Sep-01	744.17ds_stack	30 day filtration/relaxation expt	165	146	770	924	-0.0590	-0.0815	1	1.47
02-Oct-01	744.17_Iia	30 day filtration/relaxation expt	167	146	688	896	-0.0600	-0.0620	1	1
02-Oct-01	744.17_Iia_zstack	30 day filtration/relaxation expt	167	146	688	896	-0.0600	-0.0620	1	1
02-Oct-01	744.17_IIB	30 day filtration/relaxation expt	167	146	707	929	-0.1180	-0.1140	1	1
02-Oct-01	744.17_IIB	30 day filtration/relaxation expt		153		719		-0.0970		1
02-Oct-01	744.17_IIB	30 day filtration/relaxation expt	166	146	725	903	-0.0890	-0.1490	1	1.4
02-Oct-01	744.17_IIB	30 day filtration/relaxation expt	166	146	725	903	-0.0890	-0.1490	1	1.4
02-Oct-01	744.17_IIC	30 day filtration/relaxation expt	166	146	719	747	-0.0640	-0.0990	1	1.8
02-Oct-01	744.17_IIC	30 day filtration/relaxation expt	166	146	719	747	-0.0640	-0.0990	1	1.8
02-Oct-01	744.17_IID	30 day filtration/relaxation expt	166	146	750	871	-0.0655	-0.0520	1	1
02-Oct-01	744.17_IID	30 day filtration/relaxation expt	166	146	750	871	-0.0655	-0.0520	1	1

Appendix D: Preliminary Study - CLSM Image Data

Date	File Name	Specimen	Z-step size (um)	# of Z sections	Total Z depth (um)
29-Mar-01	controlMar29	clean membrane sample			
05-Jul-01	Test1	test membrane sample			71.00
05-Jul-01	Test2	test membrane sample			189.00
05-Jul-01	Test3	test membrane sample			
05-Jul-01	wholemembrane	test membrane sample			68.30
10-Jul-01	xsection	test membrane sample			42.00
17-Jul-01	clean_xsection	clean membrane sample			
17-Jul-01	clean_xsection2	clean membrane sample			
17-Jul-01	clean_xsection3	clean membrane sample			
17-Jul-01	clean_xsection4	clean membrane sample			
17-Jul-01	clean_xsection5	clean membrane sample			
17-Jul-01	clean_xsection6	clean membrane sample			
17-Jul-01	clean_xsection7	clean membrane sample			
17-Jul-01	clean_xsection8	clean membrane sample			
17-Jul-01	clean_zstack	clean membrane sample			30.50
29-Aug-01	Sample2	3 day filtration/relaxation expt			
29-Aug-01	Sample2b	3 day filtration/relaxation expt			
29-Aug-01	Sample2c	3 day filtration/relaxation expt	1.00	22	21.00
30-Aug-01	Sample2d	3 day filtration/relaxation expt			
30-Aug-01	Sample2e	3 day filtration/relaxation expt	1.10	18	19.80
30-Aug-01	Sample3a	3 day filtration/relaxation expt			
30-Aug-01	Sample3b	3 day filtration/relaxation expt	1.00	24	23.00
28-Sep-01	744.13_single1	30 day filtration/relaxation expt			
28-Sep-01	744.13ds_single	30 day filtration/relaxation expt			
28-Sep-01	744.13ds_single2	30 day filtration/relaxation expt			
28-Sep-01	744.13ds_single3	30 day filtration/relaxation expt			
28-Sep-01	744.17ds_single1	30 day filtration/relaxation expt			
28-Sep-01	744.17ds_stack	30 day filtration/relaxation expt	1.00	23	22.00
02-Oct-01	744.17_Iia	30 day filtration/relaxation expt			
02-Oct-01	744.17_Iia_zstack	30 day filtration/relaxation expt	0.80	20	15.20
02-Oct-01	744.17_IIB	30 day filtration/relaxation expt			
02-Oct-01	744.17_IIB	30 day filtration/relaxation expt			
02-Oct-01	744.17_IIB	30 day filtration/relaxation expt			
02-Oct-01	744.17_IIB	30 day filtration/relaxation expt	1.00	28	27.00
02-Oct-01	744.17_IIC	30 day filtration/relaxation expt			
02-Oct-01	744.17_IIC	30 day filtration/relaxation expt	1	36	35.00
02-Oct-01	744.17_IID	30 day filtration/relaxation expt			
02-Oct-01	744.17_IID	30 day filtration/relaxation expt	1	36	35.00

Appendix D: Preliminary Study - CLSM Image Data

Date	File Name	Specimen	Obj/NA	Averaging	Zoom	Speed (us/pixel)	Image Size	
							Pixels	Microns
04-Oct-01	744.17_Ia	30 day filtration/relaxation expt	63X/0.9 W	2	0.7	35.84	512 x 512	146.2 x 146.2
04-Oct-01	744.17_Ia_stack	30 day filtration/relaxation expt	63X/0.9 W	2	0.7	8.96	512 x 512	146.2 x 146.2
04-Oct-01	744.17_Ib	30 day filtration/relaxation expt	63X/0.9 W	2	1.2		512 x 512	146.2 x 146.2
04-Oct-01	744.17_Ic	30 day filtration/relaxation expt	63X/0.9 W	1	1	8.96	512 x 512	146.2 x 146.2
04-Oct-01	744.17_Ic_stack	30 day filtration/relaxation expt	63X/0.9 W	1	1	8.96	512 x 512	146.2 x 146.2
04-Oct-01	744.17_Id	30 day filtration/relaxation expt	63X/0.9 W	2	1.3	35.84	512 x 512	146.2 x 146.2
04-Oct-01	744.17_Ie	30 day filtration/relaxation expt	63X/0.9 W	2	1.2	35.84	512 x 512	146.2 x 146.2
04-Oct-01	744.13_Ia_zstack	30 day filtration/relaxation expt	63X/0.9 W	2	1	35.84	512 x 512	146.2 x 146.2
25-Oct-01	744.13_stack_50uL	30 day filtration/relaxation expt - 50uL/mL	63X/0.9 W	2	1	8.96	512 x 512	146.2 x 146.2
25-Oct-01	744.13_stack_50uL1	30 day filtration/relaxation expt - 50uL/mL	63X/0.9 W	2	1	8.96	512 x 512	146.2 x 146.2
25-Oct-01	744.13_single_50uL	30 day filtration/relaxation expt - 50uL/mL	63X/0.9 W	4	1	35.84	512 x 512	146.2 x 146.2
25-Oct-01	744.13c_stack_50uL	30 day filtration/relaxation expt - 50uL/mL	63X/0.9 W	1	1	8.96	512 x 512	146.2 x 146.2
26-Oct-01	744.8_stack_20ul	3 day filtration/relaxation expt - 20uL/mL	63X/0.9 W	2	0.7	8.96	512 x 512	146.2 x 146.2
26-Oct-01	744.8b_stack_20ul	3 day filtration/relaxation expt - 20uL/mL	63X/0.9 W	2	1	8.96	512 x 512	146.2 x 146.2
26-Oct-01	744.8c_stack_20ul	3 day filtration/relaxation expt - 20uL/mL	63X/0.9 W	2	1	8.96	512 x 512	146.2 x 146.2
05-Nov-01	744.12_stack1	69 day filtration/relaxation	63X/0.9 W	2	0.7	8.96	512 x 512	146.2 x 146.2
05-Nov-01	744.12_stack2	69 day filtration/relaxation	63X/0.9 W	2	1	8.96	512 x 512	146.2 x 146.2
05-Nov-01	744.10_stack1	69 day filtration/relaxation	63X/0.9 W	2	0.7	8.96	512 x 512	146.2 x 146.2
05-Nov-01	744.10_stack2	69 day filtration/relaxation	63X/0.9 W	2	1	8.96	512 x 512	146.2 x 146.2
06-Nov-01	744.10_stack1	69 day filtration/relaxation	63X/0.9 W	2	0.7	8.96	512 x 512	146.2 x 146.2
06-Nov-01	744.10_stack2	69 day filtration/relaxation	63X/0.9 W	2	0.7	8.96	512 x 512	146.2 x 146.2
06-Nov-01	744.10_stack3	69 day filtration/relaxation	63X/0.9 W	2	0.7	8.96	512 x 512	146.2 x 146.2
06-Nov-01	744.10_stack4	69 day filtration/relaxation	63X/0.9 W	2	1	8.96	512 x 512	146.2 x 146.2
06-Nov-01	744.10_stack5	69 day filtration/relaxation	63X/0.9 W	2	0.7	8.96	512 x 512	146.2 x 146.2
06-Nov-01	744.10_stack6	69 day filtration/relaxation	63X/0.9 W	2	0.7	8.96	512 x 512	146.2 x 146.2
06-Nov-01	744.10_stack7	69 day filtration/relaxation	63X/0.9 W	2	0.7	8.96	512 x 512	146.2 x 146.2
06-Nov-01	744.10_stack8	69 day filtration/relaxation	63X/0.9 W	2	0.7	8.96	512 x 512	146.2 x 146.2
06-Nov-01	744.10_stack9	69 day filtration/relaxation	63X/0.9 W	2	0.7	8.96	512 x 512	146.2 x 146.2
07-Nov-01	744.10_single1	69 day filtration/relaxation	63X/0.9 W	2	1	35.84	512 x 512	146.2 x 146.2
07-Nov-01	744.10_single2	69 day filtration/relaxation	63X/0.9 W	2	1	35.84	512 x 512	146.2 x 146.2
07-Nov-01	744.10_stack1	69 day filtration/relaxation	63X/0.9 W	2	0.7	8.96	512 x 512	146.2 x 146.2
07-Nov-01	744.10_single1_BS	69 day filtration/relaxation	63X/0.9 W	2	1	35.84	512 x 512	146.2 x 146.2
09-Nov-01	744.10_stack1	69 day filtration/relaxation	63X/0.9 W	2	0.7	35.84	512 x 512	146.2 x 146.2
09-Nov-01	744.10_stack2	69 day filtration/relaxation	63X/0.9 W	2	0.7	35.84	512 x 512	146.2 x 146.2
09-Nov-01	744.10_stack3	69 day filtration/relaxation	63X/0.9 W	2	0.7	35.84	512 x 512	146.2 x 146.2
09-Nov-01	744.10_single1	69 day filtration/relaxation	63X/0.9 W	2	0.7	8.96	512 x 512	146.2 x 146.2
09-Nov-01	744.10_single2	69 day filtration/relaxation	10X/0.25	2	0.7	8.96	512 x 512	146.2 x 146.2
09-Nov-01	744.10_stack4	69 day filtration/relaxation	63X/0.9 W	2	0.7	35.84	512 x 512	206.8 x 206.8
09-Nov-01	744.10_stack5	69 day filtration/relaxation	63X/0.9 W	2	0.7	35.84	512 x 512	206.8 x 206.8
09-Nov-01	744.10_single3	69 day filtration/relaxation	63X/0.9 W	2	0.7	8.96	512 x 512	206.8 x 206.8
09-Nov-01	744.10_stack6	69 day filtration/relaxation	63X/0.9 W	2	0.7	35.84	512 x 512	206.8 x 206.8
Nov 10_FITC	744.10_single1	69 day filtration/relaxation	63X/1.2 W corr	2	2.6	35.84	512 x 512	57.2 x 57.2

Appendix D: Preliminary Study - CLSM Image Data

Date	File Name	Specimen	Dye/Lectin			Abs/Ex λ		
			Ch 1	Ch 2	Ch 3	Ch 1	Ch 2	Ch 3
04-Oct-01	744.17_Ia	30 day filtration/relaxation expt	WGA-tmr	ConA-Fl		555/580	494/518	
04-Oct-01	744.17_Ia_stack	30 day filtration/relaxation expt	WGA-tmr	ConA-Fl		555/580	494/518	
04-Oct-01	744.17_Ib	30 day filtration/relaxation expt	WGA-tmr	ConA-Fl		555/580	494/518	
04-Oct-01	744.17_Ic	30 day filtration/relaxation expt	WGA-tmr	ConA-Fl		555/580	494/518	
04-Oct-01	744.17_Ic_stack	30 day filtration/relaxation expt	WGA-tmr	ConA-Fl		555/580	494/518	
04-Oct-01	744.17_Id	30 day filtration/relaxation expt	WGA-tmr	ConA-Fl		555/580	494/518	
04-Oct-01	744.17_Ie	30 day filtration/relaxation expt	WGA-tmr	ConA-Fl		555/580	494/518	
04-Oct-01	744.13_Ia_zstack	30 day filtration/relaxation expt	WGA-tmr	ConA-Fl		555/580	494/518	
25-Oct-01	744.13_stack_50uL	30 day filtration/relaxation expt - 50uL/mL	BS-I-TRITC			554/576		
25-Oct-01	744.13_stack_50uL1	30 day filtration/relaxation expt - 50uL/mL	BS-I-TRITC			554/576		
25-Oct-01	744.13_single_50uL	30 day filtration/relaxation expt - 50uL/mL	BS-I-TRITC			554/576		
25-Oct-01	744.13c_stack_50uL	30 day filtration/relaxation expt - 50uL/mL	BS-I-TRITC			554/576		
26-Oct-01	744.8_stack_20ul	3 day filtration/relaxation expt - 20uL/mL	BS-I-TRITC			554/576		
26-Oct-01	744.8b_stack_20ul	3 day filtration/relaxation expt - 20uL/mL	BS-I-TRITC			554/576		
26-Oct-01	744.8c_stack_20ul	3 day filtration/relaxation expt - 20uL/mL	BS-I-TRITC			554/576		
05-Nov-01	744.12_stack1	69 day filtration/relaxation	BS-I-TRITC	WGA-TR	ConA-Fl	554/576	595/615	494/518
05-Nov-01	744.12_stack2	69 day filtration/relaxation	BS-I-TRITC	WGA-TR	ConA-Fl	554/576	595/615	494/518
05-Nov-01	744.10_stack1	69 day filtration/relaxation	BS-I-TRITC	WGA-TR	ConA-Fl	554/576	595/615	494/518
05-Nov-01	744.10_stack2	69 day filtration/relaxation	BS-I-TRITC	WGA-TR	ConA-Fl	554/576	595/615	494/518
06-Nov-01	744.10_stack1	69 day filtration/relaxation			ConA-Fl			494/518
06-Nov-01	744.10_stack2	69 day filtration/relaxation			ConA-Fl			494/518
06-Nov-01	744.10_stack3	69 day filtration/relaxation			ConA-Fl			494/518
06-Nov-01	744.10_stack4	69 day filtration/relaxation			ConA-Fl			494/518
06-Nov-01	744.10_stack5	69 day filtration/relaxation		WGA-TR			595/615	
06-Nov-01	744.10_stack6	69 day filtration/relaxation		WGA-TR			595/615	
06-Nov-01	744.10_stack7	69 day filtration/relaxation		WGA-TR			595/615	
06-Nov-01	744.10_stack8	69 day filtration/relaxation		WGA-TR			595/615	
06-Nov-01	744.10_stack9	69 day filtration/relaxation		WGA-TR			595/615	
07-Nov-01	744.10_single1	69 day filtration/relaxation		WGA-TR			595/615	
07-Nov-01	744.10_single2	69 day filtration/relaxation		WGA-TR	FITC settings		595/615	
07-Nov-01	744.10_stack1	69 day filtration/relaxation	BS-I-TRITC			554/576		
07-Nov-01	744.10_single1_BS	69 day filtration/relaxation	BS-I-TRITC		FITC settings	554/576		
09-Nov-01	744.10_stack1	69 day filtration/relaxation			ConA-Fl			494/518
09-Nov-01	744.10_stack2	69 day filtration/relaxation			ConA-Fl			494/518
09-Nov-01	744.10_stack3	69 day filtration/relaxation			ConA-Fl			494/518
09-Nov-01	744.10_single1	69 day filtration/relaxation		Rhodamine settin	ConA-Fl			494/518
09-Nov-01	744.10_single2	69 day filtration/relaxation		WGA-TR			595/615	
09-Nov-01	744.10_stack4	69 day filtration/relaxation		WGA-TR			595/615	
09-Nov-01	744.10_stack5	69 day filtration/relaxation		WGA-TR			595/615	
09-Nov-01	744.10_single3	69 day filtration/relaxation		WGA-TR			595/615	
09-Nov-01	744.10_stack6	69 day filtration/relaxation		WGA-TR			595/615	
Nov 10_FITC	744.10_single1	69 day filtration/relaxation			FITC			494/518

Appendix D: Preliminary Study - CLSM Image Data

Date	File Name	Specimen	Filters			Laser Power		
			Ch 1	Ch2	Ch 3	Ch 1	Ch 2	Ch 3
04-Oct-01	744.17_Ia	30 day filtration/relaxation expt	LP560	BP 505-530		HeNe1 100%	Ar 10% of 50%	
04-Oct-01	744.17_Ia_stack	30 day filtration/relaxation expt	LP560	BP 505-530		HeNe1 100%	Ar 10% of 50%	
04-Oct-01	744.17_Ib	30 day filtration/relaxation expt	LP560	BP 505-530		HeNe1 100%	Ar 10% of 50%	
04-Oct-01	744.17_Ic	30 day filtration/relaxation expt	LP560	BP 505-530		HeNe1 100%	Ar 10% of 50%	
04-Oct-01	744.17_Ic_stack	30 day filtration/relaxation expt	LP560	BP 505-530		HeNe1 100%	Ar 22.4% of 50%	
04-Oct-01	744.17_Id	30 day filtration/relaxation expt	LP560	BP 505-530		HeNe1 100%	Ar 20% of 50%	
04-Oct-01	744.17_Ie	30 day filtration/relaxation expt	LP560	BP 505-530		HeNe1 100%	Ar 20% of 50%	
04-Oct-01	744.13_Ia_zstack	30 day filtration/relaxation expt	LP560	BP 505-530		HeNe1 100%	Ar 10% of 50%	
25-Oct-01	744.13_stack_50uL	30 day filtration/relaxation expt - 50uL/mL	LP560			HeNe1 100%		
25-Oct-01	744.13_stack_50uL1	30 day filtration/relaxation expt - 50uL/mL	LP560			HeNe1 100%		
25-Oct-01	744.13_single_50uL	30 day filtration/relaxation expt - 50uL/mL	LP560			HeNe1 100%		
25-Oct-01	744.13c_stack_50uL	30 day filtration/relaxation expt - 50uL/mL	LP560			HeNe1 100%		
26-Oct-01	744.8_stack_20ul	3 day filtration/relaxation expt - 20uL/mL	LP560			HeNe1 100%		
26-Oct-01	744.8b_stack_20ul	3 day filtration/relaxation expt - 20uL/mL	LP560			HeNe1 100%		
26-Oct-01	744.8c_stack_20ul	3 day filtration/relaxation expt - 20uL/mL	LP560			HeNe1 100%		
05-Nov-01	744.12_stack1	69 day filtration/relaxation	LP560	LP560	BP 505-530	HeNe1 100%	HeNe1 100%	Ar 10% of 50%
05-Nov-01	744.12_stack2	69 day filtration/relaxation	LP560	LP560	BP 505-530	HeNe1 100%	HeNe1 100%	Ar 10% of 50%
05-Nov-01	744.10_stack1	69 day filtration/relaxation	LP560	LP560	BP 505-530	HeNe1 100%	HeNe1 100%	Ar 10% of 50%
05-Nov-01	744.10_stack2	69 day filtration/relaxation	LP560	LP560	BP 505-530	HeNe1 100%	HeNe1 100%	Ar 10% of 50%
06-Nov-01	744.10_stack1	69 day filtration/relaxation			LP 505			Ar 10% of 50%
06-Nov-01	744.10_stack2	69 day filtration/relaxation			LP 505			Ar 10% of 50%
06-Nov-01	744.10_stack3	69 day filtration/relaxation			LP 505			Ar 10% of 50%
06-Nov-01	744.10_stack4	69 day filtration/relaxation			LP 505			Ar 10% of 50%
06-Nov-01	744.10_stack5	69 day filtration/relaxation		LP560			HeNe1 100%	
06-Nov-01	744.10_stack6	69 day filtration/relaxation		LP560			HeNe1 100%	
06-Nov-01	744.10_stack7	69 day filtration/relaxation		LP560			HeNe1 100%	
06-Nov-01	744.10_stack8	69 day filtration/relaxation		LP560			HeNe1 100%	
06-Nov-01	744.10_stack9	69 day filtration/relaxation		LP560			HeNe1 100%	
07-Nov-01	744.10_single1	69 day filtration/relaxation		LP560			HeNe1 100%	
07-Nov-01	744.10_single2	69 day filtration/relaxation		LP560	BP 505-530		HeNe1 100%	Ar 10% of 50%
07-Nov-01	744.10_stack1	69 day filtration/relaxation	LP560			HeNe1 100%		
07-Nov-01	744.10_single1_BS	69 day filtration/relaxation	LP560		BP 505-530	HeNe1 100%		Ar 10% of 50%
09-Nov-01	744.10_stack1	69 day filtration/relaxation			LP 505			Ar 10% of 50%
09-Nov-01	744.10_stack2	69 day filtration/relaxation			LP 505			Ar 10% of 50%
09-Nov-01	744.10_stack3	69 day filtration/relaxation			LP 505			Ar 10% of 50%
09-Nov-01	744.10_single1	69 day filtration/relaxation		LP560	LP 505		HeNe1 100%	Ar 10% of 50%
09-Nov-01	744.10_single2	69 day filtration/relaxation		LP560			HeNe1 100%	
09-Nov-01	744.10_stack4	69 day filtration/relaxation		LP560			HeNe1 100%	
09-Nov-01	744.10_stack5	69 day filtration/relaxation		LP560			HeNe1 100%	
09-Nov-01	744.10_single3	69 day filtration/relaxation		LP560			HeNe1 100%	
09-Nov-01	744.10_stack6	69 day filtration/relaxation		LP560			HeNe1 100%	
Nov 10_FITC	744.10_single1	69 day filtration/relaxation			BP 505			Ar 10% of 50%

Appendix D: Preliminary Study - CLSM Image Data

Date	File Name	Specimen	Pinhole (um)		Detector Gain		Amplitude Offset		Amplitude Gain	
			Ch 1	Ch 2	Ch 1	Ch 2	Ch 1	Ch 2	Ch 1	Ch 2
04-Oct-01	744.17_Ia	30 day filtration/relaxation expt	164	147	764	931	-0.0470	-0.0740	1	1.3
04-Oct-01	744.17_Ia_stack	30 day filtration/relaxation expt	164	147	764	931	-0.0470	-0.0740	1	1.3
04-Oct-01	744.17_Ib	30 day filtration/relaxation expt	164	147	896	1000	-0.2920	-0.2415	1.06	1.39
04-Oct-01	744.17_Ic	30 day filtration/relaxation expt	164	147	761	820	-0.6300	-0.4700	1	1.28
04-Oct-01	744.17_Ic_stack	30 day filtration/relaxation expt	164	147	761	820	-0.6300	-0.4700	1	1.28
04-Oct-01	744.17_Id	30 day filtration/relaxation expt	164	147	862	967	-0.3160	-0.2175	1	1
04-Oct-01	744.17_Ie	30 day filtration/relaxation expt	164	147	855	938	-0.2600	-0.1655	1	1.3
04-Oct-01	744.13_Ia_zstack	30 day filtration/relaxation expt	165	150	803	905	-0.2835	-0.2615	1.43	1.56
25-Oct-01	744.13_stack_50uL	30 day filtration/relaxation expt - 50uL/mL	167		668		-0.0250		1.46	
25-Oct-01	744.13_stack_50uL1	30 day filtration/relaxation expt - 50uL/mL	167		763		-0.0740		1.46	
25-Oct-01	744.13_single_50uL	30 day filtration/relaxation expt - 50uL/mL	162		1000		-0.1020		1.3	
25-Oct-01	744.13c_stack_50uL	30 day filtration/relaxation expt - 50uL/mL	167		887		-0.0340		1.47	
26-Oct-01	744.8_stack_20ul	3 day filtration/relaxation expt - 20uL/mL	164		888		-0.0525		1	
26-Oct-01	744.8b_stack_20ul	3 day filtration/relaxation expt - 20uL/mL	164		644		-0.0770		1.4	
26-Oct-01	744.8c_stack_20ul	3 day filtration/relaxation expt - 20uL/mL	164		833		-0.0440		1	
05-Nov-01	744.12_stack1	69 day filtration/relaxation	161	145	670	770	-0.0440	-0.0340	1.04	1
05-Nov-01	744.12_stack2	69 day filtration/relaxation	161	143	675	760	-0.1730	-0.120	1	1
05-Nov-01	744.10_stack1	69 day filtration/relaxation	160	145	627	747	-0.044	-0.022	1	1
05-Nov-01	744.10_stack2	69 day filtration/relaxation	160	145	615	747	-0.038	-0.022	1	1
06-Nov-01	744.10_stack1	69 day filtration/relaxation		145		642		-0.049		1
06-Nov-01	744.10_stack2	69 day filtration/relaxation		145		640		-0.025		1
06-Nov-01	744.10_stack3	69 day filtration/relaxation		145		566		-0.047		1
06-Nov-01	744.10_stack4	69 day filtration/relaxation		145		611		-0.0415		1.01
06-Nov-01	744.10_stack5	69 day filtration/relaxation	163		647		-0.044		1	
06-Nov-01	744.10_stack6	69 day filtration/relaxation	163		670		-0.049		1	
06-Nov-01	744.10_stack7	69 day filtration/relaxation	163		704		-0.044		1	
06-Nov-01	744.10_stack8	69 day filtration/relaxation	163		679		-0.047		1	
06-Nov-01	744.10_stack9	69 day filtration/relaxation	163		684		-0.044		1	
07-Nov-01	744.10_single1	69 day filtration/relaxation	160		868		-0.097		1	
07-Nov-01	744.10_single2	69 day filtration/relaxation	163	147	737	864	-0.1990	-0.1340	1	1
07-Nov-01	744.10_stack1	69 day filtration/relaxation	163		610		-0.0815		1.66	
07-Nov-01	744.10_single1_BS	69 day filtration/relaxation	160	147	741	842	-0.1535	-0.1125	1	1
09-Nov-01	744.10_stack1	69 day filtration/relaxation		150		643		-0.0440		1
09-Nov-01	744.10_stack2	69 day filtration/relaxation		150		643		-0.0440		1
09-Nov-01	744.10_stack3	69 day filtration/relaxation		150		624		-0.0420		1
09-Nov-01	744.10_single1	69 day filtration/relaxation	163	145	640	783	-0.1390	-0.1310		1
09-Nov-01	744.10_single2	69 day filtration/relaxation	90		769		-0.049		1	
09-Nov-01	744.10_stack4	69 day filtration/relaxation	165		650		-0.09		1	
09-Nov-01	744.10_stack5	69 day filtration/relaxation	165		705		-0.047		1	
09-Nov-01	744.10_single3	69 day filtration/relaxation	165		633		-0.042		1	
09-Nov-01	744.10_stack6	69 day filtration/relaxation	165		633		-0.042		1	
Nov 10_FITC	744.10_single1	69 day filtration/relaxation		110	726		-0.1740		1	

Appendix D: Preliminary Study - CLSM Image Data

Date	File Name	Specimen	Z-step size (um)	# of Z sections	Total Z depth (um)
04-Oct-01	744.17_Ia	30 day filtration/relaxation expt			
04-Oct-01	744.17_Ia_stack	30 day filtration/relaxation expt	0.95	36	33.25
04-Oct-01	744.17_Ib	30 day filtration/relaxation expt			
04-Oct-01	744.17_Ic	30 day filtration/relaxation expt			
04-Oct-01	744.17_Ic_stack	30 day filtration/relaxation expt	0.95	18	17.10
04-Oct-01	744.17_Id	30 day filtration/relaxation expt			
04-Oct-01	744.17_Ie	30 day filtration/relaxation expt			
04-Oct-01	744.13_Ia_zstack	30 day filtration/relaxation expt			
25-Oct-01	744.13_stack_50uL	30 day filtration/relaxation expt - 50uL/mL	2.00	40	78.00
25-Oct-01	744.13_stack_50uL1	30 day filtration/relaxation expt - 50uL/mL	0.75	23	16.50
25-Oct-01	744.13_single_50uL	30 day filtration/relaxation expt - 50uL/mL			
25-Oct-01	744.13c_stack_50uL	30 day filtration/relaxation expt - 50uL/mL	1.50	39	57.00
26-Oct-01	744.8_stack_20ul	3 day filtration/relaxation expt - 20uL/mL	0.85	26	21.25
26-Oct-01	744.8b_stack_20ul	3 day filtration/relaxation expt - 20uL/mL	0.85	26	21.25
26-Oct-01	744.8c_stack_20ul	3 day filtration/relaxation expt - 20uL/mL	0.90	31	27.00
05-Nov-01	744.12_stack1	69 day filtration/relaxation	1.00	37	36.00
05-Nov-01	744.12_stack2	69 day filtration/relaxation	0.90	29	26.10
05-Nov-01	744.10_stack1	69 day filtration/relaxation	0.95	36	33.25
05-Nov-01	744.10_stack2	69 day filtration/relaxation	0.70	37	25.20
06-Nov-01	744.10_stack1	69 day filtration/relaxation	1.00	40	39.00
06-Nov-01	744.10_stack2	69 day filtration/relaxation	0.75	27	19.50
06-Nov-01	744.10_stack3	69 day filtration/relaxation	0.65	26	16.25
06-Nov-01	744.10_stack4	69 day filtration/relaxation	1.00	25	24.00
06-Nov-01	744.10_stack5	69 day filtration/relaxation	0.90	38	33.30
06-Nov-01	744.10_stack6	69 day filtration/relaxation	0.70	39	26.60
06-Nov-01	744.10_stack7	69 day filtration/relaxation	1.00	34	33.00
06-Nov-01	744.10_stack8	69 day filtration/relaxation	0.75	40	29.25
06-Nov-01	744.10_stack9	69 day filtration/relaxation	0.70	39	26.60
07-Nov-01	744.10_single1	69 day filtration/relaxation			
07-Nov-01	744.10_single2	69 day filtration/relaxation			
07-Nov-01	744.10_stack1	69 day filtration/relaxation	0.65	28	17.55
07-Nov-01	744.10_single1_BS	69 day filtration/relaxation			
09-Nov-01	744.10_stack1	69 day filtration/relaxation	1.00	24	23.00
09-Nov-01	744.10_stack2	69 day filtration/relaxation	1.30	35	44.20
09-Nov-01	744.10_stack3	69 day filtration/relaxation	1.00	27	26.00
09-Nov-01	744.10_single1	69 day filtration/relaxation			
09-Nov-01	744.10_single2	69 day filtration/relaxation			
09-Nov-01	744.10_stack4	69 day filtration/relaxation	0.70	22	14.70
09-Nov-01	744.10_stack5	69 day filtration/relaxation	0.95	22	19.95
09-Nov-01	744.10_single3	69 day filtration/relaxation			
09-Nov-01	744.10_stack6	69 day filtration/relaxation	0.95	20	18.05
Nov 10_FITC	744.10_single1	69 day filtration/relaxation			

Appendix D: Preliminary Study - CLSM Image Data

Date	File Name	Specimen	Obj/NA	Averaging	Zoom	Speed (us/pixel)	Image Size	
							Pixels	Microns
Nov 10_FITC	744.10_stack1	69 day filtration/relaxation	63X/1.2 W corr	2	2.6	35.84	512 x 512	57.2 x 57.2
Nov 10_FITC	744.10_stack2	69 day filtration/relaxation	63X/1.2 W corr	2	4	35.84	512 x 512	36.6 x 36.6
Nov14_BSII	744.10_single1	69 day filtration/relaxation	63X/1.2 W corr	2	0.7	35.84	512 x 512	206.8 x 206.8
Nov14_BSII	744.10_stack1	69 day filtration/relaxation	63X/1.2 W corr	2	2	8.96	512 x 512	73.1 x 73.1
Nov14_BSII	744.10_stack2	69 day filtration/relaxation	63X/1.2 W corr	2	1	8.96	512 x 512	146.2 x 146.2
Nov14_BSII	744.10_stack3	69 day filtration/relaxation	63X/1.2 W corr	2	1	8.96	512 x 512	146.2 x 146.2
Nov14_BSII	744.10_stack4	69 day filtration/relaxation	63X/1.2 W corr	2	0.7	8.96	512 x 512	206.8 x 206.8
Nov14_nostain	744.10_single1	69 day filtration/relaxation	10X/0.25	4	0.7	71.68	512 x 512	1277.1 x 1277.1
Nov14_nostain	744.10_single2	69 day filtration/relaxation	63X/1.2 W corr	4	3.5	71.68	512 x 512	41.8 x 41.8
Nov14_nostain	744.10_stack1	69 day filtration/relaxation	63X/1.2 W corr	2	3.5	17.92	512 x 512	41.8 x 41.8
Nov20_WGA	744.10_single1	69 day filtration/relaxation	63X/1.2 W corr	2	0.7	35.84	512 x 512	206.8 x 206.8
Nov20_WGA	744.10_single2	69 day filtration/relaxation	63X/1.2 W corr	2	2.4	35.84	512 x 512	61.3 x 61.3
Nov20_WGA	744.10_stack1	69 day filtration/relaxation	63X/1.2 W corr	2	2.4	8.96	512 x 512	61.3 x 61.3
Nov20_WGA	744.10_stack2	69 day filtration/relaxation	63X/1.2 W corr	2	1.1	8.96	512 x 512	132.5 x 132.5
Nov20_WGA	744.10_stack3	69 day filtration/relaxation	63X/1.2 W corr	2	2	8.96	512 x 512	73.1 x 73.1
Nov20_WGA	744.10_stack4	69 day filtration/relaxation	63X/1.2 W corr	2	2.2	8.96	512 x 512	66.8 x 66.8

Appendix D: Preliminary Study - CLSM Image Data

Date	File Name	Specimen	Dye/Lectin			Abs/Ex λ		
			Ch 1	Ch 2	Ch 3	Ch 1	Ch 2	Ch 3
Nov 10_FITC	744.10_stack1	69 day filtration/relaxation			FITC			494/518
Nov 10_FITC	744.10_stack2	69 day filtration/relaxation			FITC			494/518
Nov14_BSII	744.10_single1	69 day filtration/relaxation			BS-II-FITC			494/518
Nov14_BSII	744.10_stack1	69 day filtration/relaxation			BS-II-FITC			494/518
Nov14_BSII	744.10_stack2	69 day filtration/relaxation			BS-II-FITC			494/518
Nov14_BSII	744.10_stack3	69 day filtration/relaxation			BS-II-FITC			494/518
Nov14_BSII	744.10_stack4	69 day filtration/relaxation			BS-II-FITC			494/518
Nov14_nostain	744.10_single1	69 day filtration/relaxation	none				none	
Nov14_nostain	744.10_single2	69 day filtration/relaxation	none				none	
Nov14_nostain	744.10_stack1	69 day filtration/relaxation	none				none	
Nov20_WGA	744.10_single1	69 day filtration/relaxation	WGA-tmr	FITC Settings		555/580		
Nov20_WGA	744.10_single2	69 day filtration/relaxation	WGA-tmr	FITC Settings		555/580		
Nov20_WGA	744.10_stack1	69 day filtration/relaxation	WGA-tmr	FITC Settings		555/580		
Nov20_WGA	744.10_stack2	69 day filtration/relaxation	WGA-tmr	FITC Settings		555/580		
Nov20_WGA	744.10_stack3	69 day filtration/relaxation	WGA-tmr	FITC Settings		555/580		
Nov20_WGA	744.10_stack4	69 day filtration/relaxation	WGA-tmr	FITC Settings		555/580		

Appendix D: Preliminary Study - CLSM Image Data

Date	File Name	Specimen	Filters			Laser Power		
			Ch 1	Ch2	Ch 3	Ch 1	Ch 2	Ch 3
Nov 10_FITC	744.10_stack1	69 day filtration/relaxation			BP 505			Ar 10% of 50%
Nov 10_FITC	744.10_stack2	69 day filtration/relaxation			BP 505			Ar 10% of 50%
Nov14_BSII	744.10_single1	69 day filtration/relaxation			BP 505			Ar 10% of 50%
Nov14_BSII	744.10_stack1	69 day filtration/relaxation			BP 505			Ar 10% of 50%
Nov14_BSII	744.10_stack2	69 day filtration/relaxation			BP 505			Ar 10% of 50%
Nov14_BSII	744.10_stack3	69 day filtration/relaxation			BP 505			Ar 10% of 50%
Nov14_BSII	744.10_stack4	69 day filtration/relaxation			BP 505			Ar 10% of 50%
Nov14_nostain	744.10_single1	69 day filtration/relaxation		LP475				Ar 10% of 50%
Nov14_nostain	744.10_single2	69 day filtration/relaxation		LP505				Ar 10% of 50%
Nov14_nostain	744.10_stack1	69 day filtration/relaxation		LP505				Ar 10% of 50%
Nov20_WGA	744.10_single1	69 day filtration/relaxation		LP560	LP505-530		HeNe1 100%	Ar 10% of 50%
Nov20_WGA	744.10_single2	69 day filtration/relaxation		LP560	LP505-530		HeNe1 100%	Ar 10% of 50%
Nov20_WGA	744.10_stack1	69 day filtration/relaxation		LP560	LP505-530		HeNe1 100%	Ar 10% of 50%
Nov20_WGA	744.10_stack2	69 day filtration/relaxation		LP560	LP505-530		HeNe1 100%	Ar 10% of 50%
Nov20_WGA	744.10_stack3	69 day filtration/relaxation		LP560	LP505-530		HeNe1 100%	Ar 10% of 50%
Nov20_WGA	744.10_stack4	69 day filtration/relaxation		LP560	LP505-530		HeNe1 100%	Ar 10% of 50%

Appendix D: Preliminary Study - CLSM Image Data

Date	File Name	Specimen	Pinhole (um)		Detector Gain		Amplitude Offset		Amplitude Gain	
			Ch 1	Ch 2	Ch 1	Ch 2	Ch 1	Ch 2	Ch 1	Ch 2
Nov 10_FITC	744.10_stack1	69 day filtration/relaxation		110	681		-0.1740		1	
Nov 10_FITC	744.10_stack2	69 day filtration/relaxation		110	651		-0.1200		1	
Nov14_BSII	744.10_single1	69 day filtration/relaxation		113	736		-0.0915		1	
Nov14_BSII	744.10_stack1	69 day filtration/relaxation		113	745		-0.1520		1	
Nov14_BSII	744.10_stack2	69 day filtration/relaxation		113	632		-0.0740		1.5	
Nov14_BSII	744.10_stack3	69 day filtration/relaxation		113	743		-0.0470		1	
Nov14_BSII	744.10_stack4	69 day filtration/relaxation		113	697		-0.0470		1	
Nov14_nostain	744.10_single1	69 day filtration/relaxation		91	723		-0.1670		1	
Nov14_nostain	744.10_single2	69 day filtration/relaxation		106	764		-0.2290		1	
Nov14_nostain	744.10_stack1	69 day filtration/relaxation		104	769		-0.1940		1	
Nov20_WGA	744.10_single1	69 day filtration/relaxation	124	106	780	917	-0.1420	-0.0990	1.01	1
Nov20_WGA	744.10_single2	69 day filtration/relaxation	124	106	768	900	-0.1990	-0.1040	1	1
Nov20_WGA	744.10_stack1	69 day filtration/relaxation	124	106	768	900	-0.1990	-0.1040	1	1
Nov20_WGA	744.10_stack2	69 day filtration/relaxation	124	106	719	867	-0.0970	-0.0540	1	1
Nov20_WGA	744.10_stack3	69 day filtration/relaxation	124	106	741	856	-0.1890	-0.1190	1	1.04
Nov20_WGA	744.10_stack4	69 day filtration/relaxation	124	106	714	861	-0.0720	-0.0925	1.1	1.03

Appendix D: Preliminary Study - CLSM Image Data

Date	File Name	Specimen	Z-step size (um)	# of Z sections	Total Z depth (um)
Nov 10_FITC	744.10_stack1	69 day filtration/relaxation	0.90	23	19.80
Nov 10_FITC	744.10_stack2	69 day filtration/relaxation	1.00	26	25.00
Nov14_BSII	744.10_single1	69 day filtration/relaxation			
Nov14_BSII	744.10_stack1	69 day filtration/relaxation	0.40	25	9.60
Nov14_BSII	744.10_stack2	69 day filtration/relaxation	1.00	30	29.00
Nov14_BSII	744.10_stack3	69 day filtration/relaxation	1.00	30	29.00
Nov14_BSII	744.10_stack4	69 day filtration/relaxation	0.50	34	16.50
Nov14_nostain	744.10_single1	69 day filtration/relaxation			
Nov14_nostain	744.10_single2	69 day filtration/relaxation			
Nov14_nostain	744.10_stack1	69 day filtration/relaxation			
Nov20_WGA	744.10_single1	69 day filtration/relaxation			
Nov20_WGA	744.10_single2	69 day filtration/relaxation			
Nov20_WGA	744.10_stack1	69 day filtration/relaxation	0.70	29	19.60
Nov20_WGA	744.10_stack2	69 day filtration/relaxation	0.55	20	10.45
Nov20_WGA	744.10_stack3	69 day filtration/relaxation	0.50	16	7.50
Nov20_WGA	744.10_stack4	69 day filtration/relaxation	0.50	26	12.50

APPENDIX E: Preliminary Study – Surface Charge Data

Surface Charge - August 23

Titration data

Sample	Vo (mL)	Vf (mL)	Difference (mL)	Average (mL)	Standard Deviation
1A	19.02	21.13	2.11	1.90	0.21
1B	21.13	22.82	1.69		
1C	22.82	24.71	1.89		
Blank	7.60	13.40	5.80		

where Vo and Vf are initial and final volumes respectively

MLSS Calculations

Sample	Wo (g)	Wf (g)	Difference (g)	Aliquot (mL)	Solids g/L	Average (g/L)	Standard Deviation
1A	1.1135	1.1687	0.0552	2.5	22.08	21.12	0.96
1B	1.1099	1.1603	0.0504	2.5	20.16		

where Wo and Wf are initial and final weights respectively

Vol Blank (Vo)	Titration Volume (mL)	MLSS (g/L)
5.80	1.90	21.12

Equation

Suface Charge = (-(Vo-V)*N*1000)/(aliquot mL)*MLSS(g/L) where N = 0.001

	Calculated value of Surface Charge (meq/ g MLSS)
1	-0.370

Surface Charge - September 21

Titration data

Sample	Vo (mL)	Vf (mL)	Difference (mL)	Average (mL)	Standard Deviation
1A	28.05	30.40	2.35	2.26	0.21
1B	30.40	32.80	2.40		
1C	32.80	34.82	2.02		
2A	34.82	36.92	2.10	2.17	0.05
2B	36.92	39.11	2.19		
2C	39.11	41.25	2.14		
Blank	21.81	27.75	5.94		

where Vo and Vf are initial and final volumes respectively

MLSS Calculations

Sample	Wo (g)	Wf (g)	Difference (g)	Aliquot (mL)	Solids g/L	Average (g/L)	Standard Deviation
1	1.0990	1.1750	0.0760	2.5	30.4	30.12	0.28
1	1.1017	1.1763	0.0746	2.5	29.84		
2	1.1084	1.1765	0.0681	2.5	27.24		
2	1.1232	1.1929	0.0697	2.5	27.88	27.56	0.32

where Wo and Wf are initial and final weights respectively

Vol Blank (Vo)	Sample	Titration Volume (mL)	MLSS (g/L)
5.94	1	2.26	30.12
	2	2.17	27.56

Equation

Suface Charge = (-(Vo-V)*N*1000)/(aliquot mL)*MLSS(g/L) where N = 0.001

Calculated value of Surface Charge (meq/ g MLSS)

		Average	Standard Deviation
1	-0.245		
2	-0.274	-0.259	0.021

Surface Charge - October 29

Titration data

Sample	Vo (mL)	Vf (mL)	Difference (mL)	Average (mL)	Standard Deviation
1A	17.80	21.41	3.61	3.51	0.16
1B	21.49	24.81	3.32		
1C	24.81	28.41	3.60		
2A	29.05	32.61	3.56	3.51	0.15
2B	32.70	36.35	3.65		
2C	36.35	39.71	3.36		
Blank	11.92	17.80	5.88		

where Vo and Vf are initial and final volumes respectively

MLSS Calculations

Sample	Wo (g)	Wf (g)	Difference (g)	Aliquot (mL)	Solids g/L	Average (mL)	Standard Deviation
1	1.1180	1.1507	0.0327	2.5	13.08	13.08	0
1	1.1094	1.1421	0.0327	2.5	13.08		
2	1.1174	1.1555	0.0381	2.5	15.24		
2	1.1075	1.1459	0.0384	2.5	15.36	15.3	0.06

where Wo and Wf are initial and final weights respectively

Vol Blank (Vo)	Sample	Titration Volume (mL)	MLSS (g/L)
5.88	1	3.51	13.08
	2	3.51	15.3

Equation

Suface Charge = (-(Vo-V)*N*1000)/(aliquot mL)*MLSS(g/L) where N = 0.001

Calculated value of Surface Charge (meq/ g MLSS)

		Average	Standard Deviation
1	-0.362		
2	-0.310	-0.336	0.037

APPENDIX F: Preliminary Study – Hydrophobicity Data

Hydrophobicitiy Data - Preliminary Study

Date	Sample	I_o	I	% Hydrophobicity	Average % Hydrophobicity	Standard Deviation
21-Aug-01	1	1.250	0.824	34.1	34.1	
21-Sep-01	1	1.22	0.991	18.9	20.6	2.45
21-Sep-01	2	1.23	0.955	22.3		
29-Oct-01	1	1.30	0.699	46.3	55.3	12.7
29-Oct-01	2	0.854	0.305	64.2		

where I_o and I are initial and final absorbance at 400 nm respectively

APPENDIX G: Preliminary Study – Extracellular Polymeric Substance Data

Protein Concentrations

Sampling Date	Absorbance @ 750 nm	Standard Curve y = mx	r^2	Sample	Absorbance @ 750 nm	Conc. (mg/L)	Conc. (mg/g MLSS)	Average (mg/g MLSS)	Standard Deviation
21-Aug-01	0.444	y = 0.0024x	0.9674	A1	0.886	369.19	22.45	21.07	1.96
	0.824			A2	0.886	369.19			
	1.155			A3	0.870	362.36			
	1.398			B1	1.022	425.95	19.68		
	1.602			B2	1.000	416.67			
	0			B3	0.959	399.42			
21-Sep-01	0.137	y = 0.0025x	0.9717	1A	1.398	559.18	29.28	30.12	1.18
	0.225			1B	1.456	582.37			
	0.342			1C	1.495	597.94			
	0.469			2A	1.523	609.15	30.95		
	0.052			2B	1.602	640.82			
	0			2C	1.523	609.15			
29-Oct-01	0.620	y = 0.0024x	0.9395	1A	0.699	291.24	19.70	17.95	1.72
	0.903			1B	0.721	300.52			
	0.260			1C	0.674	280.69			
	1.456			2A	0.620	258.25	17.88		
	1.745			2B	0.623	259.76			
	0			2C	0.629	262.06			
				3A	0.541	225.25	16.27		
				3B	0.545	227.15			
				3C	0.569	236.93			

Uronic Acid Concentrations

Sampling Date	Absorbance @ 750 nm	Standard Curve y = mx	r^2	Sample	Absorbance @ 750 nm	Conc. (mg/L)	Conc. (mg/g MLSS)	Average (mg/g MLSS)	Standard Deviation
21-Aug-01	0.155	y = 0.0064x	0.9768	A1	0.481	75.23	4.71	4.40	0.44
	0.398			A2	0.509	79.47			
	0.854			A3	0.488	76.27			
	0.000			B1	0.553	86.38	4.09		
				B2	0.538	84.00			
				B3	0.561	87.60			
21-Sep-01	0.137	y = 0.001x	0.852	1A	0.796	795.88	40.67	43.05	3.36
	0.225			1B	0.824	823.91			
	0.342			1C	0.796	795.88			
	0.469			2A	0.921	920.82	45.42		
	0.516			2B	0.886	886.06			
	0.000			2C	0.921	920.82			
29-Oct-01	0.264	y = 0.0067x	0.9717	1A	0.187	27.92	1.84	1.66	0.15
	0.610			1B	0.167	25.00			
	1.056			1C	0.190	28.42			
	1.260			2A	0.158	23.58	1.57		
	1.377			2B	0.161	24.05			
	0.000			2C	0.140	20.85			
				3A	0.152	22.66	1.58		
				3B	0.137	20.40			
				3C	0.161	24.05			

Carbohydrate Concentrations

Sampling Date	Absorbance @ 750 nm	Standard Curve y = mx	r^2	Sample	Absorbance @ 750 nm	Conc. (mg/L)	Conc. (mg/g MLSS)	Average (mg/g MLSS)	Standard Deviation
21-Aug-01	0.444	y = 0.0164x	0.9689	A1	1.155	70.42	4.39	3.95	0.62
	0.824			A2	1.222	74.50			
	1.155			A3	1.155	70.42			
	1.398			B1	1.187	72.38	3.51		
	1.602			B2	1.222	74.50			
	0.000			B3	1.222	74.50			
21-Sep-01	0.450	y = 0.0174x	0.9376	1A	1.347	77.40	4.13	4.34	0.30
	1.046			1B	1.523	87.52			
	1.046			1C	1.398	80.34			
	1.523			2A	1.456	83.67	4.55		
	1.699			2B	1.602	92.07			
	0.000			2C	1.699	97.64			
29-Oct-01	0.301	y = 0.0148x	0.9771	1A	0.914	61.73	4.35	3.80	0.58
	0.757			1B	0.959	64.77			
	1.022			1C	0.979	66.14			
	1.260			2A	0.830	56.06	3.87		
	1.456			2B	0.854	57.69			
	0.000			2C	0.810	54.71			
				3A	0.668	45.11	3.19		
				3B	0.668	45.11			
				3C	0.668	45.11			

DNA Concentrations

Sampling Date	Relative Fluorescence Units	Standard Curve y = mx + b	r^2	Sample	Relative Fluorescence Units	Conc. (mg/L)	Conc. (mg/g MLSS)	Average (mg/g MLSS)	Standard Deviation
29-Oct-01	0.575	y = 0.0054x + 0.6772	0.9984	1	2.97	55.0	14.8	3.72	3.39
	1.01			2	2.65	49.0	14.5	3.37	
	1.33			3	2.36	43.6	14.1	3.09	
	1.68								
	3.34								
	6.05								

APPENDIX H: Preliminary Study – Permeability Data

Membrane Loop No.	Initial Permeate (mL/min)		Initial Flux ($L/m^2/hr$)		Initial Permeability ($L/m^2/hr/bar$)		Initial Permeability @ 25°C ($L/m^2/hr/bar$)	
	5 in Hg	10 in Hg	5 in Hg	10 in Hg	5 in Hg	10 in Hg	5 in Hg	10 in Hg
4744.08	22.0	35.7	210.2	341.1	1242.3	1007.9	1311.6	1064.2
4744.16	21.6	36.0	206.4	343.9	1219.7	1016.4	1287.7	1073.1
4744.13	21.5	30.0	205.4	286.6	1214.0	847.0	1281.8	894.3
4744.17	21.0	35.0	200.6	334.4	1185.8	988.2	1252.0	1043.3
4744.11	18.0	31.5	172.0	301.0	1016.4	889.3	1073.1	939.0
4744.04	21.0	33.8	200.6	322.9	1185.8	954.3	1252.0	1007.5
4744.05	17.3	30.8	165.3	294.3	976.9	869.6	1031.4	918.1
4744.09	20.0	33.1	191.1	316.2	1129.3	934.5	1192.3	986.7
4744.10	19.0	33.5	181.5	320.1	1072.9	945.8	1132.7	998.6
4744.12	23.0	34.2	219.7	326.8	1298.7	965.6	1371.2	1019.5

Membrane Loop No.	Final Permeate (mL/min)		Final Flux ($L/m^2/hr$)		Final Permeability ($L/m^2/hr/bar$)		Final Permeability @ 25°C ($L/m^2/hr/bar$)	
	5 in Hg	10 in Hg	5 in Hg	10 in Hg	5 in Hg	10 in Hg	5 in Hg	10 in Hg
4744.08	8.1	19.5	77.4	186.3	457.4	550.5	459.6	553.2
4744.16	10.5	19.5	100.3	186.3	592.9	550.5	595.8	553.2
4744.13	3.4	6.9	32.5	65.9	192.0	194.8	179.6	182.3
4744.17	12.0	22.5	114.6	215.0	677.6	635.2	634.0	594.3
4744.11	4.0	8.1	38.2	77.4	225.9	228.7	221.6	224.3
4744.04	5.4	9.6	51.6	91.2	304.9	269.6	299.1	264.5
4744.05	3.4	6.4	32.5	61.1	192.0	180.7	188.3	177.2
4744.09	3.7	6.6	35.4	63.1	208.9	186.3	204.9	182.8
4744.10	3.4	6.6	32.5	63.1	192.0	186.3	188.3	182.8
4744.12	3.8	7.4	36.3	70.7	214.6	208.9	210.5	204.9

APPENDIX I: Preliminary Study – Reactor Data

Date	Temp (°C)	Pressure (kPa) (avg over 1 cycle)
21-Aug-01	21.4	-19.15
22-Aug-01	21.3	-19.05
23-Aug-01	21.4	-19.50
24-Aug-01	21.3	-19.45
25-Aug-01	21.1	-19.20
27-Aug-01	21.4	-19.85
29-Aug-01	21.2	-20.10
30-Aug-01	21.3	-20.50
31-Aug-01	21.8	-20.50
01-Sep-01	21.0	-20.70
03-Sep-01	21.1	-21.40
04-Sep-01	21.4	-20.45
05-Sep-01	20.7	-20.45
06-Sep-01	20.7	-20.85
07-Sep-01	21.2	-21.20
08-Sep-01	22.8	-20.35
10-Sep-01	22.1	-20.60
11-Sep-01	21.4	-20.65
12-Sep-01	21.8	-20.70
13-Sep-01	21.4	-20.25
05-Oct-01	21.0	
06-Oct-01	20.0	
08-Oct-01	20.0	
09-Oct-01	20.0	
10-Oct-01	20.0	
11-Oct-01	20.0	
12-Oct-01	18.7	
13-Oct-01	20.0	
15-Oct-01	20.0	
16-Oct-01	20.0	
17-Oct-01	20.0	
18-Oct-01	20.0	
19-Oct-01	20.0	
21-Oct-01	20.0	

APPENDIX J: Core Study - CLSM Image Data

CLSM IMAGE DATA - Unstained Membrane Fibre Samples in Fluorescent and Reflected Light Mode

Date	File Name	Specimen	Obj/NA	Averaging	Zoom	Speed (us/pixel)	Image Size			Filters			Laser Power			Pinhole (um)		
							Pixels	Microns		Ch 1	Ch2	Ch 3	488	543	633	Ch 1	Ch 2	Ch 3
07-May-02	SRT30R_nostain_1	Unstained membrane sample AR	63X/0.9 W	2	1	8.96	512 x 512	146.2 x 146.2	12 bit	LP 650	BP 505-530	BP 565-615 IR	50% of 50%	100%	100%	191	146	169
07-May-02	SRT30R_nostain_1b	Unstained membrane sample - reflected light AR	63X/0.9 W	2	1	8.96	512 x 512	146.2 x 146.2	12 bit				50% of 50%	100%	100%		161	
07-May-02	SRT30R_nostain_2	Unstained membrane sample at 60kPa	63X/0.9 W	2	1	8.96	512 x 512	146.2 x 146.2	12 bit	LP 650	BP 505-530	BP 565-615 IR	50% of 50%	100%	100%	191	146	169
07-May-02	SRT30R_nostain_2b	Unstained membrane sample at 60kPa - reflected light	63X/0.9 W	2	1	8.96	512 x 512	146.2 x 146.2	12 bit				50% of 50%	100%	100%		161	
07-May-02	SRT30R_nostain_3	Unstained membrane sample at 60kPa	63X/0.9 W	2	1	8.96	512 x 512	146.2 x 146.2	12 bit	LP 650	BP 505-530	BP 565-615 IR	50% of 50%	100%	100%	191	146	169
07-May-02	SRT30R_nostain_3b	Unstained membrane sample at 60kPa - reflected light	63X/0.9 W	2	1	8.96	512 x 512	146.2 x 146.2	12 bit				50% of 50%	100%	100%		161	
07-May-02	SRT12BW_nostain_1	Unstained membrane sample AR	63X/0.9 W	2	1	8.96	512 x 512	146.2 x 146.2	12 bit	LP 650	BP 505-530	BP 565-615 IR	50% of 50%	100%	100%	191	146	169
07-May-02	SRT12BW_nostain_1b	Unstained membrane sample - reflected light AR	63X/0.9 W	2	1	17.92	512 x 512	146.2 x 146.2	12 bit				50% of 50%	100%	100%		161	
07-May-02	SRT12BW_nostain_2	Unstained membrane sample AR	63X/0.9 W	2	1	8.96	512 x 512	146.2 x 146.2	12 bit	LP 650	BP 505-530	BP 565-615 IR	50% of 50%	100%	100%	191	146	169
07-May-02	SRT12BW_nostain_2b	Unstained membrane sample - reflected light AR	63X/0.9 W	2	1	17.92	512 x 512	146.2 x 146.2	12 bit				50% of 50%	100%	100%		161	
07-May-02	SRT12BW_nostain_3	Unstained membrane sample at 60kPa	63X/0.9 W	2	1	8.96	512 x 512	146.2 x 146.2	12 bit	LP 650	BP 505-530	BP 565-615 IR	50% of 50%	100%	100%	191	146	169
07-May-02	SRT12BW_nostain_3b	Unstained membrane sample at 60kPa - reflected light	63X/0.9 W	2	1	8.96	512 x 512	146.2 x 146.2	12 bit				50% of 50%	100%	100%		161	
07-May-02	SRT12BW_nostain_4	Unstained membrane sample at 60kPa	63X/0.9 W	2	1	8.96	512 x 512	146.2 x 146.2	12 bit	LP 650	BP 505-530	BP 565-615 IR	50% of 50%	100%	100%	191	146	169
07-May-02	SRT12R_nostain_1b	Unstained membrane sample - reflected light AR	63X/0.9 W	2	1	17.92	512 x 512	146.2 x 146.2	12 bit				50% of 50%	100%	100%		161	
07-May-02	SRT12R_nostain_2	Unstained membrane sample at 60kPa	63X/0.9 W	2	1	8.96	512 x 512	146.2 x 146.2	12 bit	LP 650	BP 505-530	BP 565-615 IR	50% of 50%	100%	100%	191	146	169
07-May-02	SRT12R_nostain_2b	Unstained membrane sample - reflected light at 60kPa	63X/0.9 W	2	1	8.96	512 x 512	146.2 x 146.2	12 bit				50% of 50%	100%	100%		161	
08-May-02	SRT12R_nostain_3	Unstained membrane sample at 60kPa	63X/0.9 W	2	1	8.96	512 x 512	146.2 x 146.2	12 bit	LP 650	BP 505-530	BP 565-615 IR	50% of 50%	100%	100%	191	146	169
08-May-02	SRT12R_nostain_3b	Unstained membrane sample - reflected light at 60kPa	63X/0.9 W	2	1	8.96	512 x 512	146.2 x 146.2	12 bit				50% of 50%	100%	100%		161	
08-May-02	SRT12R_nostain_4	Unstained membrane sample at 60kPa	63X/0.9 W	2	1	8.96	512 x 512	146.2 x 146.2	12 bit	LP 650	BP 505-530	BP 565-615 IR	50% of 50%	100%	100%	191	146	169
08-May-02	SRT12R_nostain_4b	Unstained membrane sample - reflected light at 60kPa	63X/0.9 W	2	1	8.96	512 x 512	146.2 x 146.2	12 bit				50% of 50%	100%	100%		161	

Date	File Name	Specimen	Detector Gain			Amplitude Offset			Amplitude Gain			Z-step size (um)	# of Z sections	Total Z depth (um)
			Ch 1	Ch 2	Ch 3	Ch 1	Ch 2	Ch 3	Ch 1	Ch 2	Ch 3			
07-May-02	SRT30R_nostain_1	Unstained membrane sample	1000	1000	1000	-0.145	-0.067	-0.059	-0.052	1.75	1.28	0.85	22	17.85
07-May-02	SRT30R_nostain_1b	Unstained membrane sample - reflected light		371			-0.017			1		0.8	20	15.2
07-May-02	SRT30R_nostain_2	Unstained membrane sample at 60kPa	1000	1000	1000	-0.132	-0.057	-0.049	1.5	1.68	1.87	1.4	26	36.3
07-May-02	SRT30R_nostain_2b	Unstained membrane sample at 60kPa - reflected light		350			-0.027			1.35		1.4	26	36.3
07-May-02	SRT30R_nostain_3	Unstained membrane sample at 60kPa	827	928	919	-0.1665	-0.084	-0.119	1	1.54	1.73	0.75	25	18
07-May-02	SRT30R_nostain_3b	Unstained membrane sample at 60kPa - reflected light		337			-0.055			1.53		0.8	23	18.4
07-May-02	SRT12BW_nostain_1	Unstained membrane sample AR	961	949	964	-0.042	-0.059	-0.0925	1.45	1.77	1.7	23	55	12.1
07-May-02	SRT12BW_nostain_1b	Unstained membrane sample - reflected light AR		377			-0.069			1.43		0.5	22	10.5
07-May-02	SRT12BW_nostain_2	Unstained membrane sample AR	928	936	925	-0.074	-0.057	-0.08	1.39	1.65	1.6	0.5	22	10.5
07-May-02	SRT12BW_nostain_2b	Unstained membrane sample - reflected light AR		326			-0.059			1.54		0.55	22	11.55
07-May-02	SRT12BW_nostain_3	Unstained membrane sample at 60kPa	960	1000	1000	-0.044	-0.067	-0.0865	1.48	1.7	1.68	1.85	30	53.65
07-May-02	SRT12BW_nostain_3b	Unstained membrane sample at 60kPa - reflected light		450			-0.06			1.8		1.8	30	53.7
07-May-02	SRT12BW_nostain_4	Unstained membrane sample at 60kPa	889	901	930	-0.104	-0.072	-0.099	1	1.48	1.47	0.8	26	20
07-May-02	SRT12R_nostain_1b	Unstained membrane sample - reflected light AR		339			-0.099			1.65		0.75	27	19.5
07-May-02	SRT12R_nostain_2	Unstained membrane sample at 60kPa	928	940	945	-0.029	-0.057	-0.0845	1	1.7	1.7	1	39	38
07-May-02	SRT12R_nostain_2b	Unstained membrane sample - reflected light at 60kPa		412			-0.029			1.62		1	39	38
08-May-02	SRT12R_nostain_3	Unstained membrane sample at 60kPa	900	930	955	-0.012	-0.077	-0.08	1	1.6	1.7	1.4	26	35
08-May-02	SRT12R_nostain_3b	Unstained membrane sample - reflected light at 60kPa		361			-0.034			1.3		1.4	26	35
08-May-02	SRT12R_nostain_4	Unstained membrane sample at 60kPa	861	883	920	-0.059	-0.059	-0.0675	1.1	1.59	1.3	0.85	22	17.85
08-May-02	SRT12R_nostain_4b	Unstained membrane sample - reflected light at 60kPa		363			-0.032			1.2		0.85	20	16.15

Appendix J

CLSM IMAGE DATA - Activated Sludge Floc Samples from MBR in Fluorescent and Reflected Light Mode

Date	File Name	Specimen	Obj/NA	Averaging	Zoom	Speed (us/pixel)	Image Size			Filters			Laser Power			Pinhole (um)		
							Pixels	Microns		Ch 1	Ch2	Ch 3	488	543	633	Ch 1	Ch 2	Ch 3
22-Apr-02	SRT12_1	Floc in agarose	63X/0.9 W	2	1	71.68	512 x 512	146.2 x 146.2	12 bit	LP 650	BP 505-530	BP 565-615 IR	50% of 50%	100%	100%	191	146	169
22-Apr-02	SRT12_2	Floc in agarose	63X/0.9 W	2	2	8.96	512 x 512	73.1 x 73.1	12 bit	LP 650	BP 505-530	BP 565-615 IR	50% of 50%	100%	100%	191	146	169
22-Apr-02	SRT12_3	Floc in agarose	20X/0.75	2	1	71.68	512 x 512	460.6 x 460.6	12 bit	LP 650	BP 505-530	BP 565-615 IR	50% of 55%	100%	100%	191	146	169
22-Apr-02	SRT30_1	Floc in agarose	20X/0.75	2	1	71.68	512 x 512	460.6 x 460.6	12 bit	LP 650	BP 505-530	BP 565-615 IR	50% of 50%	100%	100%	191	146	169
22-Apr-02	SRT30_2	Floc in agarose	63X/0.9 W	2	1	8.96	512 x 512	146.2 x 146.2	12 bit	LP 650	BP 505-530	BP 565-615 IR	50% of 50%	100%	100%	191	146	169
22-Apr-02	SRT30_3	Floc in agarose	63X/0.9 W	2	1.7	71.68	512 x 512	85.1 x 85.1	12 bit	LP 650	BP 505-530	BP 565-615 IR	50% of 50%	100%	100%	191	146	169
06-May-02	Floc_SRT12_1	Floc in agarose	63X/0.9 W	2	1	8.96	512 x 512	146.2 x 146.2	12 bit	LP 650	BP 505-530	BP 565-615 IR	50% of 50%	100%	100%	191	146	169
06-May-02	Floc_SRT12_1b	Floc in agarose - reflected light	63X/0.9 W	2	1	8.96	512 x 512	146.2 x 146.2	12 bit				50% of 50%	100%	100%		161	
06-May-02	Floc_SRT12_2	Floc in agarose	20X/0.75	2	1	71.68	512 x 512	460.6 x 460.6	12 bit	LP 650	BP 505-530	BP 565-615 IR	50% of 55%	100%	100%	76	57	64
06-May-02	Floc_SRT12_2b	Floc in agarose - reflected light	20X/0.75	2	1	71.68	512 x 512	460.6 x 460.6	12 bit				50% of 50%	100%	100%		61	
06-May-02	Floc_SRT12_3	Floc in agarose	20X/0.75	2	1	71.68	512 x 512	460.6 x 460.6	12 bit	LP 650	BP 505-530	BP 565-615 IR	50% of 55%	100%	100%	76	57	64
06-May-02	Floc_SRT12_3b	Floc in agarose - reflected light	20X/0.75	2	1	71.68	512 x 512	460.6 x 460.6	12 bit				50% of 50%	100%	100%		61	
06-May-02	Floc_SRT12_4	Floc in agarose	63X/0.9 W	2	1	8.96	512 x 512	146.2 x 146.2	12 bit	LP 650	BP 505-530	BP 565-615 IR	50% of 50%	100%	100%	191	146	169
06-May-02	Floc_SRT12_4b	Floc in agarose - reflected light	63X/0.9 W	2	1	8.96	512 x 512	146.2 x 146.2	12 bit				50% of 50%	100%	100%		161	
06-May-02	Floc_SRT30_1	Floc in agarose	20X/0.75	2	1	71.68	512 x 512	460.6 x 460.6	12 bit	LP 650	BP 505-530	BP 565-615 IR	50% of 50%	100%	100%	76	57	64
06-May-02	Floc_SRT30_1b	Floc in agarose - reflected light	20X/0.75	2	1	71.68	512 x 512	460.6 x 460.6	12 bit				50% of 50%	100%	100%		61	
06-May-02	Floc_SRT30_2	Floc in agarose	20X/0.75	2	1	71.68	512 x 512	460.6 x 460.6	12 bit	LP 650	BP 505-530	BP 565-615 IR	50% of 50%	100%	100%	76	57	64
06-May-02	Floc_SRT30_2b	Floc in agarose - reflected light	20X/0.75	2	1	71.68	512 x 512	460.6 x 460.6	12 bit				50% of 50%	100%	100%		61	
06-May-02	Floc_SRT30_3	Floc in agarose	63X/0.9 W	2	1	8.96	512 x 512	146.2 x 146.2	12 bit	LP 650	BP 505-530	BP 565-615 IR	50% of 50%	100%	100%	191	146	169
06-May-02	Floc_SRT30_3b	Floc in agarose - reflected light	63X/0.9 W	2	1	8.96	512 x 512	146.2 x 146.2	12 bit				50% of 50%	100%	100%		161	
06-May-02	Floc_SRT30_4	Floc in agarose	63X/0.9 W	2	1	8.96	512 x 512	146.2 x 146.2	12 bit	LP 650	BP 505-530	BP 565-615 IR	50% of 50%	100%	100%	191	146	169
06-May-02	Floc_SRT30_4b	Floc in agarose - reflected light	63X/0.9 W	2	1	8.96	512 x 512	146.2 x 146.2	12 bit				50% of 50%	100%	100%		161	
06-May-02	Floc_SRT30_5	Floc in agarose	63X/0.9 W	2	1	71.68	512 x 512	146.2 x 146.2	12 bit	LP 650	BP 505-530	BP 565-615 IR	50% of 50%	100%	100%	191	146	169
06-May-02	Floc_SRT30_5b	Floc in agarose - reflected light	63X/0.9 W	2	1	71.68	512 x 512	146.2 x 146.2	12 bit				50% of 50%	100%	100%		161	

Date	File Name	Specimen	Dye/Lectin			Abs/Em l			Detector Gain			Amplitude Offset			Amplitude Gain			Z-step size (um)	# of Z sections	Total Z depth (um)
			Ch 1	Ch 2	Ch 3	Ch 1	Ch 2	Ch 3	Ch 1	Ch 2	Ch 3	Ch 1	Ch 2	Ch 3	Ch 1	Ch 2	Ch 3			
22-Apr-02	SRT12_1	Floc in agarose	ConA-AF633	SBA-AF488	WGA-tmr	632/647	495/519	555/580	975	995	985	-0.097	-0.042	-0.069	1	1.27	1.47			
22-Apr-02	SRT12_2	Floc in agarose	ConA-AF633	SBA-AF488	WGA-tmr	632/647	495/519	555/580	724	1000	1000	-0.154	-0.032	1.25	2.63	1	-0.054	1.05	20	19.9
22-Apr-02	SRT12_3	Floc in agarose	ConA-AF633	SBA-AF488	WGA-tmr	632/647	495/519	555/580	647	728	830	-0.094	-0.039	-0.0465	1	1	1			
22-Apr-02	SRT30_1	Floc in agarose	ConA-AF633	SBA-AF488	WGA-tmr	632/647	495/519	555/580	689	797	940	-0.167	-0.047	-0.059	1	1	1			
22-Apr-02	SRT30_2	Floc in agarose	ConA-AF633	SBA-AF488	WGA-tmr	632/647	495/519	555/580	921	1000	1000	-0.049	-0.072	-0.094	1	2	2.09	1.5	31	45
22-Apr-02	SRT30_3	Floc in agarose	ConA-AF633	SBA-AF488	WGA-tmr	632/647	495/519	555/580	759	1000	1000	-0.079	-0.057	-0.069	1.5	1.61	1.67			
06-May-02	Floc_SRT12_1	Floc in agarose	ConA-AF633	SBA-AF488	WGA-tmr	632/647	495/519	555/580	946	915	985	-0.067	-0.034	-0.0915	1	1.32	1.9	0.9	26	22.5
06-May-02	Floc_SRT12_1b	Floc in agarose - reflected light								475			-0.024			1		0.9	26	22.5
06-May-02	Floc_SRT12_2	Floc in agarose	ConA-AF633	SBA-AF488	WGA-tmr	632/647	495/519	555/580	925	980	1000	-0.239	-0.039	-0.079	1	1	1.7			
06-May-02	Floc_SRT12_2b	Floc in agarose - reflected light								377			-0.057			1.7				
06-May-02	Floc_SRT12_3	Floc in agarose	ConA-AF633	SBA-AF488	WGA-tmr	632/647	495/519	555/580	852	817	1000	-0.199	-0.049	-0.089	1.58	1.5	1.77			
06-May-02	Floc_SRT12_3b	Floc in agarose - reflected light								277			-0.059			1.54				
06-May-02	Floc_SRT12_4	Floc in agarose	ConA-AF633	SBA-AF488	WGA-tmr	632/647	495/519	555/580	847	940	1000	-0.149	-0.034	-0.079	1	1	1.6	1	31	30
06-May-02	Floc_SRT12_4b	Floc in agarose - reflected light								475			-0.024			1		1	31	30
06-May-02	Floc_SRT30_1	Floc in agarose	ConA-AF633	SBA-AF488	WGA-tmr	632/647	495/519	555/580	853	920	1000	-0.17	-0.048	-0.082	1	1	1.76			
06-May-02	Floc_SRT30_1b	Floc in agarose - reflected light								461			-0.027			1				
06-May-02	Floc_SRT30_2	Floc in agarose	ConA-AF633	SBA-AF488	WGA-tmr	632/647	495/519	555/580	979	894	1000	-0.169	-0.034	-0.0925	1	1	1.73			
06-May-02	Floc_SRT30_2b	Floc in agarose - reflected light								298			-0.032			1				
06-May-02	Floc_SRT30_3	Floc in agarose	ConA-AF633	SBA-AF488	WGA-tmr	632/647	495/519	555/580	761	740	870	-0.1165	-0.054	-0.069	1	1.4	1.3	0.75	24	17.25
06-May-02	Floc_SRT30_3b	Floc in agarose - reflected light								272			-0.019			1		0.75	24	17.25
06-May-02	Floc_SRT30_4	Floc in agarose	ConA-AF633	SBA-AF488	WGA-tmr	632/647	495/519	555/580	790	716	916	-0.064	-0.052	-0.069	1	1.4	1.4	0.75	23	16.5
06-May-02	Floc_SRT30_4b	Floc in agarose - reflected light								272			-0.019			1		0.75	23	16.5
06-May-02	Floc_SRT30_5	Floc in agarose	ConA-AF633	SBA-AF488	WGA-tmr	632/647	495/519	555/580	870	716	916	-0.064	-0.052	-0.069	1	1.4	1.4			
06-May-02	Floc_SRT30_5b	Floc in agarose - reflected light								345			-0.028			1				

Appendix J

CLSM IMAGE DATA - *Bac*Light Bacterial Gram Stain of RUN 2 samples at Critical Transmembrane Pressure

Date	File Name	Specimen	Obj/NA	Averaging	Zoom	Speed (us/pixel)	Image Size			Filters	Laser Power	Pinhole (um)
							Pixels	Microns		Ch 1	488	Ch 1
09-May-02	2SRT12R_at 60kPa_1	long section of fibre at critical TMP (Run 2)	63X/0.9 W	2	1	8.96	512 x 512	146.2 x 146.2	12 bit	LP 650	50% of 50%	153
09-May-02	2SRT12R_at 60kPa_2	long section of fibre at critical TMP (Run 2)	63X/0.9 W	2	1	8.96	512 x 512	146.2 x 146.2	12 bit	LP 650	25% of 50%	153
09-May-02	2SRT12R_at 60kPa_3	long section of fibre at critical TMP (Run 2)	63X/0.9 W	2	1	8.96	512 x 512	146.2 x 146.2	12 bit	LP 650	25% of 50%	153
09-May-02	2SRT12BW_at 60kPa_1	long section of fibre at critical TMP (Run 2)	63X/0.9 W	2	1	8.96	512 x 512	146.2 x 146.2	12 bit	LP 650	25% of 50%	153
09-May-02	2SRT12BW_at 60kPa_1b	long section of fibre at critical TMP (Run 2)	63X/0.9 W	2	1	8.96	512 x 512	146.2 x 146.2	12 bit	LP 650	25% of 50%	153
09-May-02	2SRT12BW_at 60kPa_2	long section of fibre at critical TMP (Run 2)	63X/0.9 W	2	1	8.96	512 x 512	146.2 x 146.2	12 bit	LP 650	25% of 50%	153
09-May-02	2SRT12BW_at 60kPa_3	long section of fibre at critical TMP (Run 2)	63X/0.9 W	2	2	8.96	512 x 512	73.1 x 73.1	12 bit	LP 650	25% of 50%	153
09-May-02	2SRT30R_at 60kPa_1	long section of fibre at critical TMP (Run 2)	63X/0.9 W	2	1	8.96	512 x 512	146.2 x 146.2	12 bit	LP 650	25% of 50%	153
09-May-02	2SRT30R_at 60kPa_2	long section of fibre at critical TMP (Run 2)	63X/0.9 W	2	1	8.96	512 x 512	146.2 x 146.2	12 bit	LP 650	25% of 50%	153
09-May-02	2SRT30R_at 60kPa_3	long section of fibre at critical TMP (Run 2)	63X/0.9 W	2	2	8.96	512 x 512	73.1 x 73.1	12 bit	LP 650	25% of 50%	153

Date	File Name	Specimen	Dye/Lectin	Abs/Em λ	Detector Gain	Amplitude Offset	Amplitude Gain	Z-step size (um)	# of Z sections	Total Z depth (um)
			Ch 1	Ch 1	Ch 1	Ch 1	Ch 1			
09-May-02	2SRT12R_at 60kPa_1	long section of fibre at critical TMP (Run 2)	BacLight	480/500	553	-0.1765	1	0.5	13	6
09-May-02	2SRT12R_at 60kPa_2	long section of fibre at critical TMP (Run 2)	BacLight	480/500	480	-0.152	1	0.4	23	8.8
09-May-02	2SRT12R_at 60kPa_3	long section of fibre at critical TMP (Run 2)	BacLight	480/500	484	-0.039	1	1	31	30
09-May-02	2SRT12BW_at 60kPa_1	long section of fibre at critical TMP (Run 2)	BacLight	480/500	502	-0.044	1	2	35	68
09-May-02	2SRT12BW_at 60kPa_1b	long section of fibre at critical TMP (Run 2)	BacLight	480/500	642/692	1.53125	1	2	35	68
09-May-02	2SRT12BW_at 60kPa_2	long section of fibre at critical TMP (Run 2)	BacLight	480/500	481	-0.179	1	0.3	27	7.8
09-May-02	2SRT12BW_at 60kPa_3	long section of fibre at critical TMP (Run 2)	BacLight	480/500	526	-0.144	1	0.5	22	10.5
09-May-02	2SRT30R_at 60kPa_1	long section of fibre at critical TMP (Run 2)	BacLight	480/500	481	-0.179	1	0.3	27	7.8
09-May-02	2SRT30R_at 60kPa_2	long section of fibre at critical TMP (Run 2)	BacLight	480/500	527	-0.0665	1	0.4	26	10
09-May-02	2SRT30R_at 60kPa_3	long section of fibre at critical TMP (Run 2)	BacLight	480/500	583	-0.182	1	0.3	27	7.8

Appendix J

CLSM IMAGE DATA - Virgin Samples

Date	File Name	Specimen	Obj/NA	Averaging	Zoom	Speed (us/pixel)	Image Size			Filters			Laser Power			Pinhole (um)		
							Pixels	Microns		Ch 1	Ch2	Ch 3	488	543	633	Ch 1	Ch 2	Ch 3
12-Feb-02	SRT12_BW_virgin1	x-section of virgin membrane sample	10X/0.25	4	1	71.68	512 x 512	921.3 x 921.3	12 bit	LP505			Ar 70% of 50%			168		
12-Feb-02	SRT12_BW_virgin2	x-section of virgin membrane sample	63X/1.2 W	4	1	71.68	512 x 512	146.2 x 146.2	12 bit	LP505			Ar 100% of 50%			699		
12-Feb-02	SRT12_relax_virgin1	x-section of virgin membrane sample	10X/0.25	4	1	71.68	512 x 512	921.3 x 921.3	12 bit	LP505			Ar 70% of 50%			108		
12-Feb-02	SRT12_relax_virgin2	x-section of virgin membrane sample	63X/1.2 W	4	1	71.68	512 x 512	146.2 x 146.2	12 bit	LP505			Ar 70% of 50%			153		
12-Feb-02	SRT12_relax_virgin3	long section of virgin membrane sample	10X/0.25	4	1	71.68	512 x 512	921.3 x 921.3	12 bit	LP505			Ar 70% of 50%			133		
12-Feb-02	SRT30_relax_virgin1	long section of virgin membrane sample	10X/0.25	2	0.7	8.96	512 x 512	1302.7 x 1302.7	12 bit	LP505			Ar 70% of 50%			123		

Date	File Name	Specimen	Dye/Lectin			Detector Gain			Amplitude Offset			Amplitude Gain			Z-step size (um)	# of Z sections	Total Z depth (um)
			Ch 1	Ch 2	Ch 3	Ch 1	Ch 2	Ch 3	Ch 1	Ch 2	Ch 3	Ch 1	Ch 2	Ch 3			
12-Feb-02	SRT12_BW_virgin1	x-section of virgin membrane sample	FITC settings			1000			-0.209			2.38					
12-Feb-02	SRT12_BW_virgin2	x-section of virgin membrane sample	FITC settings			1000			-0.227			2.86					
12-Feb-02	SRT12_relax_virgin1	x-section of virgin membrane sample	FITC settings			1000			-0.094			1.63					
12-Feb-02	SRT12_relax_virgin2	x-section of virgin membrane sample	FITC settings			995			-0.177			2.8					
12-Feb-02	SRT12_relax_virgin3	long section of virgin membrane sample	FITC settings			965			-0.177			3					
12-Feb-02	SRT30_relax_virgin1	long section of virgin membrane sample	FITC settings			1000			-0.102			1.8			2	70	138

Appendix J

CLSM IMAGE DATA - RUN 1 after 2 hours of filtration

Date	File Name	Specimen	Obj/NA	Averaging	Zoom	Speed (us/pixel)	Image Size			Filters			Laser Power			Pinhole (um)		
							Pixels	Microns		Ch 1	Ch2	Ch 3	488	543	633	Ch 1	Ch 2	Ch 3
13-Feb-02	SRT12R_2hr_1	long section of fibre at 2 hours of filtration	10X/0.25	2	1	8.96	512 x 512	921.3 x 921.3	12 bit	LP 650	BP 505-530	BP 565-615 IR	50% of 50%	100%	100%	91	107	134
13-Feb-02	SRT12_R_2hr_SBA	long section of fibre at 2 hours of filtration	63X/0.9 W	2	1	71.68	512 x 512	146.2 x 146.2	12 bit	LP505			50% of 50%			150		
13-Feb-02	SRT12_R_2hr_WGA	long section of fibre at 2 hours of filtration	63X/0.9 W	2	1	71.68	512 x 512	146.2 x 146.2	12 bit	LP560				100%		164		
13-Feb-02	SRT12_R_2hr_ConA	long section of fibre at 2 hours of filtration	63X/0.9 W	2	1	71.68	512 x 512	146.2 x 146.2	12 bit	LP650					100%	191		
13-Feb-02	SRT12_R_2hr_2	long section of fibre at 2 hours of filtration	63X/0.9 W	2	1	35.84	512 x 512	146.2 x 146.2	12 bit	LP 650	BP 505-530	BP 565-615 IR	80% of 50%	100%	80%	193	187	169
13-Feb-02	SRT12_R_2hr_4	long section of fibre at 2 hours of filtration	63X/1.2 W	2	1	8.96	512 x 512	146.2 x 146.2	12 bit	LP 650	BP 505-530	BP 565-615 IR	80% of 50%	100%	100%	143	112	129
14-Feb-02	SRT12_BW_2hr_1	long section of fibre at 2 hours of filtration	63X/1.2 W	2	1	8.96	512 x 512	146.2 x 146.2	12 bit	LP 650	BP 505-530	BP 565-615 IR	100% of 50%	100%	100%	146	111	129
14-Feb-02	SRT12_BW_2hr_2	long section of fibre at 2 hours of filtration	63X/1.2 W	2	1	8.96	512 x 512	146.2 x 146.2	12 bit	LP 650	BP 505-530	BP 565-615 IR	100% of 50%	100%	100%	146	111	129
14-Feb-02	SRT12_BW_2hr_3	long section of fibre at 2 hours of filtration	63X/1.2 W	2	1.3	8.96	512 x 512	116.9 x 116.9	12 bit	LP 650	BP 505-530	BP 565-615 IR	100% of 50%	100%	100%	146	111	129
16-Feb-02	SRT30_R_2hr_1	x-section of fibre at 2 hours of filtration	10X/0.25	2	1	17.92	512 x 512	921.3 x 921.3	12 bit	LP 650	BP 505-530	BP 565-615 IR	30% of 50%	100%	100%	146	111	129
16-Feb-02	SRT30_R_2hr_2	x-section of fibre at 2 hours of filtration	10X/0.25	2	1	17.92	512 x 512	921.3 x 921.3	12 bit	LP 650	BP 505-530	BP 565-615 IR	30% of 50%	100%	100%	146	111	129
16-Feb-02	SRT12_BW_2hr_4	long section of fibre at 2 hours of filtration	63X/1.2 W	2	1	35.84	512 x 512	146.2 x 146.2	12 bit	LP 650	BP 505-530	BP 565-615 IR	30% of 50%	100%	100%	141	111	129
16-Feb-02	SRT12_BW_2hr_5	long section of fibre at 2 hours of filtration	63X/1.2 W	2	2.4	8.96	512 x 512	60 x 60	12 bit	LP 650	BP 505-530	BP 565-615 IR	30% of 50%	100%	100%	146	111	129
16-Feb-02	SRT12_BW_2hr_6	long section of fibre at 2 hours of filtration	10X/0.25	2	3.5	71.68	512 x 512	266.3 x 266.3	12 bit	LP 650	BP 505-530	BP 565-615 IR	30% of 50%	100%	100%	146	111	129

Date	File Name	Specimen	Dye/Lectin			Abs/Em I			Detector Gain			Amplitude Offset			Amplitude Gain			Z-step size (um)	# of Z sections	Total Z depth (um)
			Ch 1	Ch 2	Ch 3	Ch 1	Ch 2	Ch 3	Ch 1	Ch 2	Ch 3	Ch 1	Ch 2	Ch 3	Ch 1	Ch 2	Ch 3			
13-Feb-02	SRT12R_2hr_1	long section of fibre at 2 hours of filtration	ConA-AF647	SBA-AF488	WGA-tmr	650/668	495/519	555/580	915	955	985	-0.084	-0.129	-0.074	1.45	2.32	1.94	2.05	42	86.1
13-Feb-02	SRT12_R_2hr_SBA	long section of fibre at 2 hours of filtration	SBA-AF488			495/519			965			-0.134			2.4					
13-Feb-02	SRT12_R_2hr_WGA	long section of fibre at 2 hours of filtration	WGA-tmr			555/580			940			-0.102			1.8					
13-Feb-02	SRT12_R_2hr_ConA	long section of fibre at 2 hours of filtration	ConA-AF647			650/668			864			-0.117			2.03					
13-Feb-02	SRT12_R_2hr_2	long section of fibre at 2 hours of filtration	ConA-AF647	SBA-AF488	WGA-tmr	650/668	495/519	555/580	819	1000	955	-0.238	-0.202	-0.235	2.86	3	2.53			
13-Feb-02	SRT12_R_2hr_4	long section of fibre at 2 hours of filtration	ConA-AF647	SBA-AF488	WGA-tmr	650/668	495/519	555/580												
14-Feb-02	SRT12_BW_2hr_1	long section of fibre at 2 hours of filtration	ConA-AF647	SBA-AF488	WGA-tmr	650/668	495/519	555/580	878	990	943	-0.064	-0.084	-0.1105	1.5	2.02	2.1	1	20	19
14-Feb-02	SRT12_BW_2hr_2	long section of fibre at 2 hours of filtration	ConA-AF647	SBA-AF488	WGA-tmr	650/668	495/519	555/580	785	839	787	-0.085	-0.0705	-0.0715	2.08	1.79	1.42	0.75	25	18
14-Feb-02	SRT12_BW_2hr_3	long section of fibre at 2 hours of filtration	ConA-AF647	SBA-AF488	WGA-tmr	650/668	495/519	555/580												19
16-Feb-02	SRT30_R_2hr_1	x-section of fibre at 2 hours of filtration	ConA-AF647	SBA-AF488	WGA-tmr	650/668	495/519	555/580	627	807	900	-0.089	-0.1305	-0.195	2.03	2.2	2.11			
16-Feb-02	SRT30_R_2hr_2	x-section of fibre at 2 hours of filtration	ConA-AF647	SBA-AF488	WGA-tmr	650/668	495/519	555/580	622	769	815	-0.052	-0.079	-0.094	1.74	2.09	1.9			
16-Feb-02	SRT12_BW_2hr_4	long section of fibre at 2 hours of filtration	ConA-AF647	SBA-AF488	WGA-tmr	650/668	495/519	555/580	795	935	770	-0.0685	-0.07	-0.1315	1.64	2	2.47			
16-Feb-02	SRT12_BW_2hr_5	long section of fibre at 2 hours of filtration	ConA-AF647	SBA-AF488	WGA-tmr	650/668	495/519	555/580	994	943	825	-0.049	-0.077	-0.079	1.59	1.75	2.2	0.45	12	5.4
16-Feb-02	SRT12_R_2hr_6	long section of fibre at 2 hours of filtration	ConA-AF647	SBA-AF488	WGA-tmr	650/668	495/519	555/580	874	944	953	-0.1935	-0.069	-0.191	1.04	2.4	2.42			

Appendix J

CLSM IMAGE DATA - RUN 1 after 3 days of filtration

Date	File Name	Specimen	Obj/NA	Averaging	Zoom	Speed (us/pixel)	Image Size			Filters			Laser Power			Pinhole (um)		
							Pixels	Microns		Ch 1	Ch2	Ch 3	488	543	633	Ch 1	Ch 2	Ch 3
18-Feb-02	SRT30R_3day_1	long section of fibre after 3 days of filtration	63X/1.2 W	2	2.3	17.92	512 x 512		12 bit	LP 650	BP 505-530	BP 565-615 IR	50% of 50%	100%	100%	146	111	129
18-Feb-02	SRT30R_3day_2	long section of fibre after 3 days of filtration	63X/1.2 W	2	1	17.92	512 x 512	146.2 x 146.2	12 bit	LP 650	BP 505-530	BP 565-615 IR	50% of 50%	100%	100%	146	111	129
19-Feb-02	SRT30R_3day_3	long section of fibre after 3 days of filtration	63X/0.9 W	2	1	8.96	512 x 512	146.2 x 146.2	12 bit	LP 650	BP 505-530	BP 565-615 IR	50% of 25%	100%	100%	191	151	204
19-Feb-02	SRT30R_3day_7	x-section of fibre after 3 days of filtration	10X/0.25	2	1	4.48	512 x 512	921.3 x 921.3	12 bit	LP 650	BP 505-530	BP 565-615 IR	50% of 50%	100%	100%	96	91	104
18-Feb-02	SRT12BW_3day_1	long section of fibre after 3 days of filtration	63X/1.2 W	2	1	17.92	512 x 512	146.2 x 146.2	12 bit	LP 650	BP 505-530	BP 565-615 IR	50% of 50%	100%	100%	146	111	129
18-Feb-02	SRT12BW_3day_2	long section of fibre after 3 days of filtration	63X/1.2 W	2	1.6	8.96	512 x 512	91.3 x 91.3	12 bit	LP 650	BP 505-530	BP 565-615 IR	50% of 50%	100%	100%	146	151	144
19-Feb-02	SRT12BW_3day_3	x-section of fibre after 3 days of filtration	10X/0.25	2	1	71.68	512 x 512	921.3 x 921.3	12 bit	LP 650	BP 505-530	BP 565-615 IR	50% of 50%	100%	100%	111	86	99
19-Feb-02	SRT12BW_3day_4	x-section of fibre after 3 days of filtration	40X/0.6	2	1	71.68	512 x 512	230.3 x 230.3	12 bit	LP 650	BP 505-530	BP 565-615 IR	50% of 50%	100%	100%	181	141	164
20-Feb-02	SRT12R_3day_1	long section of fibre after 3 days of filtration	63X/1.2 W	2	1	8.96	512 x 512	146.2 x 146.2	12 bit	LP 650	BP 505-530	BP 565-615 IR	50% of 50%	100%	100%	146	111	129
20-Feb-02	SRT12R_3day_2	long section of fibre after 3 days of filtration	63X/1.2 W	2	1	8.96	512 x 512	146.2 x 146.2	12 bit	LP 650	BP 505-530	BP 565-615 IR	50% of 50%	100%	100%	146	111	129
20-Feb-02	SRT12R_3day_3	long section of fibre after 3 days of filtration	63X/1.2 W	2	1	8.96	512 x 512	146.2 x 146.2	12 bit	LP 650	BP 505-530	BP 565-615 IR	50% of 50%	100%	100%	146	111	129
20-Feb-02	SRT12R_3day_4	x-section of fibre after 3 days of filtration	10X/0.25	2	1	71.68	512 x 512	921.3 x 921.3	12 bit	LP 650	BP 505-530	BP 565-615 IR	50% of 50%	100%	100%	146	111	129
20-Feb-02	SRT12R_3day_5	x-section of fibre after 3 days of filtration	40X/0.6	2	1	71.68	512 x 512	230.3 x 230.3	12 bit	LP 650	BP 505-530	BP 565-615 IR	50% of 50%	100%	100%	181	141	164

Date	File Name	Specimen	Dye/Lectin			Abs/Em l			Detector Gain			Amplitude Offset			Amplitude Gain			Z-step size (um)	# of Z sections	Total Z depth (um)
			Ch 1	Ch 2	Ch 3	Ch 1	Ch 2	Ch 3	Ch 1	Ch 2	Ch 3	Ch 1	Ch 2	Ch 3	Ch 1	Ch 2	Ch 3			
18-Feb-02	SRT30R_3day_1	long section of fibre after 3 days of filtration	ConA-AF647	SBA-AF488	WGA-tmr	650/668	495/519	555/580	1000	1000	990	-0.185	-0.169	-0.1865	2.39	2.59	2.71	0.5	30	14.5
18-Feb-02	SRT30R_3day_2	long section of fibre after 3 days of filtration	ConA-AF647	SBA-AF488	WGA-tmr	650/668	495/519	555/580	827	879	940	-0.049	-0.047	-0.099	1.4	1.95	1.78	0.5	14	7
19-Feb-02	SRT30R_3day_3	long section of fibre after 3 days of filtration	ConA-AF647	SBA-AF488	WGA-tmr	650/668	495/519	555/580	720	855	755	-0.019	-0.002	-0.1215	191	2.44	2.58	0.5	36	17.5
19-Feb-02	SRT30R_3day_7	x-section of fibre after 3 days of filtration	ConA-AF647	SBA-AF488	WGA-tmr	650/668	495/519	555/580	665	1000	958	-0.084	-0.052	-0.1055	1.33	1.4	1.4	5	30	145
18-Feb-02	SRT12BW_3day_1	long section of fibre after 3 days of filtration	ConA-AF647	SBA-AF488	WGA-tmr	650/668	495/519	555/580	860	950	965	-0.114	-0.112	-0.0915	2.6	2.74	2.42	0.5	19	9
18-Feb-02	SRT12BW_3day_2	long section of fibre after 3 days of filtration	ConA-AF647	SBA-AF488	WGA-tmr	650/668	495/519	555/580	902	1000	1000	-0.069	-0.1105	-0.1405	2.27	2.7	2.63	0.25	16	3.75
19-Feb-02	SRT12BW_3day_3	x-section of fibre after 3 days of filtration	ConA-AF647	SBA-AF488	WGA-tmr	650/668	495/519	555/580	629	940	931	0.006	-0.022	-0.064	1	1	1.53			
19-Feb-02	SRT12BW_3day_4	x-section of fibre after 3 days of filtration	ConA-AF647	SBA-AF488	WGA-tmr	650/668	495/519	555/580	702	1000	1000	-0.099	-0.0865	-0.091	1.5	2.39	2.38			
20-Feb-02	SRT12R_3day_1	long section of fibre after 3 days of filtration	ConA-AF647	SBA-AF488	WGA-tmr	650/668	495/519	555/580	849	930	915	-0.067	-0.084	-0.114	1.55	2.31	2.4	1	20	19
20-Feb-02	SRT12R_3day_2	long section of fibre after 3 days of filtration	ConA-AF647	SBA-AF488	WGA-tmr	650/668	495/519	555/580										0.8	22	17.6
20-Feb-02	SRT12R_3day_3	long section of fibre after 3 days of filtration	ConA-AF647	SBA-AF488	WGA-tmr	650/668	495/519	555/580	853	1000	990	-0.072	-0.089	-0.099	1.5	2.13	1.74	1	35	34
20-Feb-02	SRT12R_3day_4	x-section of fibre after 3 days of filtration	ConA-AF647	SBA-AF488	WGA-tmr	650/668	495/519	555/580	571	858	900	-0.0275	-0.0355	-0.0475	1	1	1			
20-Feb-02	SRT12R_3day_5	x-section of fibre after 3 days of filtration	ConA-AF647	SBA-AF488	WGA-tmr	650/668	495/519	555/580	725	945	990	0.006	-0.109	-0.119	1	2.57	2.35			

Appendix J

CLSM IMAGE DATA - RUN 1 after 15 days of filtration

Date	File Name	Specimen	Obj/NA	Averaging	Zoom	Speed (us/pixel)	Image Size			Filters			Laser Power			Photobit (um)		
							Pixels	Microns		Ch 1	Ch2	Ch 3	488	543	633	Ch 1	Ch 2	Ch 3
27-Feb-02	SRT30R_15dav_1	x-section section of fibre after 15 days of filtration	10X/0.25	2	1	71.68	512 x 512	921.3 x 921.3	12 bit	LP 650	BP 505-530	BP 565-615 IR	50% of 50%	100%	100%	146	111	129
27-Feb-02	SRT30R_15dav_2	x-section of fibre after 15 days of filtration	40X/0.6	2	1	71.68	512 x 512	230.3 x 230.3	12 bit	LP 650	BP 505-530	BP 565-615 IR	50% of 50%	100%	100%	181	141	164
27-Feb-02	SRT30R_15day_3	long section of fibre after 15 days of filtration	63X/1.2 W	2	2.8	8.96	512 x 512	52.5 x 52.5	12 bit	LP 650	BP 505-530	BP 565-615 IR	50% of 25%	100%	100%	146	111	129
27-Feb-02	SRT30R_15day_4	long section of fibre after 15 days of filtration	63X/1.2 W	2	1	8.96	512 x 512	146.2 x 146.2	12 bit	LP 650	BP 505-530	BP 565-615 IR	50% of 50%	100%	100%	146	111	129
27-Feb-02	SRT30R_15dav_5	long section of fibre after 15 days of filtration	63X/1.2 W	2	1	8.96	512 x 512	146.2 x 146.2	12 bit	LP 650	BP 505-530	BP 565-615 IR	50% of 50%	100%	100%	146	111	129
27-Feb-02	SRT30R_15dav_6	long section of fibre after 15 days of filtration	63X/1.2 W	2	2.2	8.96	512 x 512	67.9 x 67.9	12 bit	LP 650	BP 505-530	BP 565-615 IR	50% of 50%	100%	100%	146	111	129
28-Feb-02	SRT12R_15day_1	x-section of fibre after 15 days of filtration	10X/0.25	2	1	71.68	512 x 512	921.3 x 921.3	12 bit	LP 650	BP 505-530	BP 565-615 IR	50% of 50%	100%	100%	146	111	129
28-Feb-02	SRT12R_15day_2	x-section of fibre after 15 days of filtration	20X/0.75	2	1	8.96	512 x 512	460.6 x 460.3	12 bit	LP 650	BP 505-530	BP 565-615 IR	50% of 50%	100%	100%	146	111	129
28-Feb-02	SRT12R_15day_3	long section of fibre after 15 days of filtration	63X/1.2 W	2	1	8.96	512 x 512	146.2 x 146.2	12 bit	LP 650	BP 505-530	BP 565-615 IR	50% of 50%	100%	100%	146	111	129
01-Mar-02	SRT12R_15day_4	long section of fibre after 15 days of filtration	63X/0.9 W	2	1	8.96	512 x 512	146.2 x 146.2	12 bit	LP 650	BP 505-530	BP 565-615 IR	50% of 50%	100%	100%	196	151	169
01-Mar-02	SRT12R_15day_5	long section of fibre after 15 days of filtration	63X/0.9 W	2	2	8.96	512 x 512	73.1 x 73.1	12 bit	LP 650	BP 505-530	BP 565-615 IR	50% of 50%	100%	100%	196	151	169
01-Mar-02	SRT12BW_15day_1	long section of fibre after 15 days of filtration	63X/0.9 W	2	1	8.96	512 x 512	146.2 x 146.2	12 bit	LP 650	BP 505-530	BP 565-615 IR	50% of 50%	100%	100%	191	147	169
04-Mar-02	SRT12BW_15day_2	long section of fibre after 15 days of filtration	63X/0.9 W	2	1	8.96	512 x 512	146.2 x 146.2	12 bit	LP 650	BP 505-530	BP 565-615 IR	50% of 50%	100%	100%	191	147	169
04-Mar-02	SRT12BW_15day_3	long section of fibre after 15 days of filtration	63X/0.9 W	2	1	8.96	512 x 512	146.2 x 146.2	12 bit	LP 650	BP 505-530	BP 565-615 IR	50% of 50%	100%	100%	191	147	169
04-Mar-02	SRT12BW_15day_4	long section of fibre after 15 days of filtration	63X/0.9 W	2	1	8.96	512 x 512	146.2 x 146.2	12 bit	LP 650	BP 505-530	BP 565-615 IR	50% of 50%	100%	100%	191	147	169
04-Mar-02	SRT12BW_15day_5	x-section of fibre after 15 days of filtration	10X/0.25	2	1	8.96	512 x 512	921.3 x 921.3	12 bit	LP 650	BP 505-530	BP 565-615 IR	50% of 50%	100%	100%	191	147	169
04-Mar-02	SRT12BW_15dav_6	x-section of fibre after 15 days of filtration	40X/0.6	2	1	8.96	512 x 512	230.3 x 230.3	12 bit	LP 650	BP 505-530	BP 565-615 IR	50% of 50%	100%	100%	181	142	164

Date	File Name	Specimen	Dye/Lectin			Abs/Em I			Detector Gain			Amplitude Offset			Amplitude Gain			Z-step size (um)	# of Z sections	Total Z depth (um)
			Ch 1	Ch 2	Ch 3	Ch 1	Ch 2	Ch 3	Ch 1	Ch 2	Ch 3	Ch 1	Ch 2	Ch 3	Ch 1	Ch 2	Ch 3			
27-Feb-02	SRT30R_15dav_1	x-section of fibre after 15 days of filtration	ConA-AF647	SBA-AF488	WGA-tmr	650/668	495/519	555/580	670	782	769	-0.049	-0.062	-0.0815	1	1.7	1.5			
18-Feb-02	SRT30R_3dav_2	x-section of fibre after 15 days of filtration	ConA-AF647	SBA-AF488	WGA-tmr	650/668	495/519	555/580	873	980	975	-0.014	-0.057	-0.0775	1.42	1.66	1.7			
27-Feb-02	SRT30R_3day_3	long section of fibre after 15 days of filtration	ConA-AF647	SBA-AF488	WGA-tmr	650/668	495/519	555/580	729	930	866	-0.079	-0.112	-0.0365	1.7	2.44	2.07	0.5	23	11.5
27-Feb-02	SRT30R_15day_4	long section of fibre after 15 days of filtration	ConA-AF647	SBA-AF488	WGA-tmr	650/668	495/519	555/580	729	825	836	-0.064	0.067	-0.0565	1.7	1	1	0.75	32	23.25
27-Feb-02	SRT30R_15dav_5	long section of fibre after 15 days of filtration	ConA-AF647	SBA-AF488	WGA-tmr	650/668	495/519	555/580	677	768	780	-0.006	-0.002	-0.006	1.47	1.55	1.5	0.55	30	15.95
27-Feb-02	SRT30R_15dav_6	long section of fibre after 15 days of filtration	ConA-AF647	SBA-AF488	WGA-tmr	650/668	495/519	555/580	980	1000	1000	-0.069	-0.089	-0.1165	1.89	2.3	2.4	0.55	21	11
28-Feb-02	SRT12R_15day_1	x-section of fibre after 15 days of filtration	ConA-AF647	SBA-AF488	WGA-tmr	650/668	495/519	555/580	657	875	836	-0.024	-0.032	-0.0475	1	1	1			
28-Feb-02	SRT12R_15day_2	x-section of fibre after 15 days of filtration	ConA-AF647	SBA-AF488	WGA-tmr	650/668	495/519	555/580	417	672	684	-0.0415	-0.027	-0.029	1.55	1.3	1.01	2.3	31	69
28-Feb-02	SRT12R_15day_3	long section of fibre after 15 days of filtration	ConA-AF647	SBA-AF488	WGA-tmr	650/668	495/519	555/580	890	902	884	-0.074	-0.072	-0.129	1	1.52	2.06	1	40	39
01-Mar-02	SRT12R_15day_4	long section of fibre after 15 days of filtration	ConA-AF647	SBA-AF488	WGA-tmr	650/668	495/519	555/580	862	867	851	-0.087	-0.054	-0.084	1.01	1.47	1.55	1.5	18	25.5
01-Mar-02	SRT12R_15day_5	long section of fibre after 15 days of filtration	ConA-AF647	SBA-AF488	WGA-tmr	650/668	495/519	555/580	895	1000	1000	-0.114	-0.107	-0.139	2.7	2.6	2.7	0.6	18	10.2
01-Mar-02	SRT12BW_15day_1	long section of fibre after 15 days of filtration	ConA-AF647	SBA-AF488	WGA-tmr	650/668	495/519	555/580	768	851	840	-0.087	-0.069	-0.084	1.7	1.5	1.66	1.05	29	29.4
04-Mar-02	SRT12BW_15day_2	long section of fibre after 15 days of filtration	ConA-AF647	SBA-AF488	WGA-tmr	650/668	495/519	555/580	866	933	920	-0.062	-0.024	-0.084	1.56	1.94	1.87	1.75	29	49
04-Mar-02	SRT12BW_15day_3	long section of fibre after 15 days of filtration	ConA-AF647	SBA-AF488	WGA-tmr	650/668	495/519	555/580	875	942	955	-0.104	-0.059	-0.0875	1	1	1	1	24	23
04-Mar-02	SRT12BW_15day_4	long section of fibre after 15 days of filtration	ConA-AF647	SBA-AF488	WGA-tmr	650/668	495/519	555/580	829	898	902	-0.097	-0.084	-0.089	1	1	1	0.7	33	22.4
04-Mar-02	SRT12BW_15day_5	x-section of fibre after 15 days of filtration	ConA-AF647	SBA-AF488	WGA-tmr	650/668	495/519	555/580	593	849	815	-0.009	-0.0425	-0.054	1	1	1	3.05	35	103.7
04-Mar-02	SRT12BW_15dav_6	x-section of fibre after 15 days of filtration	ConA-AF647	SBA-AF488	WGA-tmr	650/668	495/519	555/580	850	955	960	-0.037	-0.072	-0.0845	1	2	2	2.1	36	73.5

Appendix J

CLSM IMAGE DATA - RUN 1 at Critical Transmembrane Pressure

Date	File Name	Specimen	Obj/NA	Averaging	Zoom	Speed (us/pixel)	Image Size		Filters			Laser Power			Pinhole (um)		
							Pixels	Microns	Ch 1	Ch2	Ch 3	488	543	633	Ch 1	Ch 2	Ch 3
11-Mar-02	SRT12RI_60kpa_1	long section of fibre @ 60kpa	63X/1.2 W	2	1	8.96	512 x 512	146.2 x 146.2 12 bit	LP 650	BP 505-530	BP 565-615 IR	50% of 50%	100%	100%	146	111	129
11-Mar-02	SRT12RI_60kpa_2	long section of fibre @ 60kpa	63X/1.2 W	2	1	8.96	512 x 512	146.2 x 146.2 12 bit	LP 650	BP 505-530	BP 565-615 IR	50% of 50%	100%	100%	146	111	129
11-Mar-02	SRT12RI_60kpa_3	long section of fibre @ 60kPa	63X/0.9 W	2	2.7	8.96	512 x 512	54.9 x 54.9 12 bit	LP 650	BP 505-530	BP 565-615 IR	50% of 25%	100%	100%	146	111	129
11-Mar-02	SRT12RI_60kpa_4	long section of fibre @ 60kPa	63X/1.2 W	2	1	8.96	512 x 512	146.2 x 146.2 12 bit	LP 650	BP 505-530	BP 565-615 IR	50% of 50%	100%	100%	146	111	129
11-Mar-02	SRT12RI_60kpa_5	x-section of fibre @ 60kPa	10X/0.25	2	1	17.92	512 x 512	921.3 x 921.3 12 bit	LP 650	BP 505-530	BP 565-615 IR	50% of 50%	100%	100%	111	86	99
11-Mar-02	SRT12RI_60kpa_7	x-section of fibre @ 60kPa	40X/0.6	2	1	71.68	512 x 512	230.3 x 230.3 12 bit	LP 650	BP 505-530	BP 565-615 IR	50% of 50%	100%	100%	181	141	164
11-Mar-02	SRT12RI_60kpa_8	long section of fibre @ 60kPa	63X/1.2 W	2	1	8.96	512 x 512	146.2 x 146.2 12 bit	LP 650	BP 505-530	BP 565-615 IR	50% of 50%	100%	100%	146	111	129
11-Mar-02	SRT12RI_60kpa_9	long section of fibre @ 60kPa	63X/1.2 W	2	5	17.92	512 x 512	29.2 x 29.2 12 bit	LP 650	BP 505-530	BP 565-615 IR	50% of 50%	100%	100%	146	111	129
13-Mar-02	SRT12BW_60kPa_1	long section of fibre @ 60kPa	63X/0.9 W	2	2.5	8.96	512 x 512	57.4 x 57.4 12 bit	LP 650	BP 505-530	BP 565-615 IR	50% of 50%	100%	100%	191	146	169
13-Mar-02	SRT12BW_60kPa_3	long section of fibre @ 60kPa	63X/1.2 W	2	1	8.96	512 x 512	146.2 x 146.2 12 bit	LP 650	BP 505-530	BP 565-615 IR	50% of 50%	100%	100%	146	111	129
13-Mar-02	SRT12BW_60kPa_4	long section of fibre @ 60kPa	63X/1.2 W	2	1	8.96	512 x 512	146.2 x 146.2 12 bit	LP 650	BP 505-530	BP 565-615 IR	50% of 50%	100%	100%	146	111	129
13-Mar-02	SRT12BW_60kPa_5	long section of fibre @ 60kPa	63X/1.2 W	2	1	17.92	512 x 512	146.2 x 146.2 12 bit	LP 650	BP 505-530	BP 565-615 IR	50% of 50%	100%	100%	146	111	129
13-Mar-02	SRT12BW_60kPa_6	long section of fibre @ 60kPa	63X/1.2 W	2	1	8.96	512 x 512	146.2 x 146.2 12 bit	LP 650	BP 505-530	BP 565-615 IR	50% of 50%	100%	100%	146	111	129
13-Mar-02	SRT12BW_60kPa_7	long section of fibre @ 60kPa	63X/1.2 W	2	1	8.96	512 x 512	146.2 x 146.2 12 bit	LP 650	BP 505-530	BP 565-615 IR	50% of 50%	100%	100%	146	111	129
13-Mar-02	SRT12BW_60kPa_9	x-section of fibre @ 60kPa	10X/0.25	2	1.3	71.68	512 x 512	921.3 x 921.3 12 bit	LP 650	BP 505-530	BP 565-615 IR	50% of 50%	100%	100%	146	112	129
13-Mar-02	SRT12BW_60kPa_10	x-section of fibre @ 60kPa	10X/0.25	2	1.3	17.92	512 x 512	921.3 x 921.3 12 bit	LP 650	BP 505-530	BP 565-615 IR	50% of 50%	100%	100%	146	112	129
13-Mar-02	SRT12BW_60kPa_11	x-section of fibre @ 60kPa	40X/0.6	2	1	71.68	512 x 512	230.3 x 230.3 12 bit	LP 650	BP 505-530	BP 565-615 IR	50% of 50%	100%	100%	181	142	164
13-Mar-02	SRT12BW_60kPa_12	x-section of fibre @ 60kPa	40X/0.6	2	1	8.96	512 x 512	230.3 x 230.3 12 bit	LP 650	BP 505-530	BP 565-615 IR	50% of 50%	100%	100%	181	142	164
14-Mar-02	SRT30R_60kPa_1	long section of fibre @ 60kpa	63X/1.2 W	2	1	8.96	512 x 512	146.2 x 146.2 12 bit	LP 650	BP 505-530	BP 565-615 IR	50% of 50%	100%	100%	146	111	129
14-Mar-02	SRT30R_60kPa_2	long section of fibre @ 60kpa	63X/1.2 W	2	2	8.96	512 x 512	73.1 x 73.1 12 bit	LP 650	BP 505-530	BP 565-615 IR	50% of 50%	100%	100%	146	111	129
14-Mar-02	SRT30R_60kPa_3	long section of fibre @ 60kpa	63X/1.2 W	2	1	8.96	512 x 512	146.2 x 146.2 12 bit	LP 650	BP 505-530	BP 565-615 IR	50% of 50%	100%	100%	146	111	129
14-Mar-02	SRT30R_60kPa_4	long section of fibre @ 60kpa	63X/1.2 W	2	1	8.96	512 x 512	146.2 x 146.2 12 bit	LP 650	BP 505-530	BP 565-615 IR	50% of 50%	100%	100%	146	111	129
14-Mar-02	SRT30R_60kPa_5	long section of fibre @ 60kpa	63X/0.9 W	2	1	8.96	512 x 512	146.2 x 146.2 12 bit	LP 650	BP 505-530	BP 565-615 IR	50% of 50%	100%	100%	191	146	169
14-Mar-02	SRT30R_60kPa_6	long section of fibre @ 60kpa	63X/0.9 W	2	2	8.96	512 x 512	73.1 x 73.1 12 bit	LP 650	BP 505-530	BP 565-615 IR	50% of 50%	100%	100%	191	146	169
14-Mar-02	SRT30R_60kPa_7	long section of fibre @ 60kpa	63X/0.9 W	2	1	8.96	512 x 512	146.2 x 146.2 12 bit	LP 650	BP 505-530	BP 565-615 IR	50% of 50%	100%	100%	191	146	169
14-Mar-02	SRT30R_60kPa_8	x-section of fibre @ 60kPa	10X/0.25	2	1	71.68	512 x 512	921.3 x 921.3 12 bit	LP 650	BP 505-530	BP 565-615 IR	50% of 50%	100%	100%	146	111	129
14-Mar-02	SRT30R_60kPa_9	x-section of fibre @ 60kPa	10X/0.25	2	1	8.96	512 x 512	921.3 x 921.3 12 bit	LP 650	BP 505-530	BP 565-615 IR	50% of 50%	100%	100%	146	111	129
14-Mar-02	SRT30R_60kPa_10	x-section of fibre @ 60kPa	40X/0.6	2	0.7	71.68	512 x 512	325.7 x 325.7 12 bit	LP 650	BP 505-530	BP 565-615 IR	50% of 50%	100%	100%	181	141	164
14-Mar-02	SRT30R_60kPa_11	x-section of fibre @ 60kPa	40X/0.6	2	0.7	8.96	512 x 512	325.7 x 325.7 12 bit	LP 650	BP 505-530	BP 565-615 IR	50% of 50%	100%	100%	181	141	164

Date	File Name	Specimen	Dye/Lectin			Abs/Em l			Detector Gain			Amplitude Offset			Amplitude Gain			Z-step size (um)	# of Z sections	Total Z depth (um)
			Ch 1	Ch 2	Ch 3	Ch 1	Ch 2	Ch 3	Ch 1	Ch 2	Ch 3	Ch 1	Ch 2	Ch 3	Ch 1	Ch 2	Ch 3			
11-Mar-02	SRT12RI_60kPa_1	long section of fibre @ 60kpa	ConA-AF647	SBA-AF488	WGA-tmr	650/668	495/519	555/580	945	975	975	-0.082	-0.074	-0.094	1.7	2.06	1.75	1	19	18
11-Mar-02	SRT12RI_60kPa_2	long section of fibre @ 60kpa	ConA-AF647	SBA-AF488	WGA-tmr	650/668	495/519	555/580	840	841	877	-0.057	-0.071	-0.079	1	1.5	1.32	0.75	22	15.75
11-Mar-02	SRT12RI_60kPa_3	long section of fibre @ 60kpa	ConA-AF647	SBA-AF488	WGA-tmr	650/668	495/519	555/580	886	960	967	-0.077	-0.049	-0.074	1.45	1.45	1.4	0.75	28	20.25
11-Mar-02	SRT12RI_60kPa_4	long section of fibre @ 60kpa	ConA-AF647	SBA-AF488	WGA-tmr	650/668	495/519	555/580	879	873	8.84	-0.0545	-0.069	-0.1005	1	1.58	1.8	0.7	27	18.2
11-Mar-02	SRT12RI_60kPa_5	x-section of fibre @ 60kPa	ConA-AF647	SBA-AF488	WGA-tmr	650/668	495/519	555/580	755	894	897	-0.034	-0.082	-0.0865	1	2.04	1.72			
11-Mar-02	SRT12RI_60kPa_7	x-section of fibre @ 60kPa	ConA-AF647	SBA-AF488	WGA-tmr	650/668	495/519	555/580	844	930	911	-0.044	-0.072	-0.099	1	2.06	2.05			
11-Mar-02	SRT12RI_60kPa_8	long section of fibre @ 60kPa	ConA-AF647	SBA-AF488	WGA-tmr	650/668	495/519	555/580	840	865	885	-0.054	-0.042	-0.0665	1	1	1	0.65	24	14.95
11-Mar-02	SRT12RI_60kPa_9	long section of fibre @ 60kPa	ConA-AF647	SBA-AF488	WGA-tmr	650/668	495/519	555/580	900	895	900	-0.094	-0.077	-0.0665	1	1.5	1.5			
13-Mar-02	SRT12BW_60kPa_1	long section of fibre @ 60kPa	ConA-AF647	SBA-AF488	WGA-tmr	650/668	495/519	555/580	900	955	918	-0.067	-0.064	-0.094	1.39	1.75	1.72	1.5	29	42
13-Mar-02	SRT12BW_60kPa_3	long section of fibre @ 60kPa	ConA-AF647	SBA-AF488	WGA-tmr	650/668	495/519	555/580	759	871	816	-0.037	-0.047	-0.0675	1.22	1.5	1.7	0.95	28	25.2
13-Mar-02	SRT12BW_60kPa_4	long section of fibre @ 60kPa	ConA-AF647	SBA-AF488	WGA-tmr	650/668	495/519	555/580	823	865	862	-0.049	-0.037	-0.044	1	1	1	0.9	22	18.9
13-Mar-02	SRT12BW_60kPa_5	long section of fibre @ 60kPa	ConA-AF647	SBA-AF488	WGA-tmr	650/668	495/519	555/580	785	930	840	-0.049	-0.037	-0.044	1	1	1	0.3	17	4.8
13-Mar-02	SRT12BW_60kPa_6	long section of fibre @ 60kPa	ConA-AF647	SBA-AF488	WGA-tmr	650/668	495/519	555/580	927	930	881	-0.072	-0.054	-0.0865	1	1.5	1.48	0.3	17	4.8
13-Mar-02	SRT12BW_60kPa_7	long section of fibre @ 60kPa	ConA-AF647	SBA-AF488	WGA-tmr	650/668	495/519	555/580	870	845	880	-0.064	-0.052	-0.0665	1	1.5	1.3	0.65	22	13.65
13-Mar-02	SRT12BW_60kPa_9	x-section of fibre @ 60kPa	ConA-AF647	SBA-AF488	WGA-tmr	650/668	495/519	555/580	693	915	915	-0.027	-0.029	-0.039	1	1	1			
13-Mar-02	SRT12BW_60kPa_10	x-section of fibre @ 60kPa	ConA-AF647	SBA-AF488	WGA-tmr	650/668	495/519	555/580	693	915	915	-0.027	-0.029	-0.039	1	1	1	4.05	27	105.3
13-Mar-02	SRT12BW_60kPa_11	x-section of fibre @ 60kPa	ConA-AF647	SBA-AF488	WGA-tmr	650/668	495/519	555/580	849	985	1000	-0.022	-0.068	-0.0775	1	1.8	1.5			
13-Mar-02	SRT12BW_60kPa_12	x-section of fibre @ 60kPa	ConA-AF647	SBA-AF488	WGA-tmr	650/668	495/519	555/580	849	985	1000	-0.022	-0.068	-0.0775	1	1.8	1.5	2.05	22	43.05
14-Mar-02	SRT30R_60kPa_1	long section of fibre @ 60kpa	ConA-AF647	SBA-AF488	WGA-tmr	650/668	495/519	555/580	795	855	850	-0.064	-0.052	-0.069	1	1	1	0.6	18	10.2
14-Mar-02	SRT30R_60kPa_2	long section of fibre @ 60kpa	ConA-AF647	SBA-AF488	WGA-tmr	650/668	495/519	555/580	683	851	869	-0.054	-0.059	-0.089	1	1.02	1.09	0.5	16	7.5
14-Mar-02	SRT30R_60kPa_3	long section of fibre @ 60kpa	ConA-AF647	SBA-AF488	WGA-tmr	650/668	495/519	555/580	810	863	890	-0.049	-0.029	-0.0365	1	1	1	0.45	19	8.1
14-Mar-02	SRT30R_60kPa_4	long section of fibre @ 60kpa	ConA-AF647	SBA-AF488	WGA-tmr	650/668	495/519	555/580	777	821	828	-0.0465	-0.037	-0.048	1	1	1	0.8	25	19.2
14-Mar-02	SRT30R_60kPa_5	long section of fibre @ 60kpa	ConA-AF647	SBA-AF488	WGA-tmr	650/668	495/519	555/580	799	822	807	-0.052	-0.002	-0.0365	1	1.4	1.4	0.8	25	19.2
14-Mar-02	SRT30R_60kPa_6	long section of fibre @ 60kpa	ConA-AF647	SBA-AF488	WGA-tmr	650/668	495/519	555/580	768	873	873	-0.029	-0.034	-0.04	1	1	1	1.05	25	25.2
14-Mar-02	SRT30R_60kPa_7	long section of fibre @ 60kpa	ConA-AF647	SBA-AF488	WGA-tmr	650/668	495/519	555/580	819	895	861	-0.029	-0.057	-0.045	1	1.46	1.4	1	27	26
14-Mar-02	SRT30R_60kPa_8	x-section of fibre @ 60kPa	ConA-AF647	SBA-AF488	WGA-tmr	650/668	495/519	555/580	726	861	815	-0.034	-0.032	-0.019	1	1.3	1.32			
14-Mar-02	SRT30R_60kPa_9	x-section of fibre @ 60kPa	ConA-AF647	SBA-AF488	WGA-tmr	650/668	495/519	555/580	726	861	815	-0.034	-0.032	-0.019	1	1.3	1.32	4.6	31	138
14-Mar-02	SRT30R_60kPa_10	x-section of fibre @ 60kPa	ConA-AF647	SBA-AF488	WGA-tmr	650/668	495/519	555/580	883	985	1000	-0.074	-0.067	-0.084	1.58	1.75	1.41			
14-Mar-02	SRT30R_60kPa_11	x-section of fibre @ 60kPa	ConA-AF647	SBA-AF488	WGA-tmr	650/668	495/519	555/580	883	985	1000	-0.074	-0.067	-0.084	1.58	1.75	1.41	1.5	38	55.5

Appendix J

CLSM IMAGE DATA - After First Recovery Cleaning

Date	File Name	Specimen	Obj/NA	Averaging	Zoom	Speed (us/pixel)	Image Size			Filters			Laser Power			Pinhole (um)		
							Pixels	Microns		Ch 1	Ch2	Ch 3	488	543	633	Ch 1	Ch 2	Ch 3
18-Mar-02	SRT12BW AR 1	long section of fibre after 2000 ppm NaOCl recovery cleaning	63X/1.2 W	2	1	8.96	512 x 512	146.2 x 146.2	12 bit	LP 650	BP 505-530	BP 565-615 IR	50% of 50%	100%	100%	146	111	129
18-Mar-02	SRT12BW AR 2	long section of fibre after 2000 ppm NaOCl recovery cleaning	63X/1.2 W	2	1	8.96	512 x 512	146.2 x 146.2	12 bit	LP 650	BP 505-530	BP 565-615 IR	50% of 50%	100%	100%	146	111	129
18-Mar-02	SRT12BW AR 3	long section of fibre after 2000 ppm NaOCl recovery cleaning	63X/1.2 W	2	1	8.96	512 x 512	146.2 x 146.2	12 bit	LP 650	BP 505-530	BP 565-615 IR	50% of 50%	100%	100%	146	111	129
18-Mar-02	SRT12BW AR 4	long section of fibre after 2000 ppm NaOCl recovery cleaning	63X/1.2 W	2	4	8.96	512 x 512	36.6 x 36.6	12 bit	LP 650	BP 505-530	BP 565-615 IR	50% of 50%	100%	100%	146	111	129
18-Mar-02	SRT12BW AR 5	long section of fibre after 2000 ppm NaOCl recovery cleaning	63X/1.2 W	2	1	8.96	512 x 512	146.2 x 146.2	12 bit	LP 650	BP 505-530	BP 565-615 IR	50% of 50%	100%	100%	146	111	129
18-Mar-02	SRT12BW AR 6	x-section of fibre after 2000 ppm NaOCl recovery cleaning	10X/0.25	2	1	71.68	512 x 512	921.3 x 921.3	12 bit	LP 650	BP 505-530	BP 565-615 IR	50% of 50%	100%	100%	146	111	129
18-Mar-02	SRT12BW AR 7	x-section of fibre after 2000 ppm NaOCl recovery cleaning	40X/0.6	2	1	71.68	512 x 512	230.3 x 230.3	12 bit	LP 650	BP 505-530	BP 565-615 IR	50% of 50%	100%	100%	181	141	164
18-Mar-02	SRT12BW AR 8	x-section of fibre after 2000 ppm NaOCl recovery cleaning	40X/0.6	2	1	71.68	512 x 512	230.3 x 230.3	12 bit	LP 650	BP 505-530	BP 565-615 IR	50% of 50%	100%	100%	181	141	164
18-Mar-02	SRT12R AR 1	long section of fibre after 2000 ppm NaOCl recovery cleaning	63X/1.2 W	2	1	8.96	512 x 512	146.2 x 146.2	12 bit	LP 650	BP 505-530	BP 565-615 IR	50% of 50%	100%	100%	146	111	129
18-Mar-02	SRT12R AR 2	long section of fibre after 2000 ppm NaOCl recovery cleaning	63X/1.2 W	2	1	8.96	512 x 512	146.2 x 146.2	12 bit	LP 650	BP 505-530	BP 565-615 IR	50% of 50%	100%	100%	146	111	129
18-Mar-02	SRT12R AR 3	long section of fibre after 2000 ppm NaOCl recovery cleaning	63X/1.2 W	2	1	8.96	512 x 512	146.2 x 146.2	12 bit	LP 650	BP 505-530	BP 565-615 IR	50% of 50%	100%	100%	146	111	129
18-Mar-02	SRT12R AR 4	long section of fibre after 2000 ppm NaOCl recovery cleaning	63X/1.2 W	2	3.3	8.96	512 x 512	44.4 x 44.4	12 bit	LP 650	BP 505-530	BP 565-615 IR	50% of 50%	100%	100%	146	111	129
18-Mar-02	SRT12R AR 5	long section of fibre after 2000 ppm NaOCl recovery cleaning	63X/1.2 W	2	1	8.96	512 x 512	146.2 x 146.2	12 bit	LP 650	BP 505-530	BP 565-615 IR	50% of 50%	100%	100%	146	111	129
22-Mar-02	SRT12R_AR_6	x-section of fibre after 2000 ppm NaOCl recovery cleaning	10X/0.25	2	1	71.68	512 x 512	921.3 x 921.3	12 bit	LP 650	BP 505-530	BP 565-615 IR	50% of 50%	100%	100%	144	112	129
22-Mar-02	SRT12R_AR_7	x-section of fibre after 2000 ppm NaOCl recovery cleaning	10X/0.25	2	1	8.96	512 x 512	921.3 x 921.3	12 bit	LP 650	BP 505-530	BP 565-615 IR	50% of 50%	100%	100%	144	112	129
22-Mar-02	SRT12R AR 8	x-section of fibre after 2000 ppm NaOCl recovery cleaning	40X/0.6	2	1	71.68	512 x 512	230.3 x 230.3	12 bit	LP 650	BP 505-530	BP 565-615 IR	50% of 50%	100%	100%	184	142	164
22-Mar-02	SRT12R AR 9	x-section of fibre after 2000 ppm NaOCl recovery cleaning	40X/0.6	2	1	8.96	512 x 512	230.3 x 230.3	12 bit	LP 650	BP 505-530	BP 565-615 IR	50% of 50%	100%	100%	184	142	164
25-Mar-02	SRT30R_AR_1	long section of fibre after 2000 ppm NaOCl recovery cleaning	63X/1.2 W	2	1	8.96	512 x 512	146.2 x 146.2	12 bit	LP 650	BP 505-530	BP 565-615 IR	50% of 50%	100%	100%	146	111	129
25-Mar-02	SRT30R_AR_2	long section of fibre after 2000 ppm NaOCl recovery cleaning	63X/1.2 W	2	1	8.96	512 x 512	146.2 x 146.2	12 bit	LP 650	BP 505-530	BP 565-615 IR	50% of 50%	100%	100%	146	111	129
25-Mar-02	SRT30R_AR_3	long section of fibre after 2000 ppm NaOCl recovery cleaning	63X/1.2 W	2	1	8.96	512 x 512	146.2 x 146.2	12 bit	LP 650	BP 505-530	BP 565-615 IR	50% of 50%	100%	100%	146	111	129
25-Mar-02	SRT30R_AR_4	long section of fibre after 2000 ppm NaOCl recovery cleaning	63X/1.2 W	2	1	8.96	512 x 512	146.2 x 146.2	12 bit	LP 650	BP 505-530	BP 565-615 IR	50% of 50%	100%	100%	146	111	129
25-Mar-02	SRT30R_AR_5	long section of fibre after 2000 ppm NaOCl recovery cleaning	63X/0.9 W	2	1	8.96	512 x 512	146.2 x 146.2	12 bit	LP 650	BP 505-530	BP 565-615 IR	50% of 50%	100%	100%	191	146	169
25-Mar-02	SRT30R_AR_6	x-section of fibre after 2000 ppm NaOCl recovery cleaning	63X/0.9 W	2	1	71.68	512 x 512	146.2 x 146.2	12 bit	LP 650	BP 505-530	BP 565-615 IR	50% of 50%	100%	100%	191	146	169
25-Mar-02	SRT30R AR 7	x-section of fibre after 2000 ppm NaOCl recovery cleaning	10X/0.25	2	1	71.68	512 x 512	921.3 x 921.3	12 bit	LP 650	BP 505-530	BP 565-615 IR	50% of 50%	100%	100%	146	111	129
25-Mar-02	SRT30R AR 8	x-section of fibre after 2000 ppm NaOCl recovery cleaning	10X/0.25	2	1	8.96	512 x 512	921.3 x 921.3	12 bit	LP 650	BP 505-530	BP 565-615 IR	50% of 50%	100%	100%	146	111	129
25-Mar-02	SRT30R AR 9	x-section of fibre after 2000 ppm NaOCl recovery cleaning	40X/0.6	2	1	8.96	512 x 512	230.3 x 230.3	12 bit	LP 650	BP 505-530	BP 565-615 IR	50% of 50%	100%	100%	181	141	164

Date	File Name	Specimen	Dye/Lectin			Abs/Em 1			Detector Gain			Amplitude Offset			Amplitude Gain			Z-step size (um)	# of Z sections	Total Z depth (um)
			Ch 1	Ch 2	Ch 3	Ch 1	Ch 2	Ch 3	Ch 1	Ch 2	Ch 3	Ch 1	Ch 2	Ch 3	Ch 1	Ch 2	Ch 3			
18-Mar-02	SRT12BW AR 1	long section of fibre after 2000 ppm NaOCl recovery cleaning	ConA-AF647	SBA-AF488	WGA-tmr	650/668	495/519	555/580	865	960	975	-0.059	-0.074	-0.049	1.52	2.15	1.68	1	26	25
18-Mar-02	SRT12BW AR 2	long section of fibre after 2000 ppm NaOCl recovery cleaning	ConA-AF647	SBA-AF488	WGA-tmr	650/668	495/519	555/580	642	924	916	-0.065	-0.064	-0.091	1	1.61	1.6	0.5	14	6.5
18-Mar-02	SRT12BW AR 3	long section of fibre after 2000 ppm NaOCl recovery cleaning	ConA-AF647	SBA-AF488	WGA-tmr	650/668	495/519	555/580	778	957	951	-0.037	-0.069	-0.089	1	1.74	1.66	0.5	18	8.5
18-Mar-02	SRT12BW AR 4	long section of fibre after 2000 ppm NaOCl recovery cleaning	ConA-AF647	SBA-AF488	WGA-tmr	650/668	495/519	555/580	767	975	963	-0.084	-0.064	-0.0865	1.78	1.67	1.62	0.5	18	8.5
18-Mar-02	SRT12BW AR 5	long section of fibre after 2000 ppm NaOCl recovery cleaning	ConA-AF647	SBA-AF488	WGA-tmr	650/668	495/519	555/580	684	950	920	-0.044	-0.054	-0.079	1	1.58	1.68	0.5	18	8.5
18-Mar-02	SRT12BW AR 6	x-section of fibre after 2000 ppm NaOCl recovery cleaning	ConA-AF647	SBA-AF488	WGA-tmr	650/668	495/519	555/580	669	869	939	-0.034	-0.042	-0.069	1	1.37	1.44			
18-Mar-02	SRT12BW AR 7	x-section of fibre after 2000 ppm NaOCl recovery cleaning	ConA-AF647	SBA-AF488	WGA-tmr	650/668	495/519	555/580	790	980	1000	-0.049	-0.097	-0.119	1	2.07	2.05			
18-Mar-02	SRT12BW AR 8	x-section of fibre after 2000 ppm NaOCl recovery cleaning	ConA-AF647	SBA-AF488	WGA-tmr	650/668	495/519	555/580	790	980	1000	-0.049	-0.097	-0.119	1	2.07	2.05	1.4	34	46.2
18-Mar-02	SRT12R AR 1	long section of fibre after 2000 ppm NaOCl recovery cleaning	ConA-AF647	SBA-AF488	WGA-tmr	650/668	495/519	555/580	425	865	918	-0.062	-0.062	-0.0475	1.7	1.45	1	1	37	36
18-Mar-02	SRT12R AR 2	long section of fibre after 2000 ppm NaOCl recovery cleaning	ConA-AF647	SBA-AF488	WGA-tmr	650/668	495/519	555/580	615	929	935	-0.064	-0.052	-0.069	1.57	1.51	1.61	0.55	22	11.55
18-Mar-02	SRT12R AR 3	long section of fibre after 2000 ppm NaOCl recovery cleaning	ConA-AF647	SBA-AF488	WGA-tmr	650/668	495/519	555/580	710	977	955	-0.024	-0.042	-0.0525	1.01	1.69	1.6	0.9	25	21.6
18-Mar-02	SRT12R AR 4	long section of fibre after 2000 ppm NaOCl recovery cleaning	ConA-AF647	SBA-AF488	WGA-tmr	650/668	495/519	555/580	859	980	1000	-0.024	-0.047	-0.044	1.25	2.11	2.08	0.65	20	12.35
18-Mar-02	SRT12R AR 5	long section of fibre after 2000 ppm NaOCl recovery cleaning	ConA-AF647	SBA-AF488	WGA-tmr	650/668	495/519	555/580	840	1000	1000	-0.0345	-0.079	-0.0865	1	2.69	1.88	1	24	23
22-Mar-02	SRT12R_AR_6	x-section of fibre after 2000 ppm NaOCl recovery cleaning	ConA-AF647	SBA-AF488	WGA-tmr	650/668	495/519	555/580	733	1000	960	-0.077	-0.074	-0.084	1.55	1.5	1.51			
22-Mar-02	SRT12R_AR_7	x-section of fibre after 2000 ppm NaOCl recovery cleaning	ConA-AF647	SBA-AF488	WGA-tmr	650/668	495/519	555/580	518	861	913	-0.047	-0.035	-0.039	1	1	1	3.1	30	89.9
22-Mar-02	SRT12R AR 8	x-section of fibre after 2000 ppm NaOCl recovery cleaning	ConA-AF647	SBA-AF488	WGA-tmr	650/668	495/519	555/580	858	1000	970	-0.054	-0.094	-0.1225	1	1.96	1.9			
22-Mar-02	SRT12R AR 9	x-section of fibre after 2000 ppm NaOCl recovery cleaning	ConA-AF647	SBA-AF488	WGA-tmr	650/668	495/519	555/580	803	1000	970	-0.029	-0.064	-0.0975	1	1.96	1.9	2.1	30	60.9
25-Mar-02	SRT30R_AR_1	long section of fibre after 2000 ppm NaOCl recovery cleaning	ConA-AF647	SBA-AF488	WGA-tmr	650/668	495/519	555/580	725	918	936	-0.049	-0.049	-0.094	1	1.53	1.85	0.7	26	17.5
25-Mar-02	SRT30R_AR_2	long section of fibre after 2000 ppm NaOCl recovery cleaning	ConA-AF647	SBA-AF488	WGA-tmr	650/668	495/519	555/580	735	908	944	-0.049	-0.059	-0.104	1	1.85	1.88	0.5	25	12
25-Mar-02	SRT30R_AR_3	long section of fibre after 2000 ppm NaOCl recovery cleaning	ConA-AF647	SBA-AF488	WGA-tmr	650/668	495/519	555/580	716	907	891	-0.054	-0.039	-0.089	1	1.44	1.55	0.55	22	11.55
25-Mar-02	SRT30R_AR_4	long section of fibre after 2000 ppm NaOCl recovery cleaning	ConA-AF647	SBA-AF488	WGA-tmr	650/668	495/519	555/580	724	893	906	-0.07	-0.044	-0.073	1	1.55	1.6	0.5	20	9.5
25-Mar-02	SRT30R_AR_5	long section of fibre after 2000 ppm NaOCl recovery cleaning	ConA-AF647	SBA-AF488	WGA-tmr	650/668	495/519	555/580	628	146	908	-0.044	-0.0635	-0.0725	1	1.6	1.6	1.5	27	39
25-Mar-02	SRT30R_AR_6	x-section of fibre after 2000 ppm NaOCl recovery cleaning	ConA-AF647	SBA-AF488	WGA-tmr	650/668	495/519	555/580	559	892	881	-0.024	-0.039	-0.064	1	1.5	1.49			
25-Mar-02	SRT30R AR 7	x-section of fibre after 2000 ppm NaOCl recovery cleaning	ConA-AF647	SBA-AF488	WGA-tmr	650/668	495/519	555/580	536	891	940	-0.049	-0.047	-0.054	1	1	1			
25-Mar-02	SRT30R AR 8	x-section of fibre after 2000 ppm NaOCl recovery cleaning	ConA-AF647	SBA-AF488	WGA-tmr	650/668	495/519	555/580	546	901	950	-0.034	-0.032	-0.039	1	1	1	3	27	78
25-Mar-02	SRT30R AR 9	x-section of fibre after 2000 ppm NaOCl recovery cleaning	ConA-AF647	SBA-AF488	WGA-tmr	650/668	495/519	555/580	877	965	935	-0.039	-0.092	-0.1215	1.1	2.51	2.72	1	23	22

Appendix J

CLSM IMAGE DATA - RUN 2 after 2 hours of filtration

Date	File Name	Specimen	Obj/NA	Averaging	Zoom	Speed (us/pixel)	Image Size			Filters			Laser Power			Pinhole (um)		
							Pixels	Microns		Ch 1	Ch2	Ch 3	488	543	633	Ch 1	Ch 2	Ch 3
26-Mar-02	2SRT30R_2hrs_1	long section of fibre after 2 hours of filtration (Run 2)	63X/0.9 W	2	2	8.96	512 x 512	73.1 x 73.1	12 bit	LP 650	BP 505-530	BP 565-615 IR	50% of 50%	100%	100%	191	146	169
26-Mar-02	2SRT30R_2hrs_2	long section of fibre after 2 hours of filtration (Run 2)	63X/1.2 W	2	1	8.96	512 x 512	146.2 x 146.2	12 bit	LP 650	BP 505-530	BP 565-615 IR	50% of 50%	100%	100%	146	111	129
26-Mar-02	2SRT30R_2hrs_3	long section of fibre after 2 hours of filtration (Run 2)	63X/1.2 W	2	1	8.96	512 x 512	146.2 x 146.2	12 bit	LP 650	BP 505-530	BP 565-615 IR	50% of 50%	100%	100%	146	111	129
26-Mar-02	2SRT30R_2hrs_4	long section of fibre after 2 hours of filtration (Run 2)	63X/1.2 W	2	1	8.96	512 x 512	146.2 x 146.2	12 bit	LP 650	BP 505-530	BP 565-615 IR	50% of 50%	100%	100%	146	111	129
26-Mar-02	2SRT30R_2hrs_5	long section of fibre after 2 hours of filtration (Run 2)	63X/0.9 W	2	2	8.96	512 x 512	73.1 x 73.1	12 bit	LP 650	BP 505-530	BP 565-615 IR	50% of 50%	100%	100%	191	146	169
26-Mar-02	2SRT30R_2hrs_6	x-section of fibre after 2 hours of filtration (Run 2)	10X/0.25	2	1	71.68	512 x 512	921.3 x 921.3	12 bit	LP 650	BP 505-530	BP 565-615 IR	50% of 50%	100%	100%	146	111	129
26-Mar-02	2SRT30R_2hrs_7	x-section of fibre after 2 hours of filtration (Run 2)	40X/0.6	2	1	8.96	512 x 512	230.3 x 230.3	12 bit	LP 650	BP 505-530	BP 565-615 IR	50% of 50%	100%	100%	181	141	164
26-Mar-02	2SRT30R_2hrs_8	x-section of fibre after 2 hours of filtration (Run 2)	40X/0.6	2	1	8.96	512 x 512	230.3 x 230.3	12 bit	LP 650	BP 505-530	BP 565-615 IR	50% of 50%	100%	100%	181	141	164
26-Mar-02	2SRT12R_2hrs_1	long section of fibre after 2 hours of filtration (Run 2)	63X/0.9 W	2	1	8.96	512 x 512	146.2 x 146.2	12 bit	LP 650	BP 505-530	BP 565-615 IR	50% of 50%	100%	100%	191	146	169
26-Mar-02	2SRT12R_2hrs_2	long section of fibre after 2 hours of filtration (Run 2)	63X/0.9 W	2	1	8.96	512 x 512	146.2 x 146.2	12 bit	LP 650	BP 505-530	BP 565-615 IR	50% of 50%	100%	100%	191	146	169
26-Mar-02	2SRT12R_2hrs_3	long section of fibre after 2 hours of filtration (Run 2)	63X/0.9 W	2	1	8.96	512 x 512	146.2 x 146.2	12 bit	LP 650	BP 505-530	BP 565-615 IR	50% of 50%	100%	100%	191	146	169
26-Mar-02	2SRT12R_2hrs_4	x-section of fibre after 2 hours of filtration (Run 2)	10X/0.25	2	1	71.68	512 x 512	921.3 x 921.3	12 bit	LP 650	BP 505-530	BP 565-615 IR	50% of 50%	100%	100%	146	111	129
26-Mar-02	2SRT12R_2hrs_5	x-section of fibre after 2 hours of filtration (Run 2)	40X/0.6	2	1	8.96	512 x 512	230.3 x 230.3	12 bit	LP 650	BP 505-530	BP 565-615 IR	50% of 50%	100%	100%	181	141	164
27-Mar-02	2SRT12BW_2hrs_1	long section of fibre after 2 hours of filtration (Run 2)	63X/1.2 W	2	1	8.96	512 x 512	146.2 x 146.2	12 bit	LP 650	BP 505-530	BP 565-615 IR	50% of 50%	100%	100%	146	111	129
27-Mar-02	2SRT12BW_2hrs_2	long section of fibre after 2 hours of filtration (Run 2)	63X/0.9 W	2	1	8.96	512 x 512	146.2 x 146.2	12 bit	LP 650	BP 505-530	BP 565-615 IR	50% of 50%	100%	100%	191	146	169
27-Mar-02	2SRT12BW_2hrs_3	long section of fibre after 2 hours of filtration (Run 2)	63X/0.9 W	2	1	8.96	512 x 512	146.2 x 146.2	12 bit	LP 650	BP 505-530	BP 565-615 IR	50% of 50%	100%	100%	191	146	169
27-Mar-02	2SRT12BW_2hrs_4	long section of fibre after 2 hours of filtration (Run 2)	63X/0.9 W	2	1	8.96	512 x 512	146.2 x 146.2	12 bit	LP 650	BP 505-530	BP 565-615 IR	50% of 50%	100%	100%	191	146	169
27-Mar-02	2SRT12BW_2hrs_5	x-section of fibre after 2 hours of filtration (Run 2)	10X/0.25	2	1	71.68	512 x 512	921.3 x 921.3	12 bit	LP 650	BP 505-530	BP 565-615 IR	50% of 50%	100%	100%	146	111	129
27-Mar-02	2SRT12BW_2hrs_6	x-section of fibre after 2 hours of filtration (Run 2)	40X/0.6	2	1	8.96	512 x 512	230.3 x 230.3	12 bit	LP 650	BP 505-530	BP 565-615 IR	50% of 50%	100%	100%	181	141	164
27-Mar-02	2SRT12BW_2hrs_7	x-section of fibre after 2 hours of filtration (Run 2)	63X/0.9 W	2	1	8.96	512 x 512	146.2 x 146.2	12 bit	LP 650	BP 505-530	BP 565-615 IR	50% of 50%	100%	100%	191	146	169

Date	File Name	Specimen	Dye/Lectin			Abs/Em			Detector Gain			Amplitude Offset			Amplitude Gain			Z-step size (um)	# of Z sections	Total Z depth (um)
			Ch 1	Ch 2	Ch 3	Ch 1	Ch 2	Ch 3	Ch 1	Ch 2	Ch 3	Ch 1	Ch 2	Ch 3	Ch 1	Ch 2	Ch 3			
26-Mar-02	2SRT30R_2hrs_1	long section of fibre after 2 hours of filtration (Run 2)	ConA-AF647	SBA-AF488	WGA-tmr	650/668	495/519	555/580	801	990	980	-0.032	-0.049	-0.074	1.35	1.38	1.65	1.55	28	41.85
26-Mar-02	2SRT30R_2hrs_2	long section of fibre after 2 hours of filtration (Run 2)	ConA-AF647	SBA-AF488	WGA-tmr	650/668	495/519	555/580	742	937	900	-0.0435	-0.044	-0.091	1	1.56	1.5	0.5	28	13.5
26-Mar-02	2SRT30R_2hrs_3	long section of fibre after 2 hours of filtration (Run 2)	ConA-AF647	SBA-AF488	WGA-tmr	650/668	495/519	555/580	740	923	907	-0.057	-0.054	-0.074	1	1.52	1.56	0.8	30	23.2
26-Mar-02	2SRT30R_2hrs_4	long section of fibre after 2 hours of filtration (Run 2)	ConA-AF647	SBA-AF488	WGA-tmr	650/668	495/519	555/580	680	908	904	-0.047	-0.059	-0.084	1	1.5	1.61	0.5	27	13
26-Mar-02	2SRT30R_2hrs_5	long section of fibre after 2 hours of filtration (Run 2)	ConA-AF647	SBA-AF488	WGA-tmr	650/668	495/519	555/580	657	941	953	-0.034	-0.042	-0.077	1	1.65	1.53	1.4	34	46.2
26-Mar-02	2SRT30R_2hrs_6	x-section of fibre after 2 hours of filtration (Run 2)	ConA-AF647	SBA-AF488	WGA-tmr	650/668	495/519	555/580	?	?	?	?	?	?	?	?	?			
26-Mar-02	2SRT30R_2hrs_7	x-section of fibre after 2 hours of filtration (Run 2)	ConA-AF647	SBA-AF488	WGA-tmr	650/668	495/519	555/580	708	1000	1000	-0.034	-0.052	-0.077	1	1.73	1.58	1.95	28	52.65
26-Mar-02	2SRT30R_2hrs_8	x-section of fibre after 2 hours of filtration (Run 2)	ConA-AF647	SBA-AF488	WGA-tmr	650/668	495/519	555/580	588	924	931	-0.039	-0.057	-0.077	1	1.72	1.55	1.75	28	47.25
26-Mar-02	2SRT12R_2hrs_1	long section of fibre after 2 hours of filtration (Run 2)	ConA-AF647	SBA-AF488	WGA-tmr	650/668	495/519	555/580	710	965	904	-0.039	-0.052	-0.092	1	1.6	1.97	3.95	30	114.55
26-Mar-02	2SRT12R_2hrs_2	long section of fibre after 2 hours of filtration (Run 2)	ConA-AF647	SBA-AF488	WGA-tmr	650/668	495/519	555/580	601	940	906	-0.079	-0.062	-0.113	1	1.5	1.5	0.6	26	15
26-Mar-02	2SRT12R_2hrs_3	long section of fibre after 2 hours of filtration (Run 2)	ConA-AF647	SBA-AF488	WGA-tmr	650/668	495/519	555/580	571	945	940	-0.039	-0.042	-0.047	1	1.16	1.06	1.05	34	34.65
26-Mar-02	2SRT12R_2hrs_4	x-section of fibre after 2 hours of filtration (Run 2)	ConA-AF647	SBA-AF488	WGA-tmr	650/668	495/519	555/580	564	910	901	-0.039	-0.022	-0.017	1.2	1	1			
26-Mar-02	2SRT12R_2hrs_5	x-section of fibre after 2 hours of filtration (Run 2)	ConA-AF647	SBA-AF488	WGA-tmr	650/668	495/519	555/580	714	985	965	-0.039	-0.047	-0.082	1	1.93	1.9	1.4	38	51.8
27-Mar-02	2SRT12BW_2hrs_1	long section of fibre after 2 hours of filtration (Run 2)	ConA-AF647	SBA-AF488	WGA-tmr	650/668	495/519	555/580	818	1000	1000	-0.034	-0.062	-0.068	1	1.61	1.5	0.95	28	25.65
27-Mar-02	2SRT12BW_2hrs_2	long section of fibre after 2 hours of filtration (Run 2)	ConA-AF647	SBA-AF488	WGA-tmr	650/668	495/519	555/580	606	908	900	-0.0515	-0.064	-0.075	1	1.48	1.5	0.7	29	19.6
27-Mar-02	2SRT12BW_2hrs_3	long section of fibre after 2 hours of filtration (Run 2)	ConA-AF647	SBA-AF488	WGA-tmr	650/668	495/519	555/580	729	943	970	-0.039	-0.054	-0.069	1	1.42	1.63	0.6	26	15
27-Mar-02	2SRT12BW_2hrs_4	long section of fibre after 2 hours of filtration (Run 2)	ConA-AF647	SBA-AF488	WGA-tmr	650/668	495/519	555/580	590	945	906	-0.069	-0.047	-0.074	1.7	1.5	1.66	0.6	28	16.2
27-Mar-02	2SRT12BW_2hrs_5	x-section of fibre after 2 hours of filtration (Run 2)	ConA-AF647	SBA-AF488	WGA-tmr	650/668	495/519	555/580	598	938	946	-0.044	-0.032	-0.047	1	1.2	1.18			
27-Mar-02	2SRT12BW_2hrs_6	x-section of fibre after 2 hours of filtration (Run 2)	ConA-AF647	SBA-AF488	WGA-tmr	650/668	495/519	555/580	761	970	1000	-0.009	-0.042	-0.089	1	1.65	1.73	1.85	34	61.05
27-Mar-02	2SRT12BW_2hrs_7	x-section of fibre after 2 hours of filtration (Run 2)	ConA-AF647	SBA-AF488	WGA-tmr	650/668	495/519	555/580	577	895	907	-0.034	-0.042	-0.065	1	1.34	1.3	1	36	35

Appendix J

CLSM IMAGE DATA - RUN 2 after 3 days of filtration

Date	File Name	Specimen	Obj/NA	Averaging	Zoom	Speed (us/pixel)	Image Size			Filters			Laser Power			Pinhole (um)		
							Pixels	Microns		Ch 1	Ch2	Ch 3	488	543	633	Ch 1	Ch 2	Ch 3
03-Apr-02	2SRT12R_3days_1	long section of fibre after 3 days of filtration (Run 2)	63X/0.9 W	2	0.7	8.96	512 x 512	206.8 x 206.8	12 bit	LP 650	BP 505-530	BP 565-615 IR	50% of 50%	100%	100%	191	147	169
03-Apr-02	2SRT12R_3days_3	long section of fibre after 3 days of filtration (Run 2)	63X/0.9 W	2	1	8.96	512 x 512	146.2 x 146.2	12 bit	LP 650	BP 505-530	BP 565-615 IR	50% of 50%	100%	100%	191	146	169
03-Apr-02	2SRT12R_3days_4	long section of fibre after 3 days of filtration (Run 2)	63X/0.9 W	2	1	8.96	512 x 512	146.2 x 146.2	12 bit	LP 650	BP 505-530	BP 565-615 IR	50% of 50%	100%	100%	191	146	169
03-Apr-02	2SRT12R_3days_7	x-section of fibre after 3 days of filtration (Run 2)	63X/0.9 W	2	1	8.96	512 x 512	146.2 x 146.2	12 bit	LP 650	BP 505-530	BP 565-615 IR	50% of 50%	100%	100%	191	146	169
01-Apr-02	2SRT30R_3days_1	long section of fibre after 3 days of filtration (Run 2)	63X/0.9 W	2	1	8.96	512 x 512	146.2 x 146.2	12 bit	LP 650	BP 505-530	BP 565-615 IR	50% of 50%	100%	100%	191	146	169
01-Apr-02	2SRT30R_3days_3	long section of fibre after 3 days of filtration (Run 2)	63X/0.9 W	2	1	8.96	512 x 512	146.2 x 146.2	12 bit	LP 650	BP 505-530	BP 565-615 IR	50% of 50%	100%	100%	191	146	169
01-Apr-02	2SRT30R_3days_4	long section of fibre after 3 days of filtration (Run 2)	63X/0.9 W	2	1	8.96	512 x 512	146.2 x 146.2	12 bit	LP 650	BP 505-530	BP 565-615 IR	50% of 50%	100%	100%	191	146	169
01-Apr-02	2SRT30R_3days_5	long section of fibre after 3 days of filtration (Run 2)	63X/0.9 W	2	1	8.96	512 x 512	146.2 x 146.2	12 bit	LP 650	BP 505-530	BP 565-615 IR	50% of 50%	100%	100%	191	146	169
01-Apr-02	2SRT30R_3days_6	x-section of fibre after 3 days of filtration (Run 2)	40X/0.6	2	0.7	8.96	512 x 512	230.3 x 230.3	12 bit	LP 650	BP 505-530	BP 565-615 IR	50% of 50%	100%	100%	186	141	164
01-Apr-02	2SRT30R_3days_7	x-section of fibre after 3 days of filtration (Run 2)	63X/0.9 W	2	0.7	8.96	512 x 512	206.8 x 206.8	12 bit	LP 650	BP 505-530	BP 565-615 IR	50% of 50%	100%	100%	191	146	169
01-Apr-02	2SRT12BW_3days_1	long section of fibre after 3 days of filtration (Run 2)	63X/0.9 W	2	1	8.96	512 x 512	146.2 x 146.2	12 bit	LP 650	BP 505-530	BP 565-615 IR	50% of 50%	100%	100%	191	146	169
01-Apr-02	2SRT12BW_3days_2	long section of fibre after 3 days of filtration (Run 2)	63X/0.9 W	1	1	17.92	512 x 512	146.2 x 146.2	12 bit	LP 650	BP 505-530	BP 565-615 IR	50% of 50%	100%	100%	191	146	169
01-Apr-02	2SRT12BW_3days_3	long section of fibre after 3 days of filtration (Run 2)	63X/1.2 W	2	1	8.96	512 x 512	146.2 x 146.2	12 bit	LP 650	BP 505-530	BP 565-615 IR	50% of 50%	100%	100%	191	146	169
01-Apr-02	2SRT12BW_3days_4	long section of fibre after 3 days of filtration (Run 2)	63X/1.2 W	2	2	8.96	512 x 512	146.2 x 146.2	12 bit	LP 650	BP 505-530	BP 565-615 IR	50% of 50%	100%	100%	146	111	129
01-Apr-02	2SRT12BW_3days_5	x-section of fibre after 3 days of filtration (Run 2)	63X/0.9 W	2	1	8.96	512 x 512	146.2 x 146.2	12 bit	LP 650	BP 505-530	BP 565-615 IR	50% of 50%	100%	100%	191	146	169
01-Apr-02	2SRT12BW_3days_7	x-section of fibre after 3 days of filtration (Run 2)	10X/0.25	2	1	71.68	512 x 512	921.3 x 921.3	12 bit	LP 650	BP 505-530	BP 565-615 IR	50% of 50%	100%	100%	146	111	129

Date	File Name	Specimen	Dye/Lectin			Abs/Em 1			Detector Gain			Amplitude Offset			Amplitude Gain			Z-step size (um)	# of Z sections	Total Z depth (um)
			Ch 1	Ch 2	Ch 3	Ch 1	Ch 2	Ch 3	Ch 1	Ch 2	Ch 3	Ch 1	Ch 2	Ch 3	Ch 1	Ch 2	Ch 3			
03-Apr-02	2SRT12R_3days_1	long section of fibre after 3 days of filtration (Run 2)	ConA-AF647	SBA-AF488	WGA-tmr	650/668	495/519	555/580	825	970	960	-0.034	-0.089	-0.089	1	2.19	1.87	2	34	66
03-Apr-02	2SRT12R_3days_3	long section of fibre after 3 days of filtration (Run 2)	ConA-AF647	SBA-AF488	WGA-tmr	650/668	495/519	555/580	676	942	902	-0.049	-0.037	-0.064	1	1.31	1.49	1	38	37
03-Apr-02	2SRT12R_3days_4	long section of fibre after 3 days of filtration (Run 2)	ConA-AF647	SBA-AF488	WGA-tmr	650/668	495/519	555/580	645	906	891	-0.049	-0.069	-0.089	1	1.65	1.65	0.5	37	18
03-Apr-02	2SRT12R_3days_7	x-section of fibre after 3 days of filtration (Run 2)	ConA-AF647	SBA-AF488	WGA-tmr	650/668	495/519	555/580	655	896	933	-0.044	-0.057	-0.0475	1	1.44	1	1	36	35
01-Apr-02	2SRT30R_3days_1	long section of fibre after 3 days of filtration (Run 2)	ConA-AF647	SBA-AF488	WGA-tmr	650/668	495/519	555/580	774	868	904	-0.052	-0.069	-0.079	1	1.59	1.53	1.9	31	58.9
01-Apr-02	2SRT30R_3days_3	long section of fibre after 3 days of filtration (Run 2)	ConA-AF647	SBA-AF488	WGA-tmr	650/668	495/519	555/580	728	960	895	-0.057	-0.054	-0.074	1	1.48	1.48	0.85	34	28.05
01-Apr-02	2SRT30R_3days_4	long section of fibre after 3 days of filtration (Run 2)	ConA-AF647	SBA-AF488	WGA-tmr	650/668	495/519	555/580	725	838	853	-0.059	-0.049	-0.074	1	1.36	1.34	1	31	30
01-Apr-02	2SRT30R_3days_5	long section of fibre after 3 days of filtration (Run 2)	ConA-AF647	SBA-AF488	WGA-tmr	650/668	495/519	555/580	850	925	915	-0.064	-0.064	-0.094	1	1.55	1.5	0.5	34	16.5
01-Apr-02	2SRT30R_3days_6	x-section of fibre after 3 days of filtration (Run 2)	ConA-AF647	SBA-AF488	WGA-tmr	650/668	495/519	555/580	690	1000	1000	-0.029	-0.074	-0.094	1	1.85	1.86	1	36	35
01-Apr-02	2SRT30R_3days_7	x-section of fibre after 3 days of filtration (Run 2)	ConA-AF647	SBA-AF488	WGA-tmr	650/668	495/519	555/580	732	984	896	-0.039	-0.034	-0.0325	1	1	1	1	34	33
01-Apr-02	2SRT12BW_3days_1	long section of fibre after 3 days of filtration (Run 2)	ConA-AF647	SBA-AF488	WGA-tmr	650/668	495/519	555/580	769	900	917	-0.119	-0.114	-0.144	1	1.61	1.63	0.5	31	15
01-Apr-02	2SRT12BW_3days_2	long section of fibre after 3 days of filtration (Run 2)	ConA-AF647	SBA-AF488	WGA-tmr	650/668	495/519	555/580	646	941	879	-0.039	-0.057	-0.0675	1	1.57	1.3	1.65	38	61.05
01-Apr-02	2SRT12BW_3days_3	long section of fibre after 3 days of filtration (Run 2)	ConA-AF647	SBA-AF488	WGA-tmr	650/668	495/519	555/580	710	898	892	-0.044	-0.039	-0.049	1	1.27	1.03	0.45	28	12.15
01-Apr-02	2SRT12BW_3days_4	long section of fibre after 3 days of filtration (Run 2)	ConA-AF647	SBA-AF488	WGA-tmr	650/668	495/519	555/580	578	889	869	-0.047	-0.049	-0.064	1	1.32	1.3	0.4	24	9.2
01-Apr-02	2SRT12BW_3days_5	x-section of fibre after 3 days of filtration (Run 2)	ConA-AF647	SBA-AF488	WGA-tmr	650/668	495/519	555/580	555	958	899	-0.034	-0.057	-0.069	1	1.49	1.47	0.6	31	18
01-Apr-02	2SRT12BW_3days_7	x-section of fibre after 3 days of filtration (Run 2)	ConA-AF647	SBA-AF488	WGA-tmr	650/668	495/519	555/580	533	887	824	-0.064	-0.057	-0.084	1.5	1.5	1.56			

Appendix J

CLSM IMAGE DATA - RUN 2 at Critical Transmembrane Pressure

Date	File Name	Specimen	Obj/NA	Averaging	Zoom	Speed (us/pixel)	Image Size			Filters			Laser Power			Pinhole (um)		
							Pixels	Microns		Ch 1	Ch2	Ch 3	488	543	633	Ch 1	Ch 2	Ch 3
05-Apr-02	2SRT12R_@60kPa_1	long section of fibre at critical TMP (Run 2)	63X/0.9 W	2	1	8.96	512 x 512	146.2 x 146.2	12 bit	LP 650	BP 505-530	BP 565-615 IR	50% of 50%	100%	100%	191	146	169
05-Apr-02	2SRT12R_@60kPa_2	long section of fibre at critical TMP (Run 2)	63X/0.9 W	2	1	8.96	512 x 512	146.2 x 146.2	12 bit	LP 650	BP 505-530	BP 565-615 IR	50% of 50%	100%	100%	191	146	169
05-Apr-02	2SRT12R_@60kPa_3	long section of fibre at critical TMP (Run 2)	63X/0.9 W	2	2	8.96	512 x 512	73.1 x 73.1	12 bit	LP 650	BP 505-530	BP 565-615 IR	50% of 50%	100%	100%	191	146	169
05-Apr-02	2SRT12R_@60kPa_4	long section of fibre at critical TMP (Run 2)	63X/0.9 W	2	2	8.96	512 x 512	73.1 x 73.1	12 bit	LP 650	BP 505-530	BP 565-615 IR	50% of 50%	100%	100%	191	146	169
05-Apr-02	2SRT12R_@60kPa_5	x-section of fibre at critical TMP (Run 2)	10X/0.25	2	1	71.68	512 x 512	921.3 x 921.3	12 bit	LP 650	BP 505-530	BP 565-615 IR	50% of 50%	100%	100%	146	111	129
05-Apr-02	2SRT12R_@60kPa_6	x-section of fibre at critical TMP (Run 2)	63X/0.9 W	2	1	8.96	512 x 512	146.2 x 146.2	12 bit	LP 650	BP 505-530	BP 565-615 IR	50% of 50%	100%	100%	191	146	169
04-Apr-02	2SRT30R_@60kPa_1	long section of fibre at critical TMP (Run 2)	63X/0.9 W	2	1	8.96	512 x 512	146.2 x 146.2	12 bit	LP 650	BP 505-530	BP 565-615 IR	50% of 50%	100%	100%	191	146	169
04-Apr-02	2SRT30R_@60kPa_2	long section of fibre at critical TMP (Run 2)	63X/0.9 W	2	1	8.96	512 x 512	146.2 x 146.2	12 bit	LP 650	BP 505-530	BP 565-615 IR	50% of 50%	100%	100%	191	146	169
04-Apr-02	2SRT30R_@60kPa_3	long section of fibre at critical TMP (Run 2)	63X/0.9 W	2	1	8.96	512 x 512	146.2 x 146.2	12 bit	LP 650	BP 505-530	BP 565-615 IR	50% of 50%	100%	100%	191	146	169
04-Apr-02	2SRT30R_@60kPa_4	long section of fibre at critical TMP (Run 2)	63X/0.9 W	2	1	8.96	512 x 512	146.2 x 146.2	12 bit	LP 650	BP 505-530	BP 565-615 IR	50% of 50%	100%	100%	191	146	169
04-Apr-02	2SRT30R_@60kPa_5	x-section of fibre at critical TMP (Run 2)	10X/0.25	2	1	71.68	512 x 512	921.3 x 921.3	12 bit	LP 650	BP 505-530	BP 565-615 IR	50% of 50%	100%	100%	146	111	129
04-Apr-02	2SRT30R_@60kPa_6	x-section of fibre at critical TMP (Run 2)	63X/0.9 W	2	1	8.96	512 x 512	146.2 x 146.2	12 bit	LP 650	BP 505-530	BP 565-615 IR	50% of 50%	100%	100%	191	146	169
04-Apr-02	2SRT12BW_@60kPa_1	long section of fibre at critical TMP (Run 2)	63X/0.9 W	2	1	8.96	512 x 512	146.2 x 146.2	12 bit	LP 650	BP 505-530	BP 565-615 IR	50% of 50%	100%	100%	191	146	169
04-Apr-02	2SRT12BW_@60kPa_2	long section of fibre at critical TMP (Run 2)	63X/0.9 W	2	1	8.96	512 x 512	146.2 x 146.2	12 bit	LP 650	BP 505-530	BP 565-615 IR	50% of 50%	100%	100%	146	111	129
04-Apr-02	2SRT12BW_@60kPa_3	long section of fibre at critical TMP (Run 2)	63X/0.9 W	2	1	8.96	512 x 512	146.2 x 146.2	12 bit	LP 650	BP 505-530	BP 565-615 IR	50% of 50%	100%	100%	191	116	129
04-Apr-02	2SRT12BW_@60kPa_4	long section of fibre at critical TMP (Run 2)	63X/0.9 W	2	1	8.96	512 x 512	146.2 x 146.2	12 bit	LP 650	BP 505-530	BP 565-615 IR	50% of 50%	100%	100%	191	146	169
04-Apr-02	2SRT12BW_@60kPa_5	x-section of fibre at critical TMP (Run 2)	63X/0.9 W	2	1	8.96	512 x 512	146.2 x 146.2	12 bit	LP 650	BP 505-530	BP 565-615 IR	50% of 50%	100%	100%	191	146	169
04-Apr-02	2SRT12BW_@60kPa_6	x-section of fibre at critical TMP (Run 2)	10X/0.25	2	1	71.68	512 x 512	921.3 x 921.3	12 bit	LP 650	BP 505-530	BP 565-615 IR	50% of 50%	100%	100%	146	111	129

Date	File Name	Specimen	Dye/Lectin			Abs/Em l			Detector Gain			Amplitude Offset			Amplitude Gain			Z-step size (um)	# of Z sections	Total Z depth (um)
			Ch 1	Ch 2	Ch 3	Ch 1	Ch 2	Ch 3	Ch 1	Ch 2	Ch 3	Ch 1	Ch 2	Ch 3	Ch 1	Ch 2	Ch 3			
05-Apr-02	2SRT12R_@60kPa_1	long section of fibre at critical TMP (Run 2)	ConA-AF647	SBA-AF488	WGA-tmr	650/668	495/519	555/580	863	900	914	-0.124	-0.062	-0.08	1	1.61	1.4	0.6	34	19.8
05-Apr-02	2SRT12R_@60kPa_2	long section of fibre at critical TMP (Run 2)	ConA-AF647	SBA-AF488	WGA-tmr	650/668	495/519	555/580	903	969	932	-0.034	-0.049	-0.07	1	1.44	1.5	2.1	36	73.5
05-Apr-02	2SRT12R_@60kPa_3	long section of fibre at critical TMP (Run 2)	ConA-AF647	SBA-AF488	WGA-tmr	650/668	495/519	555/580	844	965	945	-0.044	-0.062	-0.09	1	1.79	1.75	1.4	36	49
05-Apr-02	2SRT12R_@60kPa_4	long section of fibre at critical TMP (Run 2)	ConA-AF647	SBA-AF488	WGA-tmr	650/668	495/519	555/580	865	885	884	-0.1065	-0.082	-0.11	1	1.57	1.6	0.55	20	10.45
05-Apr-02	2SRT12R_@60kPa_5	x-section of fibre at critical TMP (Run 2)	ConA-AF647	SBA-AF488	WGA-tmr	650/668	495/519	555/580	669	904	865	-0.034	-0.052	-0.07	1	1.51	1.48			
05-Apr-02	2SRT12R_@60kPa_6	x-section of fibre at critical TMP (Run 2)	ConA-AF647	SBA-AF488	WGA-tmr	650/668	495/519	555/580	574	939	735	-0.039	-0.034	-0.04	1	1	1	1.1	29	31.9
04-Apr-02	2SRT30R_@60kPa_1	long section of fibre at critical TMP (Run 2)	ConA-AF647	SBA-AF488	WGA-tmr	650/668	495/519	555/580	774	868	904	-0.052	-0.069	-0.08	1	1.59	1.53	0.65	31	19.5
04-Apr-02	2SRT30R_@60kPa_2	long section of fibre at critical TMP (Run 2)	ConA-AF647	SBA-AF488	WGA-tmr	650/668	495/519	555/580	777	910	895	-0.05	-0.064	-0.08	1	1.53	1.4	2.1	31	63
04-Apr-02	2SRT30R_@60kPa_3	long section of fibre at critical TMP (Run 2)	ConA-AF647	SBA-AF488	WGA-tmr	650/668	495/519	555/580	780	846	920	-0.044	-0.057	-0.08	1	1.63	1.72	2.5	45	110
04-Apr-02	2SRT30R_@60kPa_4	long section of fibre at critical TMP (Run 2)	ConA-AF647	SBA-AF488	WGA-tmr	650/668	495/519	555/580	676	901	914	-0.061	-0.059	-0.07	1	1.42	1.3	0.45	26	11.25
04-Apr-02	2SRT30R_@60kPa_5	x-section of fibre at critical TMP (Run 2)	ConA-AF647	SBA-AF488	WGA-tmr	650/668	495/519	555/580	659	863	844	-0.044	-0.092	-0.1	1	1.63	1.56			
04-Apr-02	2SRT30R_@60kPa_6	x-section of fibre at critical TMP (Run 2)	ConA-AF647	SBA-AF488	WGA-tmr	650/668	495/519	555/580	520	837	844	-0.049	-0.067	-0.07	1.3	1.75	1.52	0.95	20	18.05
04-Apr-02	2SRT12BW_@60kPa_1	long section of fibre at critical TMP (Run 2)	ConA-AF647	SBA-AF488	WGA-tmr	650/668	495/519	555/580	760	900	915	-0.051	-0.062	-0.08	1	1.5	1.7	1	40	41
04-Apr-02	2SRT12BW_@60kPa_2	long section of fibre at critical TMP (Run 2)	ConA-AF647	SBA-AF488	WGA-tmr	650/668	495/519	555/580	837	950	921	-0.054	-0.062	-0.08	1.3	1.56	1.75	2.05	39	77.9
04-Apr-02	2SRT12BW_@60kPa_3	long section of fibre at critical TMP (Run 2)	ConA-AF647	SBA-AF488	WGA-tmr	650/668	495/519	555/580	684	909	918	-0.039	-0.057	-0.07	1	1.65	1.5	1	41	40
04-Apr-02	2SRT12BW_@60kPa_4	long section of fibre at critical TMP (Run 2)	ConA-AF647	SBA-AF488	WGA-tmr	650/668	495/519	555/580	788	902	848	-0.049	-0.064	-0.07	1	1.67	1.59	1	48	47
04-Apr-02	2SRT12BW_@60kPa_5	x-section of fibre at critical TMP (Run 2)	ConA-AF647	SBA-AF488	WGA-tmr	650/668	495/519	555/580	547	854	853	-0.039	-0.052	-0.07	1	1.5	1.45	0.7	34	23.1
04-Apr-02	2SRT12BW_@60kPa_6	x-section of fibre at critical TMP (Run 2)	ConA-AF647	SBA-AF488	WGA-tmr	650/668	495/519	555/580	626	908	863	-0.039	-0.052	-0.07	1	1.48	1.48			

Appendix J

CLSM IMAGE DATA - After Second Recovery Cleaning

Date	File Name	Specimen	Obj/NA	Averaging	Zoom	Speed (us/pixel)	Image Size			Filters			Laser Power			Pinhole (um)		
							Pixels	Microns		Ch 1	Ch2	Ch 3	488	543	633	Ch 1	Ch 2	Ch 3
08-Apr-02	2SRT12R_AR_1	long section of fibre after recovery cleaning (2nd time)	63X/1.2 W	2	1	8.96	512 x 512	146.2 x 146.2	12 bit	LP 650	BP 505-530	BP 565-615 IR	50% of 50%	100%	100%	146	111	129
08-Apr-02	2SRT12R_AR_2	long section of fibre after recovery cleaning (2nd time)	63X/1.2 W	2	2	8.96	512 x 512	73.1 x 73.1	12 bit	LP 650	BP 505-530	BP 565-615 IR	50% of 50%	100%	100%	146	111	129
08-Apr-02	2SRT12R_AR_3	long section of fibre after recovery cleaning (2nd time)	63X/1.2 W	2	1.4	8.96	512 x 512	103.4 x 103.4	12 bit	LP 650	BP 505-530	BP 565-615 IR	50% of 50%	100%	100%	146	111	129
08-Apr-02	2SRT12R_AR_4	long section of fibre after recovery cleaning (2nd time)	63X/0.9 W	2	1	8.96	512 x 512	146.2 x 146.2	12 bit	LP 650	BP 505-530	BP 565-615 IR	50% of 50%	100%	100%	191	146	169
08-Apr-02	2SRT12R_AR_5	long section of fibre after recovery cleaning (2nd time)	63X/0.9 W	2	1	8.96	512 x 512	146.2 x 146.2	12 bit	LP 650	BP 505-530	BP 565-615 IR	50% of 50%	100%	100%	191	146	169
08-Apr-02	2SRT12R_AR_6	long section of fibre after recovery cleaning (2nd time)	63X/0.9 W	2	1	8.96	512 x 512	146.2 x 146.2	12 bit	LP 650	BP 505-530	BP 565-615 IR	50% of 50%	100%	100%	191	146	169
08-Apr-02	2SRT12R_AR_7	x-section of fibre after recovery cleaning (2nd time)	63X/0.9 W	2	0.7	8.96	512 x 512	206.8 x 206.8	12 bit	LP 650	BP 505-530	BP 565-615 IR	50% of 50%	100%	100%	191	146	169
08-Apr-02	2SRT12R_AR_8	x-section of fibre after recovery cleaning (2nd time)	63X/0.9 W	2	0.7	8.96	512 x 512	206.8 x 206.8	12 bit	LP 650	BP 505-530	BP 565-615 IR	50% of 50%	100%	100%	191	146	169
08-Apr-02	2SRT12R_AR_9	x-section of fibre after recovery cleaning (2nd time)	10X/0.25	2	1	71.68	512 x 512	921.3 x 921.3	12 bit	LP 650	BP 505-530	BP 565-615 IR	50% of 50%	100%	100%	146	111	129
08-Apr-02	2SRT12R_AR_10	x-section of fibre after recovery cleaning (2nd time)	10X/0.25	2	1	71.68	512 x 512	921.3 x 921.3	12 bit	LP 650	BP 505-530	BP 565-615 IR	50% of 50%	100%	100%	146	111	129
08-Apr-02	2SRT30R_AR_1	long section of fibre after recovery cleaning (2nd time)	63X/0.9 W	2	1	8.96	512 x 512	146.2 x 146.2	12 bit	LP 650	BP 505-530	BP 565-615 IR	50% of 50%	100%	100%	191	146	169
08-Apr-02	2SRT30R_AR_2	long section of fibre after recovery cleaning (2nd time)	63X/0.9 W	2	1	8.96	512 x 512	146.2 x 146.2	12 bit	LP 650	BP 505-530	BP 565-615 IR	50% of 50%	100%	100%	191	146	169
08-Apr-02	2SRT30R_AR_3	long section of fibre after recovery cleaning (2nd time)	63X/0.9 W	2	1	8.96	512 x 512	146.2 x 146.2	12 bit	LP 650	BP 505-530	BP 565-615 IR	50% of 50%	100%	100%	191	146	169
08-Apr-02	2SRT30R_AR_4	long section of fibre after recovery cleaning (2nd time)	63X/0.9 W	2	2	8.96	512 x 512	73.1 x 73.1	12 bit	LP 650	BP 505-530	BP 565-615 IR	50% of 50%	100%	100%	191	146	169
08-Apr-02	2SRT30R_AR_5	long section of fibre after recovery cleaning (2nd time)	63X/0.9 W	2	1	8.96	512 x 512	146.2 x 146.2	12 bit	LP 650	BP 505-530	BP 565-615 IR	50% of 50%	100%	100%	191	146	169
08-Apr-02	2SRT30R_AR_6	x-section of fibre after recovery cleaning (2nd time)	63X/0.9 W	2	0.7	8.96	512 x 512	206.8 x 206.8	12 bit	LP 650	BP 505-530	BP 565-615 IR	50% of 50%	100%	100%	191	146	169
08-Apr-02	2SRT30R_AR_7	x-section of fibre after recovery cleaning (2nd time)	63X/0.9 W	2	0.7	8.96	512 x 512	206.8 x 206.8	12 bit	LP 650	BP 505-530	BP 565-615 IR	50% of 50%	100%	100%	191	146	169
08-Apr-02	2SRT30R_AR_8	x-section of fibre after recovery cleaning (2nd time)	63X/0.9 W	2	2	8.96	512 x 512	73.1 x 73.1	12 bit	LP 650	BP 505-530	BP 565-615 IR	50% of 50%	100%	100%	191	146	169
08-Apr-02	2SRT12BW_AR_1	long section of fibre after recovery cleaning (2nd time)	63X/0.9 W	2	1	8.96	512 x 512	146.2 x 146.2	12 bit	LP 650	BP 505-530	BP 565-615 IR	50% of 50%	100%	100%	191	146	169
08-Apr-02	2SRT12BW_AR_2	long section of fibre after recovery cleaning (2nd time)	63X/0.9 W	2	2	8.96	512 x 512	73.1 x 73.1	12 bit	LP 650	BP 505-530	BP 565-615 IR	50% of 50%	100%	100%	191	146	169
08-Apr-02	2SRT12BW_AR_3	long section of fibre after recovery cleaning (2nd time)	63X/0.9 W	2	1	8.96	512 x 512	146.2 x 146.2	12 bit	LP 650	BP 505-530	BP 565-615 IR	50% of 50%	100%	100%	191	146	169
08-Apr-02	2SRT12BW_AR_4	long section of fibre after recovery cleaning (2nd time)	63X/0.9 W	2	1	8.96	512 x 512	146.2 x 146.2	12 bit	LP 650	BP 505-530	BP 565-615 IR	50% of 50%	100%	100%	191	146	169
08-Apr-02	2SRT12BW_AR_5	long section of fibre after recovery cleaning (2nd time)	63X/0.9 W	2	1	8.96	512 x 512	146.2 x 146.2	12 bit	LP 650	BP 505-530	BP 565-615 IR	50% of 50%	100%	100%	191	146	169
08-Apr-02	2SRT12BW_AR_6	x-section of fibre after recovery cleaning (2nd time)	63X/0.9 W	2	0.7	8.96	512 x 512	206.8 x 206.8	12 bit	LP 650	BP 505-530	BP 565-615 IR	50% of 50%	100%	100%	191	146	169

Date	File Name	Specimen	Dye/Lectin			Abs/Em 1			Detector Gain			Amplitude Offset			Amplitude Gain			Z-step size (um)	# of Z sections	Total Z depth (um)
			Ch 1	Ch 2	Ch 3	Ch 1	Ch 2	Ch 3	Ch 1	Ch 2	Ch 3	Ch 1	Ch 2	Ch 3	Ch 1	Ch 2	Ch 3			
08-Apr-02	2SRT12R_AR_1	long section of fibre after recovery cleaning (2nd time)	ConA-AF647	SBA-AF488	WGA-tmr	650/668	495/519	555/580	905	970	1000	-0.034	-0.119	-0.104	1	2.8	2.1	0.5	26	12.5
08-Apr-02	2SRT12R_AR_2	long section of fibre after recovery cleaning (2nd time)	ConA-AF647	SBA-AF488	WGA-tmr	650/668	495/519	555/580	523	813	843	-0.039	-0.037	-0.0515	1	1	1	0.25	26	6.25
08-Apr-02	2SRT12R_AR_3	long section of fibre after recovery cleaning (2nd time)	ConA-AF647	SBA-AF488	WGA-tmr	650/668	495/519	555/580	522	788	821	-0.034	-0.039	-0.0505	1	1	1	0.4	26	10
08-Apr-02	2SRT12R_AR_4	long section of fibre after recovery cleaning (2nd time)	ConA-AF647	SBA-AF488	WGA-tmr	650/668	495/519	555/580	814	1000	965	-0.082	-0.099	-0.109	2	2.37	2.23	1.55	30	44.95
08-Apr-02	2SRT12R_AR_5	long section of fibre after recovery cleaning (2nd time)	ConA-AF647	SBA-AF488	WGA-tmr	650/668	495/519	555/580	541	893	827	-0.074	-0.049	-0.0915	1	1	1	0.4	28	10.8
08-Apr-02	2SRT12R_AR_6	long section of fibre after recovery cleaning (2nd time)	ConA-AF647	SBA-AF488	WGA-tmr	650/668	495/519	555/580	567	858	852	-0.0555	-0.091	-0.094	1	1.4	1	0.5	20	9.5
08-Apr-02	2SRT12R_AR_7	x-section of fibre after recovery cleaning (2nd time)	ConA-AF647	SBA-AF488	WGA-tmr	650/668	495/519	555/580	617	854	926	-0.029	-0.059	-0.0675	1	1.56	1.5	1.5	22	31.5
08-Apr-02	2SRT12R_AR_8	x-section of fibre after recovery cleaning (2nd time)	ConA-AF647	SBA-AF488	WGA-tmr	650/668	495/519	555/580	530	820	797	-0.032	-0.029	-0.034	1	1	1	1.6	22	33.6
08-Apr-02	2SRT12R_AR_9	x-section of fibre after recovery cleaning (2nd time)	ConA-AF647	SBA-AF488	WGA-tmr	650/668	495/519	555/580	550	723	772	-0.037	-0.034	-0.039	1	1	1			
08-Apr-02	2SRT12R_AR_10	x-section of fibre after recovery cleaning (2nd time)	ConA-AF647	SBA-AF488	WGA-tmr	650/668	495/519	555/580	581	833	883	-0.042	-0.039	-0.039	1	1	1			
08-Apr-02	2SRT30R_AR_1	long section of fibre after recovery cleaning (2nd time)	ConA-AF647	SBA-AF488	WGA-tmr	650/668	495/519	555/580	561	864	903	-0.064	-0.062	-0.0805	1	1.54	1.5	0.5	24	11.5
08-Apr-02	2SRT30R_AR_2	long section of fibre after recovery cleaning (2nd time)	ConA-AF647	SBA-AF488	WGA-tmr	650/668	495/519	555/580	508	845	798	-0.044	-0.059	-0.077	1	1.49	1.32	0.5	32	15.5
08-Apr-02	2SRT30R_AR_3	long section of fibre after recovery cleaning (2nd time)	ConA-AF647	SBA-AF488	WGA-tmr	650/668	495/519	555/580	567	872	902	-0.064	-0.064	-0.084	1	1.48	1.55	0.8	20	15.2
08-Apr-02	2SRT30R_AR_4	long section of fibre after recovery cleaning (2nd time)	ConA-AF647	SBA-AF488	WGA-tmr	650/668	495/519	555/580	542	849	896	-0.0715	-0.064	-0.095	1	1.39	1.3	0.4	22	8.4
08-Apr-02	2SRT30R_AR_5	long section of fibre after recovery cleaning (2nd time)	ConA-AF647	SBA-AF488	WGA-tmr	650/668	495/519	555/580	509	884	792	-0.034	-0.039	-0.0565	1	1	1	1	21	20
08-Apr-02	2SRT30R_AR_6	x-section of fibre after recovery cleaning (2nd time)	ConA-AF647	SBA-AF488	WGA-tmr	650/668	495/519	555/580	433	814	742	-0.037	-0.0385	-0.0375	1	1	1	1	22	21
08-Apr-02	2SRT30R_AR_7	x-section of fibre after recovery cleaning (2nd time)	ConA-AF647	SBA-AF488	WGA-tmr	650/668	495/519	555/580	479	864	795	-0.034	-0.029	-0.039	1	1	1	1.05	28	28.35
08-Apr-02	2SRT30R_AR_8	x-section of fibre after recovery cleaning (2nd time)	ConA-AF647	SBA-AF488	WGA-tmr	650/668	495/519	555/580	535	817	826	-0.039	-0.054	-0.065	1	1.52	1.3	0.95	18	16.15
08-Apr-02	2SRT12BW_AR_1	long section of fibre after recovery cleaning (2nd time)	ConA-AF647	SBA-AF488	WGA-tmr	650/668	495/519	555/580	580	909	925	-0.0725	-0.069	-0.064	1	1.65	1.5	0.5	19	9
08-Apr-02	2SRT12BW_AR_2	long section of fibre after recovery cleaning (2nd time)	ConA-AF647	SBA-AF488	WGA-tmr	650/668	495/519	555/580	616	893	911	-0.064	-0.052	-0.0955	1	1.49	1.5	0.5	15	7
08-Apr-02	2SRT12BW_AR_3	long section of fibre after recovery cleaning (2nd time)	ConA-AF647	SBA-AF488	WGA-tmr	650/668	495/519	555/580	585	861	879	-0.0665	-0.074	-0.089	1	1.58	1.6	0.5	19	9
08-Apr-02	2SRT12BW_AR_4	long section of fibre after recovery cleaning (2nd time)	ConA-AF647	SBA-AF488	WGA-tmr	650/668	495/519	555/580	580	847	870	-0.0615	-0.059	-0.095	1	1.52	1.2	0.5	25	12
08-Apr-02	2SRT12BW_AR_5	long section of fibre after recovery cleaning (2nd time)	ConA-AF647	SBA-AF488	WGA-tmr	650/668	495/519	555/580	610	908	893	-0.052	-0.054	-0.094	1	1.53	1.49	0.55	26	13.75
08-Apr-02	2SRT12BW_AR_6	x-section of fibre after recovery cleaning (2nd time)	ConA-AF647	SBA-AF488	WGA-tmr	650/668	495/519	555/580	449	800	802	-0.034	-0.049	-0.064	1	1.3	1.4	1.05	24	24.15

Appendix J

CLSM IMAGE DATA - RUN 3 after 2 hours of filtration

Date	File Name	Specimen	Obj/NA	Averaging	Zoom	Speed (us/pixel)	Image Size			Filters			Laser Power			Pinhole (um)		
							Pixels	Microns		Ch 1	Ch2	Ch 3	488	543	633	Ch 1	Ch 2	Ch 3
18-Apr-02	3SRT30R_2hrs_1	long section of fibre after 2 hours of filtration (Run 3)	63X/0.9 W	2	1	8.96	512 x 512	146.2 x 146.2	12 bit	LP 650	BP 505-530	BP 565-615 IR	50% of 50%	100%	100%	191	146	169
18-Apr-02	3SRT30R_2hrs_2	long section of fibre after 2 hours of filtration (Run 3)	63X/0.9 W	2	1	8.96	512 x 512	146.2 x 146.2	12 bit	LP 650	BP 505-530	BP 565-615 IR	50% of 50%	100%	100%	191	146	169
18-Apr-02	3SRT30R_2hrs_3	long section of fibre after 2 hours of filtration (Run 3)	63X/0.9 W	2	1	8.96	512 x 512	146.2 x 146.2	12 bit	LP 650	BP 505-530	BP 565-615 IR	50% of 50%	100%	100%	191	146	169
18-Apr-02	3SRT30R_2hrs_4	long section of fibre after 2 hours of filtration (Run 3)	63X/0.9 W	2	1	8.96	512 x 512	146.2 x 146.2	12 bit	LP 650	BP 505-530	BP 565-615 IR	50% of 50%	100%	100%	191	146	169
18-Apr-02	3SRT30R_2hrs_5	long section of fibre after 2 hours of filtration (Run 3)	63X/0.9 W	2	2	8.96	512 x 512	73.1 x 73.1	12 bit	LP 650	BP 505-530	BP 565-615 IR	50% of 50%	100%	100%	191	146	169
18-Apr-02	3SRT30R_2hrs_6	x-section of fibre after 2 hours of filtration (Run 3)	63X/0.9 W	2	1	8.96	512 x 512	146.2 x 146.2	12 bit	LP 650	BP 505-530	BP 565-615 IR	50% of 50%	100%	100%	191	146	169
18-Apr-02	3SRT30R_2hrs_7	x-section of fibre after 2 hours of filtration (Run 3)	63X/0.9 W	2	0.7	8.96	512 x 512	206.8 x 206.8	12 bit	LP 650	BP 505-530	BP 565-615 IR	50% of 50%	100%	100%	191	146	169
18-Apr-02	3SRT30R_2hrs_8	x-section of fibre after 2 hours of filtration (Run 3)	10X/0.25	2	1	8.96	512 x 512	921.3 x 921.3	12 bit	LP 650	BP 505-530	BP 565-615 IR	50% of 50%	100%	100%	146	111	129
18-Apr-02	3SRT12R_2hrs_1	long section of fibre after 2 hours of filtration (Run 3)	63X/0.9 W	2	1	8.96	512 x 512	146.2 x 146.2	12 bit	LP 650	BP 505-530	BP 565-615 IR	50% of 50%	100%	100%	191	146	169
18-Apr-02	3SRT12R_2hrs_2	long section of fibre after 2 hours of filtration (Run 3)	63X/0.9 W	2	1	8.96	512 x 512	146.2 x 146.2	12 bit	LP 650	BP 505-530	BP 565-615 IR	50% of 50%	100%	100%	191	146	169
18-Apr-02	3SRT12R_2hrs_3	long section of fibre after 2 hours of filtration (Run 3)	63X/0.9 W	2	1	8.96	512 x 512	51.5 x 51.5	12 bit	LP 650	BP 505-530	BP 565-615 IR	50% of 50%	100%	100%	191	146	169
18-Apr-02	3SRT12R_2hrs_4	long section of fibre after 2 hours of filtration (Run 3)	63X/0.9 W	2	1	8.96	512 x 512	146.2 x 146.2	12 bit	LP 650	BP 505-530	BP 565-615 IR	50% of 50%	100%	100%	146	111	129
18-Apr-02	3SRT12R_2hrs_5	x-section of fibre after 2 hours of filtration (Run 3)	63X/0.9 W	2	1	8.96	512 x 512	146.2 x 146.2	12 bit	LP 650	BP 505-530	BP 565-615 IR	50% of 50%	100%	100%	146	111	129
18-Apr-02	3SRT12R_2hrs_6	x-section of fibre after 2 hours of filtration (Run 3)	10X/0.25	2	1	71.68	512 x 512	921.3 x 921.3	12 bit	LP 650	BP 505-530	BP 565-615 IR	50% of 50%	100%	100%	146	111	129
18-Apr-02	3SRT12BW_2hrs_1	long section of fibre after 2 hours of filtration (Run 3)	63X/0.9 W	2	1	8.96	512 x 512	146.2 x 146.2	12 bit	LP 650	BP 505-530	BP 565-615 IR	50% of 50%	100%	100%	146	111	129
18-Apr-02	3SRT12BW_2hrs_2	long section of fibre after 2 hours of filtration (Run 3)	63X/0.9 W	2	1	8.96	512 x 512	146.2 x 146.2	12 bit	LP 650	BP 505-530	BP 565-615 IR	50% of 50%	100%	100%	191	146	169
18-Apr-02	3SRT12BW_2hrs_3	long section of fibre after 2 hours of filtration (Run 3)	63X/0.9 W	2	1	8.96	512 x 512	146.2 x 146.2	12 bit	LP 650	BP 505-530	BP 565-615 IR	50% of 50%	100%	100%	191	146	169
18-Apr-02	3SRT12BW_2hrs_4	long section of fibre after 2 hours of filtration (Run 3)	63X/0.9 W	2	1	8.96	512 x 512	146.2 x 146.2	12 bit	LP 650	BP 505-530	BP 565-615 IR	50% of 50%	100%	100%	191	146	169
18-Apr-02	3SRT12BW_2hrs_5	x-section of fibre after 2 hours of filtration (Run 3)	63X/0.9 W	2	1	8.96	512 x 512	146.2 x 146.2	12 bit	LP 650	BP 505-530	BP 565-615 IR	50% of 50%	100%	100%	191	146	169
18-Apr-02	3SRT12BW_2hrs_6	x-section of fibre after 2 hours of filtration (Run 3)	10X/0.25	2	1	71.68	512 x 512	921.3 x 921.3	12 bit	LP 650	BP 505-530	BP 565-615 IR	50% of 50%	100%	100%	146	111	129

Date	File Name	Specimen	Dye/Lectin			Abs/Em1			Detector Gain			Amplitude Offset			Amplitude Gain			Z-step size (um)	# of Z sections	Total Z depth (um)
			Ch 1	Ch 2	Ch 3	Ch 1	Ch 2	Ch 3	Ch 1	Ch 2	Ch 3	Ch 1	Ch 2	Ch 3	Ch 1	Ch 2	Ch 3			
18-Apr-02	3SRT30R_2hrs_1	long section of fibre after 2 hours of filtration (Run 3)	ConA-AF647	SBA-AF488	WGA-tmr	650/668	495/519	555/580	583	892	854	-0.074	-0.067	-0.11	1	1.5	1.5	0.6	23	13.2
18-Apr-02	3SRT30R_2hrs_2	long section of fibre after 2 hours of filtration (Run 3)	ConA-AF647	SBA-AF488	WGA-tmr	650/668	495/519	555/580	551	879	852	-0.0615	-0.064	-0.071	1.58	1.68	1.5	2.05	32	63.55
18-Apr-02	3SRT30R_2hrs_3	long section of fibre after 2 hours of filtration (Run 3)	ConA-AF647	SBA-AF488	WGA-tmr	650/668	495/519	555/580	606	913	868	-0.047	-0.059	-0.069	1	1.54	1.52	0.9	25	21.6
18-Apr-02	3SRT30R_2hrs_4	long section of fibre after 2 hours of filtration (Run 3)	ConA-AF647	SBA-AF488	WGA-tmr	650/668	495/519	555/580	581	908	868	-0.032	-0.059	-0.079	1	1.54	1.52	2.05	34	67.7
18-Apr-02	3SRT30R_2hrs_5	long section of fibre after 2 hours of filtration (Run 3)	ConA-AF647	SBA-AF488	WGA-tmr	650/668	495/519	555/580	623	920	864	-0.0735	-0.052	-0.134	1	1.67	1.6	0.4	24	9.2
18-Apr-02	3SRT30R_2hrs_6	x-section of fibre after 2 hours of filtration (Run 3)	ConA-AF647	SBA-AF488	WGA-tmr	650/668	495/519	555/580	517	758	829	-0.034	-0.032	-0.043	1	1	1	1	26	25
18-Apr-02	3SRT30R_2hrs_7	x-section of fibre after 2 hours of filtration (Run 3)	ConA-AF647	SBA-AF488	WGA-tmr	650/668	495/519	555/580	548	884	845	-0.039	-0.052	-0.077	1.07	1.5	1.61	1	22	21
18-Apr-02	3SRT30R_2hrs_8	x-section of fibre after 2 hours of filtration (Run 3)	ConA-AF647	SBA-AF488	WGA-tmr	650/668	495/519	555/580	545	844	810	-0.032	-0.069	-0.084	1	1.92	1.78			
18-Apr-02	3SRT12R_2hrs_1	long section of fibre after 2 hours of filtration (Run 3)	ConA-AF647	SBA-AF488	WGA-tmr	650/668	495/519	555/580	683	955	763	-0.044	-0.047	-0.089	1	1.65	1.82	1.55	24	35.65
18-Apr-02	3SRT12R_2hrs_2	long section of fibre after 2 hours of filtration (Run 3)	ConA-AF647	SBA-AF488	WGA-tmr	650/668	495/519	555/580	609	909	824	-0.002	0.006	0.006	1	1.5	1.54	0.5	21	10
18-Apr-02	3SRT12R_2hrs_3	long section of fibre after 2 hours of filtration (Run 3)	ConA-AF647	SBA-AF488	WGA-tmr	650/668	495/519	555/580	680	1000	774	-0.074	-0.082	-0.089	1	1.92	1.51			
18-Apr-02	3SRT12R_2hrs_4	long section of fibre after 2 hours of filtration (Run 3)	ConA-AF647	SBA-AF488	WGA-tmr	650/668	495/519	555/580	635	884	852	-0.044	-0.074	-0.074	1	1.98	1.38	0.4	27	10.4
18-Apr-02	3SRT12R_2hrs_5	x-section of fibre after 2 hours of filtration (Run 3)	ConA-AF647	SBA-AF488	WGA-tmr	650/668	495/519	555/580	?	?	?	?	?	?	?	?	?	0.5	28	13.5
18-Apr-02	3SRT12R_2hrs_6	x-section of fibre after 2 hours of filtration (Run 3)	ConA-AF647	SBA-AF488	WGA-tmr	650/668	495/519	555/580	556	886	822	-0.032	-0.027	-0.044	1	1	1			
18-Apr-02	3SRT12BW_2hrs_1	long section of fibre after 2 hours of filtration (Run 3)	ConA-AF647	SBA-AF488	WGA-tmr	650/668	495/519	555/580	878	965	763	0.006	0.006	-0.019	1	1.61	1.3	1.5	28	40.5
18-Apr-02	3SRT12BW_2hrs_2	long section of fibre after 2 hours of filtration (Run 3)	ConA-AF647	SBA-AF488	WGA-tmr	650/668	495/519	555/580	704	932	881	-0.037	-0.054	-0.079	1	1.59	1.5	1	20	19
18-Apr-02	3SRT12BW_2hrs_3	long section of fibre after 2 hours of filtration (Run 3)	ConA-AF647	SBA-AF488	WGA-tmr	650/668	495/519	555/580	712	960	893	-0.0505	-0.049	-0.074	1	1.44	1.48	0.8	29	22.4
18-Apr-02	3SRT12BW_2hrs_4	long section of fibre after 2 hours of filtration (Run 3)	ConA-AF647	SBA-AF488	WGA-tmr	650/668	495/519	555/580	802	960	903	-0.037	-0.067	-0.079	1	1.89	1.7	2.6	27	67.6
18-Apr-02	3SRT12BW_2hrs_5	x-section of fibre after 2 hours of filtration (Run 3)	ConA-AF647	SBA-AF488	WGA-tmr	650/668	495/519	555/580	561	927	911	-0.037	-0.044	-0.064	1	1.3	1.46	1.55	23	34.1
18-Apr-02	3SRT12BW_2hrs_6	x-section of fibre after 2 hours of filtration (Run 3)	ConA-AF647	SBA-AF488	WGA-tmr	650/668	495/519	555/580	761	970	1000	-0.009	-0.042	-0.089	1	1.65	1.73			

Appendix J

CLSM IMAGE DATA - RUN 3 after 13 days of filtration

Date	File Name	Specimen	Obj/NA	Averaging	Zoom	Speed (us/pixel)	Image Size			Filters			Laser Power			Pinhole (um)		
							Pixels	Microns		Ch 1	Ch2	Ch 3	488	543	633	Ch 1	Ch 2	Ch 3
24-Apr-02	3SRT30R_13days_1	long section of fibre after 13 days of filtration (Run 3)	63X/0.9 W	2	1	8.96	512 x 512	146.2 x 146.2	12 bit	LP 650	BP 505-530	BP 565-615 IR	50% of 50%	100%	100%	191	146	169
24-Apr-02	3SRT30R_13days_2	long section of fibre after 13 days of filtration (Run 3)	63X/0.9 W	2	2	8.96	512 x 512	73.1 x 73.1	12 bit	LP 650	BP 505-530	BP 565-615 IR	50% of 50%	100%	100%	191	146	169
24-Apr-02	3SRT30R_13days_3	long section of fibre after 13 days of filtration (Run 3)	63X/0.9 W	2	1	8.96	512 x 512	146.2 x 146.2	12 bit	LP 650	BP 505-530	BP 565-615 IR	50% of 50%	100%	100%	191	146	169
24-Apr-02	3SRT30R_13days_4	long section of fibre after 13 days of filtration (Run 3)	63X/0.9 W	2	1	8.96	512 x 512	146.2 x 146.2	12 bit	LP 650	BP 505-530	BP 565-615 IR	50% of 50%	100%	100%	191	146	169
24-Apr-02	3SRT30R_13days_5	long section of fibre after 13 days of filtration (Run 3)	63X/0.9 W	2	1	8.96	512 x 512	146.2 x 146.2	12 bit	LP 650	BP 505-530	BP 565-615 IR	50% of 50%	100%	100%	191	146	169
24-Apr-02	3SRT30R_13days_6	x-section of fibre after 13 days of filtration (Run 3)	10X/0.25	2	1	71.68	512 x 512	921.3 x 921.3	12 bit	LP 650	BP 505-530	BP 565-615 IR	50% of 50%	100%	100%	191	146	169
24-Apr-02	3SRT30R_13days_7	x-section of fibre after 13 days of filtration (Run 3)	40X/0.6	2	1	8.96	512 x 512	230.3 x 230.3	12 bit	LP 650	BP 505-530	BP 565-615 IR	50% of 50%	100%	100%	191	146	169
25-Apr-02	3SRT12BW_13days_1	long section of fibre after 13 days of filtration (Run 3)	63X/0.9 W	2	1	8.96	512 x 512	146.2 x 146.2	12 bit	LP 650	BP 505-530	BP 565-615 IR	50% of 50%	100%	100%	191	146	169
25-Apr-02	3SRT12BW_13days_2	long section of fibre after 13 days of filtration (Run 3)	63X/0.9 W	2	1	8.96	512 x 512	146.2 x 146.2	12 bit	LP 650	BP 505-530	BP 565-615 IR	50% of 50%	100%	100%	191	146	169
25-Apr-02	3SRT12BW_13days_3	long section of fibre after 13 days of filtration (Run 3)	63X/0.9 W	2	1	8.96	512 x 512	146.2 x 146.2	12 bit	LP 650	BP 505-530	BP 565-615 IR	50% of 50%	100%	100%	191	146	169
25-Apr-02	3SRT12BW_13days_4	long section of fibre after 13 days of filtration (Run 3)	63X/0.9 W	2	2.7	17.92	512 x 512	53.4 x 53.4	12 bit	LP 650	BP 505-530	BP 565-615 IR	50% of 50%	100%	100%	191	146	169
25-Apr-02	3SRT12BW_13days_5	long section of fibre after 13 days of filtration (Run 3)	63X/0.9 W	2	1	8.96	512 x 512	146.2 x 146.2	12 bit	LP 650	BP 505-530	BP 565-615 IR	50% of 50%	100%	100%	191	146	169
25-Apr-02	3SRT12BW_13days_6	x-section of fibre after 13 days of filtration (Run 3)	63X/0.9 W	2	1	8.96	512 x 512	146.2 x 146.2	12 bit	LP 650	BP 505-530	BP 565-615 IR	50% of 50%	100%	100%	191	146	169
25-Apr-02	3SRT12BW_13days_7	x-section of fibre after 13 days of filtration (Run 3)	10X/0.25	2	1	71.68	512 x 512	921.3 x 921.3	12 bit	LP 650	BP 505-530	BP 565-615 IR	50% of 50%	100%	100%	146	111	129
25-Apr-02	3RT12R_13days_1	long section of fibre after 13 days of filtration (Run 3)	63X/0.9 W	2	1	8.96	512 x 512	146.2 x 146.2	12 bit	LP 650	BP 505-530	BP 565-615 IR	50% of 50%	100%	100%	191	146	169
25-Apr-02	3RT12R_13days_2	long section of fibre after 13 days of filtration (Run 3)	63X/0.9 W	2	1	8.96	512 x 512	146.2 x 146.2	12 bit	LP 650	BP 505-530	BP 565-615 IR	50% of 50%	100%	100%	191	146	169
25-Apr-02	3RT12R_13days_3	long section of fibre after 13 days of filtration (Run 3)	63X/0.9 W	2	1	8.96	512 x 512	146.2 x 146.2	12 bit	LP 650	BP 505-530	BP 565-615 IR	50% of 50%	100%	100%	191	146	169
25-Apr-02	3RT12R_13days_4	long section of fibre after 13 days of filtration (Run 3)	63X/0.9 W	2	1	8.96	512 x 512	146.2 x 146.2	12 bit	LP 650	BP 505-530	BP 565-615 IR	50% of 50%	100%	100%	191	146	169
25-Apr-02	3RT12R_13days_5	long section of fibre after 13 days of filtration (Run 3)	10X/0.25	2	1	71.68	512 x 512	921.3 x 921.3	12 bit	LP 650	BP 505-530	BP 565-615 IR	50% of 50%	100%	100%	191	146	169
25-Apr-02	3RT12R_13days_6	x-section of fibre after 13 days of filtration (Run 3)	10X/0.25	2	1	71.68	512 x 512	921.3 x 921.3	12 bit	LP 650	BP 505-530	BP 565-615 IR	50% of 50%	100%	100%	191	146	169
25-Apr-02	3RT12R_13days_7	x-section of fibre after 13 days of filtration (Run 3)	63X/0.9 W	2	0.7	71.68	512 x 512	921.3 x 921.3	12 bit	LP 650	BP 505-530	BP 565-615 IR	50% of 50%	100%	100%	191	146	169

Date	File Name	Specimen	Dye/Lectin			Abs/Em 1			Detector Gain			Amplitude Offset			Amplitude Gain			Z-step size (um)	# of Z sections	Total Z depth (um)
			Ch 1	Ch 2	Ch 3	Ch 1	Ch 2	Ch 3	Ch 1	Ch 2	Ch 3	Ch 1	Ch 2	Ch 3	Ch 1	Ch 2	Ch 3			
24-Apr-02	3SRT30R_13days_1	long section of fibre after 13 days of filtration (Run 3)	ConA-AF647	SBA-AF488	WGA-tmr	650/668	495/519	555/580	650	855	853	-0.059	-0.059	-0.074	1	1.52	1.53	1.55	30	44.95
24-Apr-02	3SRT30R_13days_2	long section of fibre after 13 days of filtration (Run 3)	ConA-AF647	SBA-AF488	WGA-tmr	650/668	495/519	555/580	739	831	828	-0.0815	-0.059	-0.069	1	1.48	1.5	0.7	29	19.6
24-Apr-02	3SRT30R_13days_3	long section of fibre after 13 days of filtration (Run 3)	ConA-AF647	SBA-AF488	WGA-tmr	650/668	495/519	555/580	671	838	842	-0.1205	-0.079	-0.104	1	1.5	1.5	0.5	23	11
24-Apr-02	3SRT30R_13days_4	long section of fibre after 13 days of filtration (Run 3)	ConA-AF647	SBA-AF488	WGA-tmr	650/668	495/519	555/580	731	834	849	-0.057	-0.044	-0.074	1	1.35	1.35	1	29	28
24-Apr-02	3SRT30R_13days_5	long section of fibre after 13 days of filtration (Run 3)	ConA-AF647	SBA-AF488	WGA-tmr	650/668	495/519	555/580	585	827	862	-0.074	-0.057	-0.064	1.3	1.4	1.4	0.95	30	27.55
24-Apr-02	3SRT30R_13days_6	x-section of fibre after 13 days of filtration (Run 3)	ConA-AF647	SBA-AF488	WGA-tmr	650/668	495/519	555/580	519	710	766	-0.042	-0.102	-0.074	1	2.5	1.56			
24-Apr-02	3SRT30R_13days_7	x-section of fibre after 13 days of filtration (Run 3)	ConA-AF647	SBA-AF488	WGA-tmr	650/668	495/519	555/580	715	1000	1000	-0.047	-0.057	-0.073	1	1.59	1.5	1.5	32	46.5
25-Apr-02	3SRT12BW_13days_1	long section of fibre after 13 days of filtration (Run 3)	ConA-AF647	SBA-AF488	WGA-tmr	650/668	495/519	555/580	751	865	888	-0.0825	-0.062	-0.098	1	1.48	1.5	0.8	27	20.8
25-Apr-02	3SRT12BW_13days_2	long section of fibre after 13 days of filtration (Run 3)	ConA-AF647	SBA-AF488	WGA-tmr	650/668	495/519	555/580	692	816	792	-0.069	-0.067	-0.067	1	1.53	1.4	1.05	27	27.3
25-Apr-02	3SRT12BW_13days_3	long section of fibre after 13 days of filtration (Run 3)	ConA-AF647	SBA-AF488	WGA-tmr	650/668	495/519	555/580	715	851	869	-0.064	-0.0635	-0.076	1	1.57	1.4	0.6	30	17.4
25-Apr-02	3SRT12BW_13days_4	long section of fibre after 13 days of filtration (Run 3)	ConA-AF647	SBA-AF488	WGA-tmr	650/668	495/519	555/580	854	852	854	-0.0965	-0.069	-0.097	1.58	1.61	1.58	0.5	23	11
25-Apr-02	3SRT12BW_13days_5	long section of fibre after 13 days of filtration (Run 3)	ConA-AF647	SBA-AF488	WGA-tmr	650/668	495/519	555/580	618	656	831	-0.037	-0.032	-0.049	1	1	1.15	1	31	30
25-Apr-02	3SRT12BW_13days_6	x-section of fibre after 13 days of filtration (Run 3)	ConA-AF647	SBA-AF488	WGA-tmr	650/668	495/519	555/580	555	861	874	-0.034	-0.064	-0.074	1	1.82	1.55	1	23	22
25-Apr-02	3SRT12BW_13days_7	x-section of fibre after 13 days of filtration (Run 3)	ConA-AF647	SBA-AF488	WGA-tmr	650/668	495/519	555/580	579	866	841	-0.024	-0.052	-0.067	1	1.43	1.46			
25-Apr-02	3RT12R_13days_1	long section of fibre after 13 days of filtration (Run 3)	ConA-AF647	SBA-AF488	WGA-tmr	650/668	495/519	555/580	588	623	791	-0.059	-0.094	-0.094	1	2.92	1.7	0.8	30	23.2
25-Apr-02	3RT12R_13days_2	long section of fibre after 13 days of filtration (Run 3)	ConA-AF647	SBA-AF488	WGA-tmr	650/668	495/519	555/580	629	837	851	-0.117	-0.079	-0.099	1	1.53	1.5	0.4	27	10.4
25-Apr-02	3RT12R_13days_3	long section of fibre after 13 days of filtration (Run 3)	ConA-AF647	SBA-AF488	WGA-tmr	650/668	495/519	555/580	700	940	940	-0.049	-0.049	-0.068	1	1.48	1.3	0.7	28	18.9
25-Apr-02	3RT12R_13days_4	long section of fibre after 13 days of filtration (Run 3)	ConA-AF647	SBA-AF488	WGA-tmr	650/668	495/519	555/580	649	884	864	-0.047	-0.039	-0.068	1	1.41	1.4	3	28	81
25-Apr-02	3RT12R_13days_5	long section of fibre after 13 days of filtration (Run 3)	ConA-AF647	SBA-AF488	WGA-tmr	650/668	495/519	555/580	654	851	827	-0.074	-0.049	-0.064	1	1	1.04			
25-Apr-02	3RT12R_13days_6	x-section of fibre after 13 days of filtration (Run 3)	ConA-AF647	SBA-AF488	WGA-tmr	650/668	495/519	555/580	544	782	788	-0.042	-0.05	-0.073	1	1.54	1.4			
25-Apr-02	3RT12R_13days_7	x-section of fibre after 13 days of filtration (Run 3)	ConA-AF647	SBA-AF488	WGA-tmr	650/668	495/519	555/580	480	781	840	-0.034	-0.054	-0.073	1	1.5	1.5	1.05	29	29.4

Appendix J

CLSM IMAGE DATA - RUN 3 at Shutdown

Date	File Name	Specimen	Obj/NA	Averaging	Zoom	Speed (us/pixel)	Image Size			Filters			Laser Power			Pinhole (um)		
							Pixels	Microns		Ch 1	Ch2	Ch 3	488	543	633	Ch 1	Ch 2	Ch 3
29-Apr-02	SRT30R_shutdown_1	long section of fibre at shutdown - Run 3 after 28 days	63X/0.9 W	2	1	8.96	512 x 512	146.2 x 146.2	12 bit	LP 650	BP 505-530	BP 565-615 IR	50% of 50%	100%	100%	191	146	169
29-Apr-02	SRT30R_shutdown_2	long section of fibre at shutdown - Run 3 after 28 days	63X/0.9 W	2	1	8.96	512 x 512	146.2 x 146.2	12 bit	LP 650	BP 505-530	BP 565-615 IR	50% of 50%	100%	100%	191	146	169
29-Apr-02	SRT30R_shutdown_4	long section of fibre at shutdown - Run 3 after 28 days	63X/0.9 W	2	2	8.96	512 x 512	73.1 x 73.1	12 bit	LP 650	BP 505-530	BP 565-615 IR	50% of 50%	100%	100%	191	146	169
29-Apr-02	SRT30R_shutdown_5	long section of fibre at shutdown - Run 3 after 28 days	63X/0.9 W	2	2	8.96	512 x 512	73.1 x 73.1	12 bit	LP 650	BP 505-530	BP 565-615 IR	50% of 50%	100%	100%	191	146	169
29-Apr-02	SRT30R_shutdown_6	long section of fibre at shutdown - Run 3 after 28 days	63X/0.9 W	2	1	8.96	512 x 512	146.2 x 146.2	12 bit	LP 650	BP 505-530	BP 565-615 IR	50% of 50%	100%	100%	191	146	169
29-Apr-02	SRT30R_shutdown_7	x-section of fibre at shutdown - Run 3 after 28 days	10X/0.25	2	1	71.68	512 x 512	921.3 x 921.3	12 bit	LP 650	BP 505-530	BP 565-615 IR	50% of 50%	100%	100%	191	146	169
29-Apr-02	SRT30R_shutdown_8	x-section of fibre at shutdown - Run 3 after 28 days	63X/0.9 W	2	1	8.96	512 x 512	146.2 x 146.2	12 bit	LP 650	BP 505-530	BP 565-615 IR	50% of 50%	100%	100%	191	146	169
29-Apr-02	SRT12BW_shutdown_1	long section of fibre at shutdown - Run 3 after 32 days	63X/0.9 W	2	1	8.96	512 x 512	146.2 x 146.2	12 bit	LP 650	BP 505-530	BP 565-615 IR	50% of 50%	100%	100%	191	146	169
29-Apr-02	SRT12BW_shutdown_2	long section of fibre at shutdown - Run 3 after 32 days	63X/0.9 W	2	1	8.96	512 x 512	146.2 x 146.2	12 bit	LP 650	BP 505-530	BP 565-615 IR	50% of 50%	100%	100%	191	146	169
29-Apr-02	SRT12BW_shutdown_3	long section of fibre at shutdown - Run 3 after 32 days	63X/0.9 W	2	1	8.96	512 x 512	146.2 x 146.2	12 bit	LP 650	BP 505-530	BP 565-615 IR	50% of 50%	100%	100%	191	146	169
29-Apr-02	SRT12BW_shutdown_4	long section of fibre at shutdown - Run 3 after 32 days	63X/0.9 W	2	1	8.96	512 x 512	146.2 x 146.2	12 bit	LP 650	BP 505-530	BP 565-615 IR	50% of 50%	100%	100%	191	146	169
29-Apr-02	SRT12BW_shutdown_5	long section of fibre at shutdown - Run 3 after 32 days	63X/0.9 W	2	1	8.96	512 x 512	146.2 x 146.2	12 bit	LP 650	BP 505-530	BP 565-615 IR	50% of 50%	100%	100%	191	146	169
29-Apr-02	SRT12BW_shutdown_6	x-section of fibre at shutdown - Run 3 after 32 days	10X/0.25	2	1	71.68	512 x 512	921.3 x 921.3	12 bit	LP 650	BP 505-530	BP 565-615 IR	50% of 50%	100%	100%	146	111	129
29-Apr-02	SRT12BW_shutdown_7	x-section of fibre at shutdown - Run 3 after 32 days	63X/0.9 W	2	1	8.96	512 x 512	146.2 x 146.2	12 bit	LP 650	BP 505-530	BP 565-615 IR	50% of 50%	100%	100%	191	146	169
29-Apr-02	SRT12R_shutdown_1	long section of fibre at shutdown - Run 3 after 34 days	63X/0.9 W	2	1	8.96	512 x 512	146.2 x 146.2	12 bit	LP 650	BP 505-530	BP 565-615 IR	50% of 50%	100%	100%	191	146	169
29-Apr-02	SRT12R_shutdown_2	long section of fibre at shutdown - Run 3 after 34 days	63X/0.9 W	2	1	8.96	512 x 512	146.2 x 146.2	12 bit	LP 650	BP 505-530	BP 565-615 IR	50% of 50%	100%	100%	191	146	169
29-Apr-02	SRT12R_shutdown_3	long section of fibre at shutdown - Run 3 after 34 days	63X/0.9 W	2	1	8.96	512 x 512	146.2 x 146.2	12 bit	LP 650	BP 505-530	BP 565-615 IR	50% of 50%	100%	100%	191	146	169
29-Apr-02	SRT12R_shutdown_4	long section of fibre at shutdown - Run 3 after 34 days	63X/0.9 W	2	1	8.96	512 x 512	146.2 x 146.2	12 bit	LP 650	BP 505-530	BP 565-615 IR	50% of 50%	100%	100%	191	146	169
29-Apr-02	SRT12R_shutdown_5	long section of fibre at shutdown - Run 3 after 34 days	63X/0.9 W	2	1	8.96	512 x 512	146.2 x 146.2	12 bit	LP 650	BP 505-530	BP 565-615 IR	50% of 50%	100%	100%	191	146	169
29-Apr-02	SRT12R_shutdown_6	x-section of fibre at shutdown - Run 3 after 34 days	10X/0.25	2	1	71.68	512 x 512	921.3 x 921.3	12 bit	LP 650	BP 505-530	BP 565-615 IR	50% of 50%	100%	100%	146	111	129
29-Apr-02	SRT12R_shutdown_7	x-section of fibre at shutdown - Run 3 after 34 days	63X/0.9 W	2	1	8.96	512 x 512	146.2 x 146.2	12 bit	LP 650	BP 505-530	BP 565-615 IR	50% of 50%	100%	100%	191	146	169

Date	File Name	Specimen	Dye/Lectin			Abs/Em l			Detector Gain			Amplitude Offset			Amplitude Gain			Z-step size (um)	# of Z sections	Total Z depth (um)
			Ch 1	Ch 2	Ch 3	Ch 1	Ch 2	Ch 3	Ch 1	Ch 2	Ch 3	Ch 1	Ch 2	Ch 3	Ch 1	Ch 2	Ch 3			
29-Apr-02	SRT30R_shutdown_1	long section of fibre at shutdown - Run 3 after 28 days	ConA-AF633	SBA-AF488	WGA-tmr	632/647	495/519	555/580	748	792	853	-0.1715	-0.0865	-0.154	1	1	1	0.7	25	16.8
29-Apr-02	SRT30R_shutdown_2	long section of fibre at shutdown - Run 3 after 28 days	ConA-AF633	SBA-AF488	WGA-tmr	632/647	495/519	555/580	734	772	825	-0.059	-0.054	-0.0775	1	1.74	1.4	1	31	30
29-Apr-02	SRT30R_shutdown_4	long section of fibre at shutdown - Run 3 after 28 days	ConA-AF633	SBA-AF488	WGA-tmr	632/647	495/519	555/580	774	812	879	-0.092	-0.062	-0.05	1	1.41	1	0.8	22	16.8
29-Apr-02	SRT30R_shutdown_5	long section of fibre at shutdown - Run 3 after 28 days	ConA-AF633	SBA-AF488	WGA-tmr	632/647	495/519	555/580	768	816	858	-0.047	-0.054	-0.07	1	1.45	1.4	1	30	29
29-Apr-02	SRT30R_shutdown_6	long section of fibre at shutdown - Run 3 after 28 days	ConA-AF633	SBA-AF488	WGA-tmr	632/647	495/519	555/580	728	806	829	-0.0139	-0.064	-0.079	1	1	1	0.8	26	20
29-Apr-02	SRT30R_shutdown_7	x-section of fibre at shutdown - Run 2 after 28 days	ConA-AF633	SBA-AF488	WGA-tmr	632/647	495/519	555/580	564	678	642	-0.014	-0.104	-0.149	1	2.55	2.87			
29-Apr-02	SRT30R_shutdown_8	x-section of fibre at shutdown - Run 2 after 28 days	ConA-AF633	SBA-AF488	WGA-tmr	632/647	495/519	555/580	637	736	768	-0.039	-0.079	-0.094	1	2.08	1.77	1	31	30
29-Apr-02	SRT12BW_shutdown_1	long section of fibre at shutdown - Run 3 after 32 days	ConA-AF633	SBA-AF488	WGA-tmr	632/647	495/519	555/580	717	771	791	-0.069	-0.0785	-0.095	1	1.7	1.7	1.1	37	39.6
29-Apr-02	SRT12BW_shutdown_2	long section of fibre at shutdown - Run 3 after 32 days	ConA-AF633	SBA-AF488	WGA-tmr	632/647	495/519	555/580	715	822	844	-0.0965	-0.042	-0.06	1	1	1	0.4	23	8.8
29-Apr-02	SRT12BW_shutdown_3	long section of fibre at shutdown - Run 3 after 32 days	ConA-AF633	SBA-AF488	WGA-tmr	632/647	495/519	555/580	698	784	804	-0.164	-0.094	-0.1	1	1	1	0.45	26	11.25
29-Apr-02	SRT12BW_shutdown_4	long section of fibre at shutdown - Run 3 after 32 days	ConA-AF633	SBA-AF488	WGA-tmr	632/647	495/519	555/580	676	763	745	-0.0915	-0.051	-0.0765	1	1	1.22	0.5	29	14
29-Apr-02	SRT12BW_shutdown_5	long section of fibre at shutdown - Run 3 after 32 days	ConA-AF633	SBA-AF488	WGA-tmr	632/647	495/519	555/580	718	824	822	-0.067	-0.034	-0.05	1	1	1	0.7	34	23.1
29-Apr-02	SRT12BW_shutdown_6	x-section of fibre at shutdown - Run 2 after 32 days	ConA-AF633	SBA-AF488	WGA-tmr	632/647	495/519	555/580	647	794	790	-0.034	-0.047	-0.054	1	1.42	1.29			
29-Apr-02	SRT12BW_shutdown_7	x-section of fibre at shutdown - Run 2 after 32 days	ConA-AF633	SBA-AF488	WGA-tmr	632/647	495/519	555/580	735	791	808	-0.032	-0.057	-0.044	1	1.5	1.23	1.25	26	32.5
29-Apr-02	SRT12R_shutdown_1	long section of fibre at shutdown - Run 3 after 34 days	ConA-AF633	SBA-AF488	WGA-tmr	632/647	495/519	555/580	833	743	915	-0.049	-0.057	-0.0725	1	1.4	1.4	1	33	32
29-Apr-02	SRT12R_shutdown_2	long section of fibre at shutdown - Run 3 after 34 days	ConA-AF633	SBA-AF488	WGA-tmr	632/647	495/519	555/580	739	800	808	-0.074	-0.054	-0.079	1	1.2	1.2	0.7	28	18.9
29-Apr-02	SRT12R_shutdown_3	long section of fibre at shutdown - Run 3 after 34 days	ConA-AF633	SBA-AF488	WGA-tmr	632/647	495/519	555/580	768	802	826	-0.0415	-0.047	-0.0565	1	1.3	1.31	1	35	34
29-Apr-02	SRT12R_shutdown_4	long section of fibre at shutdown - Run 3 after 34 days	ConA-AF633	SBA-AF488	WGA-tmr	632/647	495/519	555/580	765	798	793	-0.1625	-0.1205	-0.1235	1	1.5	1.4	0.5	30	14.5
29-Apr-02	SRT12R_shutdown_5	long section of fibre at shutdown - Run 3 after 34 days	ConA-AF633	SBA-AF488	WGA-tmr	632/647	495/519	555/580	766	797	814	-0.089	-0.064	-0.08	1	1.3	1.3	1	24	23
29-Apr-02	SRT12R_shutdown_6	x-section of fibre at shutdown - Run 3 after 34 days	ConA-AF633	SBA-AF488	WGA-tmr	632/647	495/519	555/580	643	820	821	-0.034	-0.042	-0.057	1	1.23	1.16			
29-Apr-02	SRT12R_shutdown_7	x-section of fibre at shutdown - Run 3 after 34 days	ConA-AF633	SBA-AF488	WGA-tmr	632/647	495/519	555/580	819	895	861	-0.029	-0.057	-0.045	1	1.46	1.4	1	31	30

Appendix J

CLSM IMAGE DATA - After Final Recovery Cleaning

Date	File Name	Specimen	Obj/NA	Averaging	Zoom	Speed (us/pixel)	Image Size			Filters			Laser Power			Pinhole (um)		
							Pixels	Microns		Ch 1	Ch2	Ch 3	488	543	633	Ch 1	Ch 2	Ch 3
30-Apr-02	3SRT12R_AR_1	long section of fibre after final recovery cleaning	63X/0.9 W	2	1	8.96	512 x 512	146.2 x 146.2	12 bit	LP 650	BP 505-530	BP 565-615 IR	50% of 50%	100%	100%	191	146	169
30-Apr-02	3SRT12R_AR_2	long section of fibre after final recovery cleaning	63X/0.9 W	2	1.7	8.96	512 x 512	88.6 x 88.6	12 bit	LP 650	BP 505-530	BP 565-615 IR	50% of 50%	100%	100%	191	146	169
30-Apr-02	3SRT12R_AR_3	long section of fibre after final recovery cleaning	63X/0.9 W	2	1	8.96	512 x 512	146.2 x 146.2	12 bit	LP 650	BP 505-530	BP 565-615 IR	50% of 50%	100%	100%	191	146	169
30-Apr-02	3SRT12R_AR_4	long section of fibre after final recovery cleaning	63X/0.9 W	2	1	8.96	512 x 512	146.2 x 146.2	12 bit	LP 650	BP 505-530	BP 565-615 IR	50% of 50%	100%	100%	191	146	169
30-Apr-03	3SRT12R_AR_5	x-section of fibre after final recovery cleaning	10X/0.25	2	1	71.68	512 x 512	921.3 x 921.3	12 bit	LP 650	BP 505-530	BP 565-615 IR	50% of 50%	100%	100%	146	111	129
30-Apr-03	3SRT12R_AR_6	x-section of fibre after final recovery cleaning	63X/0.9 W	2	1	8.96	512 x 512	146.2 x 146.2	12 bit	LP 650	BP 505-530	BP 565-615 IR	50% of 50%	100%	100%	191	146	169
30-Apr-02	3SRT12BW_AR_1	long section of fibre after final recovery cleaning	63X/0.9 W	2	1	8.96	512 x 512	146.2 x 146.2	12 bit	LP 650	BP 505-530	BP 565-615 IR	50% of 50%	100%	100%	191	146	169
30-Apr-02	3SRT12BW_AR_2	long section of fibre after final recovery cleaning	63X/0.9 W	2	2	8.96	512 x 512	73.1 x 73.1	12 bit	LP 650	BP 505-530	BP 565-615 IR	50% of 50%	100%	100%	191	146	169
30-Apr-02	3SRT12BW_AR_3	long section of fibre after final recovery cleaning	63X/0.9 W	2	1	8.96	512 x 512	146.2 x 146.2	12 bit	LP 650	BP 505-530	BP 565-615 IR	50% of 50%	100%	100%	191	146	169
30-Apr-02	3SRT12BW_AR_4	long section of fibre after final recovery cleaning	63X/0.9 W	2	1	8.96	512 x 512	146.2 x 146.2	12 bit	LP 650	BP 505-530	BP 565-615 IR	50% of 50%	100%	100%	191	146	169
30-Apr-02	3SRT12BW_AR_5	x-section of fibre after final recovery cleaning	10X/0.25	2	1	71.68	512 x 512	921.3 x 921.3	12 bit	LP 650	BP 505-530	BP 565-615 IR	50% of 50%	100%	100%	146	111	129
30-Apr-02	3SRT12BW_AR_6	x-section of fibre after final recovery cleaning	63X/0.9 W	2	0.7	8.96	512 x 512	206.8 x 206.8	12 bit	LP 650	BP 505-530	BP 565-615 IR	50% of 50%	100%	100%	191	146	169
30-Apr-02	3SRT30R_AR_1	long section of fibre after final recovery cleaning	63X/0.9 W	2	1	8.96	512 x 512	146.2 x 146.2	12 bit	LP 650	BP 505-530	BP 565-615 IR	50% of 50%	100%	100%	191	146	169
30-Apr-02	3SRT30R_AR_2	long section of fibre after final recovery cleaning	63X/0.9 W	2	1	8.96	512 x 512	146.2 x 146.2	12 bit	LP 650	BP 505-530	BP 565-615 IR	50% of 50%	100%	100%	191	146	169
30-Apr-02	3SRT30R_AR_3	long section of fibre after final recovery cleaning	63X/0.9 W	2	1	8.96	512 x 512	146.2 x 146.2	12 bit	LP 650	BP 505-530	BP 565-615 IR	50% of 50%	100%	100%	191	146	169
30-Apr-02	3SRT30R_AR_4	long section of fibre after final recovery cleaning	63X/0.9 W	2	2	8.96	512 x 512	73.1 x 73.1	12 bit	LP 650	BP 505-530	BP 565-615 IR	50% of 50%	100%	100%	191	146	169
30-Apr-02	3SRT30R_AR_5	x-section of fibre after final recovery cleaning	10X/0.25	2	1	71.68	512 x 512	921.3 x 921.3	12 bit	LP 650	BP 505-530	BP 565-615 IR	50% of 50%	100%	100%	146	111	129
30-Apr-02	3SRT30R_AR_6	x-section of fibre after final recovery cleaning	63X/0.9 W	2	0.7	8.96	512 x 512	206.8 x 206.8	12 bit	LP 650	BP 505-530	BP 565-615 IR	50% of 50%	100%	100%	191	146	169

Date	File Name	Specimen	Dye/Lectin			Abs/Em l			Detector Gain			Amplitude Offset			Amplitude Gain			Z-step size (um)	# of Z sections	Total Z depth (um)
			Ch 1	Ch 2	Ch 3	Ch 1	Ch 2	Ch 3	Ch 1	Ch 2	Ch 3	Ch 1	Ch 2	Ch 3	Ch 1	Ch 2	Ch 3			
30-Apr-02	3SRT12R_AR_1	long section of fibre after final recovery cleaning	ConA-AF633	SBA-AF488	WGA-tmr	632/647	495/519	555/580	583	827	802	-0.1015	-0.074	-0.099	1	1.39	1	0.55	13	6.6
30-Apr-02	3SRT12R_AR_2	long section of fibre after final recovery cleaning	ConA-AF633	SBA-AF488	WGA-tmr	632/647	495/519	555/580	591	847	827	-0.1315	-0.0835	-0.1205	1	1	1	0.35	12	3.85
30-Apr-02	3SRT12R_AR_3	long section of fibre after final recovery cleaning	ConA-AF633	SBA-AF488	WGA-tmr	632/647	495/519	555/580	581	773	792	-0.1285	-0.1	-0.125	1	1.3	1.2	0.45	16	6.75
30-Apr-02	3SRT12R_AR_4	long section of fibre after final recovery cleaning	ConA-AF633	SBA-AF488	WGA-tmr	632/647	495/519	555/580	603	797	771	-0.144	-0.119	-0.1065	1	1.35	1.3	0.6	21	12
30-Apr-03	3SRT12R_AR_5	x-section of fibre after final recovery cleaning	ConA-AF633	SBA-AF488	WGA-tmr	632/647	495/519	555/580	583	878	776	-0.024	-0.032	-0.039	1	1	1			
30-Apr-03	3SRT12R_AR_6	x-section of fibre after final recovery cleaning	ConA-AF633	SBA-AF488	WGA-tmr	632/647	495/519	555/580	546	832	752	-0.029	-0.037	-0.054	1	1.16	1.09	1.25	21	25
30-Apr-02	3SRT12BW_AR_1	long section of fibre after final recovery cleaning	ConA-AF633	SBA-AF488	WGA-tmr	632/647	495/519	555/580	568	789	787	-0.1365	-0.084	-0.1165	1	1.46	1	0.5	8	3.5
30-Apr-02	3SRT12BW_AR_2	long section of fibre after final recovery cleaning	ConA-AF633	SBA-AF488	WGA-tmr	632/647	495/519	555/580	650	780	760	-0.1205	-0.077	-0.117	1	1.5	1.4	0.7	12	9.8
30-Apr-02	3SRT12BW_AR_3	long section of fibre after final recovery cleaning	ConA-AF633	SBA-AF488	WGA-tmr	632/647	495/519	555/580	770	801	914	-0.039	-0.037	-0.07	1	1.3	1.4	1.4	33	44.8
30-Apr-02	3SRT12BW_AR_4	long section of fibre after final recovery cleaning	ConA-AF633	SBA-AF488	WGA-tmr	632/647	495/519	555/580	595	857	842	-0.122	-0.092	-0.124	1	1.38	1.12	0.5	22	10.5
30-Apr-02	3SRT12BW_AR_5	x-section of fibre after final recovery cleaning	ConA-AF633	SBA-AF488	WGA-tmr	632/647	495/519	555/580	568	864	756	-0.039	-0.032	-0.074	1	1.05	1.48			
30-Apr-02	3SRT12BW_AR_6	x-section of fibre after final recovery cleaning	ConA-AF633	SBA-AF488	WGA-tmr	632/647	495/519	555/580	532	765	720	-0.039	-0.054	-0.074	1	1.47	1.63	0.8	25	19.2
30-Apr-02	3SRT30R_AR_1	long section of fibre after final recovery cleaning	ConA-AF633	SBA-AF488	WGA-tmr	632/647	495/519	555/580	589	797	795	-0.132	-0.104	-0.124	1	1.3	1.3	0.55	10	4.95
30-Apr-02	3SRT30R_AR_2	long section of fibre after final recovery cleaning	ConA-AF633	SBA-AF488	WGA-tmr	632/647	495/519	555/580	607	821	840	-0.0815	-0.077	-0.1245	1	1.46	1.4	0.45	17	7.2
30-Apr-02	3SRT30R_AR_3	long section of fibre after final recovery cleaning	ConA-AF633	SBA-AF488	WGA-tmr	632/647	495/519	555/580	615	806	853	-0.127	-0.059	-0.094	1	1	1	0.45	17	7.2
30-Apr-02	3SRT30R_AR_4	long section of fibre after final recovery cleaning	ConA-AF633	SBA-AF488	WGA-tmr	632/647	495/519	555/580	587	710	774	-0.115	-0.112	-0.1375	1	1.93	1.26	0.6	17	9..6
30-Apr-02	3SRT30R_AR_5	x-section of fibre after final recovery cleaning	ConA-AF633	SBA-AF488	WGA-tmr	632/647	495/519	555/580	555	837	691	-0.039	-0.034	-0.0765	1	1	1.5			
30-Apr-02	3SRT30R_AR_6	x-section of fibre after final recovery cleaning	ConA-AF633	SBA-AF488	WGA-tmr	632/647	495/519	555/580	533	765	735	-0.034	-0.042	-0.039	1	1.3	1	1	19	18

APPENDIX K: Core Study – Surface Charge Data

SRT 12 - February 5, 2002

Titration data

Sample	Vo (mL)	Vf (mL)	Difference (mL)	Average (mL)	Standard Deviation
A1	25.10	29.11	4.01	3.91	0.10
A2	29.30	33.20	3.90		
A3	33.20	37.02	3.82		
Blank 1	6.65	15.69	9.04	9.15	0.15
Blank 2	15.80	25.05	9.25		

where Vo and Vf are initial and final volumes respectively

MLSS Calculations

Sample	Wo (g)	Wf (g)	Difference (g)	Aliquot (mL)	Solids g/L	Average	Standard Deviation
1	1.1183	1.1289	0.0106	2	5.30	5.35	0.0707
2	1.1122	1.1230	0.0108	2	5.40		

where Wo and Wf are initial and final weights respectively

Vol Blank(Vo)	Titration Volume (mL)	MLSS (g/L)
9.15	3.91	5.35

Equation

Suface Charge = (-(Vo-V)*N*1000)/(aliquot mL)*MLSS(g/L) where N = 0.001

	Calculated value of Surface Charge (meq/ g MLSS)
1	-0.489

SRT 12 - February 11, 2002

Titration data

Sample	Vo (mL)	Vf (mL)	Difference (mL)	Average (mL)	Standard Deviation
A1	34.60	37.89	3.29	3.60	0.28
A2	38.10	42.02	3.92		
A3	42.02	45.75	3.73		
A4	45.75	49.21	3.46		
Blank 1	5.29	14.61	9.32	9.21	0.16
Blank 2	14.61	23.70	9.09		

where Vo and Vf are initial and final volumes respectively

MLSS Calculations

Sample	Wo (g)	Wf (g)	Difference (g)	Aliquot (mL)	Solids g/L
1	1.1120	1.1269	0.0149	2.5	5.96

where Wo and Wf are initial and final weights respectively

Vol Blank(Vo)	Titration Volume (mL)	MLSS (g/L)
9.21	3.60	5.96

Calculated value of Surface Charge (meq/ g MLSS)	
1	-0.470

SRT 12 - February 26, 2002

Titration data

Sample	Vo (mL)	Vf (mL)	Difference (mL)	Average (mL)	Standard Deviation
1	21.81	24.30	2.49	2.52	0.04
2	24.30	26.84	2.54		
Blank 1	1.10	9.72	8.62	8.40	0.31
Blank 2	9.72	17.90	8.18		

where Vo and Vf are initial and final volumes respectively

MLSS Calculations

Sample	Wo (g)	Wf (g)	Difference (g)	Aliquot (mL)	Solids (g/L)	Average (g/L)	Standard Deviation
1	1.1133	1.1218	0.0085	2.5	3.40	3.64	0.339
2	1.1066	1.1163	0.0097	2.5	3.88		

where Wo and Wf are initial and final weights respectively

Vol Blank(Vo)	Titration Volume (V)	MLSS (g/L)
8.40	2.52	3.64

	Calculated value of Surface Charge (meq/ g MLSS)
1	-0.808

SRT 12 - March 8, 2002

Titration data

Sample	Vo (mL)	Vf (mL)	Difference (mL)	Average (mL)	Standard Deviation
1A	18.35	19.80	1.45	1.46	0.02
1B	21.75	23.21	1.46		
1C	22.70	24.18	1.48		
Blank 1	2.00	10.30	8.30	8.15	0.21
Blank 2	10.35	18.35	8.00		

where Vo and Vf are initial and final volumes respectively

MLSS Calculations

Sample	Wo (g)	Wf (g)	Difference (g)	Aliquot (mL)	Solids (g/L)	Average (g/L)	Standard Deviation
1	1.1135	1.1270	0.0135	2.50	5.40	5.24	0.226
2	1.0972	1.1099	0.0127	2.50	5.08		

where Wo and Wf are initial and final weights respectively

Vol Blank(Vo)	Titration Volume (V)	MLSS (g/L)
8.15	1.46	5.24

	Calculated value of Surface Charge (meq/ g MLSS)
1	-0.638

SRT 12 - March 20, 2002

Titration data

Sample	Vo (mL)	Vf (mL)	Difference (mL)	Average (mL)	Standard Deviation
1A	35.50	38.15	2.65	2.64	0.05
1B	38.15	40.83	2.68		
1C	40.43	43.02	2.59		
Blank 1	18.12	26.71	8.59	8.69	0.14
Blank 2	26.71	35.50	8.79		

where Vo and Vf are initial and final volumes respectively

MLSS Calculations

Sample	Wo (g)	Wf (g)	Difference (g)	Aliquot (mL)	Solids (g/L)	Average (g/L)	Standard Deviation
1	1.1154	1.1254	0.0100	2.5	4.00	4.42	0.594
2	1.1201	1.1322	0.0121	2.5	4.84		

where Wo and Wf are initial and final weights respectively

Vol Blank(Vo)	Titration Volume (V)	MLSS (g/L)
8.69	2.64	4.42

	Calculated value of Surface Charge (meq/ g MLSS)
1	-0.684

SRT 12 - April 2, 2002

Titration data

Sample	Vo (mL)	Vf (mL)	Difference (mL)	Average (mL)	Standard Deviation
1A	33.11	35.70	2.59	2.64	0.08
1B	35.70	38.29	2.59		
1C	38.29	41.02	2.73		
Blank 1	14.65	23.20	8.55	8.64	0.13
Blank 2	23.20	31.93	8.73		

where Vo and Vf are initial and final volumes respectively

MLSS Calculations

Sample	Wo (g)	Wf (g)	Difference (g)	Aliquot (mL)	Solids (g/L)	Average (g/L)	Standard Deviation
1	1.1155	1.1281	0.0126	2.5	5.04	5.04	0
2	1.1190	1.1316	0.0126	2.5	5.04		

where Wo and Wf are initial and final weights respectively

Vol Blank (Vo)	Titration Volume (V)	MLSS (g/L)
8.64	2.64	5.04

	Calculated value of Surface Charge (meq/ g MLSS)
1	-0.596

SRT 12 - April 17, 2002

Titration data

Sample	Vo (mL)	Vf (mL)	Difference (mL)	Average (mL)	Standard Deviation
1A	26.21	29.40	3.19	3.09	0.09
1B	29.40	32.45	3.05		
1C	32.45	35.48	3.03		
Blank 1	8.45	17.25	8.80	8.75	0.07
Blank 2	17.41	26.11	8.70		

where Vo and Vf are initial and final volumes respectively

MLSS Calculations

Sample	Wo (g)	Wf (g)	Difference (g)	Aliquot (mL)	Solids (g/L)	Average (g/L)	Standard Deviation
1	1.1135	1.1283	0.0148	2.5	5.92	6.48	0.792
2	1.1173	1.1349	0.0176	2.5	7.04		

where Wo and Wf are initial and final weights respectively

Vol Blank (Vo)	Titration Volume (V)	MLSS (g/L)
8.75	3.09	6.48

Calculated value of Surface Charge (meq/ g MLSS)	
1	-0.437

SRT 30 - February 11, 2002

Titration data

Sample	Vo (mL)	Vf (mL)	Difference (mL)	Average (mL)	Standard Deviation
1	23.70	27.40	3.70	3.22	0.49
2	28.55	31.27	2.72		
3	31.30	34.54	3.24		
Blank 1	5.29	14.61	9.32	9.21	0.16
Blank 2	14.61	23.70	9.09		

where Vo and Vf are initial and final volumes respectively

MLSS Calculations

Sample	Wo (g)	Wf (g)	Difference (g)	Aliquot (mL)	Solids (g/L)
1	1.0964	1.1163	0.0199	2.5	7.96

where Wo and Wf are initial and final weights respectively

Vol Blank (Vo)	Titration Volume (V)	MLSS
9.21	3.22	7.96

Calculated value of Surface Charge (meq/ g MLSS)	
1	-0.376

SRT 30 - February 26, 2002

Titration data

Sample	Vo (mL)	Vf (mL)	Difference (mL)	Average (mL)	Standard Deviation
1	30.20	34.09	3.89	3.71	0.26
2	34.09	37.61	3.52		
Blank 1	1.10	9.72	8.62	8.40	0.31
Blank 2	9.72	17.90	8.18		

where Vo and Vf are initial and final volumes respectively

MLSS Calculations

Sample	Wo (g)	Wf (g)	Difference (g)	Aliquot (mL)	Solids (g/L)	Average (g/L)	Standard Deviation
1	1.0996	1.112	0.0124	2.5	4.96	5.34	0.537
2	1.1099	1.1242	0.0143	2.5	5.72		

where Wo and Wf are initial and final weights respectively

Vol Blank (Vo)	Titration Volume (V)	MLSS (g/L)
8.4	3.705	5.34

	Calculated value of Surface Charge (meq/ g MLSS)
1	-0.440

SRT 30 - March 8, 2002

Titration data

Sample	Vo (mL)	Vf (mL)	Difference (mL)	Average (mL)	Standard Deviation
1A	25.12	26.68	1.56	1.67	0.15
1B	26.68	28.28	1.60		
1C	29.58	31.42	1.84		
Blank 1	2.00	10.30	8.30	8.15	0.21
Blank 2	10.35	18.36	8.01		

where Vo and Vf are initial and final volumes respectively

MLSS Calculations

Sample	Wo (g)	Wf (g)	Difference (g)	Aliquot (mL)	Solids (g/L)	Average (g/L)	Standard Deviation
1	1.1003	1.1173	0.0170	2.50	6.80	7.02	0.311
2	1.1103	1.1284	0.0181	2.50	7.24		

where Wo and Wf are initial and final weights respectively

Vol Blank (Vo)	Titration Volume (V)	MLSS (g/L)
8.15	1.67	7.02

	Calculated value of Surface Charge (meq/ g MLSS)
1	-0.462

SRT 30 - March 20, 2002

Titration data

Sample	Vo (mL)	Vf (mL)	Difference (mL)	Average (mL)	Standard Deviation
1A	43.02	46.02	3.00	3.10	0.17
1B	39.79	42.80	3.01		
1C	42.80	46.10	3.30		
Blank 1	18.12	26.71	8.59	8.69	0.14
Blank 2	26.71	35.50	8.79		

where Vo and Vf are initial and final volumes respectively

MLSS Calculations

Sample	Wo (g)	Wf (g)	Difference (g)	Aliquot (mL)	Solids (g/L)	Average (g/L)	Standard Deviation
1	1.1030	1.1116	0.0086	2.5	3.44	3.88	0.622
2	1.1234	1.1342	0.0108	2.5	4.32		

where Wo and Wf are initial and final weights respectively

Vol Blank (Vo)	Titration Volume (V)	MLSS (g/L)
8.69	3.10	3.88

Calculated value of Surface Charge (meq/ g MLSS)	
1	-0.720

SRT 30 - April 2, 2002

Titration data

Sample	Vo (mL)	Vf (mL)	Difference (mL)	Average (mL)	Standard Deviation
1A	41.62	44.10	2.48	2.43	0.12
1B	27.21	29.51	2.30		
1C	29.51	32.03	2.52		
Blank 1	14.65	23.20	8.55	8.64	0.13
Blank 2	23.20	31.93	8.73		

where Vo and Vf are initial and final volumes respectively

MLSS Calculations

Sample	Wo (g)	Wf (g)	Difference (g)	Aliquot (mL)	Solids (g/L)	Average (g/L)	Standard Deviation
1	1.1049	1.1200	0.0151	2.5	6.04	5.96	0.113
2	1.1241	1.1388	0.0147	2.5	5.88		

where Wo and Wf are initial and final weights respectively

Vol Blank (Vo)	Titration Volume (V)	MLSS (g/L)
8.64	2.43	5.96

	Calculated value of Surface Charge (meq/ g MLSS)
1	-0.521

SRT 30 - April 17, 2002

Titration data

Sample	Vo (mL)	Vf (mL)	Difference (mL)	Average (mL)	Standard Deviation
1A	35.48	38.69	3.21	3.23	0.03
1B	38.69	41.91	3.22		
1C	41.91	45.18	3.27		
Blank 1	8.45	17.25	8.80	8.75	0.07
Blank 2	17.41	26.11	8.70		

where Vo and Vf are initial and final volumes respectively

MLSS Calculations

Sample	Wo (g)	Wf (g)	Difference (g)	Aliquot (mL)	Solids (g/L)	Average (g/L)	Standard Deviation
1	1.1015	1.1208	0.0193	2.5	7.72	7.18	0.764
2	1.1204	1.1370	0.0166	2.5	6.64		

where Wo and Wf are initial and final weights respectively

Vol Blank (Vo)	Titration Volume (V)	MLSS (g/L)
8.75	3.23	7.18

	Calculated value of Surface Charge (meq/ g MLSS)
1	-0.384

APPENDIX L: Core Study – Hydrophobicity Data

Hydrophobicitiy Data – SRT 12

Date	Day #	Sample	Io	I	% Hydrophobicity	Average % Hydrophobicity	Standard Deviation
11-Feb-02	0	1	1.30	1.07	17.7	15.6	2.95
11-Feb-02		2	1.30	1.12	13.5		
26-Feb-02	15	1	1.35	1.15	14.2	11.8	3.51
26-Feb-02		2	1.35	1.22	9.28		
08-Mar-02	25	1	0.955	0.883	7.54	8.88	1.91
08-Mar-02		2	0.955	0.857	10.2		
20-Mar-02	37	1	0.979	0.793	19.0	12.4	9.22
20-Mar-02		2	0.979	0.921	5.92		
02-Apr-02	50	1	1.19	0.870	26.7	26.0	0.976
02-Apr-02		2	1.19	0.886	25.4		
17-Apr-02	65	1	1.05	0.569	45.6	45.2	0.549
17-Apr-02		2	1.05	0.577	44.8		

where Io and I are initial and final absorbance at 400 nm respectively

Hydrophobicitiy Data – SRT 30

Date	Day #	Sample	Io	I	% Hydrophobicity	Average % Hydrophobicity	Standard Deviation
11-Feb-02	0	1	1.398	1.071	23.4	19.3	5.89
11-Feb-02		2	1.398	1.187	15.1		
26-Feb-02	15	1	1.52	1.02	32.9	30.4	3.47
26-Feb-02		2	1.52	1.10	28.0		
08-Mar-02	25	1	1.51	1.19	21.3	22.2	1.22
08-Mar-02		2	1.51	1.16	23.0		
20-Mar-02	37	1	1.39	1.00	27.6	27.9	0.443
20-Mar-02		2	1.39	0.996	28.2		
02-Apr-02	50	1	1.46	0.939	35.5	34.8	0.938
02-Apr-02		2	1.46	0.959	34.2		
17-Apr-02	65	1	1.05	0.462	55.8	52.9	4.10
17-Apr-02		2	1.05	0.523	50.0		

where Io and I are initial and final absorbance at 400 nm respectively

APPENDIX M: Core Study – Extracellular Polymeric Substance Data

Protein Concentrations – SRT 12 days

Day	Day #	Absorbance @ 750 nm	Standard Curve y = mx	r^2	Sample	Absorbance @ 750 nm	Conc. (mg/L)	Average Conc. (mg/L)	Final Conc. (mg/g MLSS)	Average Conc. (mg/g MLSS)	Std. Dev.
5-Feb-02		0.000	y = 0.0033x	0.9754	1A	0.456	138	140	25.1	22.0	4.46
		0.076			1B	0.495	150				
		0.187			1C	0.438	133				
		0.252			2A	0.284	86.1	91.3	18.8		
		0.314			2B	0.319	96.6				
		0.488			2C	0.301	91.2				
11-Feb-02	0	0.000	y = 0.0029x	0.9848	1A	0.337	116	117	17.0	18.6	2.26
		0.0132			1B	0.337	116				
		0.146			1C	0.342	118				
		0.229			2A	0.450	155	154	20.2		
		0.328			2B	0.432	149				
		0.409			2C	0.456	157				
26-Feb-02	15	0.000	y = 0.0022x	0.8096	1A	0.328	149	156	30.4	25.8	6.51
		0.0550			1B	0.382	174				
		0.125			1C	0.319	145				
		0.180			2A	0.267	121	113	21.2		
		0.403			2B	0.244	111				
					2C	0.237	108				
8-Mar-02	25	0	y = 0.0031x	0.9975	1A	0.259	83.5	79.8	12.0	11.4	0.794
		0.120			1B	0.243	78.3				
		0.260			1C	0.240	77.5				
		0.393			2A	0.244	78.8	79.7	10.9		
		0.509			2B	0.253	81.5				
		0.611			2C	0.244	78.8				
20-Mar-02	37	0	y = 0.0031x	0.9975	1A	0.287	92.4	90.5	15.6	14.9	0.921
		0.120			1B	0.280	90.3				
		0.260			1C	0.275	88.7				
		0.393			2A	0.223	71.8	74.0	14.3		
		0.509			2B	0.245	79.0				
		0.611			2C	0.221	71.3				
2-Apr-02	50	0.000	y = 0.0036x	0.9745	1A	0.264	73.2	68.4	9.75	8.78	1.37
		0.181			1B	0.243	67.4				
		0.310			1C	0.233	64.7				
		0.481			2A	0.229	63.7	63.4	7.81		
		0.592			2B	0.237	65.9				
		0.660			2C	0.218	60.6				
17-Apr-02	65	0.000	y = 0.0036x	0.9745	1A	0.506	141	147	18.2	18.1	0.161
		0.181			1B	0.553	154				
		0.310			1C	0.524	146				
		0.481			2A	0.488	136	127	18.0		
		0.592			2B	0.398	111				
		0.660			2C	0.483	134				

Uronic Acid Concentrations – SRT 12 days

Day	Day #	Absorbance @ 750 nm	Standard Curve y = mx	r^2	Sample	Absorbance @ 750 nm	Conc. (mg/L)	Average Conc. (mg/L)	Final Conc. (mg/g MLSS)	Average Conc. (mg/g MLSS)	Std. Dev.
5-Feb-02		1.000	y = 0.0077x	0.9586	1A	0.102	13.3	16.1	2.88	2.66	0.322
		0.990			1B	0.164	21.3				
		0.945			1C	0.105	13.7				
		0.880			2A	0.102	13.3	11.8	2.43		
		0.810			2B	0.0809	10.5				
		0.720			2C	0.0888	11.5				
11-Feb-02	0	0.000	y = 0.0072x	0.9908	1A	0.114	15.8		2.07	2.11	0.0599
		0.00877			1B	0.114	15.8		2.07		
		0.0155			1C	0.119	16.6		2.18		
		0.0269									
		0.0706									
		0.149									
26-Feb-02	15	0.000	y = 0.009x	0.8883	1A	0.122	13.6	16.6	3.24	3.01	0.319
		0.0501			1B	0.177	19.6				
		0.996			2A	0.126	13.9	14.9	2.79		
		0.173			2B	0.131	14.5				
					2C	0.146	16.2				
8-Mar-02	25	0.000	y = 0.0067x	0.9703	1A	0.109	16.3	17.0	2.56	2.39	0.238
		0.0269			1B	0.108	16.2				
		0.0862			1C	0.125	18.6				
		0.107			2A	0.112	16.7	16.3	2.22		
		0.131			2B	0.114	16.9				
		0.158			2C	0.102	15.3				
20-Mar-02	37	0.000	y = 0.0067x	0.9703	1A	0.0531	7.92	8.68	1.50	1.23	0.380
		0.0269			1B	0.0482	7.19				
		0.0862			1C	0.0731	10.9				
		0.107			2A	0.0320	4.77	4.96	0.958		
		0.131			2B	0.0315	4.70				
		0.158			2C	0.0362	5.40				
2-Apr-02	50	0.000	0.0095x	0.9561	1A	0.0511	5.38	6.48	0.923	0.922	0.000495
		0.0410			1B	0.0680	7.16				
		0.119			1C	0.0655	6.89				
		0.149			2A	0.0655	6.89	7.49	0.922		
		0.173			2B	0.0580	6.10				
					2C	0.0899	9.46				
17-Apr-02	65	0.000	0.0095x	0.9561	1A	0.161	16.9	15.0	1.87	1.88	0.0204
		0.0410			1B	0.136	14.3				
		0.119			1C	0.131	13.8				
		0.149			2A	0.125	13.2	13.4	1.90		
		0.173			2B	0.142	15.0				
					2C	0.114	11.9				

Carbohydrate Concentrations – SRT 12 days

Day	Day #	Absorbance @ 750 nm	Standard Curve y = mx	r^2	Sample	Absorbance @ 750 nm	Conc. (mg/L)	Average Conc. (mg/L)	Final Conc. (mg/g MLSS)	Average Conc. (mg/g MLSS)	Std. Dev.
5-Feb-02		0.000	y = 0.0173x	0.9944	1A	0.648	37.4	36.0	6.46	5.14	1.85
		0.268			1B	0.699	40.4				
		0.678			1C	0.523	30.2				
		1.05			2A	0.301	17.4	18.6	3.83		
		1.46			2B	0.292	16.9				
		1.70			2C	0.372	21.5				
11-Feb-02	0	0.000	y = 0.0153x	0.9798	1A	0.745	48.7	45.3	6.60	6.27	0.460
		0.237			1B	0.523	34.2				
		0.757			1C	0.810	52.9				
		0.921			2A	0.620	40.5	45.2	5.95		
		1.26			2B	0.569	37.2				
		1.46			2C	0.886	57.9				
26-Feb-02	15	0.000	y = 0.0139x	0.9774	1A	0.442	31.8	30.9	6.03	5.24	1.11
		0.0969			1B	0.438	31.5				
		0.580			1C	0.408	29.3				
		0.851			2A	0.355	25.5	23.8	4.46		
		1.14			2B	0.329	23.7				
		1.38			2C	0.309	22.2				
8-Mar-02	25	0.000	y = 0.0047x	0.9906	1A	0.293	62.4	59.7	8.96	8.29	0.948
		0.102			1B	0.268	57.1				
		0.192			1C	0.280	59.5				
		0.302			2A	0.252	53.6	55.9	7.62		
		0.387			2B	0.268	56.9				
		0.442			2C	0.269	57.3				
20-Mar-02	37	0.000	y = 0.0047x	0.9906	1A	0.355	75.4	73.0	12.6	11.8	1.04
		0.102			1B	0.346	73.6				
		0.192			1C	0.329	70.0				
		0.302			2A	0.300	63.9	57.6	11.1		
		0.387			2B	0.248	52.8				
		0.442			2C	0.264	56.1				
2-Apr-02	50	0.000	y = 0.0156x	0.9958	1A	0.162	10.4	10.2	1.45	1.22	0.325
		0.342			1B	0.149	9.57				
		0.678			1C	0.164	10.5				
		0.951			2A	0.120	7.68	8.02	0.99		
		1.26			2B	0.131	8.38				
		1.51			2C	0.125	8.01				
17-Apr-02	65	0.000	y = 0.0156x	0.9958	1A	0.368	23.6	24.4	3.04	3.13	0.133
		0.342			1B	0.398	25.5				
		0.678			1C	0.377	24.2				
		0.951			2A	0.342	21.9	22.7	3.22		
		1.26			2B	0.382	24.5				
		1.51			2C	0.338	21.7				

DNA Concentrations – SRT 12 days

Day	Day #	Relative Fluorescence Units	Standard Curve y = mx + b	r^2	Sample	Relative Fluorescence Units	Conc. (mg/L)	Final Conc. (mg/g MLSS)	Average Conc. (mg/g MLSS)	Std. Dev.
5-Feb-02		0.0551	y=0.0003x + 0.0586	0.9952	1	0.1751	38.8	6.96	6.88	0.114
		0.1182			2	0.1575	33.0	6.80		
		0.2337								
		0.3734								
11-Feb-02	0	0.0551	y=0.0003x + 0.0586	0.9952	1	0.1437	28.4	4.14	4.04	0.135
		0.1182			2	0.1485	30.0	3.94		
		0.2337								
		0.3734								
26-Feb-02	15	0.0551	y=0.0003x + 0.0586	0.9952	1	0.1412	27.5	5.38	5.71	0.470
		0.1182			2	0.1554	32.3	6.04		
		0.2337								
		0.3734								
8-Mar-02	25	88.6	y=0.2321x + 91.192	0.9962	1	102.9	5.0	0.76	1.11	0.497
		196.0			2	116.0	10.7	1.46		
		347.0								
		432.7								
		668.1								
20-Mar-02	37	88.6	y=0.2321x + 91.192	0.9962	1	161.6	30.3	5.23	5.84	0.865
		196.0			2	168.8	33.4	6.46		
		347.0								
		432.7								
		668.1								
2-Apr-02	50	0	y=0.6321x	0.9930	1	158.0	25.0	3.56	2.36	1.691
		206			2	60.0	9.5	1.17		
		520								
		916								
		3393								
		6165								
17-Apr-02	65	0	y=0.6321x	0.9930	1	194.0	30.7	3.82	3.71	0.157
		206			2	160.0	25.3	3.60		
		520								
		916								
		3393								
		6165								

Protein Concentrations – SRT 30 days

Day	Day #	Absorbance @ 750 nm	Standard Curve y = mx	r^2	Sample	Absorbance @ 750 nm	Conc. (mg/L)	Average Conc. (mg/L)	Final Conc. (mg/g MLSS)	Average Conc. (mg/g MLSS)	Std. Dev.
11-Feb-02	0	0.000	y = 0.0029x	0.9848	1A	0.420	145	144	18.2	18.7	0.724
		0.0132			1B	0.415	143				
		0.146			1C	0.420	145				
		0.229			2A	0.438	151	152	19.3		
		0.328			2B	0.456	157				
		0.409			2C	0.432	149				
26-Feb-02	15	0.000	y = 0.0022x	0.8096	1A	0.208	94	104	21.5	22.2	0.953
		0.0550			1B	0.231	105				
		0.125			1C	0.248	113				
		0.180			2A	0.240	109	114	22.8		
		0.403			2B	0.261	119				
					2C	0.252	114				
8-Mar-02	25	0	y = 0.0031x	0.9975	1A	0.233	75.1	72.4	10.3	9.65	0.933
		0.120			1B	0.229	73.9				
		0.260			1C	0.211	68.1				
		0.393			2A	0.237	76.3	73.0	8.99		
		0.509			2B	0.213	68.8				
		0.611			2C	0.229	73.9				
20-Mar-02	37	0	y = 0.0031x	0.9975	1A	0.287	92.4	90.5	15.6	14.9	0.92
		0.120			1B	0.280	90.3				
		0.260			1C	0.275	88.7				
		0.393			2A	0.223	71.8	74.0	14.3		
		0.509			2B	0.245	79.0				
		0.611			2C	0.221	71.3				
2-Apr-02	50	0.000	y = 0.0036x	0.9745	1A	0.502	139	142	24.4	23.4	1.45
		0.181			1B	0.509	141				
		0.310			1C	0.520	144				
		0.481			2A	0.457	127	125	22.4		
		0.592			2B	0.455	126				
		0.660			2C	0.441	123				
17-Apr-02	65	0.000	y = 0.0036x	0.9745	1A	0.282	78	71	13.6	14.4	1.14
		0.181			1B	0.240	67				
		0.310			1C	0.240	67				
		0.481			2A	0.348	97	94	15.2		
		0.592			2B	0.328	91				
		0.660			2C	0.335	93				

Uronic Acid Concentrations – SRT 30 days

Day	Day #	Absorbance @ 750 nm	Standard Curve y = mx	r^2	Sample	Absorbance @ 750 nm	Conc. (mg/L)	Average Conc. (mg/L)	Final Conc. (mg/g MLSS)	Average Conc. (mg/g MLSS)	Std. Dev.
11-Feb-02	0	0.000	y = 0.0072x	0.9908	1A	0.108	14.99		1.89	3.00	0.983
		0.00877			1B	0.215	29.82		3.77		
		0.0155			1C	0.190	26.45		3.34		
		0.0269									
		0.0706									
		0.149									
26-Feb-02	15	0.000	y = 0.009x	0.8883	1A	0.0809	8.99	10.4	2.15	2.06	0.130
		0.0501			1B	0.110	12.2				
		0.996			1C	0.0904	10.0				
		0.173			2A	0.0867	9.64	9.83	1.97		
					2B	0.0867	9.64				
					2C	0.0921	10.2				
8-Mar-02	25	0.000	y = 0.0067x	0.9703	1A	0.109	16.3	17.0	2.56	2.39	0.238
		0.0269			1B	0.108	16.2				
		0.0862			1C	0.125	18.6				
		0.107			2A	0.112	16.7	16.3	2.22		
		0.131			2B	0.114	16.9				
		0.158			2C	0.102	15.3				
20-Mar-02	37	0.000	y = 0.0067x	0.9703	1A	0.0975	14.5	13.2	1.89	1.61	0.392
		0.0269			1B	0.0783	11.7				
		0.0862			1C	0.0904	13.5				
		0.107			2A	0.0757	11.3	10.8	1.33		
		0.131			2B	0.0660	9.85				
		0.158			2C	0.0757	11.3				
2-Apr-02	50	0.000	0.0095x	0.9561	1A	0.130	13.7	13.4	2.32	2.22	0.137
		0.0410			1B	0.134	14.1				
		0.119			1C	0.119	12.5				
		0.149			2A	0.107	11.2	11.9	2.12		
		0.173			2B	0.119	12.5				
					2C	0.113	11.9				
17-Apr-02	65	0.000	0.0095x	0.9561	1A	0.108	11.4	11.2	2.15	2.14	0.007
		0.0410			1B	0.097	10.3				
		0.119			1C	0.112	11.8				
		0.149			2A	0.120	12.6	13.2	2.14		
		0.173			2B	0.128	13.5				
					2C	0.128	13.5				

Carbohydrate Concentrations – SRT 30 days

Day	Day #	Absorbance @ 750 nm	Standard Curve y = mx	r^2	Sample	Absorbance @ 750 nm	Conc. (mg/L)	Average Conc. (mg/L)	Final Conc. (mg/g MLSS)	Average Conc. (mg/g MLSS)	Std. Dev.
11-Feb-02	0	0.000	y = 0.0153x	0.9798	1A	0.602	39.4	42.1	5.33	5.04	0.410
		0.237			1B	0.721	47.1				
		0.757			1C	0.611	39.9				
		0.921			2A	0.561	36.6	37.5	4.75		
		1.26			2B	0.602	39.4				
		1.46			2C	0.561	36.6				
26-Feb-02	15	0.000	y = 0.0139x	0.9774	1A	0.229	16.5	16.5	3.40	3.38	0.03
		0.0969			1B	0.236	17.0				
		0.580			1C	0.221	15.9				
		0.851			2A	0.252	18.1	16.8	3.35		
		1.14			2B	0.197	14.2				
		1.38			2C	0.250	18.0				
8-Mar-02	25	0.000	y = 0.0047x	0.9906	1A	0.269	57.3	53.5	7.61	7.22	0.561
		0.102			1B	0.240	51.0				
		0.192			1C	0.245	52.1				
		0.302			2A	0.275	58.5	55.4	6.82		
		0.387			2B	0.258	54.9				
		0.442			2C	0.248	52.8				
20-Mar-02	37	0.000	y = 0.0047x	0.9906	1A	0.355	75.4	73.0	12.6	11.8	1.04
		0.102			1B	0.346	73.6				
		0.192			1C	0.329	70.0				
		0.302			2A	0.300	63.9	57.6	11.1		
		0.387			2B	0.248	52.8				
		0.442			2C	0.264	56.1				
2-Apr-02	50	0.000	y = 0.0156x	0.9958	1A	0.367	23.5	23.3	4.03	3.80	0.321
		0.342			1B	0.365	23.4				
		0.678			1C	0.362	23.2				
		0.951			2A	0.320	20.5	20.0	3.57		
		1.26			2B	0.302	19.4				
		1.51			2C	0.314	20.1				
17-Apr-02	65	0.000	y = 0.0156x	0.9958	1A	0.223	14.3	14.6	2.81	2.94	0.182
		0.342			1B	0.236	15.1				
		0.678			1C	0.225	14.5				
		0.951			2A	0.292	18.7	18.9	3.07		
		1.26			2B	0.288	18.5				
		1.51			2C	0.305	19.6				

DNA Concentrations – SRT 30 days

Day	Day #	Relative Fluorescence Units	Standard Curve y = mx + b	r^2	Sample	Relative Fluorescence Units	Conc. (mg/L)	Final Conc. (mg/g MLSS)	Average Conc. (mg/g MLSS)	Std. Dev.
11-Feb-02	0	0.0551	y=0.0003x + 0.0586	0.9952	1	0.3183	86.6	10.9	10.2	0.983
		0.1182			2	0.2853	75.6	9.55		
		0.2337								
		0.3734								
26-Feb-02	15	0.0551	y=0.0003x + 0.0586	0.9952	1	0.2486	63.3	13.1	11.7	2.02
		0.1182			2	0.2121	51.2	10.2		
		0.2337								
		0.3734								
8-Mar-02	25	88.6	y=0.2321x + 91.192	0.9962	1	106.4	6.57	0.936	0.876	0.0845
		196.0			2	106.6	6.63	0.816		
		347.0								
		432.7								
		668.1								
20-Mar-02	37	88.6	y=0.2321x + 91.192	0.9962	1	178.6	37.6	8.59	8.09	0.711
		196.0			2	174.7	36.0	7.59		
		347.0								
		432.7								
		668.1								
2-Apr-02	50	0	y=0.6321x	0.9930	1	193.0	30.5	5.26	5.87	0.852
		206			2	229.0	36.2	6.47		
		520								
		916								
		3393								
		6165								
17-Apr-02	65	0	y=0.6321x	0.9930	1	297.0	47.0	9.04	8.36	0.959
		206			2	299.0	47.3	7.68		
		520								
		916								
		3393								
		6165								

Appendix N: Core Study - Reactor Data

Date	Day No.	Temp (oC)		MLSS (g/L)		DO (mg/L)		TMP (kPa)					
		Reactor 1 SRT 30	Reactor 2 SRT12	Reactor 1 SRT 30	Reactor 2 SRT12	Reactor 1 SRT 30	Reactor 2 SRT12	Reactor 1 SRT 30 before relaxation	Reactor 1 SRT 30 after relaxation	Average TMP (kPa)	Average TMP (bar)	Permeability ($L/m^2/hr/bar$)	Permeability @ 25oC ($L/m^2/hr/bar$)
Mon. Feb 11	0												
Tues. Feb 12	1	12.3	12.3	20.49	21.3	4.81	5.6	-16.2	-15.1	-15.7	-0.157	223.6	309.4
Wed. Feb 13	2	10.8	10.8	20.05		3.29	4.35	-19.4	-19.4	-19.4	-0.194	180.4	256.7
Thurs. Feb 14	3	8.2	8.2	21.8	22.52			-20.2	-20.3	-20.3	-0.203	172.8	268.1
Fri. Feb 15	4	9	9	18.87	14.35	1.95	5.84	-18.6	-17	-17.8	-0.178	196.6	296.2
Sat. Feb 16	5	13.1	13.1					-18	-17.2	-17.6	-0.176	198.9	267.7
Mon. Feb 18	7	12.7	12.7	21.48	18.87	4.62	4.88	-21.4	-21.2	-21.3	-0.213	164.3	221.2
Tues. Feb 19	8	11.6	11.6	20.83	9.79			-22.4	-21.6	-22.0	-0.220	159.1	220.1
Wed. Feb 20	9	8.3	8.3	20.57	21.8	4.33	5.75	-23.8	-22.8	-23.3	-0.233	150.2	208.2
Thurs. Feb 21	10	8.7	8.7	19.06	18.89	4.06	2.77	-20.6	-20.1	-20.4	-0.204	172.0	231.5
Fri. Feb 22	11	8.8	8.8	17.51	21.63			-18.8	-18.9	-18.9	-0.189	185.7	249.9
Sat. Feb 23	12	8.9	8.9					-28.9	-28.6	-28.8	-0.288	121.7	163.8
Mon. Feb 25	14	9.4	9.4	19.84	13.77			-32.2	-31.3	-31.8	-0.318	110.2	148.4
Tues. Feb 26	15	9.1	9.1	20.92	20.19			-37	-35.5	-36.3	-0.363	96.6	129.9
Wed. Feb 27	16	9.1	9.1	20.6	22.04			-45.4	-42.7	-44.1	-0.441	79.5	106.9
Thurs. Feb 28	17	8.5	8.5	21.46	18.44			-47	-45	-46.0	-0.460	76.1	102.4
Fri. Mar. 1	18	9.2	9.2	21.25	20.72			-48.1	-48	-48.1	-0.481	72.8	98.0
Sat. Mar. 2	19	8.8	8.8					-49.9	-48	-49.0	-0.490	71.5	96.2
Mon. Mar. 4	21	8	8	17.3	27.94			-56.9	-53.7	-55.3	-0.553	63.3	87.7
Tues. Mar. 5	22			18.28	13.71			At Critical TMP Recovery Cleaning on all modules					
Wed. Mar. 6	23	8.5	8.5	19.55	13.14	5.13	5.16	-26	-25.7	-25.9	-0.259	135.4	182.2
Thurs. Mar. 7	24	8.7	8.7	20.44	14.38	4.88	1.98	-29.72	-28.4	-29.1	-0.291	120.4	162.1
Fri. Mar. 8	25	8.9	8.9	16.53	21.36			-33.5	-32.3	-32.9	-0.329	106.4	143.2
Sat. Mar. 9	26	9	9					-33.8	-33.1	-33.5	-0.335	104.6	140.8
Mon. Mar. 11	28	9.2	9.2	15.91	19.28			-50.5	-49.2	-49.9	-0.499	70.2	94.5
Tues. Mar. 12	29	8.4	8.4	18.08	20.16	5.19	1.16	-53.9	-50.9	-52.4	-0.524	66.8	92.6
Wed. Mar. 13	30	9.5	9.5	19.9	21.17	1.72	2.13	-43.5	-42.6	-43.1	-0.431	81.3	106.3
Thurs. Mar. 14	31	10.7	10.7	21.19	16.89			-43.7	-43.7	-43.7	-0.437	80.1	101.8
Fri. Mar. 15	32	8.9	8.9	28.35	20.36			-43.7	-59.7	-51.7	-0.517	67.7	91.1
Sat. Mar. 16	33	8.3	8.3					-66.1	-63.4	-64.8	-0.648	54.1	74.9
Mon. Mar. 18	35	8.4	8.4	20.98	16.12			At critical TMP					
Tues. Mar. 19	36	8.7	8.7	17.7	18.08	4.75	7.51	Recovery Cleaning					
Wed.. Mar. 20	37	8.9	8.9	12.66	17.78	1.62	3.27	-14.9	-15.1	-15.0	-0.150	133.3	179.5
Thurs. Mar. 21	38	8.9	8.9	12.02	17.38			-15.9	-12.2	-14.1	-0.141	142.3	191.6
Fri. Mar. 22	39	7.8	7.8	13.36	18.66			-17.2	-17.4	-17.3	-0.173	115.6	160.2
Sat. Mar. 23	40	7	7					-17.8	-18	-17.9	-0.179	111.7	159.6
Mon. Mar. 25	42	7.8	7.8	16.06	18.96			-19.5	-19.5	-19.5	-0.195	102.6	142.2
Tues. Mar. 26	43	8.9	8.9	11.54	19.11	1.95	2.44	-19.7	-19.4	-19.6	-0.196	102.3	137.7
Wed. Mar. 27	44	8.6	8.6	15.42	22.16			-20.4	-20.1	-20.3	-0.203	98.8	132.9
Thurs. Mar. 28	45	8.7	8.7	14.88	20.04	1.4	3.82	-21.5	-21.4	-21.5	-0.215	93.2	125.5
Fri. Mar. 29	46	12.1	12.1	16.46	18.46			-20.3	-20.2	-20.3	-0.203	98.8	122.1
Sat. Mar. 30	48	12.4	12.4					-21.7	-21.6	-21.7	-0.217	92.4	114.2
Mon. Apr. 1	49	13	13	15.06	18.01			-20.5	-20.3	-20.4	-0.204	98.0	117.9
Tues. Apr. 2	50	9.2	9.2	13.77	17.95	3.86	1.97	-22	-21.8	-21.9	-0.219	91.3	122.9
Wed. Apr. 3	51	13.3	13.3	15.41	19.46			-23.2	-22.5	-22.9	-0.229	87.5	105.3
Thurs. Apr. 4	52	13.1	13.1	13.13	20.22	5.03	4.61	-23.2	-23.1	-23.2	-0.232	86.4	103.9
Fri. Apr. 5	53	10.2	10.2	17.3	18.22	3.75	4.25	-23.8	-23.7	-23.8	-0.238	84.2	110.1
Sat Apr. 6	54	10.3	10.3					-24.1	-23.7	-23.9	-0.239	83.7	109.4
Mon. Apr. 8	56	10.8	10.8	19.5	20.89			-22.3	-22.1	-22.2	-0.222	90.1	114.5
Tues. Apr. 9	57	11.1	11.1	23.08	18.58	2.79	5.6	-28.2	-27.1	-27.7	-0.277	72.3	91.9
Wed. Apr. 10	58	9.6	9.6	21.71	18.63	4.44	4.17	-27.1	-26.6	-26.9	-0.269	74.5	97.4
Thur. Apr. 11	59	10.9	10.9	20.24	19.14			-26	-25.8	-25.9	-0.259	77.2	98.2
Fri Apr 12	60	15.3	15.3	14.6	18.88			-23.2	-23.4	-23.3	-0.233	85.8	97.9
Sat Apr. 13	61	12.8	12.8					-26.4	-26.3	-26.4	-0.264	75.9	91.3
Mon Apr. 15	63	11.7	11.7	14.29	19.12			-25.3	-25	-25.2	-0.252	79.5	98.3
Tues Apr 16	64	13.4	13.4	15.34	21.04	4.94	4.62	-27.3	-27.4	-27.4	-0.274	73.1	88.0

Appendix N

Date	Day No.	TMP (kPa)											
		Reactor 2 SRT 12 before relaxation	Reactor 2 SRT 12 after relaxation	Average TMP (kPa)	Average TMP (bar)	Permeability ($L/m^2/hr/bar$)	Permeability @ 25oC ($L/m^2/hr/bar$)	Reactor 2 SRT 12 before backwash	Reactor 2 SRT 12 after backwash	Average TMP (kPa)	Average TMP (bar)	Permeability ($L/m^2/hr/bar$)	Permeability @ 25oC ($L/m^2/hr/bar$)
Mon. Feb 11	0												
Tues. Feb 12	1	-12.1	-12.1	-12.1	-0.121	289.3	400.2	-14.8	-14.1	-14.5	-0.145	242.2	335.1
Wed. Feb 13	2	-14.3	-14.1	-14.2	-0.142	246.5	350.7	-15.2	-14.7	-15.0	-0.150	234.1	333.1
Thurs. Feb 14	3	-15.6	-15.5	-15.6	-0.156	225.1	349.1	-16.3	-16.3	-16.3	-0.163	214.7	333.1
Fri. Feb 15	4	-16.1	-15.6	-15.9	-0.159	220.8	332.6	-15.8	-14.8	-15.3	-0.153	228.8	344.6
Sat. Feb 16	5	-17.4	-16.9	-17.2	-0.172	204.1	274.8	-15.2	-13.4	-14.3	-0.143	244.8	329.5
Mon. Feb 18	7	-14.4	-14	-14.2	-0.142	246.5	331.8	-22.4	-21.1	-21.8	-0.218	160.9	216.6
Tues. Feb 19	8	-17.7	-17.4	-17.6	-0.176	199.4	275.9	-24.4	-23.1	-23.8	-0.238	147.4	203.9
Wed. Feb 20	9	-15.7	-17.1	-16.4	-0.164	213.4	295.8	-28.5	-26.7	-27.6	-0.276	126.8	175.8
Thurs. Feb 21	10	-22.3	-21	-21.7	-0.217	161.7	217.6	-30	-26.7	-28.4	-0.284	123.5	166.2
Fri. Feb 22	11	-32.4	-31.2	-31.8	-0.318	110.1	148.1	-39.9	-34.7	-37.3	-0.373	93.8	126.3
Sat. Feb 23	12	-38.3	-35.7	-37.0	-0.370	94.6	127.3	-39.2	-35.8	-37.5	-0.375	93.3	125.6
Mon. Feb 25	14	-49.3	-45	-47.2	-0.472	74.2	99.9	-42.1	-38.1	-40.1	-0.401	87.3	117.5
Tues. Feb 26	15	-56.2	-58.3	-57.3	-0.573	61.1	82.3	-48	-42.2	-45.1	-0.451	77.6	104.4
Wed. Feb 27	16	-49.4	-43.9	-46.7	-0.467	75.0	101.0	-47.5	-42.8	-45.2	-0.452	77.5	104.3
Thurs. Feb 28	17	-61.2	-54.4	-57.8	-0.578	60.6	81.5	-51.3	-46.2	-48.8	-0.488	71.8	96.6
Fri. Mar. 1	18	-62.1	-58	-60.1	-0.601	58.3	78.4	-50	-45.8	-47.9	-0.479	73.1	98.3
Sat. Mar. 2	19	Recovery Cleaning						-53.3	-48.7	-51.0	-0.510	68.6	92.4
Mon. Mar. 4	21	-58	-51.5	-54.8	-0.548	63.9		-66.6	-58.8	-62.7	-0.627	55.8	77.4
Tues. Mar. 5	22	At Critical TMP Recovery Cleaning on all modules											
Wed. Mar. 6	23	-35.3	-32.5	-33.9	-0.339	103.2	139.0	-29.7	-29.9	-29.8	-0.298	117.4	158.1
Thurs. Mar. 7	24	-38.2	-37.1	-37.7	-0.377	93.0	125.1	-32.8	-30.6	-31.7	-0.317	110.4	148.6
Fri. Mar. 8	25	-49.5	-45.8	-47.7	-0.477	73.5	98.9	-36.4	-33.7	-35.1	-0.351	99.9	134.4
Sat. Mar. 9	26	-45.9	-44.3	-45.1	-0.451	77.6	104.4	-36.4	-33.3	-34.9	-0.349	100.4	135.2
Mon. Mar. 11	28	-62.5	-63.4	-63.0	-0.630	55.6	74.8	-42.6	-39.2	-40.9	-0.409	85.6	115.2
Tues. Mar. 12	29	At critical TMP						-45.2	-41.4	-43.3	-0.433	80.8	112.0
Wed. Mar. 13	30	Recovery Cleaning						-48.7	-48.1	-48.4	-0.484	72.3	94.6
Thurs. Mar. 14	31	-10.2	-11.5	-10.9	-0.109	184.3	234.3	At critical TMP					
Fri. Mar. 15	32	-9.9	-10	-10.0	-0.100	201.0	270.5	Recovery Cleaning					
Sat. Mar. 16	33	-14.6	-14.3	-14.5	-0.145	138.4	191.8	-11.3	-15	-13.2	-0.132	152.1	210.8
Mon. Mar. 18	35	-17.8	-17.1	-17.5	-0.175	114.6	158.9	-20.3	-19	-19.7	-0.197	101.8	141.1
Tues. Mar. 19	36	-17.5	-17.2	-17.4	-0.174	115.3	155.1	-19.4	-19.3	-19.4	-0.194	103.4	139.1
Wed.. Mar. 20	37	-17.2	-17.5	-17.4	-0.174	115.3	155.1	-21.2	-20.7	-21.0	-0.210	95.5	128.5
Thurs. Mar. 21	38	-17.5	-16.7	-17.1	-0.171	117.0	157.4	-19.4	-18.2	-18.8	-0.188	106.4	143.2
Fri. Mar. 22	39	-18.8	-19	-18.9	-0.189	105.8	146.7	-21.6	-20.8	-21.2	-0.212	94.3	130.8
Sat. Mar. 23	40	-19.5	-19.6	-19.6	-0.196	102.3	146.1	-22.4	-22.4	-22.4	-0.224	89.3	127.5
Mon. Mar. 25	42	-21.7	-20.7	-21.2	-0.212	94.3	130.8	-22.7	-23.2	-23.0	-0.230	87.1	120.8
Tues. Mar. 26	43	-21.8	-20.5	-21.2	-0.212	94.6	127.3	-24.1	-23	-23.6	-0.236	84.9	114.3
Wed. Mar. 27	44	-21.7	-21.8	-21.8	-0.218	92.0	123.8	-24.7	-24	-24.4	-0.244	82.1	110.5
Thurs. Mar. 28	45	-22.6	-22.4	-22.5	-0.225	88.9	119.6	-24.8	-23.3	-24.1	-0.241	83.2	111.9
Fri. Mar. 29	46	-21.4	-21.6	-21.5	-0.215	93.0	115.0	-20.4	-17.9	-19.2	-0.192	104.4	129.1
Sat. Mar. 30	48	-23.6	-23.3	-23.5	-0.235	85.3	105.4	-20	-19.9	-20.0	-0.200	100.3	123.9
Mon. Apr. 1	49	-23.7	-23	-23.4	-0.234	85.7	103.0	-23.7	-21.4	-22.6	-0.226	88.7	106.7
Tues. Apr. 2	50	-25.7	-25.6	-25.7	-0.257	78.0	104.9	-17.6	-17.4	-17.5	-0.175	114.3	153.8
Wed. Apr. 3	51	-26.9	-26.5	-26.7	-0.267	74.9	90.1	-22.1	-21.5	-21.8	-0.218	91.7	110.4
Thurs. Apr. 4	52	-27.5	-27.4	-27.5	-0.275	72.9	87.6	-26.7	-27.1	-26.9	-0.269	74.3	89.4
Fri. Apr. 5	53	-29.3	-28.6	-29.0	-0.290	69.1	90.3	-26.8	-25.7	-26.3	-0.263	76.2	99.6
Sat Apr. 6	54	-29.6	-29.2	-29.4	-0.294	68.0	89.0	-27.5	-26.6	-27.1	-0.271	73.9	96.7
Mon. Apr. 8	56	-30.7	-30.2	-30.5	-0.305	65.7	83.5	-29.6	-28.4	-29.0	-0.290	69.0	87.7
Tues. Apr. 9	57	-27.5	-26.8	-27.2	-0.272	73.7	93.6	-29.1	-26	-27.6	-0.276	72.6	92.3
Wed. Apr. 10	58	-28.6	-28.2	-28.4	-0.284	70.4	92.1	-32.6	-29.5	-31.1	-0.311	64.4	84.2
Thur. Apr. 11	59	-28.9	-29	-29.0	-0.290	69.1	87.8	-32.1	-29.6	-30.9	-0.309	64.8	82.4
Fri Apr 12	60	-28.4	-28.2	-28.3	-0.283	70.7	80.6	-29.9	-29.1	-29.5	-0.295	67.8	77.3
Sat Apr. 13	61	-29.7	-29.3	-29.5	-0.295	67.8	81.6	-31.5	-30.4	-31.0	-0.310	64.6	77.7
Mon Apr. 15	63	-27.7	-27.4	-27.6	-0.276	72.6	89.7	-31.2	-30.8	-31.0	-0.310	64.5	79.8
Tues Apr 16	64	-30.8	-30.5	-30.7	-0.307	65.3	78.5	-32.1	-31	-31.6	-0.316	63.4	76.3

Appendix N

Feed Sewage Sample

Date	Day No.	TSS (mg/L)	pH	TCOD (mg/L)	FCOD (mg/L)	Total P (mg/L)	Ammonia N (mg/L)
Wed. Feb 13	2	340	6.92	1074	63	22.1	13.7
Wed. Feb 20	9	343	7.14	568	113	26.8	14
Wed. Mar. 6	23	216	7.18	379	71	18.2	17
Thurs. Mar. 14	31	233	7.25	391	67	25.2	17.6
Thurs. Mar. 21	38	280	7.19	371	59	21.8	21.2
Wed. Mar. 27	44	320	7.46	449	48	24.2	18
Thurs. Apr. 4	52	273	7.41	624	44	17.2	7.8
Thur. Apr. 11	59	403	7.38	1424	69	48.5	15.3
Average		301	7.24	660	67	25.5	15.6
Standard Deviation		62.2	0.175	386	21	9.86	3.97

Permeate Analysis

		Permeate pH			Permeate COD (mg/L)		
Date	Day No.	Reactor 1 SRT 30 Relaxation	Reactor 2 SRT 12 Backwash	Reactor 2 SRT12 Relaxation	Reactor 1 SRT 30 Relaxation	Reactor 2 SRT 12 Backwash	Reactor 2 SRT12 Relaxation
Wed. Feb 13	2	7.16	7.07	7.16	9	15	10
Wed. Feb 20	9	7.25	7.28	7.3	23	28	35
Wed. Mar. 6	23	7.23	7.34	7.25	11	13	11
Thurs. Mar. 14	31	7.3		7.2	9		5
Thurs. Mar. 21	38	7.1	7.13	7.11	8	4	8
Wed. Mar. 27	44	7.17	7.22	7.25	22	18	13
Thurs. Apr. 4	52	7.34	7.34	7.42	8	12	13
Thur. Apr. 11	59	7.33	7.4	7.4	10	8	19
Average		7.24	7.25	7.26	12.5	14	14
Standard Deviation		0.0867	0.121	0.109	6.3	7.7	9.3

Appendix O: Core Study - Clean Water Flux Data

Reactor 1 SRT 30 permeate/relaxation

Date	Day No.	Temp. (°C)	Flow (mL/min)	Flow (L/hr)	Flux ($L/m^2/hr$)	TMP @ 1 minute (kPa)	TMP @ 5 minutes (kPa)	Average TMP over 4 minutes (kPa)	Average TMP over 4 minutes (bar)	Permeability ($L/m^2/hr/bar$)	Permeability @ 25oC ($L/m^2/hr/bar$)	Sample
Mon. Feb 11	0	9	595	35.7	39.7	-17.1	-18.9	-18.0	-0.180	220.4	331.9	virgin membrane
Thurs. Feb 14	3	10	635	38.1	42.3	-15.8	-15.1	-15.5	-0.155	274.0	401.0	Run 1: after 3 days of filtration
Tues. Feb 26	15	12	605	36.3	40.3	-19.4	-21.6	-20.5	-0.205	196.7	272.2	Run 1: after 15 days of filtration
Mon. Mar. 4	21	11.4	610	36.6	40.7	-22.6	-21.6	-22.1	-0.221	184.0	261.8	Run 1: at critical TMP
Tues. Mar. 5	22	9.3	610	36.6	40.7	-7.4	-9.9	-8.7	-0.087	470.1	708.2	After first 2000 ppm NaOCl recovery cleaning
Tues. Mar. 5	22	9.3	610	36.6	40.7	-14.6	-14.7	-14.7	-0.147	277.6	418.1	Run 2: after 2 hours of filtration
Mon. Mar. 18	35	10.2	600	36.0	40.0	-40.3	-40.2	-40.3	-0.403	99.4	145.4	Run 2: at critical TMP
Tues. Mar. 19	36	11.1	610	36.6	40.7	-26	-26.2	-26.1	-0.261	155.8	221.7	After second 2000 ppm NaOCl recovery cleaning
Tues. Mar. 19	36	13.1	650	39.0	43.3	-15.3	-16.4	-15.9	-0.159	273.4	368.1	Run 3: after 2 hours of filtration
Tues Apr 16	64	17.9	640	38.4	42.7	-13.4	-15.7	-14.6	-0.146	293.2	346.5	Run 3: after 28 days of filtration

Reactor 2 SRT 12 permeate/backwash

Date	Day No.	Temp. (°C)	Flow (mL/min)	Flow (L/hr)	Flux ($L/m^2/hr$)	TMP @ 1 minute (kPa)	TMP @ 5 minutes (kPa)	Average TMP over 4 minutes (kPa)	Average TMP over 4 minutes (bar)	Permeability ($L/m^2/hr/bar$)	Permeability @ 25oC ($L/m^2/hr/bar$)	Sample
Mon. Feb 11	0	9	570	34.2	38.0	-11.0	-9.8	-10.4	-0.104	365.4	491.8	virgin membrane
Thurs. Feb 14	3	10	610	36.6	40.7	-8.9	-9.1	-9.0	-0.090	451.9	590.9	Run 1: after 3 days of filtration
Tues. Feb 26	15	12	610	36.6	40.7	-34.8	-35.7	-35.3	-0.353	115.4	142.6	Run 1: after 15 days of filtration
Mon. Mar. 4	21	11.2	620	37.2	41.3	-31.0	-33.2	-32.1	-0.321	128.8	163.7	Run 1: at critical TMP
Tues. Mar. 5	22	9.3	605	36.3	40.3	-9.0	-9.4	-9.2	-0.092	438.4	590.1	After first 2000 ppm NaOCl recovery cleaning
Tues. Mar. 5	22	14	610	36.6	40.7	-16.1	-17.1	-16.6	-0.166	245.0	286.8	Run 2: after 2 hours of filtration
Thurs. Mar. 14	31	11.9	620	37.2	41.3	-31.5	-31.7	-31.6	-0.316	130.8	161.7	Run 2: at critical TMP
Fri. Mar. 15	32	9.5	620	37.2	41.3	-21.1	-12.9	-17.0	-0.170	243.1	318.0	After second 2000 ppm NaOCl recovery cleaning
Fri. Mar. 15	32	15	630	37.8	42.0	-8.8	-11.4	-10.1	-0.101	415.8	474.2	Run 3: after 2 hours of filtration
Tues Apr 16	64	18	620	37.2	41.3	-19.2	-19.4	-19.3	-0.193	214.2	226.1	Run 3: after 32 days of filtration

Appendix O

Reactor 2 SRT 12 permeate/relaxation

Date	Day No.	Temp. (°C)	Flow (mL/min)	Flow (L/hr)	Flux ($L/m^2/hr$)	TMP @ 1 minute (kPa)	TMP @ 5 minutes (kPa)	Average TMP over 4 minutes (kPa)	Average TMP over 4 minutes (bar)	Permeability ($L/m^2/hr/bar$)	Permeability @ 25oC ($L/m^2/hr/bar$)	Sample
Mon. Feb 11	0	9	595	35.7	39.7	-11.3	-12.1	-11.7	-0.117	339.0	456.3	virgin membrane
Thurs. Feb 14	3	10	620	37.2	41.3	-8.8	-9.4	-9.1	-0.091	454.2	594.0	Run 1: after 3 days of filtration
Fri. Mar. 1	18	12	610	36.6	40.7	-26.8	-27.6	-27.2	-0.272	149.5	184.8	Run 1: at critical TMP
Tues. Mar. 5	22	9.3	610	36.6	40.7	-10.7	-11.7	-11.2	-0.112	363.1	488.7	After first 2000 ppm NaOCl recovery cleaning
Tues. Mar. 12	29	9.4	620	37.2	41.3	-40.4	-40.3	-40.4	-0.404	102.4	137.9	Run 2: at critical TMP
Wed. Mar. 13	30	12.7	620	37.2	41.3	-12.0	-9.2	-10.6	-0.106	389.9	469.1	After second 2000 ppm NaOCl recovery cleaning
Wed. Mar. 13	30	16	640	38.4	42.7	-10.7	-11.6	-11.2	-0.112	382.7	425.1	Run 3: after 2 hours of filtration
Tues Apr 16	64	18	650	39.0	43.3	-18.5	-18.6	-18.6	-0.186	233.6	246.6	Run 3: after 34 days of filtration

Appendix P: Core Study - Estimation of Membrane Fouling

Reactor 1 SRT 30 permeate/relaxation

Date	Day No.	Temp. (°C)	Flow (mL/min)	Flow (m^3/s)	Flux ($m^3/m^2/s$)	TMP @ 1 minute (kPa)	TMP @ 5 minutes (kPa)	Average TMP over 4 minutes (kPa)	Average TMP over 4 minutes (Pa)	Viscosity (Pa s)	Resistance (R_t) (m^{-1})	Resistance ($R_t - R_m$) (m^{-1})	Sample
Mon. Feb 11	Install	9	595	9.92E-06	1.10E-05	-17.1	-18.9	-18.0	18000.0	0.00134	1.21E+12	0.00E+00	virgin membrane
Thurs. Feb 14	3	10	635	1.06E-05	1.18E-05	-15.8	-15.1	-15.5	15450.0	0.00131	1.01E+12	-2.09E+11	Run 1: after 3 days of filtration
Tues. Feb 26	15	12	605	1.01E-05	1.12E-05	-19.4	-21.6	-20.5	20500.0	0.00124	1.48E+12	2.66E+11	Run 1: after 15 days of filtration
Mon. Mar. 4	21	11.4	610	1.02E-05	1.13E-05	-22.6	-21.6	-22.1	22100.0	0.00126	1.56E+12	3.43E+11	Run 1: at critical TMP
Tues. Mar. 5	22	9.3	610	1.02E-05	1.13E-05	-7.4	-9.9	-8.7	8650.0	0.00133	5.74E+11	-6.40E+11	After first 2000 ppm NaOCl recovery cleaning
Tues. Mar. 5	22	9.3	610	1.02E-05	1.13E-05	-14.6	-14.7	-14.7	14650.0	0.00133	9.73E+11	-2.42E+11	Run 2: after 2 hours of filtration
Mon. Mar. 18	35	10.2	600	1.00E-05	1.11E-05	-40.3	-40.2	-40.3	40250.0	0.00130	2.79E+12	1.57E+12	Run 2: at critical TMP
Tues. Mar. 19	36	11.1	610	1.02E-05	1.13E-05	-26	-26.2	-26.1	26100.0	0.00127	1.82E+12	6.09E+11	After second 2000 ppm NaOCl recovery cleaning
Tues. Mar. 19	36	13.1	650	1.08E-05	1.20E-05	-15.3	-16.4	-15.9	15850.0	0.00120	1.10E+12	-1.16E+11	Run 3: after 2 hours of filtration
Tues Apr 16	64	17.9	640	1.07E-05	1.19E-05	-13.4	-15.7	-14.6	14550.0	0.00106	1.16E+12	-5.53E+10	Run 3: after 28 days of filtration

Reactor 2 SRT 12 permeate/backwash

Date	Day No.	Temp. (°C)	Flow (mL/min)	Flow (m^3/s)	Flux ($m^3/m^2/s$)	TMP @ 1 minute (kPa)	TMP @ 5 minutes (kPa)	Average TMP over 4 minutes (kPa)	Average TMP over 4 minutes (Pa)	Viscosity (Pa s)	Resistance (R_t) (m^{-1})	Resistance ($R_t - R_m$) (m^{-1})	Sample
Mon. Feb 11	Install	9	570	9.50E-06	1.06E-05	-11.0	-9.8	-10.4	10400.0	0.00134	7.33E+11	0.00E+00	virgin membrane
Thurs. Feb 14	3	10	610	1.02E-05	1.13E-05	-8.9	-9.1	-9.0	9000.0	0.00131	6.10E+11	-1.23E+11	Run 1: after 3 days of filtration
Tues. Feb 26	15	12	610	1.02E-05	1.13E-05	-34.8	-35.7	-35.3	35250.0	0.00124	2.53E+12	1.79E+12	Run 1: after 15 days of filtration
Mon. Mar. 4	21	11.2	620	1.03E-05	1.15E-05	-31.0	-33.2	-32.1	32100.0	0.00126	2.21E+12	1.48E+12	Run 1: at critical TMP
Tues. Mar. 5	22	9.3	605	1.01E-05	1.12E-05	-9.0	-9.4	-9.2	9200.0	0.00133	6.16E+11	-1.17E+11	After first 2000 ppm NaOCl recovery cleaning
Tues. Mar. 5	22	14	610	1.02E-05	1.13E-05	-16.1	-17.1	-16.6	16600.0	0.00117	1.26E+12	5.23E+11	Run 2: after 2 hours of filtration
Thurs. Mar. 14	31	11.9	620	1.03E-05	1.15E-05	-31.5	-31.7	-31.6	31600.0	0.00124	2.22E+12	1.49E+12	Run 2: at critical TMP
Fri. Mar. 15	32	9.5	620	1.03E-05	1.15E-05	-21.1	-12.9	-17.0	17000.0	0.00133	1.12E+12	3.84E+11	After second 2000 ppm NaOCl recovery cleaning
Fri. Mar. 15	32	15	630	1.05E-05	1.17E-05	-8.8	-11.4	-10.1	10100.0	0.00114	7.59E+11	2.68E+10	Run 3: after 2 hours
Tues Apr 16	64	18	620	1.03E-05	1.15E-05	-19.2	-19.4	-19.3	19300.0	0.00106	1.59E+12	8.59E+11	Run 3: after 32 days of filtration

Appendix P

Reactor 2 SRT 12 permeate/relaxation

Date	Day No.	Temp. (°C)	Flow (mL/min)	Flow (m^3/s)	Flux ($m^3/m^2/s$)	TMP @ 1 minute (kPa)	TMP @ 5 minutes (kPa)	Average TMP over 4 minutes (kPa)	Average TMP over 4 minutes (Pa)	Viscosity (Pa s)	Resistance (R_t) (m^{-1})	Resistance ($R_t - R_m$) (m^{-1})	Sample
Mon. Feb 11	Install	9	595	9.92E-06	1.10E-05	-11.3	-12.1	-11.7	11700.0	0.00134	7.90E+11	0.00E+00	virgin membrane
Thurs. Feb 14	3	10	620	1.03E-05	1.15E-05	-8.8	-9.4	-9.1	9100.0	0.00131	6.07E+11	-1.83E+11	Run 1: after 3 days of filtration
Fri. Mar. 1	18	12	610	1.02E-05	1.13E-05	-26.8	-27.6	-27.2	27200.0	0.00124	1.95E+12	1.16E+12	Run 1: at critical TMP
Tues. Mar. 5	22	9.3	610	1.02E-05	1.13E-05	-10.7	-11.7	-11.2	11200.0	0.00133	7.44E+11	-4.59E+10	After first 2000 ppm NaOCl recovery cleaning
Tues. Mar. 12	29	9.4	620	1.03E-05	1.15E-05	-40.4	-40.3	-40.4	40350.0	0.00133	2.64E+12	1.85E+12	Run 2: at critical TMP
Wed. Mar. 13	30	12.7	620	1.03E-05	1.15E-05	-12.0	-9.2	-10.6	10600.0	0.00121	7.62E+11	-2.78E+10	After second 2000 ppm NaOCl recovery cleaning
Wed. Mar. 13	30	16	640	1.07E-05	1.19E-05	-10.7	-11.6	-11.2	11150.0	0.00111	8.47E+11	5.73E+10	Run 3: after 2 hours of filtration
Tues Apr 16	64	18	650	1.08E-05	1.20E-05	-18.5	-18.6	-18.6	18550.0	0.00106	1.46E+12	6.70E+11	Run 3: after 34 days of filtration

APPENDIX Q: Statistical Analysis

T-Test

t-test for 2 independent samples for equal variance, based on Pagano (1993).

1. Calculate the means (μ_1, μ_2 in each group)
2. Calculate the variance (S_1^2, S_2^2 in each group)
3. Calculate S_p^2

$$S_p^2 = [(n_1-1)\, S_1^2+(n_2-1)\, S_2^2]/\, (n_1+n_2-2)$$

4. Calculate t, test the null hypothesis, H_o, that all observations come from the same population

$$H_o: \mu_1=\mu_2$$

$$t= \mu_1-\mu_2/\, [S_p^2(1/n_1+1/n_2)]^{1/2} \qquad \text{for } n_1+n_2-2 \text{ df (degrees of freedom)}$$

5. Compare with t-table (Table A.2, Pagano, 1993) to see if $p<0.05$.
6. If $p<0.05$ reject the null hypothesis, H_o.

Note: t-test was calculated by using Excel Software (for Windows 2000) and sample results are presented below.

Sample results of t-test (two-sample assuming equal variance) to determine if any difference in % relative hydrophobicity of microbial flocs exists between microbial flocs at a sludge retention time of 12 days and 30 days.

Sludge Age	**12 days**	**30 days**
Mean	19.98	31.25
Variance	187.8104	143.595
Observations	6	6
Pooled Variance	165.7027	
Hypothesized Mean Difference	0	
df	10	
t stat	-1.516420863	
P(T<=t) one-tail	0.080183936	
t Critical one-tail	1.812461505	
P(T<=t) two-tail*	0.160367872	
t Critical two-tail	2.228139238	

* not significantly different, $p>0.05$.